In-depth functional analysis of heterochromatin protein 1 in *Plasmodium falciparum*

INAUGURALDISSERTATION

zur

Erlangung der Würde eines Doktors der Philosophie

vorgelegt der

Philosophisch--Naturwissenschaftlichen Fakultät

der Universität Basel

von

Thi Ngoc Hai BUI

aus

Vietnam (VN)

Basel, 2020

Genehmigt von der Philosophisch-Naturwissenschaftlichen Fakultät auf Antrag von

---

Prof. Dr. Till S. Voss und Prof. Dr. Gabriele Pradel

Basel, den 17. Sep 2019

Prof. Dr. Martin Spiess

Dekan der Philosophisch-

Naturwissenschaftlichen Fakultät

Summary

The most severe form of malaria, caused by *Plasmodium falciparum,* is an enormous burden for the endemic countries without any commercial vaccine available currently. *P. falciparum* possesses a complex life cycle, changing from different hosts and environmental conditions, and hence requires intensive and essential mechanisms for regulation of gene expression to survive and take advantage from external environments. In recent years, epigenetic control of gene expression emerged as an important mechanism to regulate expression of genes involved in virulence and sexual differentiation. Among epigenetic histone marks, histone 3 lysine 9 trimethylation (H3K9me3), which is considered the hallmark of heterochromatin formation, is recognized by an evolutionary conserved silencing factor called heterochromatin protein 1 (HP1). HP1 is a small protein consisting of three domains: two conserved domains at the N and C-terminus, namely the chromo domain (CD) and chromoshadow domain (CSD), respectively, and a variable hinge or linker domain in between them. The CD recognizes and binds to H3K9me3 to establish heterochromatin while the CSD interacts with a large number of effector proteins. HP1 possesses a number of posttranslational modifications, among which phosphorylation is highly important in regulating its functions. *P. falciparum* encodes only one HP1 isoform in contrast to most other eukaryotes that contain two to five HP1 paralogs. Although HP1 has been well studied in model eukaryotes, the detailed functions of each PfHP1 domain as well as PfHP1 phosphorylation in *P. falciparum* are poorly understood. My PhD project aimed to investigate PfHP1 function in detail using CRISPR/Cas9-based gene editing combined with the DiCre/loxP system for conditional mutagenesis. The two specific objectives were (1) to uncover the roles of the individual PfHP1 domains in PfHP1 function and (2) to understand if and how phosphorylation of PfHP1 regulates its function. Both objectives focused on the three known PfHP1-dependent cellular processes: (1) the maintenance of heritable silencing and mutually exclusive expression of *var* genes, (2) mitotic progression of asexual blood stage parasites, and (3) sexual commitment.

In the first project, I aimed to analyse the functional contribution and conservation of the CD, Hinge and CSD domains of PfHP1 using the approach mentioned above to generate PfHP1 truncation and hybrid mutant lines. I found that nuclear localization ability of PfHP1 is underlined in the N-terminal 29 amino acids (1-29) and the C-terminal

76 amino acids (191-266). The former polypeptide is supposed to have weak ability of nuclear delivery while the later one is necessary for fully targeting PfHP1 to nucleus. I also showed that an intact PfHP1 containing all three structural domains is required for heterochromatin localization and the normal asexual growth pathway of blood stage malaria parasites. Third, I successfully generated a PfHP1 knock out cell line with more pronounced phenotype that allowed massive production of more than 82% of sexual commitment rate once induced and suggested a PfHP1-independent regulatory pathway of *var* gene silencing during gametocytogenesis. Finally, I showed that the HP1 Hinge and CSD domains are functionally conserved between human – and rodent malaria parasites.

In the second project, I aimed to address (1) the kinases phosphorylating PfHP1 and their target residues and (2) the role of selected phosphorylated residues in regulating PfHP1 function using similar approach mentioned above to generate conditional PfHP1 phosphomutant cell lines. Liquid chromatography tandem mass spectrometry (LC-MS/MS) analysis of immunoprecipitated native PfHP1 showed that PfHP1 is phosphorylated mostly in the CD and hinge domains. *In vitro* kinase assays revealed that PfHP1 is a substrate of *P. falciparum* CK2 (PfCK2). LC-MS/MS analysis showed that PfCK2 targets three clustered serine residues within the PfHP1 hinge region *in vitro*. By generating conditional PfHP1 phosphomutant cell lines using CRISPR/Cas9-mediated genome editing and the DiCre/LoxP system, I found that PfCK2-dependent phosphorylation of PfHP1, and phosphorylation of the PfHP1 hinge domain in general, is dispensable for proper PfHP1 localization, gene silencing, parasite growth and sexual conversion.

In summary, for the first time, in-depth function and functional conservation of PfHP1domains as well as phosphorylation of PfHP1 have been studied in detail in the three main PfHP1-dependent processes (*var* gene silencing, mitotic proliferation, sexual commitment). The experimental pipeline established in this study provides an elegant approach to interrogate function of other essential proteins. In addition, the study also provides a tool for robust production of gametocytes used in further studies on gametocyte biology or high-throughput anti-malaria gametocyte drug screen. This study is highly relevant to study pathogenesis and transmission as well as underlying epigenetic mechanisms in some other unicellular pathogenic eukaryotes since they also share common features such as changing living environments and mutually exclusive expression of surface antigens.

Acknowledgement

First of all, I would like to express my deepest gratitude to my advisor, Prof. Dr. Till Voss, who offered me interesting projects, gave me useful advice, developed my ideas and nurtured my aspiration in all the time of research and writing of this thesis. Till is not only an excellent and dedicated scientist that inspires students but also a good friend to share many experiences of life.

Further, I highly appreciate that Prof. Gabriele Pradel is part of my PhD committee and thank her for her useful conversations and evaluations during my PhD committee meetings as well as for her long trip from Aachen to Basel.

In addition, my gratefulness is for Prof. Hans-Peter Beck, who is not only joining my PhD committee, but also contributed valuable inputs during lab meetings, PhD student meetings and throughout my study at the Swiss TPH.

Moreover, I cannot say thank you enough for Prof. Christian Doerig and Prof. Isabelle Lucet for their intensive support, training and teaching during my collaboration in Australia, 2015. I am also thankful to have an opportunity to work with very skilful collaborators from the Monash University and the Walter and Eliza Hall Institute of Medical Research such as Megan J. Bird, Weiwen Dai, Mitchell B Batty, Simona John Von Freyend, Belinda Morahan, Teresa Carvalho.

I want to thank Dr. Paul Jenoe and Suzzette Moes for their enthusiastic assistance in MS/MS analysis during my study at the University of Basel.

I would also like to thank all the former and present members of the Gene Regulation family. Especially, I thank Igor Niederwieser for all of his help, training in recombinant protein expression as well as his useful advice for troubleshooting and problem solving. Additionally, my great appreciation is for Nicolas Brancucci, Eilidh Carrington who have supported me with completing unfinished experiments as well as provided me valuable scientific experience. Another special thank is dedicated to Elvira Carrio Gaspar for sharing whatever early or latter, daily or weekend, happy or difficult time in the lab. Further, I do not forget Eva Hitz, Travis Basson, Armin Passecker for their scientific discussions, helps with experiments at weekend, holiday and relaxing times outside the lab. I also greatly appreciate Nicole Bertschi, Michael Filarsky and Sylwia Dorota Niederwieser who have supported me with scientific experience when I was in

the laboratory. Nicole, thank you so much for your kind words and encouragement. You were always a good companion in the lab and a sister to me since I was the first time in the GR lab.

Besides, I am also grateful to have opportunities to work and receive enthusiastic supports from other members of the Swiss TPH institute: Prof. Ingrid Felger, Rahel Wampfler, Raphel Bieri, Julia Hauser, Liliana Rutaihwa, Jan Warncke, Francoise Brand, Sebastian Marco Rush...

Finally, I cherish and thank my family in Vietnam, and all of my friends, my former teachers and lectures who abundantly lighted up my spirit, and supplied me strength to overcome times of hardship! I appreciate my mum for all of her love, scarification and encouragement for me. In addition, my special thank is devoted to my husband that he always stays beside me, shares happiness and difficulties, answers my questions in biology and helps me with this thesis. Last but not least, during many years after graduation that I was committed to seek a so-called success; finally, I found it simply and not far away to reach. Since our little Vy came, she is the sweetest and the most successful outcome of my long PhD journey and my life that her shining smiles and endless naïve love for me always bring me strength and happiness. At this stage, I am proud not only to be a PhD but also a PhD Mom!

Table of Contents

Abbreviations

aa	amino acid
ADP	adenosine di-phosphate
ApiAP2	Apicomplexa apetala2
ATP	adenosine tri-phosphate
ATS	acid termial segment
BSA	bovine serum albumin
BSD	blasticidin S deaminase
Cas9	CRISPR associated protein 9
CD	chromo domain
CD-36	cluster of differentiation 36
Chp2	Chromodomain-containing protein 2
chr	chromosome
CK2	casein kinase 2
CRISPR	clustered regularly interspaced short palindromic repeat
CSD	chromoshadow domain
C-terminus	carboxy-terminus
CV	column volume
DAPI	4' 6'-diamindino-2-2phenyldole
DBL	Duffy binding ligand
DIC	differential interference contrast
DMSO	Dimethyl sulfoxide
DTT	DL-Dithiothreitol
EACA	Aminocaproic acid
EDTA	Ethylenediaminetetraacetic acid
G2/M	Gap 2/mitosis
GB1	B1 domain of Streptococcal protein G
GFP	green fluorescent protein
GlcNAC	N-acetyl-glucosamine
GSK3	glycogen synthase kinase-3
H3K9me3	trimethylation of lysine 9 on histone H3 protein subunit
HA	hemaglutinin

HDAC	histone deacetylase
hDHFR	human dehydrofolate reductase
HMT	histone methyltransferase
HP1	heterochromatin protein 1
hpi	hours post infection
HR	homology region
ICAM-1	Intercellular Adhesion Molecule 1
IDC	intraerythrocytic development cycle
IFA	indirect immunofluorescence assay
IP	immunoprecipitation
iRBC	infected red blood cell
KAHRP	knob-associated histidine-rich protein
LC-MS/MS	liquid chromatography tandem mass spectrometry
lncRNA	long non-coding RNA
LR	late ring
LS	late schizont
M31	heterochromatin protein 1 homolog beta
MBP	maltose-binding protein
NEK2/4	NIMA (Never In Mitosis Gene A)-Related Kinase 2/4
NLS	Nuclear localization signal
N-terminus	amino-terminus
PBS	phosphate-buffered saline
PfEMP1	*Plasmodium falciparum* erythrocyte membrane 1
PK6	protein kinase 6
PKA	protein kinase A
RAP	rapamycin
RT	room temperature
SD	standard deviation
SDS	Dodecyl sodium sulfate
sgRNA	single guide RNA
SHREC	Snf2/Hdac-containing Repressor Complex
SUMO	Small Ubiquitin-like Modifier
Swi6	Switching 6 protein
TBB	4,5,6,7-tetrabromobenzotriazole

TCA	trichloroacetic acid
TCEP	tris(2-carboxyethyl)phosphine hydrochloride
TF	transcription factor
TFA	trifluoroacetic acid
TSS	transcription starting site
WB	wash buffer
WHO	World Health Organization
wt	wild type
yFCU	yeast cytosine deaminase and uridyl phosphoribosyl transferase

Chapter 1. Introduction

1.1 Malaria and *Plasmodium falciparum*

Malaria is a complex parasitic disease transmitted by female *Anopheles* mosquitoes through blood feeding. In 2017, 219 million cases of malaria occurred worldwide, 2 million cases more compared with 2016 (World Health Organization – World malaria report 2018 at https://www.who.int/malaria/publications/world-malaria-report-2018/report/en/).

Five species of the *Plasmodium* genus infect humans, namely *P. vivax*, *P. ovale*, *P. malaria, P. knowlesi* and *P. falciparum* (Cox-Singh et al., 2008). Among them, *P. falciparum* causes the most lethal and severe malaria, especially among children under five years old (Elliott and Beeson, 2008). The massive proliferation of intra-erythrocytic parasites during blood stage infection is responsible for all malaria-related symptoms. A number of surface antigens on the infected red blood cell (RBC) membrane, in particular *P. falciparum* erythrocyte membrane protein 1 (PfEMP1), interact with receptors on blood endothelial cells such as ICAM-1, CD-36 and with uninfected RBCs (rosetting), resulting in cellular adherence and sequestration of infected RBC (iRBC) (Newbold et al., 1997; Rowe et al., 2009). Hence, iRBC clearance from the blood stream is reduced as the parasite escapes passage through the spleen (Yazdani et al., 2006). Furthermore, sequestration causes severe malaria outcomes such as cerebral or placental malaria by blocking blood flow, damaging tissues and triggering inflammatory responses (Miller et al., 2013). Antigenic variation and diversity of PfEMP1 and many other antigens contribute significantly to immune evasion and hence to the establishment of chronic infection (Reeder and Brown, 1996). Although acquired immune responses develop gradually after repeated exposure (Marsh and Kinyanjui, 2006), sterile immunity is not acquired even after life-long exposure to malaria parasites (Ferreira et al., 2004).

1.2 *Plasmodium falciparum* life cycle

P. falciparum has a complex life cycle in two different hosts and various environments: the sexual reproduction in mosquitoes and several cycles of asexual proliferation and development in the mosquitoes and the human host (Figure 1.1). During their blood meal, the female *Anopheles* injects sporozoites which travel to the liver where they

first infect hepatocytes (Scherf et al., 2008). The parasites then undergo asexual division to produce merozoites and are released into the blood stream to invade RBCs (Scherf et al., 2008). Within RBCs, parasites reside in a parasitophosphorous vacuole and develop into the ring stage, starting to synthesise stage-specific proteins that are actively exported into the host cell to refurnish the erythrocyte cytosol and membrane (Maier et al., 2009). Among these proteins, PfEMP1, encoded by *var* gene family, is considered the major parasite virulence factor. *var* gene expression is controlled tightly in a mutually exclusive manner that only one *var* gene is transcribed by a single parasite (Deitsch and Dzikowski, 2017; Dzikowski and Deitsch, 2009; Kyes et al., 2007; Scherf et al., 1998; Voss et al., 2014; 2006) in order to avoid exhausting the surface antigen repertoire. Once PfEMP1s is exported to the RBC membrane, the protein is assembled in so-called knob structures (Maier et al., 2009). The N-terminal (binding) region of PfEMP1 is directed on the external surface of iRBCs while the acidic C-terminal sequence (ATS) faces the erythrocyte cytosol (Baruch et al., 1995; J. D. Smith et al., 1995). The extracellular part of PfEMP1 is responsible for causing cellular adherence and antigenic variation which is the driving force of chronic infection (Bannister and Mitchell, 2003). When intra-erythrocytic parasites enter the schizont stage, the parasite nucleus divides multiple times and finally cytokinesis generates 16-32 merozoites that are released into the blood circulation to reinvade RBCs and start another 48-hour intraerythrocytic cycle. Importantly, during each round of intra-erythrocytic development, a small subpopulation of asexual parasites exits the cell cycle and undergoes sexual differentiation to form gametocytes (Ngotho et al., 2019). After 10-12 days of maturation, male and female stage V gametocytes are able to infect mosquitoes (Bruce et al., 1990; Inselburg, 1983; Silvestrini et al., 2000; T. G. Smith et al., 2000). Further in the mosquito, gamete egress, fertilization and sporogonic development occur to ultimately produce infective sporozoites ready for transmission to the next human.

During progression through the life cycle, *P. falciparum* expresses distinct global transcriptomes and proteomes (Horrocks et al., 2009). For instance, inside the mosquito, a noticeable proportion (46%) of proteins appear to be unique for the ookinete stage (Patra et al., 2008). Similarly, 49% of proteins found in sporozoites are specific for this stage and in merozoites, trophozoites and gametocytes 20-33% of all detected proteins are likely specific for the corresponding stage (Florens et al., 2002). Only a small number (6%) of proteins have been detected in all life cycle stages

(Florens et al., 2002). Even during the intraerythrocytic developmental cycle (IDC), transcription profiles during rings, trophozoites and schizonts are also stage-specific, showing that gene expression regulation during the IDC is tightly regulated in *P. falciparum* (Bozdech et al., 2003).

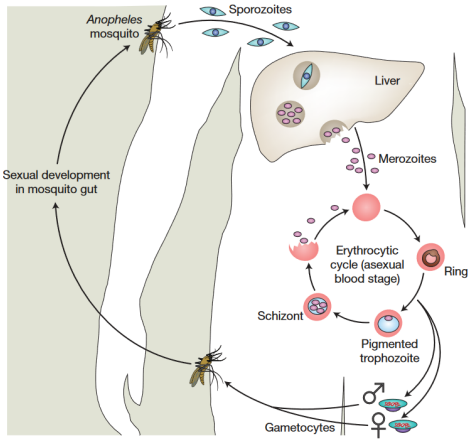

Figure 1.1. Life cycle of *P. falciparum* (Rowe et al., 2009)

It has therefore been suggested that *P. falciparum* transcribes many genes in a "just-in-time" manner where genes are only expressed when their protein products are needed (Bozdech et al., 2003). For example, genes important for the merozoite invasion process including *ama1*, *eba175*, *msp1*, *msp4* or *msp5* are transcribed in middle and late schizonts, whereas *var* genes and many genes required for host cell remodelling are expressed in ring stages, early after invasion (Bozdech et al., 2003).

1.3 Gene regulation in *Plasmodium falciparum*

As mentioned above, *P. falciparum* lives an extraordinarily complex life cycle during which morphology, function, metabolism and antigens are stage-specific. Hence, intensive and essential mechanisms for a tight regulation of gene expression are required for the parasite in order to survive and progress through vastly different environments (Horrocks et al., 2009; Voss et al., 2014). It is not surprising that *P. falciparum* controls gene expression at multiple levels (Horrocks et al., 2009) and interconnects different layers of regulation, including transcriptional regulation and epigenetic mechanisms to govern many important cellular processes, for example, the clonally variant expression of *var* genes to evade host immunity and sexual

conversion pathways in order to transform/switch from the asexual blood stage form to gametocytes, the transmissible form of the parasites.

1.3.1 Transcriptional regulation and specific transcription factors

One central mechanism of gene-specific transcriptional control in model eukaryotes is the fine-tuned interplay between *trans*-acting factors, for example transcription factors, and *cis*-regulatory elements in a sequence-specific manner at promoter regions (Horrocks et al., 2009). Compared to other eukaryotes, *P. falciparum* possesses a unique small set of specific transcription factors (TFs) (Coulson et al., 2004).

There have been few *P. falciparum* transcription factors (TFs) characterized so far including Myb1 protein (Gissot et al., 2005; Komaki-Yasuda et al., 2013) and several Apicomplexa apetala2 (ApiAP2) family factors (Balaji et al., 2005; Jeninga et al., 2019; Modrzynska et al., 2017; Painter et al., 2011).

While the mechanisms that *P. falciparum* uses to tightly control transcription are not well understood, several lines of evidences imply an important role of ApiAP2 factors in this type of regulation. ApiAP2 is a phylum-specific family of sequence-specific DNA-binding proteins in Apicomplexa phylum (De Silva et al., 2008). The proteins are varied in size but the AP2-intergrase DNA binding like domain containing 60 amino acids is highly conserved between ApiAP2 members (Balaji et al., 2005). Each of ApiAP2-family members has one to four AP2 domains (Balaji et al., 2005). Using protein binding microarrays (PBMs), a large number of these AP2 domains were shown to bind to specific DNA motifs that are also found in the promoter regions of subsets of parasite genes (Campbell et al., 2010; De Silva et al., 2008). As AP2 domains from particular ApiAp2 proteins are able to bind several DNA sequence motifs, this feature highly likely increases the number of genes regulated by one transcription factor (Campbell et al., 2010).

Most of *P. falciparum apiap2* genes (22/27 genes) are expressed in a stage-specific manner during the 48-hour IDC (Balaji et al., 2005). As presumed master regulators of parasite development, ApiAP2 factors have been shown to take part in developmental transition processes such as ookinete formation (Yuda et al., 2009), sporozoite formation (Yuda et al., 2010), liver stage development (Iwanaga et al., 2012) and gametocyte commitment within the human blood stream (Kafsack et al., 2014; Sinha et al., 2014). Up to date, there have been a number of ApiAP2 proteins characterized in detail. There are some ApiAP2 proteins functioning as transcription

factors that mediate gene expression, including five that have been characterized in the rodent malaria parasite, *P. berghei* and three have been characterized in *P. falciparum*. They are PbAP2-O (ortholog of PF3D7_1143100) (Yuda et al., 2009), PbAP2-L (ortholog of PF3D7_0730300) (Iwanaga et al., 2012), PbAP2-G2 (no otholog in *P. falciparum*) (Modrzynska et al., 2017; Yuda et al., 2015), PbAp2-SP (otholog of PF3D7_1466400 or PfAP2-exp) (Modrzynska et al., 2017; Yuda et al., 2010), PbAP2-G (ortholog of PfAP2-G) (Sinha et al., 2014), PfAP2-exp (Martins et al., 2017), PfAp2-I (Santos et al., 2017) and the PfAP2-G (Kafsack et al., 2014).

In the rodent malaria parasite *P. berghei*, PbAP2-L has a wide range of expression including salivary gland sporozoites, erythrocytic trophozoites and liver stages (Iwanaga et al., 2012). Depletion of PbAP2-L resulted in the arrest of parasites at mid-schizont development (36 hpi) in hepatocytes, thus decreasing the ability of liver infection (Iwanaga et al., 2012). Meanwhile, PbAP2-O and PbAP2-SP transcription factors were described to be exclusively expressed in mosquito stages (Yuda et al., 2010; 2009). PbAP2-O is highly expressed in ookinetes, the mosquito midgut-invading stage and plays an essential role for the normal morphogenesis of oocyst development (Yuda et al., 2009). The PbAP2-SP is expressed in oocyst and salivary gland sporozoites and disruption of *pbap2-sp* caused loss of sporozoite formation in oocyst (Yuda et al., 2010). Orthologs of PbAP2-L, PbAP2-O and PbAP2-SP in *P. falciparum*, in contrast, are all expressed during IDC (Balaji et al., 2005; Bozdech et al., 2003; Iwanaga et al., 2012; Le Roch et al., 2003; Otto et al., 2010; Yuda et al., 2009), suggesting that they might have IDC-related functions. To be specific, the disruption of *pfap2-exp* (ortholog of *pbap2-sp*) resulted in the alteration of the knob-morphology (rougher and larger) and an upregulation of some clonally variant gene families at sub-telomeric regions such as *rif, stevor* and *Pfmc-2TM* (Martins et al., 2017). Recently, PfAP2-I has been found to associate with the promoters of genes involved in wide range of functions in *P. falciparum* such as invasion genes (*msp*, *rap*, and *rhopH* gene families), nucleosome and chromatin-related genes, cell division/cell-cycle-related genes and genes related to vesicle formation and host cell remodelling (Santos et al., 2017).

In 2014, whole genome sequencing of gametocyte non-producer lines in both *P. falciparum* and *P. berghei* has discovered mutations in *ap2-g*, a conserved member of the ApiAp2 family among all species in Apicomplexa phylum (Sinha et al., 2014), connected to this phenotype (Kafsack et al., 2014; Sinha et al., 2014). Knock out of

ap2-g in the two parasites resulted in the complete loss of gametocyte producibility (Kafsack et al., 2014; Sinha et al., 2014). The correction of AP2-G mutations or complementation of an *ap2-g* deletion mutant in *P. berghei* restores gametocyte reducibility to that of wildtype parasites (Sinha et al., 2014). A number of gametocyte-specific genes have been found to be deregulated in the gametocyte non-producer *ap2-g* mutant lines by qRT-PCR and microarray (Kafsack et al., 2014; Sinha et al., 2014). Both of PfAP2-G and PbAP2-G DNA binding domain binds to a 6-mer palindrome motifs (GxGTAC and GTACxC) which occur frequently within promoters of genes upregulated in gametocytes (Kafsack et al., 2014; Sinha et al., 2014). These binding motifs are also found in the upstream region of the *pfap2-g* and *pbap2-g* genes, suggesting that the expression of AP2-G might follow an auto feedback regulatory mechanism (Kafsack et al., 2014; Sinha et al., 2014). In addition, *pfap2-g* locus was found associated with histone silencing marker (H3K9me3) (Kafsack et al., 2014; Lopez-Rubio et al., 2009) and is the only PfHP1-regulated member of the *apiap2* family (Brancucci et al., 2014; Flueck et al., 2009), implying that *pfap2-g* expression is also controlled by epigenetic mechanisms.

PbAP2-G2 (PBANKA_103430, no ortholog in *P. falciparum*) was first addressed as a transcription factor that is significantly associated with sexual commitment but acts downstream of this irreversible commitment point to rather modulate gametocyte maturation (Kafsack et al., 2014). PbAP2-G2 was later shown to bind to 5-mer motifs in the promoters of a series of genes that are required for asexual proliferation (Yuda et al., 2015). Many of these genes were found to be upregulated in PbAP2-G2 depleted cell line (Yuda et al., 2015), suggesting that PbAP2-G2 plays as a suppressor of genes important for asexual stages in gametocytes. Further, in a pure asexual population due to *pbap2-g* depletion, an upregulation in gene transcription and protein translation of gametocyte-specific and ookinete-specific genes was found upon *pbap2-g2* depletion (double knockout) (Modrzynska et al., 2017). The later study suggested that PbAP2-G2 plays as a suppressor of transmission genes in asexual parasites (Modrzynska et al., 2017). Together, these studies revealed PbAP2-G2 as a transcriptional repressor in both asexual and sexual blood stages in the rodent malaria parasites (Modrzynska et al., 2017; Yuda et al., 2015).

In addition to the transcription factors above, there are also ApiAp2 members that play other general functions, of which two have been characterized in *P. falciparum*, PfSIP2 (Flueck et al., 2010) and PfAP2-Tel (Sierra-Miranda et al., 2017). PfSIP2

(*Plasmodium falciparum* SPE2-interacting protein) was shown to interact preferentially with SPE2 motifs located in telomere-associated repetitive elements (TAREs) 2/3 regions and directly upstream of *upsB*-type *var* genes (Flueck et al., 2010; Voss et al., 2003). While orthologs of PfSIP2 were found in other sequenced *Plasmodium* species, sub-telomeric SPE2 elements were exclusively found in *P. falciparum* (Flueck et al., 2010; Voss et al., 2003). The protein was proposed to play multiple functional roles including *var* gene silencing, heterochromatin formation and organization, genome integrity, chromosome replication and segregation (Flueck et al., 2010) but the exact function of PfSIP2 remains unknown. Recently, in 2017, Sierra-Miranda M. and colleagues have reported PfAP2-Tel as a component of a telomere-binding complex in *P. falciparum* (Sierra-Miranda et al., 2017). The protein was identified with one canonical DNA-binding domain and conserved among all *Plasmodium* spp. (Sierra-Miranda et al., 2017). PfAP2-Tel localizes to telomeric clusters throughout all parasite stages in the IDC (Sierra-Miranda et al., 2017). Genome-wide profiling using ChIP-Seq revealed its predominant distribution at 14 telomere ends and protein binding assays revealed its direct binding to the GGGTT(T/C)A conserved telomeric tandem repeat (Mancio-Silva et al., 2008; Sierra-Miranda et al., 2017). It is interesting that this telomere repeat-binding factor (TRF) does not contain a sequence-specific MYB-type DNA-binding domain as all known TRFs have in other model eukaryotes (Giraud-Panis et al., 2010), but uses AP2 binding domain instead, thus opening a new insight into telomere biology in *P. falciparum* as well as set a novel function of ApiAP2 members.

Up to date, only two transcription factors outside the ApiAp2 family have been characterized in detail, namely PfMyb1 (Gissot et al., 2005) and PfPREBP (Kornberg, 2007). The PfMyb1 protein contains three Myb domains with DNA binding ability at the C-terminal region (Boschet et al., 2004). PfMyb1 protein was shown to be an essential transcription factor for the erythrocytic cycle of *P. falciparum* and for regulating key genes, such as *pfpk5* and *PFL1285c*, a homologue of proliferating cell nuclear antigen (PCNA) which is involved in cell cycle regulation and progression (Gissot et al., 2005). In addition, the transcription factor PREBP in *P. falciparum* was discovered as a novel and unique transcription factor by possessing four K-homology (KH) domains that are usually found in RNA- and single-stranded DNA-binding proteins (Valverde et al., 2008). The binding of PREBP to a 102 bp-*cis* enhancer region of the *pf1-cys-prx* gene regulates the expression timing of this antioxidant protein exclusively in trophozoites and schizont stages (Komaki-Yasuda et al., 2013).

1.3.2 Epigenetic regulation

Another alternative primary mode of transcriptional regulation is epigenetic control, which *P. falciparum* utilizes to govern nutrient uptake, clonally variant gene expression of virulence genes in blood stage parasites and sexual differentiation (Voss et al., 2014). Epigenetics is a biological term referring to the heritable, reversible change in phenotype occurring through changes in chromatin structure without changes in the underlying DNA sequence (Berger et al., 2009). The two major states of chromatin are known as euchromatin and heterochromatin. Euchromatin is rather loosely packed chromatin, allowing transcriptional activation of genes located in these regions. In contrast, heterochromatin consists of a more condensed chromatin structure related to gene inactivation/heritable silencing (Woodcock and Ghosh, 2010). In eukaryotes, DNA methylation, non-coding RNA and chromatin modifications are favourable processes involved in epigenetic regulation of gene expression (A. D. Goldberg et al., 2007; Handy et al., 2011).

In *Plasmodium falciparum*, DNA methylation is still an enigma. It has been reported that only a small proportion of the cytosines was asymmetrically methylated and non-CG methylations also occurs in the *P. falciparum* genome during its IDC (Ponts et al., 2013). While a potentially putative C5 DNA methytransferase gene (PF3D7_0727300, encoding for PfTRDMT1) was detected computationally (Ponts et al., 2013), the DNA methyltransferase activity of this protein was still controversial as a recent study has shown that PfTRDMT1 only methylated endogenous aspartic acid tRNA at cytosine position 38 but not DNA (Govindaraju et al., 2017). These results, together with an extreme A+T richness (80.6%) in the genome (Gardner et al., 2002) suggest that the parasite has lost its DNA methylation machinery during evolution, just like the other apicomplexan parasites *Toxoplasma gondii* and *Cryptosporidium parvum* (Gissot et al., 2008).

Another epigenetic mode to control gene expression in *P. falciparum* is the non-coding RNA machinery. As its name suggests, such RNAs are transcribed but not translated into proteins. Although *P. falciparum* lacks functional small RNA-interference machinery (RNAi) (Baum et al., 2009), long non-coding (lncRNAs) and antisense long non-coding RNAs (aslncRNAs) are observed in the parasite during its IDC (Gunasekera et al., 2004; López-Barragán et al., 2011; Patankar et al., 2001; Siegel et al., 2014; Vembar et al., 2014; Wei et al., 2014). lncRNAs have been controversially

shown to associate with either inactive or active *var* genes (Epp et al., 2009; Jiang et al., 2013; Ralph et al., 2005). To date, there have been more and more evidences revealing the association of aslncRNAs with the active *var* gene in a sequence-specific and dose-dependent manner (Amit-Avraham et al., 2015; Jing et al., 2018). Interestingly, while Voss and colleagues revealed an exogenous *var* promoter is sufficient to repress endogenous *var* gene transcription, thus controlling the singular choice of *var* gene expression (Voss et al., 2006), Q Jing and colleagues in contrast showed the co-transcription of both dominant endogenous and the newly induced *var* genes by an exogenous aslncRNA in one single parasite, thus breaking *var* gene mutually exclusive expression in short-term culture of parasites (Jing et al., 2018). Therefore, the *var* gene activation by aslncRNA is considered as a relative independent intermediary step of the regulation of singular *var* gene expression (Jing et al., 2018). Currently, antisense RNA transcript has been indicated as negative regulator for the expression of the gametocyte development 1 gene (*Pfgdv1*) which plays an important role in regulating sexual commitment (Filarsky et al., 2018). Deletion of *pfgdv1* aslncRNAs resulted in the expression of GDV1 and consequently the upregulation of *pfap2-g*, which in turns triggers sexual commitment and gametocytogenesis (Filarsky et al., 2018). The AP2-G, encoded by *pfap2-g, is* a conserved member of the ApiAp2 family and was previously discovered as a master regulator of gametocytogenesis in both *P. falciparum* and *P. berghei* (Kafsack et al., 2014; Sinha et al., 2014). The activation of *ap2-g* resulted in subsequent expression of genes encoding earliest known gametocyte markers, for example Pfs16, Pfg27/25, Pfg14.744 (Kafsack et al., 2014) and genes required for early gametocyte development such as several members of the PHIST family (Eksi et al., 2005).

Furthermore, chromatin modification is a well-known mode of chromatin-based epigenetic mechanisms mediating gene expression in a wide range of organisms from yeast to human. Because of the lack of apparent DNA methylation and a functional RNAi pathway, the malaria parasite seems to largely exploit the pool of histone posttranslational modifications (PTMs) and histone variants to modulate chromatin accessibility. Beside the four canonical histone components (H2A, H2B, H3.1 and H4) making up nucleosomes as in other eukaryotes, four histone variants have been identified so far in *P. falciparum* (H3.3, centromere-specific H3 (cenH3), H2A.Z, H2B.Z (H2B.v)) (Miao et al., 2006). While H2A.Z was found at promoters and transcription starting sites (TSSs) of euchromatic genes in other eukaryotic models (Raisner et al.,

2005; Schones et al., 2008), PfH2A.Z was constantly found at 5'and 3' flanking regions, marking its presence at the intergenic regions throughout the IDC, especially with the colocalization of some particular histone PTMs such as H3K4me3 and H3K9ac (Bartfai et al., 2010). The double variant PfH2A.Z/H2B.Z was found at the same nucleosomes with H3K4me3 that occupied most 5' flanking regions (Petter et al., 2013). The enrichment of the double variant Pf H2A.Z/Pf H2B.Z at A-T rich intergenic and promoter regions of the actively transcribed *var* gene (Hoeijmakers et al., 2013; Petter et al., 2013) was shown to be correlated with *var* gene transcription and developmentally regulated (Petter et al., 2013). As the euchromatic intergenic region is especially rich in AT content (~90%) (Gardner et al., 2002), which is considered relative rigid and not easy to wrap around histone core, it seems the parasite has taken advantage of histone variants H2A.Z and H2B.Z to bind AT-rich DNA more effectively (Batugedara et al., 2017). Meanwhile, the PfH3.3 was discovered as a GC-content dependent histone variant that associates with euchromatic coding regions and sub-telomeric regions where the GC content is higher (Fraschka et al., 2016). Interestingly, PfH3.3 occupies promoter and coding regions of activated and poised *var* genes, raising a possibility of its epigenetic role in the memory of *var* gene expression (Fraschka et al., 2016).

At least 106 individual histone PTMs have been identified so far in *P. falciparum* (Coetzee et al., 2017; Gupta et al., 2013; Saraf et al., 2016) and many of those have been found in other eukaryote models. Among those modifications, histone acetylation and histone methylation are the most abundant and widely studied.

At least four histone acetyl transferases (HATs) and three classes of histone deacetylases (HDACs) have been identified in *P. falciparum* (Liwang Cui and Miao, 2010). Acetylated lysines on histone tails such as lysine 9 at histone 3 (H3K9ac) and its associated HAT, PfGCN5 - a yeast GCN5 homologue involved in chromatin remodelling (Fan et al., 2004) were found at putative transcriptional starting sites (TSSs) and associated with gene activation (Long Cui et al., 2007). In contrast, PfSIR2, a *P. falciparum* HDAC homolog of yeast SIR2 protein (silent information regulator 2), which is responsible for the deacetylation of acetylated lysines on histone 3 and 4 (Merrick and Duraisingh, 2007), was found at promoters of the silenced *var2csa* gene and has been shown to mediate the mutually exclusive expression of sub-telomeric virulent genes including *var* and *rifin* (Duraisingh et al., 2005).

While histone acetylation is involved in gene activation, histone methylation could be involved in both gene activation and silencing. To be specific, H3K4me3 is associated with actively transcribed genes in *P. falciparu*m (Salcedo-Amaya et al., 2009), PfSET2-dependent H3K36me3 is enriched at the TSSs and associated with transcriptional repression, specifically with *var* gene silencing, controlling the singular choice of *var* gene expression (Jiang et al., 2013). Hence, by incorporating these modifications, histones can dictate higher order structure of chromatin, regulating transcriptional accessibility through recruitment of non-histone proteins (Kouzarides, 2007). To fulfil this function, histone PTM patterns (so-called histone codes) need to be recognized or read by histone code "reader" proteins containing specific domains binding to histone PTMs.

In *P. falciparum*, there have been several histone code readers discovered including the phosphorylated histone reader - Pf14-3-3I (Dastidar et al., 2013), the acetylated histone reader - PfBDP1 (Josling et al., 2015) and the methylated histone reader - PfHP1 (Brancucci et al., 2014; Flueck et al., 2009; Pérez-Toledo et al., 2009). Among those, PfBDP1 and PfHP1 have been functionally characterized *in vivo*.

The PfBDP1 or bromodomain protein encoded by PF3D7_1033700 contains one bromodomain at the C-terminus and binds preferentially to H3K9ac and H3K14ac (Josling et al., 2015). PfBDP1 was found to interact with another bromodomain-containing protein namely PfBDP2 (Josling et al., 2015). PfBDP1 was enriched near the transcriptional starting sites at the promoter regions of a number of genes important for invasion (Josling et al., 2015). Moreover, PfBDP1 depletion resulted in the downregulation of genes involved in invasion ligands and motility during invasion in schizont stage (Josling et al., 2015). Thus, these findings imply a role of PfBDP1 in invasion gene recognition and regulation (Josling et al., 2015).

Plasmodium falciparum heterochromatin protein 1 (PfHP1), a reader of H3K9me3 is a conserved protein from fission yeast to human (Voss et al., 2014). The protein has stood out for its functions in epigenetically regulatory mechanisms in various cellular processes including antigenic variation, life cycle progression and sexual differentiation (Brancucci et al., 2014). As its name suggests, HP1 is an essential component of heterochromatin (Kwon and Workman, 2011). *P. falciparum* heterochromatin protein 1 (PfHP1) specifically recognizes the H3K9me3 mark and plays a central role in gene silencing (Voss et al., 2014). The vast majority of parasite

genes located within heterochromatin are clonally variant genes such as *var, rifin, stevor* (Rovira-Graells et al., 2012). Recently, Brancucci and colleagues have revealed a central role of PfHP1 in controlling the mutually exclusive expression of the *var* gene family (Brancucci et al., 2014). In addition, this study also showed that PfHP1 is required for the parasite to enter S phase and mitotic proliferation during the IDC (Brancucci et al., 2014). Interestingly, PfHP1 also orchestrates at the *ap2-g* locus, which encodes for the transcription factor AP2-G that is essential for sexual commitment in *P. falciparum* (Brancucci et al., 2014; Kafsack et al., 2014). Because of the important functions of PfHP1 in these crucial processes, PfHP1 should be studied in more detail on the functional level in order to acquire a deeper insight into antigenic variation, parasite proliferation and sexual commitment.

1.4 Heterochromatin protein 1 in eukaryotes

HP1 was originally identified in *Drosophila melanogaster* as a non-histone chromosomal protein associated with heterochromatin (Eissenberg et al., 1990; James and Elgin, 1986). It is well conserved in eukaryotes and has been studied extensively in fission yeast (*Schizosaccharomyces pombe*), *D. melanogaster* and mammals (Lomberk et al., 2006b).

HP1 is a main component of heterochromatin structure. Heterochromatin is generally enriched at centromeric and telomeric regions and localises at the nuclear periphery (Lomberk et al., 2006b). Other studies also revealed the association of HP1 with some euchromatic regions and this somehow depends on specific isoforms of HP1 (Hiragami and Festenstein, 2005).

The major and well-known function of HP1 lies in heterochromatin formation and gene silencing. HP1 recognizes and binds to H3K9me3 (Lomberk et al., 2006b). In turn, HP1 forms a homodimer, which recruits a H3K9me-specific histone methyltransferase (HKMT) (Lomberk et al., 2006b). As a consequence, heterochromatin and gene silencing can spread *in cis* along the chromatin fibre. Other functions of HP1 include the silencing of euchromatic genes, enhancing DNA repair by relaxing the heterochromatin structure in response to DNA damage, targeting and protecting telomeres, up-regulating genes located at heterochromatin regions or stabilizing transcript processing and elongation (Kwon and Workman, 2011).

In mammals, there are three HP1 variants encoded by a class of genes called *chromobox* (*cbx*) genes. They are *cbx5*/HP1a, *cbx1*/HP1β and *cbx3*/HP1γ, which are

highly similar in the amino acid sequence (Hayakawa et al., 2003). While HP1α and HP1β localize at centromeric and telomeric heterochromatin (Dialynas et al., 2007; Zeng et al., 2010), HP1γ associates with both heterochromatic and euchromatic regions (Minc et al., 2000).

In *S. pombe*, Switching 6 (Swi6) and Chromo domain-containing protein 2 (Chp2) are two important homologs of HP1 protein involved in gene silencing and heterochromatin formation (Zeng et al., 2010). Both Chp2 and Swi6 contribute to the localization of histone deacetylase (HDAC) repressor complexes such as Clr3/Clr6-HDAC to heterochromatin loci (Fischer et al., 2009; Sugiyama et al., 2007; Yamada et al., 2005). Not only does histone deacetylation by these HP1-associated complexes prevent the transcriptional machinery from accessing heterochromatin but this also provides proper nucleosome orders required for higher chromatin structure (Sugiyama et al., 2007; Yamada et al., 2005). The double deletion of Swi6 and Chp2 caused an increase in Pol II enzyme occupancy at centromeric heterochromatin, indicating an essential role of Swi6 and Chp2 in heterochromatin silencing effects (Fischer et al., 2009).

1.4.1 HP1 structure and domain function

HP1 is a small protein containing three regions: two conserved domains at the N- and C-terminus, namely the chromo domain (CD) and the chromoshadow domain (CSD), respectively, and a variable linker or hinge domain between them (Aasland and Stewart, 1995; Kwon and Workman, 2008; Lomberk et al., 2006a).

Chromodomain – a recognizer of a specific histone mark

The chromatin organization modifier domain or chromo domain (CD) is located at the N-terminus of HP1 and this domain is highly conserved among animals, fungi and plants (Lomberk et al., 2006b). Conserved amino acid residues form the backbone of a relatively open hydrophobic groove on the beta sheet of the CD (Singh and Georgatos, 2002). The total negative charge distribution of the CD suggests that the domain is more likely to interact with proteins rather than with DNA (Eissenberg and Elgin, 2000). The CD interacts directly with H3K9me2/3 via its hydrophobic pocket, altering the chromatin structure to form heterochromatin (Lomberk et al., 2006b). Mutations at highly conserved amino acids such as Tyr24, Va26, Trp45 and Tyr48 in the CD of *Drosophila* HP1 can incapacitate the binding to H3K9me3, resulting in functional defects of HP1 (Lomberk et al., 2006b). Consistently, the substitution of some aromatic

hydrophobic amino residues in the CD of Swi6 caused Swi6 loss-of-function phenotypes, for example the abolishment in mating-type switching to the opposite allele and reducing the number of cells that can form normal zygotic asci (Wang et al., 2000).

Chromo Shadow Domain – a domain directs protein-protein interactions

The chromo shadow domain (CSD) is a unique motif of the HP1 family (Lomberk et al., 2006b). It locates at the C-terminus of HP1. Regardless of the high similarity in sequence and structure with the CD, the CSD plays different roles in self-dimerization and interaction with various non-histone proteins (Lomberk et al., 2006b). A consensus pentapeptide sequence motif (PxVxL) in this domain is required for homodimerization and is also found in proteins interacting with HP1 (Brasher et al., 2000; Cowieson et al., 2000; Lechner et al., 2000; Smothers and Henikoff, 2000). Mutations in this motif interfere with HP1 homo-dimer formation, causing defects in H3K9m3e binding and heterochromatin establishment (Brasher et al., 2000; Schultz et al., 2002).

Hinge region - more than a linker

The linker or hinge region separating the CD and CSD domains is less conserved and has a flexible structure. The domain was assumed to be exposed on the surface of HP1 (Singh and Georgatos, 2002). In a study in *S. pombe*, the length of the hinge domain was shown to be essential for the full function of Swi6 (Wang et al., 2000). When the Swi6 hinge domain was shortened by 80 amino acids down to the size of the hinge domain of mouse HP1β (M31), Swi6 was still fully functional and localized to nucleus (Wang et al., 2000). However, with a larger deletion in the hinge domain by 112 amino acids, the truncated Swi6 only retained 25% of wild type activity and was not strictly localized within the nucleus (Wang et al., 2000).

1.4.2 HP1 post-translational modifications – functional decorations

In general, HP1 possesses a number of posttranslational modifications (PTMs) that include mainly phosphorylation but also acetylation, methylation, formylation, uquibitination and sumoylation (Kwon and Workman, 2011; LeRoy et al., 2009; Lomberk et al., 2006a). The dynamics in the PTMs of HP1 is highly important in regulating its functions. In humans, HP1a was shown to be a substrate of the nuclear Dbf2-related (NDR) kinase (Chakraborty et al., 2014). In an NDR mutant, the unphosphorylated HP1a, prominently at serine 95 (S95) in the hinge domain, caused a significant increase in the proportion of cells at prometaphase while a decrease in

cells at metaphase was observed (Chakraborty et al., 2014). In the NDR-depleted cells, chromosome alignment was defective and mitotic progression was delayed, suggesting an important role of the phosphorylated S95 in mitosis (Chakraborty et al., 2014). In another study, hyperphosphorylation at the N-terminus of murine HP1a demonstrated a significant influence on the localization of HP1 to heterochromatin as well as on chromosomal stability (Hiragami-Hamada et al., 2011). When a phosphorylated residue (S14) was replaced with an unphosphorylatable alanine (A), the mutated HP1 showed weak binding to H3K9me3 and diffused heterochromatic localization(Hiragami-Hamada et al., 2011). A mutant containing multiple phosphomutations (S11A-S14A) showed multiple abnormal chromosomes such as diplochromosomes, circular chromosomes and long fused chromosomes (Hiragami-Hamada et al., 2011). The phosphomutant also showed little or no affinity to casein kinase 2 (CKII) compared to wild type HP1a which also bound strongly to H3K9me3 after being phosphorylated by CKII (Hiragami-Hamada et al., 2011). In *S. pombe,* Swi6 phosphorylation contributes to heterochromatic silencing at centromeres and phosphorylated Swi6 catalysed by CKII is required for its interaction with other effectors (Shimada et al., 2009).

1.5 Heterochromatin protein 1 in *Plasmodium falciparum*

1.5.1 Plasmodium falciparum heterochromatin protein 1 at a glance

Unlike most other eukaryotes, *P. falciparum* encodes only a single HP1 protein denoted as PfHP1 (Flueck et al., 2009; Pérez-Toledo et al., 2009). In general, PfHP1 also retains a common HP1 structure: a CD domain at the N-terminus, a hinge domain and a CSD domain at the C-terminus. Genome-wide profiling showed that PfHP1 mainly localizes to telomeric/subtelomeric regions and some chromosome-internal islands, but not in peri-centromeric regions (Flueck et al., 2009) where H3K9me3 is also absent (Lopez-Rubio et al., 2009; Salcedo-Amaya et al., 2009). This indicates that PfHP1 might not contribute to maintenance of centromere structure and function as in other eukaryotes (Flueck et al., 2009; Pérez-Toledo et al., 2009). The PfHP1-demarcated heterochromatic domains contain a large number of protein-coding genes (approx. 425) of which most belong to gene families encoding exported virulence proteins that are specific for *P. falciparum* (Flueck et al., 2009). The association of PfHP1 and H3K9me3 at these loci highlights an underlying role of PfHP1 in regulating the phenotypic/antigenic variation of virulence factors, with the best-known example

being the mutually exclusive expression of *var*/PfEMP1 (Brancucci et al., 2014; Flueck et al., 2009). Another regulatory role of PfHP1/H3K9me3 was implied in regulating invasion pathway switching involved in facultative interchanging between transcriptionally permissive and silent states of *Pfrh4* (invasion gene) and a neighbouring pseudogene, *pfeba-165* (Coleman et al., 2012). Silent state of *pfrh4* was found associated with H3K9me3-marked heterochromatin regions near TSS and ORF (Coleman et al., 2012; Jiang et al., 2010) and preferably recruited to a transcriptionally repressive heterochromatic zone at nuclear periphery (Coleman et al., 2012). Further, during gametocytogenesis, genes encoding for key components of gametocyte determinant like *pfap2-g* (Kafsack et al., 2014) and earliest gametocyte markers, for example *pfs16, pfg27, pfg 14-744/748* (Eksi et al., 2005; 2012) were reduced in PfHP1/H3K9me3 occupation (Brancucci et al., 2014; Flueck et al., 2009; Fraschka et al., 2018). In contrast, genes involving in host cell remodelling like *mesa*, *pfemp3, hsp40* and *kahrp* were found associated with PfHP1/H3K9me3 during gametocytogenesis (Fraschka et al., 2018). Interestingly, studies on genome-wide distribution of heterochromatin have shown the association of PfHP1/H3K9me3 with variance gene families and *pfap2-g* in intracellular blood stage as well as in salivary gland sporozoites with a similar enrichment (Brancucci et al., 2014; Flueck et al., 2009; Lopez-Rubio et al., 2009; Zanghì et al., 2018). Notably, mutually exclusive expression of PfEMP1 was also implied in sporozoites similarly to blood stage parasites (Brancucci et al., 2014; Voss et al., 2006) and possibly involved in sporozoite migration and hepatocyte infectivity (Zanghì et al., 2018). Thus, these understandings strengthen a role of PfHP1/H3K9me3 in stage-specific epigenetic regulation during the parasite life cycle using heterochromatin restructuring.

1.5.2 PfHP1 functions during intracellular development cycle

Recently, Brancucci and Bertschi et al. have studied the function of PfHP1 through a PfHP1 knockdown clone by targeting PfHP1 with the FKPB destabilization domain (DD) (Armstrong and D. E. Goldberg, 2007; Brancucci et al., 2014) (Figure 1.2). The DD allows the targeted degradation of DD fusion proteins when cells are cultured in absence of the stabilizing ligand Shield-1 (Armstrong and Goldberg, 2007). After Shield-1 removal at 4-12 hpi, 3D7/PfHP1-GFP-DD^{OFF} parasites can still complete the current cycle (generation 1) but showed very pronounced phenotypes after reinvasion in generation 2 (Figure 1.2). These phenotypes are summarised in the following paragraphs.

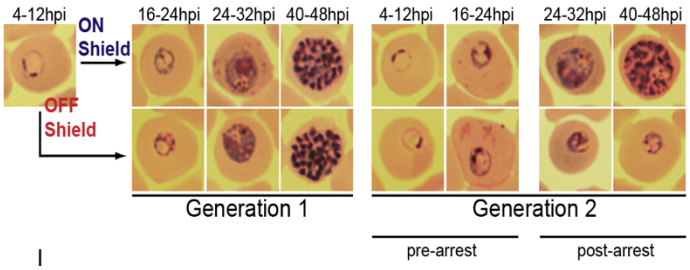

Figure 1.2. The pipeline of Shield-1 removal (at 4-12 hpi in generation 1) and light microscopic observation of Giemsa smears for 3D7/PfHP1-GPF-DD$^{ON/OFF}$ through generation 1 and 2. 3D7/ PfHP1-GFP-DD^{OFF} showed a very pronounced morphological phenotype compared to the control after reinvasion in generation 2 (Brancucci et al., 2014).

First, in the OFF Shield-1 condition, a high proportion of subtelomeric PfHP1-associated genes were up-regulated such as *rifin*, *pfmc-2tm* and especially the *var* gene family(Brancucci et al., 2014). To be specific, when Shield-1 was withdrawn at 4-12hpi in generation 1, *var* gene transcription was comparable between 3D7/PfHP1-GPF-DD^{OFF} and 3D7/PfHP1-GPF-DD^{ON} during the current cycle (Brancucci et al., 2014). However, at 16-24 hpi in generation 2, there was a massive de-repression of most *var* genes such that 52 out of 60 genes of this family were highly upregulated (Brancucci et al., 2014). In brief, these results identified a central role for PfHP1 in silencing heterochromatic genes and controlling mutually exclusive expression of *var* genes.

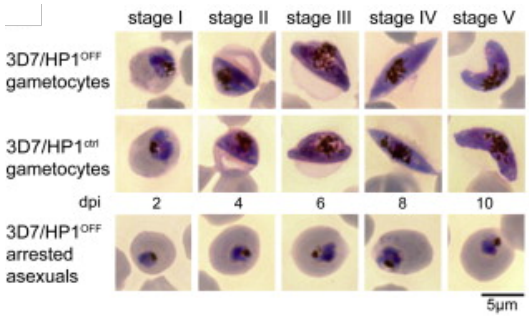

Figure1.3. Hyper-induction of gametocytogenesis and normal gametocyte maturation observed in approximately 52% of 3D7/PfHP1-GFP-DD^{OFF} parasites in generation 2 (upper panel) (Brancucci et al., 2014). The remaining subset of PfHP1-depleted parasites did not commit to sexual development but was unable to enter S-phase and arrested prior to schizogony (lower panel).

Second, a high percentage of early stage I gametocytes was observed in the 3D7/PfHP1-GFP-DD^{OFF} population in generation 2 (Brancucci et al., 2014). This striking phenotype occurred as a result of the activation of the *pfap2-g* gene in generation 1 trophozoites or schizonts (Brancucci et al., 2014). In asexual parasites, *pfap2* locus is silencing by PfHP1/H3K9me3-marked heterochromatin (Brancucci et al., 2014; Flueck et al., 2009; Josling and Llinás, 2015; Kafsack et al., 2014). Interestingly, Brancucci and colleagues found that in PfHP1-depleted parasites, PfHP1 and H3K9me3 occupancy were substantially reduced at the *pfap2-g* locus in schizonts of the same cycle of induction (generation 1) and in the ring progeny (generation 2) (Brancucci et al., 2014). The removal of H3K9me3-bound PfHP1 is mediated by the upstream regulator of sexual commitment, PfGDV1 (Gametocyte gene development 1), which results in the derepression of *pfap2-g*, thus triggering sexual commitment (Filarsky et al., 2018). The depletion of PfHP1 initiates de-repression of *pfap2-g* in committed schizonts which then release sexually committed merozoites that re-invade and undergo full gametocyte maturation over the next 8-10 days (Figure 1.3, upper and middle panel) (Brancucci et al., 2014). Approximately 52% of the 3D7/PfHP1-GFP-DD^{OFF} population committed to gametocytes in comparison to ~2% in the control (Brancucci et al., 2014). The sexual commitment process driven by this PfHP1-dependent pathway is considered as a canonical next cycle conversion (NCC) route in which an additional round of replication occurs after sexual commitment (Bancells et al., 2019).

Third, a role for PfHP1 in mitotic proliferation was revealed through PfHP1 depletion. After 24 hpi in generation 2, the approx. 45% of 3D7/PfHP1-GFP-DD^{OFF} parasites that did not undergo sexual commitment arrested at the trophozoite stage and were unable to enter schizogony because of a failure in DNA replication (Figure 1.3, lower panel, Brancucci et al., 2014). Interestingly, these arrested trophozoites remained in a dormant state (Figure 1.3, lower panel) and were able to re-accumulate PfHP1 and re-enter replication cycles when Shield-1 was added back to the culture medium (Brancucci et al., 2014). Indeed, delayed replication timing and cell cycle progression at the S and G2/M phase have been observed in other eukaryote models like *S. pombe* and *D. melanogaster* when HP1 was depleted (De Lucia et al., 2005; Hayashi et al., 2009; Schwaiger et al., 2010).

Taken together, the study of Brancucci and colleagues has identified essential functions of PfHP1 in (1) the maintenance of heritable silencing and mutually exclusive expression of *var* genes, (2) in mitotic progression of asexual blood stage parasites,

and (3) in the sexual differentiation switch (Brancucci et al., 2014). This study hence provides a fundamental basis for further investigation on detailed functions of PfHP1 in these processes.

1.5.3 PfHP1 phosphorylation

Large-scale phosphoproteomics studies in *P. falciparum* so far identified several phosphorylated residues in PfHP1. They include T2, S4, S33, S57, S89, S92, S108, T110, S122, S125, S174 (Collins et al., 2014; Filarsky et al., 2018; Lasonder et al., 2012; 2015; Pease et al., 2013; Solyakov et al., 2011; Treeck et al., 2011), and the Y32 and S136 residues that have been identified as additional phosphosites in a recent study investigating native PfHP1 complexes (Filarsky et al., 2018). Unsurprisingly, PfHP1 is mainly phosphorylated in the hinge domain as observed in HP1s from other eukaryotes (Lomberk et al., 2006b). As mentioned above, mutations in the hinge region have been shown to hamper the location and functions of HP1. Therefore, we considered it worthy to study in detail whether phosphorylation controls some of the known functions of PfHP1. Moreover, the kinases that phosphorylate PfHP1 and their target phosphosites on PfHP1 are still elusive.

1.6 Main aims and objectives

My research pursued in this PhD project aimed to investigate PfHP1 function in detail using CRISPR/Cas9-based gene editing combined with the DiCre/loxP system for conditional mutagenesis. The two specific objectives were:

Objective 1: To uncover the roles of the individual PfHP1 domains in PfHP1 function.

Objective 2: To understand if and how phosphorylation of PfHP1 regulates its function.

Both objectives focused on the three known PfHP1-dependent cellular processes: (1) the maintenance of heritable silencing and mutually exclusive expression of *var* genes, (2) mitotic progression of asexual blood stage parasites, and (3) sexual commitment (Brancucci et al., 2014). The first study analysed the functional contribution and conservation of the CD, hinge and CSD domains of PfHP1. The main results from this project were presented in Chapter 3 (manuscript in preparation). Some preliminary results related to this project were presented in Chapter 4. Some initial results obtained during this study using functional complementation assays were presented in Chapter 5. The second project addressed (1) the kinases phosphorylating PfHP1 and their target residues (in collaboration with Prof. C. Doerig, Monash University, Melbourne, Australia and Prof. Isabel Lucet, Walter and Eliza Hall Institute of Medical Research, Melbourne, Australia); and (2) the role of selected phosphorylated residues in regulating PfHP1 function. The main results from this study were presented in Chapter 2 (Bui et al., manuscript submitted).

1.7 References

Aasland, R., Stewart, A.F., 1995. The chromo shadow domain, a second chromo domain in heterochromatin-binding protein 1, HP1. Nucleic Acids Res. 23, 3168–3173.

Amit-Avraham, I., Pozner, G., Eshar, S., Fastman, Y., Kolevzon, N., Yavin, E., Dzikowski, R., 2015. Antisense long noncoding RNAs regulate var gene activation in the malaria parasite Plasmodium falciparum. Proc. Natl. Acad. Sci. U.S.A. 112, E982–91. doi:10.1073/pnas.1420855112

Armstrong, C.M., Goldberg, D.E., 2007. An FKBP destabilization domain modulates protein levels in Plasmodium falciparum. Nat Meth. 4, 1007–1009. doi:10.1038/nmeth1132

Balaji, S., Babu, M.M., Iyer, L.M., Aravind, L., 2005. Discovery of the principal specific transcription factors of Apicomplexa and their implication for the evolution of the AP2-integrase DNA binding domains. Nucleic Acids Res. 33, 3994–4006. doi:10.1093/nar/gki709

Bancells, C., Llorà-Batlle, O., Poran, A., Nötzel, C., Rovira-Graells, N., Elemento, O., Kafsack, B.F.C., Cortés, A., 2019. Revisiting the initial steps of sexual development in the malaria parasite Plasmodium falciparum. Nat Microbiol 4, 144–154. doi:10.1038/s41564-018-0291-7

Bannister, L., Mitchell, G., 2003. The ins, outs and roundabouts of malaria. Trends Parasitol. 19, 209–213.

Bartfai, R., Hoeijmakers, W.A.M., Salcedo-Amaya, A.M., Smits, A.H., Janssen-Megens, E., Kaan, A., Treeck, M., Gilberger, T.-W., Françoijs, K.-J., Stunnenberg, H.G., 2010. H2A.Z demarcates intergenic regions of the plasmodium falciparum epigenome that are dynamically marked by H3K9ac and H3K4me3. PLoS Pathog. 6, e1001223. doi:10.1371/journal.ppat.1001223

Baruch, D.I., Pasloske, B.L., Singh, H.B., Bi, X., Ma, X.C., Feldman, M., Taraschi, T.F., Howard, R.J., 1995. Cloning the P. falciparum gene encoding PfEMP1, a malarial variant antigen and adherence receptor on the surface of parasitized human erythrocytes. Cell 82, 77–87.

Batugedara, G., Lu, X.M., Bunnik, E.M., Le Roch, K.G., 2017. The Role of Chromatin Structure in Gene Regulation of the Human Malaria Parasite. Trends Parasitol. 33, 364–377. doi:10.1016/j.pt.2016.12.004

Baum, J., Papenfuss, A.T., Mair, G.R., Janse, C.J., Vlachou, D., Waters, A.P., Cowman, A.F., Crabb, B.S., de Koning-Ward, T.F., 2009. Molecular genetics and comparative genomics reveal RNAi is not functional in malaria parasites. Nucleic Acids Res. 37, 3788–3798. doi:10.1093/nar/gkp239

Berger, S.L., Kouzarides, T., Shiekhattar, R., Shilatifard, A., 2009. An operational definition of epigenetics. Genes Dev. 23, 781–783. doi:10.1101/gad.1787609

Boschet, C., Gissot, M., Briquet, S., Hamid, Z., Claudel-Renard, C., Vaquero, C., 2004. Characterization of PfMyb1 transcription factor during erythrocytic development of 3D7 and F12 Plasmodium falciparum clones. Mol. Biochem. Parasitol. 138, 159–163. doi:10.1016/j.molbiopara.2004.07.011

Bozdech, Z., Llinás, M., Pulliam, B.L., Wong, E.D., Zhu, J., DeRisi, J.L., 2003. The transcriptome of the intraerythrocytic developmental cycle of Plasmodium falciparum. PLoS Biol 1, E5. doi:10.1371/journal.pbio.0000005

Brancucci, N.M.B., Bertschi, N.L., Zhu, L., Niederwieser, I., Chin, W.H., Wampfler, R., Freymond, C., Rottmann, M., Felger, I., Bozdech, Z., Voss, T.S., 2014. Heterochromatin protein 1 secures survival and transmission of malaria parasites. Cell Host Microbe 16, 165–176. doi:10.1016/j.chom.2014.07.004

Brasher, S.V., Smith, B.O., Fogh, R.H., Nietlispach, D., Thiru, A., Nielsen, P.R., Broadhurst, R.W., Ball, L.J., Murzina, N.V., Laue, E.D., 2000. The structure of mouse HP1 suggests a unique mode of single peptide recognition by the shadow chromo domain dimer. EMBO J. 19, 1587–1597. doi:10.1093/emboj/19.7.1587

Bruce, M.C., Alano, P., Duthie, S., Carter, R., 1990. Commitment of the malaria parasite Plasmodium falciparum to sexual and asexual development. Parasitology 100 Pt 2, 191–200.

Campbell, T.L., De Silva, E.K., Olszewski, K.L., Elemento, O., Llinás, M., 2010. Identification and genome-wide prediction of DNA binding specificities for the ApiAP2 family of regulators from the malaria parasite. PLoS Pathog. 6, e1001165. doi:10.1371/journal.ppat.1001165

Chakraborty, A., Prasanth, K.V., Prasanth, S.G., 2014. Dynamic phosphorylation of HP1a regulates mitotic progression in human cells. Nat Commun 5, 3445. doi:10.1038/ncomms4445

Coetzee, N., Sidoli, S., van Biljon, R., Painter, H., Llinás, M., Garcia, B.A., Birkholtz, L.-M., 2017. Quantitative chromatin proteomics reveals a dynamic histone post-translational modification landscape that defines asexual and sexual Plasmodium falciparum parasites. Sci Rep 7, 607–12. doi:10.1038/s41598-017-00687-7

Coleman, B.I., Ribacke, U., Manary, M., Bei, A.K., Winzeler, E.A., Wirth, D.F., Duraisingh, M.T., 2012. Nuclear repositioning precedes promoter accessibility and is linked to the switching frequency of a Plasmodium falciparum invasion gene. Cell Host Microbe 12, 739–750. doi:10.1016/j.chom.2012.11.004

Collins, M.O., Wright, J.C., Jones, M., Rayner, J.C., Choudhary, J.S., 2014. Confident and sensitive phosphoproteomics using combinations of collision induced dissociation and electron transfer dissociation. J Proteomics 103, 1–14. doi:10.1016/j.jprot.2014.03.010

Coulson, R.M.R., Hall, N., Ouzounis, C.A., 2004. Comparative genomics of transcriptional control in the human malaria parasite Plasmodium falciparum. Genome Res. 14, 1548–1554. doi:10.1101/gr.2218604

Cowieson, N.P., Partridge, J.F., Allshire, R.C., McLaughlin, P.J., 2000. Dimerisation of a chromo shadow domain and distinctions from the chromodomain as revealed by structural analysis. Curr. Biol. 10, 517–525.

Cox-Singh, J., Davis, T.M.E., Lee, K.-S., Shamsul, S.S.G., Matusop, A., Ratnam, S., Rahman, H.A., Conway, D.J., Singh, B., 2008. Plasmodium knowlesi malaria in humans is widely distributed and potentially life threatening. Clin. Infect. Dis. 46, 165–171. doi:10.1086/524888

Cui, Liwang, Miao, J., 2010. Chromatin-mediated epigenetic regulation in the malaria parasite Plasmodium falciparum. Eukaryotic Cell 9, 1138–1149. doi:10.1128/EC.00036-10

Cui, Long, Miao, J., Furuya, T., Li, X., Su, X.-Z., Cui, L., 2007. PfGCN5-mediated histone H3 acetylation plays a key role in gene expression in Plasmodium falciparum. Eukaryotic Cell 6, 1219–1227. doi:10.1128/EC.00062-07

Dastidar, E.G., Dzeyk, K., Krijgsveld, J., Malmquist, N.A., Doerig, C., Scherf, A., Lopez-Rubio, J.J., 2013. Comprehensive histone phosphorylation analysis and identification of Pf14-3-3 protein as a histone H3 phosphorylation reader in malaria parasites. PLoS ONE 8, e53179. doi:10.1371/journal.pone.0053179

De Lucia, F., Ni, J.-Q., Vaillant, C., Sun, F.-L., 2005. HP1 modulates the transcription of cell-cycle regulators in Drosophila melanogaster. Nucleic Acids Res. 33, 2852–2858. doi:10.1093/nar/gki584

De Silva, E.K., Gehrke, A.R., Olszewski, K., León, I., Chahal, J.S., Bulyk, M.L., Llinás, M., 2008. Specific DNA-binding by apicomplexan AP2 transcription factors. Proc. Natl. Acad. Sci. U.S.A. 105, 8393–8398. doi:10.1073/pnas.0801993105

Deitsch, K.W., Dzikowski, R., 2017. Variant Gene Expression and Antigenic Variation by Malaria Parasites. Annu. Rev. Microbiol. 71, 625–641. doi:10.1146/annurev-micro-090816-093841

Dialynas, G.K., Terjung, S., Brown, J.P., Aucott, R.L., Baron-Luhr, B., Singh, P.B., Georgatos, S.D., 2007. Plasticity of HP1 proteins in mammalian cells. J. Cell. Sci. 120, 3415–3424. doi:10.1242/jcs.012914

Duraisingh, M.T., Voss, T.S., Marty, A.J., Duffy, M.F., Good, R.T., Thompson, J.K., Freitas-Junior, L.H., Scherf, A., Crabb, B.S., Cowman, A.F., 2005. Heterochromatin silencing and locus repositioning linked to regulation of virulence genes in Plasmodium falciparum. Cell 121, 13–24. doi:10.1016/j.cell.2005.01.036

Dzikowski, R., Deitsch, K.W., 2009. Genetics of antigenic variation in Plasmodium falciparum. Curr. Genet. 55, 103–110. doi:10.1007/s00294-009-0233-2

Eissenberg, J.C., Elgin, S.C., 2000. The HP1 protein family: getting a grip on chromatin. Curr. Opin. Genet. Dev. 10, 204–210.

Eissenberg, J.C., James, T.C., Foster-Hartnett, D.M., Hartnett, T., Ngan, V., Elgin, S.C., 1990. Mutation in a heterochromatin-specific chromosomal protein is associated with suppression of position-effect variegation in Drosophila melanogaster. Proc. Natl. Acad. Sci. U.S.A. 87, 9923–9927.

Eksi, S., Haile, Y., Furuya, T., Ma, L., Su, X., Williamson, K.C., 2005. Identification of a subtelomeric gene family expressed during the asexual-sexual stage transition in Plasmodium falciparum. Mol. Biochem. Parasitol. 143, 90–99. doi:10.1016/j.molbiopara.2005.05.010

Eksi, S., Morahan, B.J., Haile, Y., Furuya, T., Jiang, H., Ali, O., Xu, H., Kiattibutr, K., Suri, A., Czesny, B., Adeyemo, A., Myers, T.G., Sattabongkot, J., Su, X.-Z., Williamson, K.C., 2012. Plasmodium falciparum gametocyte development 1 (Pfgdv1) and gametocytogenesis early gene identification and commitment to sexual development. PLoS Pathog. 8, e1002964. doi:10.1371/journal.ppat.1002964

Elliott, S.R., Beeson, J.G., 2008. Estimating the burden of global mortality in children aged <5 years by pathogen-specific causes. Clin. Infect. Dis. 46, 1794–1795. doi:10.1086/588049

Epp, C., Li, F., Howitt, C.A., Chookajorn, T., Deitsch, K.W., 2009. Chromatin associated sense and antisense noncoding RNAs are transcribed from the var gene family of virulence genes of the malaria parasite Plasmodium falciparum. RNA 15, 116–127. doi:10.1261/rna.1080109

Fan, Q., An, L., Cui, L., 2004. Plasmodium falciparum histone acetyltransferase, a yeast GCN5 homologue involved in chromatin remodeling. Eukaryotic Cell 3, 264–276. doi:10.1128/ec.3.2.264-276.2004

Ferreira, M.U., da Silva Nunes, M., Wunderlich, G., 2004. Antigenic diversity and immune evasion by malaria parasites. Clin. Diagn. Lab. Immunol. 11, 987–995. doi:10.1128/CDLI.11.6.987-995.2004

Filarsky, M., Fraschka, S.A., Niederwieser, I., Brancucci, N.M.B., Carrington, E., Carrió, E., Moes, S., Jenoe, P., Bartfai, R., Voss, T.S., 2018. GDV1 induces sexual commitment of malaria parasites by antagonizing HP1-dependent gene silencing. Science 359, 1259–1263. doi:10.1126/science.aan6042

Fischer, T., Cui, B., Dhakshnamoorthy, J., Zhou, M., Rubin, C., Zofall, M., Veenstra, T.D., Grewal, S.I.S., 2009. Diverse roles of HP1 proteins in heterochromatin assembly and functions in fission yeast. Proc. Natl. Acad. Sci. U.S.A. 106, 8998–9003. doi:10.1073/pnas.0813063106

Florens, L., Washburn, M.P., Raine, J.D., Anthony, R.M., Grainger, M., Haynes, J.D., Moch, J.K., Muster, N., Sacci, J.B., Tabb, D.L., Witney, A.A., Wolters, D., Wu, Y., Gardner, M.J., Holder, A.A., Sinden, R.E., Yates, J.R., Carucci, D.J., 2002. A proteomic view of the Plasmodium falciparum life cycle. Nature 419, 520–526. doi:10.1038/nature01107

Flueck, C., Bartfai, R., Niederwieser, I., Witmer, K., Alako, B.T.F., Moes, S., Bozdech, Z., Jenoe, P., Stunnenberg, H.G., Voss, T.S., 2010. A major role for the Plasmodium falciparum ApiAP2 protein PfSIP2 in chromosome end biology. PLoS Pathog. 6, e1000784. doi:10.1371/journal.ppat.1000784

Flueck, C., Bartfai, R., Volz, J., Niederwieser, I., Salcedo-Amaya, A.M., Alako, B.T.F., Ehlgen, F., Ralph, S.A., Cowman, A.F., Bozdech, Z., Stunnenberg, H.G., Voss, T.S., 2009. Plasmodium falciparum heterochromatin protein 1 marks genomic loci linked to phenotypic variation of exported virulence factors. PLoS Pathog. 5, e1000569. doi:10.1371/journal.ppat.1000569

Fraschka, S.A., Filarsky, M., Hoo, R., Niederwieser, I., Yam, X.Y., Brancucci, N.M.B., Mohring, F., Mushunje, A.T., Huang, X., Christensen, P.R., Nosten, F., Bozdech, Z., Russell, B., Moon, R.W., Marti, M., Preiser, P.R., Bartfai, R., Voss, T.S., 2018. Comparative Heterochromatin Profiling Reveals Conserved and Unique Epigenome Signatures Linked to Adaptation and Development of Malaria Parasites. Cell Host Microbe 23, 407–420.e8. doi:10.1016/j.chom.2018.01.008

Fraschka, S.A.-K., Henderson, R.W.M., Bartfai, R., 2016. H3.3 demarcates GC-rich coding and subtelomeric regions and serves as potential memory mark for virulence gene expression in Plasmodium falciparum. Sci Rep 6, 31965. doi:10.1038/srep31965

Gardner, M.J., Hall, N., Fung, E., White, O., Berriman, M., Hyman, R.W., Carlton, J.M., Pain, A., Nelson, K.E., Bowman, S., Paulsen, I.T., James, K., Eisen, J.A., Rutherford, K., Salzberg, S.L., Craig, A., Kyes, S., Chan, M.-S., Nene, V., Shallom, S.J., Suh, B., Peterson, J., Angiuoli, S., Pertea, M., Allen, J., Selengut, J., Haft, D., Mather, M.W., Vaidya, A.B., Martin, D.M.A., Fairlamb, A.H., Fraunholz, M.J., Roos, D.S., Ralph, S.A., McFadden, G.I., Cummings, L.M., Subramanian, G.M., Mungall, C., Venter, J.C., Carucci, D.J., Hoffman, S.L., Newbold, C., Davis, R.W., Fraser, C.M., Barrell, B., 2002. Genome sequence of the human malaria parasite Plasmodium falciparum. Nature 419, 498–511. doi:10.1038/nature01097

Giraud-Panis, M.-J., Pisano, S., Poulet, A., Le Du, M.-H., Gilson, E., 2010. Structural identity of telomeric complexes. FEBS Lett. 584, 3785–3799. doi:10.1016/j.febslet.2010.08.004

Gissot, M., Briquet, S., Refour, P., Boschet, C., Vaquero, C., 2005. PfMyb1, a Plasmodium falciparum transcription factor, is required for intra-erythrocytic growth and controls key genes for cell cycle regulation. J. Mol. Biol. 346, 29–42. doi:10.1016/j.jmb.2004.11.045

Gissot, M., Choi, S.-W., Thompson, R.F., Greally, J.M., Kim, K., 2008. Toxoplasma gondii and Cryptosporidium parvum lack detectable DNA cytosine methylation. Eukaryotic Cell 7, 537–540. doi:10.1128/EC.00448-07

Goldberg, A.D., Allis, C.D., Bernstein, E., 2007. Epigenetics: a landscape takes shape. Cell 128, 635–638. doi:10.1016/j.cell.2007.02.006

Govindaraju, G., Jabeena, C.A., Sethumadhavan, D.V., Rajaram, N., Rajavelu, A., 2017. DNA methyltransferase homologue TRDMT1 in Plasmodium falciparum specifically methylates endogenous aspartic acid tRNA. Biochim Biophys Acta Gene Regul Mech 1860, 1047–1057. doi:10.1016/j.bbagrm.2017.08.003

Gunasekera, A.M., Patankar, S., Schug, J., Eisen, G., Kissinger, J., Roos, D., Wirth, D.F., 2004. Widespread distribution of antisense transcripts in the Plasmodium falciparum genome. Mol. Biochem. Parasitol. 136, 35–42. doi:10.1016/j.molbiopara.2004.02.007

Gupta, A.P., Chin, W.H., Zhu, L., Mok, S., Luah, Y.-H., Lim, E.-H., Bozdech, Z., 2013. Dynamic epigenetic regulation of gene expression during the life cycle of malaria parasite Plasmodium falciparum. PLoS Pathog. 9, e1003170. doi:10.1371/journal.ppat.1003170

Handy, D.E., Castro, R., Loscalzo, J., 2011. Epigenetic modifications: basic mechanisms and role in cardiovascular disease. Circulation 123, 2145–2156. doi:10.1161/CIRCULATIONAHA.110.956839

Hayakawa, T., Haraguchi, T., Masumoto, H., Hiraoka, Y., 2003. Cell cycle behavior of human HP1 subtypes: distinct molecular domains of HP1 are required for their centromeric localization during interphase and metaphase. J. Cell. Sci. 116, 3327–3338. doi:10.1242/jcs.00635

Hayashi, M.T., Takahashi, T.S., Nakagawa, T., Nakayama, J.-I., Masukata, H., 2009. The heterochromatin protein Swi6/HP1 activates replication origins at the pericentromeric region and silent mating-type locus. Nat. Cell Biol. 11, 357–362. doi:10.1038/ncb1845

Hiragami, K., Festenstein, R., 2005. Heterochromatin protein 1: a pervasive controlling influence. Cell. Mol. Life Sci. 62, 2711–2726. doi:10.1007/s00018-005-5287-9

Hiragami-Hamada, K., Shinmyozu, K., Hamada, D., Tatsu, Y., Uegaki, K., Fujiwara, S., Nakayama, J.-I., 2011. N-terminal phosphorylation of HP1{alpha} promotes its chromatin binding. Mol. Cell. Biol. 31, 1186–1200. doi:10.1128/MCB.01012-10

Hoeijmakers, W.A.M., Salcedo-Amaya, A.M., Smits, A.H., Françoijs, K.-J., Treeck, M., Gilberger, T.-W., Stunnenberg, H.G., Bartfai, R., 2013. H2A.Z/H2B.Z double-variant nucleosomes inhabit the AT-rich promoter regions of the Plasmodium falciparum genome. Mol. Microbiol. 87, 1061–1073. doi:10.1111/mmi.12151

Horrocks, P., Wong, E., Russell, K., Emes, R.D., 2009. Control of gene expression in Plasmodium falciparum - ten years on. Mol. Biochem. Parasitol. 164, 9–25. doi:10.1016/j.molbiopara.2008.11.010

Inselburg, J., 1983. Gametocyte formation by the progeny of single Plasmodium falciparum schizonts. J. Parasitol. 69, 584–591.

Iwanaga, S., Kaneko, I., Kato, T., Yuda, M., 2012. Identification of an AP2-family protein that is critical for malaria liver stage development. PLoS ONE 7, e47557. doi:10.1371/journal.pone.0047557

James, T.C., Elgin, S.C., 1986. Identification of a nonhistone chromosomal protein associated with heterochromatin in Drosophila melanogaster and its gene. Mol. Cell. Biol. 6, 3862–3872.

Jeninga, M.D., Quinn, J.E., Petter, M., 2019. ApiAP2 Transcription Factors in Apicomplexan Parasites. Pathogens 8, 47. doi:10.3390/pathogens8020047

Jiang, L., López-Barragán, M.J., Jiang, H., Mu, J., Gaur, D., Zhao, K., Felsenfeld, G., Miller, L.H., 2010. Epigenetic control of the variable expression of a Plasmodium falciparum receptor protein for erythrocyte invasion. Proc. Natl. Acad. Sci. U.S.A. 107, 2224–2229. doi:10.1073/pnas.0913396107

Jiang, L., Mu, J., Zhang, Q., Ni, T., Srinivasan, P., Rayavara, K., Yang, W., Turner, L., Lavstsen, T., Theander, T.G., Peng, W., Wei, G., Jing, Q., Wakabayashi, Y., Bansal, A., Luo, Y., Ribeiro, J.M.C., Scherf, A., Aravind, L., Zhu, J., Zhao, K., Miller, L.H., 2013. PfSETvs methylation of histone H3K36 represses virulence genes in Plasmodium falciparum. Nature 499, 223–227. doi:10.1038/nature12361

Jing, Q., Cao, L., Zhang, L., Cheng, X., Gilbert, N., Dai, X., Sun, M., Liang, S., Jiang, L., 2018. Plasmodium falciparumvar Gene Is Activated by Its Antisense Long Noncoding RNA. Front Microbiol 9, 3117. doi:10.3389/fmicb.2018.03117

Josling, G.A., Llinás, M., 2015. Sexual development in Plasmodium parasites: knowing when it's time to commit. Nat. Rev. Microbiol. 13, 573–587. doi:10.1038/nrmicro3519

Josling, G.A., Petter, M., Oehring, S.C., Gupta, A.P., Dietz, O., Wilson, D.W., Schubert, T., Längst, G., Gilson, P.R., Crabb, B.S., Moes, S., Jenoe, P., Lim, S.W., Brown, G.V., Bozdech, Z., Voss, T.S., Duffy, M.F., 2015. A Plasmodium Falciparum Bromodomain Protein Regulates Invasion Gene Expression. Cell Host Microbe 17, 741–751. doi:10.1016/j.chom.2015.05.009

Kafsack, B.F.C., Rovira-Graells, N., Clark, T.G., Bancells, C., Crowley, V.M., Campino, S.G., Williams, A.E., Drought, L.G., Kwiatkowski, D.P., Baker, D.A., Cortés, A., Llinás, M., 2014. A transcriptional switch underlies commitment to sexual development in malaria parasites. Nature 507, 248–252. doi:10.1038/nature12920

Komaki-Yasuda, K., Okuwaki, M., Nagata, K., Kawazu, S.-I., Kano, S., 2013. Identification of a novel and unique transcription factor in the intraerythrocytic stage of Plasmodium falciparum. PLoS ONE 8, e74701. doi:10.1371/journal.pone.0074701

Kornberg, R.D., 2007. The molecular basis of eukaryotic transcription. Proc. Natl. Acad. Sci. U.S.A. 104, 12955–12961. doi:10.1073/pnas.0704138104

Kouzarides, T., 2007. Chromatin modifications and their function. Cell 128, 693–705. doi:10.1016/j.cell.2007.02.005

Kwon, S.H., Workman, J.L., 2011. The changing faces of HP1: From heterochromatin formation and gene silencing to euchromatic gene expression: HP1 acts as a positive regulator of transcription. Bioessays 33, 280–289. doi:10.1002/bies.201000138

Kwon, S.H., Workman, J.L., 2008. The heterochromatin protein 1 (HP1) family: put away a bias toward HP1. Mol. Cells 26, 217–227.

Kyes, S.A., Kraemer, S.M., Smith, J.D., 2007. Antigenic variation in Plasmodium falciparum: gene organization and regulation of the var multigene family. Eukaryotic Cell 6, 1511–1520. doi:10.1128/EC.00173-07

Lasonder, E., Green, J.L., Camarda, G., Talabani, H., Holder, A.A., Langsley, G., Alano, P., 2012. The Plasmodium falciparum schizont phosphoproteome reveals extensive phosphatidylinositol and cAMP-protein kinase A signaling. J. Proteome Res. 11, 5323–5337. doi:10.1021/pr300557m

Lasonder, E., Green, J.L., Grainger, M., Langsley, G., Holder, A.A., 2015. Extensive differential protein phosphorylation as intraerythrocytic Plasmodium falciparum schizonts develop into extracellular invasive merozoites. Proteomics 15, 2716–2729. doi:10.1002/pmic.201400508

Le Roch, K.G., Zhou, Y., Blair, P.L., Grainger, M., Moch, J.K., Haynes, J.D., La Vega, De, P., Holder, A.A., Batalov, S., Carucci, D.J., Winzeler, E.A., 2003. Discovery of gene function by expression profiling of the malaria parasite life cycle. Science 301, 1503–1508. doi:10.1126/science.1087025

Lechner, M.S., Begg, G.E., Speicher, D.W., Rauscher, F.J., 2000. Molecular determinants for targeting heterochromatin protein 1-mediated gene silencing: direct chromoshadow domain-KAP-1 corepressor interaction is essential. Mol. Cell. Biol. 20, 6449–6465.

Lomberk, G., Bensi, D., Fernandez-Zapico, M.E., Urrutia, R., 2006a. Evidence for the existence of an HP1-mediated subcode within the histone code. Nat. Cell Biol. 8, 407–415. doi:10.1038/ncb1383

Lomberk, G., Wallrath, L., Urrutia, R., 2006b. The Heterochromatin Protein 1 family. Genome Biol. 7, 228. doi:10.1186/gb-2006-7-7-228

Lopez-Rubio, J.J., Mancio-Silva, L., Scherf, A., 2009. Genome-wide analysis of heterochromatin associates clonally variant gene regulation with perinuclear repressive centers in malaria parasites. Cell Host Microbe 5, 179–190. doi:10.1016/j.chom.2008.12.012

López-Barragán, M.J., Lemieux, J., Quiñones, M., Williamson, K.C., Molina-Cruz, A., Cui, K., Barillas-Mury, C., Zhao, K., Su, X.-Z., 2011. Directional gene expression and antisense transcripts in sexual and asexual stages of Plasmodium falciparum. BMC Genomics 12, 587–13. doi:10.1186/1471-2164-12-587

Maier, A.G., Cooke, B.M., Cowman, A.F., Tilley, L., 2009. Malaria parasite proteins that remodel the host erythrocyte. Nat. Rev. Microbiol. 7, 341–354. doi:10.1038/nrmicro2110

Mancio-Silva, L., Rojas-Meza, A.P., Vargas, M., Scherf, A., Hernandez-Rivas, R., 2008. Differential association of Orc1 and Sir2 proteins to telomeric domains in Plasmodium falciparum. J. Cell. Sci. 121, 2046–2053. doi:10.1242/jcs.026427

Marsh, K., Kinyanjui, S., 2006. Immune effector mechanisms in malaria. Parasite Immunol. 28, 51–60. doi:10.1111/j.1365-3024.2006.00808.x

Martins, R.M., Macpherson, C.R., Claes, A., Scheidig-Benatar, C., Sakamoto, H., Yam, X.Y., Preiser, P., Goel, S., Wahlgren, M., Sismeiro, O., Coppée, J.-Y., Scherf, A., 2017. An ApiAP2 member regulates expression of clonally variant genes of the human malaria parasite Plasmodium falciparum. Sci Rep 7, 14042–10. doi:10.1038/s41598-017-12578-y

Merrick, C.J., Duraisingh, M.T., 2007. Plasmodium falciparum Sir2: an unusual sirtuin with dual histone deacetylase and ADP-ribosyltransferase activity. Eukaryotic Cell 6, 2081–2091. doi:10.1128/EC.00114-07

Miao, J., Fan, Q., Cui, L., Li, J., Li, J., Cui, L., 2006. The malaria parasite Plasmodium falciparum histones: organization, expression, and acetylation. Gene 369, 53–65. doi:10.1016/j.gene.2005.10.022

Miller, L.H., Ackerman, H.C., Su, X.-Z., Wellems, T.E., 2013. Malaria biology and disease pathogenesis: insights for new treatments. Nat. Med. 19, 156–167. doi:10.1038/nm.3073

Minc, E., Courvalin, J.C., Buendia, B., 2000. HP1gamma associates with euchromatin and heterochromatin in mammalian nuclei and chromosomes. Cytogenet. Cell Genet. 90, 279–284.

Modrzynska, K., Pfander, C., Chappell, L., Yu, L., Suarez, C., Dundas, K., Gomes, A.R., Goulding, D., Rayner, J.C., Choudhary, J., Billker, O., 2017. A Knockout Screen of ApiAP2 Genes Reveals Networks of Interacting Transcriptional Regulators Controlling the Plasmodium Life Cycle. Cell Host Microbe 21, 11–22. doi:10.1016/j.chom.2016.12.003

Newbold, C., Warn, P., Black, G., Berendt, A., Craig, A., Snow, B., Msobo, M., Peshu, N., Marsh, K., 1997. Receptor-specific adhesion and clinical disease in Plasmodium falciparum. Am. J. Trop. Med. Hyg. 57, 389–398. doi:10.4269/ajtmh.1997.57.389

Ngotho, P., Soares, A.B., Hentzschel, F., Achcar, F., Bertuccini, L., Marti, M., 2019. Revisiting gametocyte biology in malaria parasites. FEMS Microbiol. Rev. 43, 401–414. doi:10.1093/femsre/fuz010

Otto, T.D., Wilinski, D., Assefa, S., Keane, T.M., Sarry, L.R., Böhme, U., Lemieux, J., Barrell, B., Pain, A., Berriman, M., Newbold, C., Llinás, M., 2010. New insights into the blood-stage transcriptome of Plasmodium falciparum using RNA-Seq. Mol. Microbiol. 76, 12–24. doi:10.1111/j.1365-2958.2009.07026.x

Painter, H.J., Campbell, T.L., Llinás, M., 2011. The Apicomplexan AP2 family: integral factors regulating Plasmodium development. Mol. Biochem. Parasitol. 176, 1–7. doi:10.1016/j.molbiopara.2010.11.014

Patankar, S., Munasinghe, A., Shoaibi, A., Cummings, L.M., Wirth, D.F., 2001. Serial analysis of gene expression in Plasmodium falciparum reveals the global expression profile of erythrocytic stages and the presence of anti-sense transcripts in the malarial parasite. Mol. Biol. Cell 12, 3114–3125. doi:10.1091/mbc.12.10.3114

Patra, K.P., Johnson, J.R., Cantin, G.T., Yates, J.R., Vinetz, J.M., 2008. Proteomic analysis of zygote and ookinete stages of the avian malaria parasite Plasmodium gallinaceum delineates the homologous proteomes of the lethal human malaria parasite Plasmodium falciparum. Proteomics 8, 2492–2499. doi:10.1002/pmic.200700727

Pease, B.N., Huttlin, E.L., Jedrychowski, M.P., Talevich, E., Harmon, J., Dillman, T., Kannan, N., Doerig, C., Chakrabarti, R., Gygi, S.P., Chakrabarti, D., 2013. Global analysis of protein expression and phosphorylation of three stages of Plasmodium falciparum intraerythrocytic development. J. Proteome Res. 12, 4028–4045. doi:10.1021/pr400394g

Petter, M., Selvarajah, S.A., Lee, C.C., Chin, W.H., Gupta, A.P., Bozdech, Z., Brown, G.V., Duffy, M.F., 2013. H2A.Z and H2B.Z double-variant nucleosomes define intergenic regions and dynamically occupy var gene promoters in the malaria parasite Plasmodium falciparum. Mol. Microbiol. 87, 1167–1182. doi:10.1111/mmi.12154

Pérez-Toledo, K., Rojas-Meza, A.P., Mancio-Silva, L., Hernández-Cuevas, N.A., Delgadillo, D.M., Vargas, M., Martínez-Calvillo, S., Scherf, A., Hernandez-Rivas, R., 2009. Plasmodium falciparum heterochromatin protein 1 binds to tri-methylated histone 3 lysine 9 and is linked to mutually exclusive expression of var genes. Nucleic Acids Res. 37, 2596–2606. doi:10.1093/nar/gkp115

Ponts, N., Fu, L., Harris, E.Y., Zhang, J., Chung, D.-W.D., Cervantes, M.C., Prudhomme, J., Atanasova-Penichon, V., Zehraoui, E., Bunnik, E.M., Rodrigues, E.M., Lonardi, S., Hicks, G.R., Wang, Y., Le Roch, K.G., 2013. Genome-wide mapping of DNA methylation in the human malaria parasite Plasmodium falciparum. Cell Host Microbe 14, 696–706. doi:10.1016/j.chom.2013.11.007

Raisner, R.M., Hartley, P.D., Meneghini, M.D., Bao, M.Z., Liu, C.L., Schreiber, S.L., Rando, O.J., Madhani, H.D., 2005. Histone variant H2A.Z marks the 5' ends of both active and inactive genes in euchromatin. Cell 123, 233–248. doi:10.1016/j.cell.2005.10.002

Ralph, S.A., Bischoff, E., Mattei, D., Sismeiro, O., Dillies, M.-A., Guigon, G., Coppée, J.-Y., David, P.H., Scherf, A., 2005. Transcriptome analysis of antigenic variation in Plasmodium falciparum--var silencing is not dependent on antisense RNA. Genome Biol. 6, R93–12. doi:10.1186/gb-2005-6-11-r93

Reeder, J.C., Brown, G.V., 1996. Antigenic variation and immune evasion in Plasmodium falciparum malaria. Immunol. Cell Biol. 74, 546–554. doi:10.1038/icb.1996.88

Rovira-Graells, N., Gupta, A.P., Planet, E., Crowley, V.M., Mok, S., Ribas de Pouplana, L., Preiser, P.R., Bozdech, Z., Cortés, A., 2012. Transcriptional variation in the malaria parasite Plasmodium falciparum. Genome Res. 22, 925–938. doi:10.1101/gr.129692.111

Rowe, J.A., Claessens, A., Corrigan, R.A., Arman, M., 2009. Adhesion of Plasmodium falciparum-infected erythrocytes to human cells: molecular mechanisms and therapeutic implications. Expert Rev Mol Med 11, e16. doi:10.1017/S1462399409001082

Salcedo-Amaya, A.M., van Driel, M.A., Alako, B.T., Trelle, M.B., van den Elzen, A.M.G., Cohen, A.M., Janssen-Megens, E.M., van de Vegte-Bolmer, M., Selzer, R.R., Iniguez, A.L., Green, R.D., Sauerwein, R.W., Jensen, O.N., Stunnenberg, H.G., 2009. Dynamic histone H3 epigenome marking during the intraerythrocytic cycle of Plasmodium falciparum. Proc. Natl. Acad. Sci. U.S.A. 106, 9655–9660. doi:10.1073/pnas.0902515106

Santos, J.M., Josling, G., Ross, P., Joshi, P., Orchard, L., Campbell, T., Schieler, A., Cristea, I.M., Llinás, M., 2017. Red Blood Cell Invasion by the Malaria Parasite Is Coordinated by the PfAP2-I Transcription Factor. Cell Host Microbe 21, 731–741.e10. doi:10.1016/j.chom.2017.05.006

Saraf, A., Cervantes, S., Bunnik, E.M., Ponts, N., Sardiu, M.E., Chung, D.-W.D., Prudhomme, J., Varberg, J.M., Wen, Z., Washburn, M.P., Florens, L., Le Roch, K.G., 2016. Dynamic and Combinatorial Landscape of Histone Modifications during the Intraerythrocytic Developmental Cycle of the Malaria Parasite. J. Proteome Res. 15, 2787–2801. doi:10.1021/acs.jproteome.6b00366

Scherf, A., Hernandez-Rivas, R., Buffet, P., Bottius, E., Benatar, C., Pouvelle, B., Gysin, J., Lanzer, M., 1998. Antigenic variation in malaria: in situ switching, relaxed and mutually exclusive transcription of var genes during intra-erythrocytic development in Plasmodium falciparum. EMBO J. 17, 5418–5426. doi:10.1093/emboj/17.18.5418

Scherf, A., Lopez-Rubio, J.J., Riviere, L., 2008. Antigenic variation in Plasmodium falciparum. Annu. Rev. Microbiol. 62, 445–470. doi:10.1146/annurev.micro.61.080706.093134

Schones, D.E., Cui, K., Cuddapah, S., Roh, T.-Y., Barski, A., Wang, Z., Wei, G., Zhao, K., 2008. Dynamic regulation of nucleosome positioning in the human genome. Cell 132, 887–898. doi:10.1016/j.cell.2008.02.022

Schultz, D.C., Ayyanathan, K., Negorev, D., Maul, G.G., Rauscher, F.J., 2002. SETDB1: a novel KAP-1-associated histone H3, lysine 9-specific methyltransferase that contributes to HP1-mediated silencing of euchromatic genes by KRAB zinc-finger proteins. Genes Dev 16, 919–932. doi:10.1101/gad.973302

Schwaiger, M., Kohler, H., Oakeley, E.J., Stadler, M.B., Schübeler, D., 2010. Heterochromatin protein 1 (HP1) modulates replication timing of the Drosophila genome. Genome Res. 20, 771–780. doi:10.1101/gr.101790.109

Shimada, A., Dohke, K., Sadaie, M., Shinmyozu, K., Nakayama, J.-I., Urano, T., Murakami, Y., 2009. Phosphorylation of Swi6/HP1 regulates transcriptional gene silencing at heterochromatin. Genes Dev. 23, 18–23. doi:10.1101/gad.1708009

Siegel, T.N., Hon, C.-C., Zhang, Q., Lopez-Rubio, J.J., Scheidig-Benatar, C., Martins, R.M., Sismeiro, O., Coppée, J.-Y., Scherf, A., 2014. Strand-specific RNA-Seq reveals widespread and developmentally regulated transcription of natural antisense transcripts in Plasmodium falciparum. BMC Genomics 15, 150–16. doi:10.1186/1471-2164-15-150

Sierra-Miranda, M., Vembar, S.-S., Delgadillo, D.M., Ávila-López, P.A., Herrera-Solorio, A.-M., Lozano Amado, D., Vargas, M., Hernandez-Rivas, R., 2017. PfAP2Tel, harbouring a non-canonical DNA-binding AP2 domain, binds to Plasmodium falciparum telomeres. Cell. Microbiol. 19, e12742. doi:10.1111/cmi.12742

Silvestrini, F., Alano, P., Williams, J.L., 2000. Commitment to the production of male and female gametocytes in the human malaria parasite Plasmodium falciparum. Parasitology 121 Pt 5, 465–471.

Singh, P.B., Georgatos, S.D., 2002. HP1: facts, open questions, and speculation. J. Struct. Biol. 140, 10–16.

Sinha, A., Hughes, K.R., Modrzynska, K.K., Otto, T.D., Pfander, C., Dickens, N.J., Religa, A.A., Bushell, E., Graham, A.L., Cameron, R., Kafsack, B.F.C., Williams, A.E., Llinás, M., Berriman, M., Billker, O., Waters, A.P., 2014. A cascade of DNA-binding proteins for sexual commitment and development in Plasmodium. Nature. 507, 253-257 doi:10.1038/nature12970

Smith, J.D., Chitnis, C.E., Craig, A.G., Roberts, D.J., Hudson-Taylor, D.E., Peterson, D.S., Pinches, R., Newbold, C.I., Miller, L.H., 1995. Switches in expression of Plasmodium falciparum var genes correlate with changes in antigenic and cytoadherent phenotypes of infected erythrocytes. Cell 82, 101–110.

Smith, T.G., Lourenço, P., Carter, R., Walliker, D., Ranford-Cartwright, L.C., 2000. Commitment to sexual differentiation in the human malaria parasite, Plasmodium falciparum. Parasitology 121 (Pt 2), 127–133.

Smothers, J.F., Henikoff, S., 2000. The HP1 chromo shadow domain binds a consensus peptide pentamer. Curr. Biol. 10, 27–30.

Solyakov, L., Halbert, J., Alam, M.M., Semblat, J.-P., Dorin-Semblat, D., Reininger, L., Bottrill, A.R., Mistry, S., Abdi, A., Fennell, C., Holland, Z., Demarta, C., Bouza, Y., Sicard, A., Nivez, M.-P., Eschenlauer, S., Lama, T., Thomas, D.C., Sharma, P., Agarwal, S., Kern, S., Pradel, G., Graciotti, M., Tobin, A.B., Doerig, C., 2011. Global kinomic and phospho-proteomic analyses of the human malaria parasite Plasmodium falciparum. Nat Commun 2, 565. doi:10.1038/ncomms1558

Sugiyama, T., Cam, H.P., Sugiyama, R., Noma, K.-I., Zofall, M., Kobayashi, R., Grewal, S.I.S., 2007. SHREC, an effector complex for heterochromatic transcriptional silencing. Cell 128, 491–504. doi:10.1016/j.cell.2006.12.035

Treeck, M., Sanders, J.L., Elias, J.E., Boothroyd, J.C., 2011. The phosphoproteomes of Plasmodium falciparum and Toxoplasma gondii reveal unusual adaptations within and beyond the parasites' boundaries. Cell Host Microbe 10, 410–419. doi:10.1016/j.chom.2011.09.004

Valverde, R., Edwards, L., Regan, L., 2008. Structure and function of KH domains. FEBS J. 275, 2712–2726. doi:10.1111/j.1742-4658.2008.06411.x

Vembar, S.S., Scherf, A., Siegel, T.N., 2014. Noncoding RNAs as emerging regulators of Plasmodium falciparum virulence gene expression. Curr. Opin. Microbiol. 20, 153–161. doi:10.1016/j.mib.2014.06.013

Voss, T.S., Bozdech, Z., Bartfai, R., 2014. Epigenetic memory takes center stage in the survival strategy of malaria parasites. Curr. Opin. Microbiol. 20, 88–95. doi:10.1016/j.mib.2014.05.007

Voss, T.S., Healer, J., Marty, A.J., Duffy, M.F., Thompson, J.K., Beeson, J.G., Reeder, J.C., Crabb, B.S., Cowman, A.F., 2006. A var gene promoter controls allelic exclusion of virulence genes in Plasmodium falciparum malaria. Nature 439, 1004–1008. doi:10.1038/nature04407

Voss, T.S., Kaestli, M., Vogel, D., Bopp, S., Beck, H.-P., 2003. Identification of nuclear proteins that interact differentially with Plasmodium falciparum var gene promoters. Mol. Microbiol. 48, 1593–1607. doi:10.1046/j.1365-2958.2003.03528.x

Wang, G., Ma, A., Chow, C.M., Horsley, D., Brown, N.R., Cowell, I.G., Singh, P.B., 2000. Conservation of heterochromatin protein 1 function. Mol. Cell. Biol. 20, 6970–6983.

Wei, C., Xiao, T., Zhang, P., Wang, Z., Chen, X., Zhang, L., Yao, M., Chen, R., Wang, H., 2014. Deep profiling of the novel intermediate-size noncoding RNAs in intraerythrocytic Plasmodium falciparum. PLoS ONE 9, e92946. doi:10.1371/journal.pone.0092946

Woodcock, C.L., Ghosh, R.P., 2010. Chromatin higher-order structure and dynamics. Cold Spring Harb Perspect Biol 2, a000596–a000596. doi:10.1101/cshperspect.a000596

Yamada, T., Fischle, W., Sugiyama, T., Allis, C.D., Grewal, S.I.S., 2005. The nucleation and maintenance of heterochromatin by a histone deacetylase in fission yeast. Mol. Cell 20, 173–185. doi:10.1016/j.molcel.2005.10.002

Yazdani, S.S., Mukherjee, P., Chauhan, V.S., Chitnis, C.E., 2006. Immune responses to asexual blood-stages of malaria parasites. Curr. Mol. Med. 6, 187–203.

Yuda, M., Iwanaga, S., Kaneko, I., Kato, T., 2015. Global transcriptional repression: An initial and essential step for Plasmodium sexual development. Proc. Natl. Acad. Sci. U.S.A. 112, 12824–12829. doi:10.1073/pnas.1504389112

Yuda, M., Iwanaga, S., Shigenobu, S., Kato, T., Kaneko, I., 2010. Transcription factor AP2-Sp and its target genes in malarial sporozoites. Mol. Microbiol. 75, 854–863. doi:10.1111/j.1365-2958.2009.07005.x

Yuda, M., Iwanaga, S., Shigenobu, S., Mair, G.R., Janse, C.J., Waters, A.P., Kato, T., Kaneko, I., 2009. Identification of a transcription factor in the mosquito-invasive stage of malaria parasites. Mol. Microbiol. 71, 1402–1414. doi:10.1111/j.1365-2958.2009.06609.x

Zanghì, G., Vembar, S.S., Baumgarten, S., Ding, S., Guizetti, J., Bryant, J.M., Mattei, D., Jensen, A.T.R., Rénia, L., Goh, Y.S., Sauerwein, R., Hermsen, C.C., Franetich, J.-F., Bordessoulles, M., Silvie, O., Soulard, V., Scatton, O., Chen, P., Mecheri, S., Mazier, D., Scherf, A., 2018. A Specific PfEMP1 Is Expressed in P. falciparum Sporozoites and Plays a Role in Hepatocyte Infection. Cell Rep 22, 2951–2963. doi:10.1016/j.celrep.2018.02.075

Zeng, W., Ball, A.R., Yokomori, K., 2010. HP1: heterochromatin binding proteins working the genome. Epigenetics 5, 287–292.

Chapter 2. Mapping and functional analysis of heterochromatin protein 1 phosphorylation in the malaria parasite *Plasmodium falciparum*

Hai T. N. Bui[1,2], Igor Niederwieser[1,2], Megan J. Bird[3], Weiwen Dai[4,5], Nicolas M. B. Brancucci[1,2], Suzette Moes[6], Paul Jenoe[6], Isabelle S. Lucet[4,5], Christian Doerig[3,7], Till S. Voss[1,2,*]

[1]Department of Medical Parasitology and Infection Biology, Swiss Tropical and Public Health Institute, 4051 Basel, Switzerland
[2]University of Basel, 4003 Basel, Switzerland
[3]Department of Microbiology, Monash University, Clayton, Victoria 3800, Australia
[4]The Walter and Eliza Hall Institute of Medical Research, Parkville, Victoria 3052, Australia
[5]Department of Medical Biology, University of Melbourne, Parkville, Victoria, 3052, Australia
[6]Biozentrum, University of Basel, 4056 Basel, Switzerland
[7]Centre for Chronic Inflammatory and Infectious Diseases, School for Health and Biomedical Sciences, RMIT University, Bundoora Victoria 3083, Australia

[*]Corresponding author: till.voss@swisstph.ch

Manuscript submitted (see Author contributions)

2.1 Abstract

Previous studies in model eukaryotes have demonstrated that phosphorylation of heterochromatin protein 1 (HP1) is important for dynamically regulating its various functions. However, in the malaria parasite *Plasmodium falciparum* both the function of HP1 phosphorylation and the identity of the protein kinases targeting HP1 are still elusive. In order to functionally analyze phosphorylation of *P. falciparum* HP1 (PfHP1), we first mapped PfHP1 phosphorylation sites by liquid chromatography tandem mass spectrometry (LC-MS/MS) analysis of native PfHP1, which identified motifs from which potential kinases could be predicted; in particular, several phosphorylated residues were embedded in motifs rich in acidic residues, reminiscent of targets for *P. falciparum* casein kinase 2 (PfCK2). Secondly, we tested recombinant PfCK2 and a number of additional protein kinases for their ability to phosphorylate PfHP1 in *in vitro* kinase assays. These experiments validated our prediction that PfHP1 acts as a substrate for PfCK2. Furthermore, LC-MS/MS analysis showed that PfCK2 phosphorylates three clustered serine residues in an acidic motif within the central hinge region of PfHP1. To study the role of PfHP1 phosphorylation in live parasites we used CRISPR/Cas9-mediated genome editing to generate a number of conditional PfHP1 phosphomutants based on the DiCre/LoxP system. Our studies revealed that neither PfCK2-dependent phosphorylation of PfHP1, nor phosphorylation of the hinge domain in general, affect PfHP1's ability to localize to heterochromatin, and that PfHP1 phosphorylation in this region is dispensable for the proliferation and sexual differentiation of *P. falciparum* blood stage parasites.

2.2 Introduction

Euchromatin and heterochromatin are the two main structures of chromatin in eukaryotes. While euchromatin is associated with active gene transcription, heterochromatin is associated with heritable gene silencing. Heterochromatin is characterized by the enrichment of heterochromatin protein 1 (HP1) bound to trimethylated histone 3 lysine 9 (H3K9me3) (Bannister et al., 2001; Lachner et al., 2001; Lomberk et al., 2006). HP1 recruits chromatin modifiers such as H3K9me-specific histone methyltransferases, which in turn methylate H3K9 in neighbouring nucleosomes, thus facilitating the binding of further HP1 proteins and consequently the regional spreading of heterochromatin in a sequence-independent manner (Grewal and Moazed, 2003; Lomberk et al., 2006). In addition to promoting gene silencing and heterochromatin maintenance HP1 also plays roles in centromere function in fission yeast and humans and in DNA replication and repair (Kwon and Workman, 2008; Zeng et al., 2010).

HP1 is widely conserved among eukaryotes and consists of three functional domains, namely the N-terminal chromo domain (CD) that binds H3K9me3 (Jacobs et al., 2001; Lachner et al., 2001; Platero et al., 1995), the C-terminal chromoshadow domain (CSD) that mediates HP1 homodimerisation and specific interactions with other regulatory proteins (Brasher et al., 2000; Cowieson et al., 2000; Schotta et al., 2002), and a variable hinge region located between the CD and CSD domains that has been shown to interact with DNA and/or RNA (Meehan et al., 2003; Muchardt et al., 2002; Sugimoto et al., 1996). Some eukaryotes have several HP1 paralogs; for instance, *Schizosaccharomyces pombe* encodes two HP1 variants (Swi6 and Chp2) and mammals possess three HP1 variants (HP1α, HP1β and HP1γ) (Kwon and Workman, 2008; Lomberk et al., 2006).

The parasitic protist *Plasmodium falciparum*, the causative agent of the most severe form of malaria in humans, possesses a single HP1 ortholog (PfHP1). PfHP1 binds to and co-localizes with H3K9me3 to heterochromatic domains in the subtelomeric regions of all 14 chromosomes and to internal heterochromatic islands on some chromosomes (Flueck et al., 2009; Fraschka et al., 2018; Lopez-Rubio et al., 2009; Perez-Toledo et al., 2009; Salcedo-Amaya et al., 2010). There is no evidence for the presence of either PfHP1 or H3K9me3 in peri-centromeric regions, suggesting that PfHP1 does not contribute to the maintenance of centromere structure and function in this organism (Flueck et al., 2009; Fraschka et al., 2018; Hoeijmakers et al., 2012; Lopez-Rubio et al.,

2009; Salcedo-Amaya et al., 2010). The subtelomeric and chromosome-internal heterochromatic domains collectively cover over 400 protein-coding genes, most of which belong to *P. falciparum*-specific gene families that encode virulence factors exported to the host erythrocyte (Flueck et al., 2009; Fraschka et al., 2018; Lopez-Rubio et al., 2009; Salcedo-Amaya et al., 2010). In addition, PfHP1 also binds to a small number of euchromatic loci, including the gene encoding the master transcription factor of sexual differentiation PfAP2-G (Flueck et al., 2009; Fraschka et al., 2018). Consistent with a role for PfHP1 in heritable gene silencing, almost all PfHP1-associated genes are expressed in a clonally variant manner (Rovira-Graells et al., 2012). The best-studied example is provided by the *var* gene family that consists of approximately 60 members, each encoding a variant of the erythrocyte membrane protein 1 (PfEMP1) antigen that is exposed on the surface of infected red blood cells (iRBCs) (Baruch et al., 1995; Gardner et al., 2002; Smith et al., 1995; Su et al., 1995). The PfEMP1-dependent binding of iRBCs to endothelial cells and uninfected RBCs leads to parasite sequestration in the microvasculature, which strongly contributes to severe disease (Hviid and Jensen, 2015; Scherf et al., 2008). Importantly, expression of the *var* gene family is controlled in a mutually exclusive manner (aka singular gene choice), such that at any given time only a single *var* gene is transcribed while all other family members are epigenetically silenced in a PfHP1-dependent manner (Brancucci et al., 2014; Deitsch and Dzikowski, 2017; Guizetti and Scherf, 2013; Scherf et al., 1998). Switches in *var* gene transcription then lead to clonal antigenic variation of PfEMP1, allowing the parasite to evade adaptive immune responses and establish chronic infection (Scherf et al., 2008; Smith et al., 1995).

Using an inducible PfHP1 loss-of-function parasite line, where PfHP1 expression levels can be modulated via the FKBP/DD-Shield-1 conditional expression system (Armstrong and Goldberg, 2007; Banaszynski et al., 2006), we recently identified three important roles for PfHP1 in the biology of blood stage parasites (Brancucci et al., 2014). First, we found that PfHP1 is essential for the heritable silencing of heterochromatic gene families as PfHP1 depletion resulted in the de-repression of almost all *var* genes and many other subtelomeric gene families in the progeny. Second, we demonstrated that PfHP1 depletion leads to a 25-fold increase in sexual conversion rates, with over 50% of parasites in the progeny differentiating into gametocytes (which are required for malaria transmission via the mosquito vector). This striking phenotype was linked to de-repression of the *ap2-g* locus in absence of PfHP1. Third, we showed that the remaining

asexual parasites in the PfHP1-depleted progeny failed to enter S-phase, revealing a crucial role for PfHP1 in the control of proliferation (Brancucci et al., 2014).

Studies in model eukaryotes have shown that HP1 is post-translationally modified, particularly by phosphorylation. Phosphorylation of HP1 regulates various functions in a number of cellular processes in fission yeast and mammals, including heterochromatic gene silencing, mitosis and DNA repair (Kwon and Workman, 2011; Shimada and Murakami, 2010). For instance, casein kinase 2 (CK2)-dependent phosphorylation of serine residues in the N-terminal part of Swi6 is important for transcriptional silencing and the recruitment of the histone deacetylase complex SHREC in *S. pombe* (Shimada et al., 2009). Similarly, in mice the N-terminal phosphorylation of HP1a by CK2 is important for targeting HP1 to heterochromatin as well as for chromosomal stability. While a single substitution of serine 14 with alanine (S14A) impaired the binding of HP1 a to H3K9me3 and caused diffuse heterochromatic localization, multiple substitutions of clustered serines (S11A to S14A) hampered chromosomal integrity (Hiragami-Hamada et al., 2011). In humans, HP1 phosphorylation has been shown to play a role in progression through mitosis. Human HP1a is a substrate of the nuclear Dbf2-related (NDR) kinase; in an NDR-depleted cell line, the lack of HP1a phosphorylation at serine 95 in the hinge domain resulted in chromosome alignment defects, aberrant spindle morphology and a delay in metaphase progression (Chakraborty and Prasanth, 2014). Furthermore, HP1 phosphorylation has also been shown to play a role the DNA damage response in humans. CK2-dependent phosphorylation of HP1β at threonine 51 was shown to modulate the dispersion of HP1 from chromatin, which in turns facilitates histone H2AX phosphorylation and recruitment of downstream regulators involved in repairing chromosomal DNA breaks (Ayoub et al., 2008).

In contrast to model eukaryotes, the functional role of HP1 phosphorylation in *P. falciparum* and the kinases involved are still unknown. Hence, to begin understanding how PfHP1 function is regulated in *P. falciparum,* we studied PfHP1 phosphorylation using *in vitro* and *in vivo* assays. Liquid chromatography tandem mass spectrometry (LC-MS/MS) analysis of immunoprecipitated native PfHP1 showed that PfHP1 is phosphorylated in its CD and hinge domains. *In vitro* kinase assays revealed that PfHP1 is a substrate of *P. falciparum* CK2 (PfCK2). LC-MS/MS analysis showed that PfCK2 targets three clustered serine residues within the PfHP1 hinge region *in vitro*. By generating conditional PfHP1 phosphomutant cell lines using CRISPR/Cas9-mediated genome editing combined with the DiCre/LoxP system (Collins et al., 2013; Jones et

al., 2016), we found that PfCK2-dependent phosphorylation of PfHP1, and phosphorylation of the PfHP1 hinge domain in general, is dispensable for proper PfHP1 localisation, gene silencing, parasite growth and sexual conversion.

2.3 Results

Identification of phosphorylated PfHP1 residues and parasite kinases phosphorylating PfHP1

Several large-scale phosphoproteomics studies in *P. falciparum* collectively detected 13 phosphorylated residues in PfHP1 (T2, S4, S33, T38, S57, S89, S92, S108, T110, S122, S125, S129, S174) (Collins et al., 2014; Lasonder et al., 2012; Lasonder et al., 2015; Pease et al., 2013; Solyakov et al., 2011; Treeck et al., 2011). The Y32 and S136 residues have been identified as additional phosphosites in a recent study investigating native PfHP1 complexes (Filarsky et al., 2018). To confirm and possibly expand these results, we used LC-MS/MS experiments to map phosphorylated residues in native PfHP1. To this end, we purified PfHP1-GFP by immunoprecipitation (IP) from nuclear extracts prepared from 3D7/HP1-GFP parasites (Brancucci et al., 2014) in four independent biological replicate experiments (Figure 1A). LC-MS/MS analysis of the eluted protein samples identified a total of eleven phosphosites in PfHP1 (Figure 1B and Table S1). One of these phosphosites (S206) has not been identified in any of the earlier studies, and five previously mapped phosphosites (T38, S57, S92, S108 and T110) have not been identified here (Figure 1B). Two of the sites identified in our study are located in the first few residues preceding the CD domain (T2, S4), two are located within the CD domain in a predicted flexible loop (Y32, S33), six are located in the hinge region (S89, S122, S125, S129, S136, S174) and one is located in a predicted loop in the CSD domain (S206) (Figure 1B).

Several of the identified phosphosites conform to CK2 target sites in view of their richness in acidic residues (e.g. S129; SDEE), while others appear as potential targets of proline-directed kinases such as CDK, GSK3 or MAPK (e.g. S174; ESP), or of basic residues-directed kinases such as AGC kinases (e.g. S89; SIK) (Table S1) [see Amanchy and colleagues for a comprehensive list of phosphorylation motifs (Amanchy et al., 2007)]. To identify candidate kinases possibly phosphorylating PfHP1, we screened a set of six recombinant functional parasite kinases, namely PfCK2 (Holland et al., 2009), PfGSK3 (Droucheau et al., 2004), PfMAP2 (Dorin et al., 1999), PfNEK2 (Reininger et al., 2009), PfNEK4 (Reininger et al., 2005) and PfPK6 (Bracchi-Ricard et al., 2000), for their ability to phosphorylate recombinant PfHP1 *in vitro*, which includes the potential

candidates PfCK2, PfGSK3 and PfMAP2 predicted by the phosphorylation site motifs outlined above. For this purpose, we expressed recombinant full-length PfHP1 and a truncated PfHP1 polypeptide encompassing the CD domain and hinge region (PfCD.H) in *Escherichia coli* and purified them by fast protein liquid chromatography (Figure 2A). To perform the kinase reactions, we used an *in vitro* assay based on luminescence signal detection (ADP-Glo™, Promega). The enzymatic reaction starts when a kinase is added into a mixture containing the substrate and ATP. Upon completion of the reaction, the ADP-Glo™ assay quantifies the levels of ADP released from consumed ATP as a measure of kinase activity. Among the recombinant parasite kinases screened, PfMAP2, PfPK6, PfNEK2 and PfNEK4 showed little or no activity on PfHP1 (Figure S1). PfGSK3 showed some positive enzymatic activity on PfHP1 but this result was inconclusive due to the high level of autophosphorylation exerted by this kinase both in the ADP-Glo assay as well as in a radioactive kinase activity assay employing γ-P^{32}-ATP (Figure S2). Importantly, however, PfCK2 displayed remarkable activity in phosphorylating PfHP1 *in vitro*. In the ADP-Glo assay, PfCK2 showed autophosphorylation activity and was able to phosphorylate the control substrate β-casein. In absence of PfCK2, PfHP1 and PfCD.H exhibited no signals of phosphorylation activity as expected. In contrast, when PfCK2 was added to the PfHP1 and PfCD.H substrates, ADP conversion increased substantially compared to PfCK2 alone or PfCK2 with β-casein (Figure 2B). Consistent results were obtained for PfCK2 using the *in vitro* γ-P^{32}-ATP kinase assay. PfCK2 again showed auto-phosphorylation activity but was clearly capable of phosphorylating β-casein as a positive control and, at substantially higher levels, the PfHP1 and PfCD.H substrates (Figure 2C). To further probe the specificity of the CK2-dependent kinase reaction towards PfHP1 and PfCD.H, 4,5,6,7-tetrabromobenzimidazole (TBB), a selective ATP-competitive inhibitor of CK2 across species (Sarno et al., 2001), was added to the kinase reactions. The treatment with 20 μM TBB resulted in a significant drop of phosphorylation signal intensity in the reactions containing the substrates (Figure 2C). Finally, to identify the residues in PfHP1 targeted by PfCK2 *in vitro*, we performed LC-MS/MS analysis of the ADP-Glo™ kinase assay reactions. The results revealed that PfCK2 phosphorylated a cluster of three serine residues in the hinge domain (S122, S125 and S129). Three additional predicted CK2 target residues in the PfHP1 N-terminus (T2, S4, S33; see Table S1), however, where not detected in their phosphorylated form. As expected, no phosphorylated sites were detected in recombinant PfHP1 prior to the phosphorylation assay (Table S2). We also

failed to detect any phosphorylated residues in PfHP1 after incubation with PfGSK3 (Table S2).

Overall, using three independent approaches, we demonstrate that PfHP1 is phosphorylated at least at eleven residues during intra-erythrocytic development, that most of these residues are located either at the N-terminus, in predicted loop regions in the CD and CSD domains or in the hinge domain, and that three residues in the hinge region (S122, S125 and S129) are phosphorylated by PfCK2 in *in vitro*.

Generation of conditional PfHP1 phosphomutant parasite lines

To address the *in vivo* functional significance of PfHP1 phosphorylation, we used two subsequent CRISPR-Cas9-based gene editing steps to engineer parasites that allow for the conditional expression of PfHP1 phosphomutants based on the DiCre-loxP system (Collins et al., 2013) (Figures 3A, S3 and S4). In the first step, a *sera2* intron:loxP element (Jones et al., 2016) was inserted into the 5' end of the endogenous *pfhp1* gene to obtain the 3D7/N31DC mother line. PCRs on gDNA and cDNA and Sanger sequencing confirmed the correct editing of the *pfhp1* locus and the correct splicing of the *sera2* intron:loxP element (Figure S4). In the second step, a second *sera2* intron:loxP element followed by a recodonised *pfhp1* gene fused to *gfp* was placed directly downstream of the *pfhp1* STOP codon (Figures 3A and S3). In these parasites, activation of the DiCre recombinase by rapamycin is expected to excise the floxed endogenous *pfhp1* gene and to place a recodonised version encoding a PfHP1-GFP phosphomutant under control of the endogenous promoter (Figure 3A). We generated two such conditional PfHP1 phosphomutant lines called 3D7/HP1-3M and 3D7/HP1-HIM, where either the three serine residues targeted by PfCK2 *in vitro* (S122/125/129A) or the cluster of seven phosphorylated serine residues in the hinge region (S89/92/122/125/129/136/174A), respectively, have been substituted by non-phoshorylatable alanines. We also generated a control cell line where rapamycin treatment results in the replacement of the endogenous *pfhp1* with a recodonized wild type *pfhp1-gfp* sequence (3D7/HP1-Control) (Figure 3A).

PCR on parasite genomic DNA (gDNA) was used to confirm (1) the correct integration of the recodonised *pfhp1-gfp* gene directly downstream of the endogenous *pfhp1* locus; and (2) the successful DiCre-mediated excision of the floxed endogenous *pfhp1* gene in schizont stages (24-36 hrs after rapamycin treatment) in all three cell lines (Figure 3B). To confirm correct splicing of the *sera2* intron:loxP element after rapamycin treatment and presence of the mutated codons encoding serine-to-alanine

substitutions, RT-PCR and Sanger sequencing was performed (Figure S4). Live cell fluorescence imaging in late schizonts at 40-48 hpi (40 hrs after rapamycin treatment) showed that in each of the three parasite lines, excision of the endogenous *pfhp1* gene was highly efficient and expression of the recodonised PfHP1-GFP variants was observed in close to 100% of parasites in the populations (Figure 3C). In contrast, parasites in the DMSO-treated control populations did not express GFP-tagged PfHP1 variants as expected. Consistent with the live fluorescence imaging results, analysis of whole parasite protein lysates by Western Blot showed that the rapamycin-treated parasites exclusively expressed the recodonised PfHP1-GFP fusions, while DMSO-treated control parasites exclusively expressed wild-type untagged PfHP1 (Figure 3D).

PfHP1 phosphomutants still localize to perinuclear heterochromatin

In *Drosophila melanogaster* and mice, CK2-dependent phosphorylation of HP1 is required for the correct localization of HP1 to heterochromatin (Hiragami-Hamada et al., 2011; Zhao and Eissenberg, 1999). We therefore tested if the PfHP1 phosphomutants PfHP1-3M and PfHP1-HIM still localize to subtelomeric heterochromatin. Live cell fluorescence imaging in late schizonts at 40-48 hpi and in the late ring stage progeny at 16-24 hpi in generation 2 showed that the GFP-tagged PfHP1-3M, PfHP1-HIM and control PfHP1-GFP were not expressed in DMSO-treated parasites as expected. However, in the rapamycin-treated populations the GFP-tagged PfHP1-3M and PfHP1-HIM phosphomutants were expressed and showed a punctate pattern at the nuclear periphery indistinguishable from that observed for the PfHP1-GFP control protein (Figure 4). These results demonstrate that the phosphorylation of serine residues in the PfHP1 hinge domain is not required for the correct targeting and localization of PfHP1 to heterochromatin.

Phosphorylation of serine residues in the PfHP1 hinge domain is not required for parasite multiplication and plays no obvious role in regulating sexual commitment and *var* gene silencing

In a recent study, we showed that PfHP1 is required for (1) progression through schizogony and thus parasite multiplication; (2) *var* gene silencing and mutually exclusive *var* gene expression; and (3) silencing of the *pfap2-g* locus and thus inhibition of sexual commitment (Brancucci et al., 2014). Here, we asked if phosphorylation of serine residues in the PfHP1 hinge domain is required for any of these processes.

We first monitored the proliferation rates of the PfHP1 phosphomutants and the control line over three consecutive generations after rapamycin treatment. As shown in Figure

5A, in each parasite line the multiplication of DMSO- and rapamycin-treated parasites was highly comparable. This result indicates that phosphorylation of the PfHP1 hinge domain is not required for the proliferation of asexual blood stage parasites.

To identify a possible role for PfHP1 hinge domain phosphorylation in controlling *pfap2-g* silencing, we compared the sexual conversion rates between DMSO- and rapamycin-treated parasites for all three transgenic parasite lines. Parasite populations were split at 0-8 hpi and treated either with DMSO or rapamycin. After re-invasion, ring stage progeny (16-24 hpi in generation 2; day 1 of gametocytogenesis) were cultured in medium containing 50 mM N-acetyl-glucosamine (GlcNAc) for six consecutive days to eliminate asexual parasites (Fivelman et al., 2007; Ponnudurai et al., 1986). Gametocytaemia was determined on day six by inspection of Giemsa-stained blood smears and sexual conversion rates were calculated as the fraction of gametocytaemia on day 6 in relation to the total parasitaemia observed on day 1. As shown in Figure 5B, the rapamycin-treated 3D7/HP1-3M and 3D7/HP1-HIM populations showed significantly higher sexual conversion rates compared to the DMSO-treated populations ($p<0.01$, unpaired two-tailed Student's t-test). Unexpectedly, however, rapamycin-treated 3D7/HP1-Control parasites, which express a recodonised wild-type *pfhp1* gene, also displayed significantly increased sexual conversion compared to the matched DMSO-treated population. In contrast, the 3D7/1G5DiCre mother line, which expresses the DiCre recombinase in absence of a floxed *pfhp1* locus, as well as 3D7 wild type parasites did not show increased sexual conversion rates upon rapamycin treatment, showing that rapamycin-induced expression of the DiCre recombinase *per se* or the exposure to rapamycin *per se* has no effect on sexual conversion rates. Hence, the increased sexual conversion rates observed for rapamycin-treated 3D7/HP1-3M, 3D7/HP1-HIM and the 3D7/HP1-Control parasites rather seem to be linked to the DiCre-dependent recombination events at the floxed *pfhp1* locus. Whatever the mechanisms underlying this puzzling observation, our data clearly suggest that phosphorylation of the hinge domain plays no important role in regulating *pfap2-g* silencing. Furthermore, gametocytes expressing either of the two PfHP1 phosphomutant proteins also developed into stage V gametocytes without any apparent morphological differences compared to control gametocytes (data not shown), suggesting that hinge domain phosphorylation is also dispensable for gametocytogenesis.

Finally, to test if the PfHP1 phosphomutations investigated affect *var*/PfEMP1 expression, we compared the expression of PfEMP1 in the late ring stage progeny of

DMSO- and rapamycin-treated 3D7/HP1-3M, 3D7/HP1-HIM and 3D7/HP1-Control parasites (16-24 hpi in generation 2) by IFA. We observed comparable fluorescence intensity signals for PfEMP1 and percentage of PfEMP1-positive iRBCs in the DMSO- and rapamycin-treated parasites of all three lines (Figure 5C), indicating that phosphorylation of the PfHP1 hinge domain plays no major role in regulating *var* gene expression.

2.4 Discussion

Heterochromatin-dependent gene silencing is an important mechanism employed by *P. falciparum* for clonally variant gene expression. PfHP1 is one of the critical factors in this process. In addition, PfHP1 is essential for proliferation of blood stage parasites. Phosphorylation of HP1 has been reported to dynamically regulate the function of this chromatin reader protein in a variety of eukaryotic organisms. Our study described here analysed phosphorylation of PfHP1 and its potential functional role in the biology of *P. falciparum* blood stage parasites.

Using immunoprecipitation of native PfHP1-GFP followed by LC-MS/MS analysis we identified eleven phosphorylated residues in PfHP1 purified from asexual blood stage parasites. All except one of these sites (S206) have either been identified on multiple tryptic peptides and/or in at least two of the independent IP samples analysed here, or they have been detected in previous studies by high-throughput phosphoproteomics approaches (Collins et al., 2014; Lasonder et al., 2012; Lasonder et al., 2015; Pease et al., 2013; Solyakov et al., 2011; Treeck et al., 2011) and/or the mass spectrometry-based analysis of PfHP1 complexes (Filarsky et al., 2018). Hence, we assume these residues are truly phosphorylated in intra-erythrocytic parasites. By screening a number of recombinant *P. falciparum* kinases using two independent kinase activity assays, we found that PfCK2 and PfGSK3 are able to phosphorylate PfHP1 *in vitro*. However, for PfGSK3 the phosphorylation signals obtained with the control and PfHP1 substrates were not noticeably higher compared to those obtained from auto-phosphorylation. GSK3 is a serine/threonine protein kinase preferring to catalyse substrates upon prior phosphorylation of a residue nearby the consensus sequence (S*/T*-X-X-X-S/T) (Doble and Woodgett, 2003; Fiol et al., 1990). Therefore, it is likely that GSK3 is only able to efficiently phosphorylate substrates if they have been primed by phosphorylation through another kinase, which was not applied in our *in vitro* kinase assays. Moreover, although PfGSK3 phosphorylated PfHP1 in the ADP-Glo assay and to some extent also in the radioactive kinase assays, no PfGSK3-dependent

phosphosites were detected on the *in vitro*-reacted PfHP1 substrates by LC-MS/MS analysis. Hence, additional experiments with higher sensitivity will be required to confirm if PfHP1 is indeed phosphorylated by PfGSK3.

Importantly, however, we obtained convincing results showing that PfCK2 phosphorylates PfHP1 at a cluster of three serine residues located in the hinge region (LSLS122*DNS125*LKKS129*DEE), at least *in vitro*. Serine 122 and S129 are embedded in a typical CK2 phosphorylation consensus target motif rich in acidic residues (S*/T*-D/E-X-D/E) (Pinna, 2002; Rusin et al., 2017; St-Denis et al., 2015), whereas S125 lacks the favoured acidic residue at position +1 or +3 as the most crucial specificity determinant of the phosphoacceptor site (Meggio et al., 1994). However, similar atypical CK2 recognition sites containing only one acidic residue between -1 to +5 have indeed been reported (Bian et al., 2013). In our efforts to analyse the role of PfCK2-dependent PfHP1 phosphorylation *in vivo*, however, we found that substituting the three target residues in the hinge domain with non-phosphorylatable alanines (S122/125/129A; PfHP1-3M) had no observable effect on PfHP1 function; parasites expressing the PfHP1-3M triple phosphomutant displayed no marked defects in PfHP1 localisation, *ap2-g/var* gene silencing or mitotic progression. Strikingly, we even failed to observe any silencing- or growth-related phenotypes in parasites expressing the PfHP1-HIM phosphomutant, where seven serine residues in the hinge region have been replaced with alanines (S89/92/122/125/129/136/174A).

In line with these results, it has been reported that phosphorylation of S93 within the mouse HP1a hinge region or S89/91 within the human HP1β hinge domain does not affect HP1's localization to chromatin (Ayoub et al., 2008; Hiragami-Hamada et al., 2011). In addition, co-immunoprecipitation of human HP1β with histone 3 revealed only a minor role for S89 phosphorylation in the ability of HP1β to bind H3K9me3, in spite of local conformational changes induced upon phosphorylation (Munari et al., 2014). In another study on Swi6, the HP1 ortholog in *S. pombe*, mutations of CK2-dependent phosphosites in the hinge and CSD domains (S192/212/220/268/274A) did also not affect heterochromatic gene silencing (Shimada et al., 2009). In other systems, however, essential roles of phosphorylation within the HP1 hinge region have still been reported. In humans, the Aurora A- and NDR1-dependent phosphorylation of serine residues in the hinge region of HP1γ and HP1a, respectively, both play crucial roles in mitotic progression during the G2/M phase (Chakraborty et al., 2014; Grzenda et al., 2013). Further, protein kinase A (PKA)-dependent phosphorylation of the hinge domain

of a *D. melanogaster* HP1 variant plays important roles in HP1 dimerisation, protein-protein interaction and binding to H3K9me3 (Badugu et al., 2005).

In conclusion, our study confirms that PfHP1 is phosphorylated during intra-erythrocytic development at multiple residues particularly in the CD and hinge domains. We also show that PfCK2 phosphorylates three clustered serine residues in the PfHP1 hinge region *in vitro*, but the phosphorylation of these sites is not required for proper PfHP1 function in blood stage parasites. If S122, S125, and S129 are indeed phosphorylated by PfCK2 *in vivo* and if PfCK2 phosphorylates additional target residues in PfHP1 could be tested in future experiments employing conditional PfCK2 knock-down cell lines (Tham et al., 2015). Surprisingly, we also demonstrate that the simultaneous mutation of seven phosphorylation target residues in the hinge has no observable effect on parasite viability. We therefore anticipate that phosphorylation of the PfHP1 hinge region may play an important role elsewhere in the parasite life cycle, for instance during meiosis in the mosquito vector and/or in the replicative phases during male gametogenesis, sporogony or exo-erythrocytic schizogony. While our study does not provide functional insight into the functional role of PfHP1 hinge domain phosphorylation, the experimental pipeline established in this study provides an elegant approach to interrogate protein function and the role of post-translational protein modifications in the biology of *P. falciparum* blood stage parasites.

2.5 Materials and Methods

Parasite culture and transfection

3D7/HP1-GFP parasites (Brancucci et al., 2014) were cultured at 5% hematocrit in RPMI-1640 medium supplemented with 25 mM HEPES, 100 mM hypoxanthine, 24 mM sodium bicarbonate and 0.5% Albumax II. The transgenic lines generated in this study were cultured in the same medium supplemented with 2 mM choline to reduce background sexual conversion rates as demonstrated recently (Brancucci et al., 2017). Parasite cultures were synchronized using 5% sorbitol as described (Lambros and Vanderberg, 1979). Co-transfection of CRISPR/Cas9 and donor plasmids into the DiCre-expressing line 3D7/1G5DiCre (Collins et al., 2013) and selection of transfected populations was performed as described recently (Filarsky et al., 2018).

Immunoprecipitation of native PfHP1-GFP

Parasite nuclei were isolated from 30 ml culture of 3D7/HP1-GFP parasites (5% hematocrit) as described previously (Filarsky et al., 2018). Nuclear proteins were extracted using extraction buffer (2 M L-arginine, 1.925 M HCl, 50 mM H_3PO_4, and 10

mM TCEP) for 20 min on ice. The extract was cleared by centrifugation for 20 min at 20'000 g and 4°C. The supernatant was diluted 1:5 with wash buffer 1 (WB1) (PBS containing additional 324 mM NaCl, 1 M L-proline, 1% octyl β-D-glucopyranoside and 2 mM TCEP) and spun again using the same conditions. Extraction buffer, WB1 and buffers used for nuclear isolation were supplemented with 1x protease inhibitor cocktail (Roche), 5 mM ε-aminocaproic acid (protease inhibitor), 3 mM sodium butyrate (histone deacetylase inhibitor) and 2 mM NaF, 2 mM β-glycerophosphate, 4 mM sodium tartrate, 1 mM sodium pyrophosphate and 1 mM activated $NaVO_3$ (phosphatase inhibitors). GFP-Trap®_A beads (Chromotek) were equilibrated in WB1, added to the supernatant and rotated for 1h at room temperature (RT). The beads were washed three times with WB1 and twice using WB2 (PBS containing additional 824 mM NaCl and 0.2 mM TCEP). Proteins were eluted using arginine elution buffer (2 M L-arginine, 50 mM acetic acid and HCl to pH 4). The eluate was neutralized by addition of 0.1 volumes of 1 M tris base. Next, the samples were processed and analyzed using LC-MS/MS as detailed below.

Capillary liquid chromatography-tandem mass spectrometry (LC-MS/MS)

For the PfHP1 IP experiments, the neutralised elutions were reduced with 10 mM DTT at 37°C for 1 hr and alkylated with 50 mM iodo-acetamide for 15 min at room temperature. Proteins were digested with 250 ng endoproteinase LysC (Wako, Neuss, Germany) for two hours at 37°C followed by 500 ng trypsin (Worthington, Lakewood, NJ, USA) overnight. The digest was stopped with TFA to 1% final concentration and desalted on a microspin column (The Nest Group, Southborough, MA, USA) according to the manufacturer's recommendations.

For the ADP-Glo™ *in vitro* kinase assay samples, 20 µl of the technical duplicate reactions were pooled, precipitated with 20% trichloroacetic acid (TCA) on ice for 30min, followed by washing the precipitate with 17% TCA and two acetone (ice-cold) washes before air-drying the pellets. The protein pellets were dissolved in 30 µl 100 mM Tris-HCl (pH 8.0)/6 M Urea, reduced and alkylated as above and digested with 250 ng endoproteinase LysC for two hours at 37°C. The urea concentration was diluted to 2 M with 100 mM Tris-HCl (pH 8.0) and the sample was further digested with 500 ng trypsin overnight at 37°C. The digest was acidified with 1% TFA and the sample was desalted on a MicroSpin cartridge according to the manufacturer's recommendations.

The eluted peptides were dried in a SpeedVac and dissolved in 40 µl 0.1% formic acid and analysed by capillary LC-MS/M) using a home-packed separating column (0.075

mm x 25 cm) packed with Reprosil C18 reverse-phase material (2.4 µm particle size, Dr. Maisch, Ammerbuch-Entringen, Germany). The column was connected on line to an Orbitrap Elite FT hybrid instrument (Thermo Scientific, Reinach, Switzerland). The solvents used for peptide separation were 0.1% formic acid in water (solvent A) and 0.1% formic acid and 80% acetonitrile in water (solvent B). 2 µl of peptide digest were injected with a Proxeon nLC capillary pump (Thermo Scientific) set to 0.3 µl/min. A linear gradient from 0 to 40% solvent B in solvent A in 95 min was delivered with the nano pump at a flow rate of 300 nl/min. After 95 min the percentage of solvent B was increased to 75% in ten minutes. The eluting peptides were ionized at 2.5 kV. The mass spectrometer was operated in data-dependent mode. The precursor scan was done in the Orbitrap set to 60,000 resolution, while the fragment ions were mass analyzed in the LTQ instrument. A top twenty method was run so that the twenty most intense precursors were selected for fragmentation. The MS/MS spectra of the four PfHP1-GFP IP samples were searched against a combined *P. falciparum* (www.plasmoDB.org; release 9.3)/human annotated protein database using Proteome Discoverer 2.2 (Thermo Scientific, Reinach, Switzerland) using the two search engines Mascot and SequestHT (Table S1). The PfHP1-GFP IP replicate samples 1 and 2 were additionally searched against the PfHP1-GFP sequence (Table S1). The PfCK2 and PfGSK3 ADP-Glo™ *in vitro* kinase assay samples were searched against the respective PfHP1 and PfCD.H recombinant protein sequences (Table S2). For the search, oxidized methionine, N-terminal protein acetylation and phosphorylation on serine, threonine and tyrosine were used as variable modifications. The identifications were filtered for a false discovery rate of 1%.

Generation of *E. coli* expression vectors

In order to increase the solubility strength of the SUMO tag, sequences encoding additional solubility tags were inserted upstream of the sequence encoding an N-terminal 6xHis-SUMO tag as suggested elsewhere (Malakhov et al., 2004). For this purpose, the His-SUMO-encoding sequence was PCR amplified from pETA-HS (Fraschka et al., 2018) using the primers Bsa_His_f and T7term. The *Bsa*I/*Xho*I-digested product was then cloned into *BamH*I/*Xho*I-cut pGB1 (a kind gift of S. Hiller) and pETA-MBP (Bertschi et al., 2017), yielding the GB1-His-SUMO (pETA-GHS) and MBP-His-SUMO (pETA-MHS) expression vectors, respectively. Two gene fragments were amplified from 3D7 genomic DNA; full-length *pfhp1* (using primers HP1_F and HP1_Xho_R) and a truncated version encoding the CD and hinge domains only (PfCD.H: M1-T181 (using primers HP1_F and CDH_Xho_R). *Xho*I-digested PCR products were ligated into

*Sfo*I/*Xho*I-cut expression vectors; full-length *pfhp1* was cloned into pETA-MHS and *pfcd.h* into pETA-GHS. All primer sequences are listed in Table S3.

Expression and purification of recombinant PfHP1

Both recombinant proteins were expressed in *E. coli* Rosetta2 (DE3) cells (Novagen) using auto-induction at 22°C in ZYM-5052 medium (Studier, 2005). Expression cultures were spun down at 4°C and the pellets were kept at -20°C. Both recombinant proteins were purified using nickel affinity (A), followed by dextrin affinity (MHS-HP1 only) (B) and tag removal (C). PfCD.H was further purified using hydrophobic interaction chromatography (HIC) (D). Both proteins were polished using gel filtration (E). All affinity columns used were produced by GE Healthcare. (A) Nickel affinity. *E. coli* pellets were resuspended in buffer N-A (50 mM H_3PO_4, 20 mM imidazole, 500 mM NaCl, 5 mM EACA and NaOH to pH 7.4) and lysed by sonication. The lysates were loaded on 1 ml HisTrap columns, washed with 20 column volumes (CV) of the same buffer and eluted using N-B (50 mM H_3PO_4, 225 mM imidazole, 500 mM NaCl, 5 mM EACA). For full length HP1, 2 M urea was included in the lysis buffer. The nickel eluate containing PfCD.H was buffer exchanged to subtraction buffer (0.75x concentrated N-A complemented with 10% glycerol, 1 mM TCEP and additional 125 mM NaCl) using three 5 ml HiTrap desalting columns. (B) Dextrin affinity (MHS-HP1 only). The protein was eluted from the nickel column directly on a 5 ml MBPTrap HP column placed below the HisTrap column. After elution, the nickel column was removed and the MBPTrap column was washed with 5 CV of N-A and eluted with N-A containing 2 M urea, 10 mM maltose and 1 mM TCEP. (C) Tag removal. The GHS and MHS tags were cleaved off using recombinantly expressed SUMO protease (L403-K621 of *S. cerevisiae* ULP1; expressed as GB1-ULP1-6xHis fusion and purified by nickel affinity and gel filtration) in a ratio of 1:200 and incubated for 1.5 hours at 16°C. In order to subtract the tag, the protease and other contaminants, the digest was passed through a HisTrap column. In the case of full-length HP1, guanine-HCl was added to a final concentration of 1 M for this step. (D) HIC (PfCD.H only). Ammonium sulfate from a 4 M stock (pH adjusted to 7 using NH_4OH) was added to the protein sample to 1.5 M and this mixture was loaded on a 1 ml Phenyl HP column equilibrated in buffer HIC (1.5 M ammonium sulfate, 5 mM EACA, 0.5 mM EDTA, 20 mM H_3PO_4-KOH, pH 6.8, and 10% Glycerol). The column was washed with 20 CV of the same buffer and the protein eluted using a 25 CV long linear gradient, from 1.5 M to 0 M ammonium sulfate. (E) Gel filtration. PfCD.H was polished using 10 mM MOPS-KOH, pH 7, 100 mM NaCl, 10% glycerol buffer and a Superdex75 10/300 GL column. For full-length HP1, a HiLoad 26/60 Superdex 200

column was prepared in three steps: first, it was equilibrated in storage buffer (20 mM MOPS-KOH, pH 7, 0.5 M NaCl, 10 % glycerol). Then, a gradient (1/10th CV) from storage buffer to refolding buffer (20 mM MOPS-KOH, pH 7, 800 mM arginine, 267 mM citric acid) was loaded to the column, and finally a second gradient (1/8th CV), from refolding buffer to buffer N-A containing 2 M urea and 1 M guanine-HCl was loaded. As a result, the protein passed first through refolding and later through storage buffer. Both proteins were concentrated using Amicon spin filter (Millipore) with a 10K cut-off and stored at -80°C. Their purity and concentration were determined by SDS-PAGE and NanoDrop™ 2000/2000c spectrophotometer with UV extinction coefficients calculated by protparam (https://web.expasy.org/protparam/).

***In vitro* kinase assays**

Purified recombinant *P. falciparum* kinases were prepared as described for PfCK2 (Holland et al., 2009), PfGSK3 (Droucheau et al., 2004) and PfMAP2, PfNEK2, PfNEK4, PfPK6 (Van Voorhis et al., 2016). The ADP-Glo™ *in vitro* kinase assay was performed in duplicates according to the manufacturer`s instructions (Promega, USA). The exact amount of recombinant kinase (0.6-7 µg) and PfHP1 or PfCD.H (1.8-5.8 µg) substrates used in each reaction is indicated in the corresponding figures. 10 µg of either histone from calf thymus, bovine myelin basic protein (MBP) or β-casein from bovine milk (Sigma-Aldrich) were used as positive controls. 5 µl out of 25 µl of the kinase reactions were used for the final ATP depletion and detection steps. The remaining reaction volume was used for LC-MS/MS analysis to identify phosphosites (see above).

The γ-P^{32}-ATP *in vitro* kinase assays were performed in a standard 25 µl reaction in kinase buffer (20 mM Tris HCl pH 7.5, 20 mM $MgCl_2$, 2 mM $MnCl_2$, 10 mM glycerolphosphate and 10 mM NaF) containing 10 µM ATP, 5 µCi γ-P^{32}-ATP (3000 Ci/mmol, Amersham Biosciences), substrates (5.4 µg PfHP1, 5.8 µg PfCD.H, 10 µg β-casein, 10 µg calf thymus histone, or 5 µg MBP) and recombinant kinases (0.5 µg PfCK2 or 0.6 µg PfGSK3). In the assay using PfCK2, 20 µM of 4,5,6,7-tetrabromobenzimidazole (TBB) in DMSO was use as a specific CK2 inhibitor (Holland et al., 2009; Sarno et al., 2001). The reactions were carried out for 30 min at 30 °C and stopped by the addition of Laemmli buffer. The samples were analyzed by SDS-polyacrylamide gel electrophoresis followed by autoradiography.

Transfection constructs

We applied CRISPR/Cas9-mediated genome editing and the DiCre/LoxP system (Collins et al., 2013; Jones et al., 2016) to generate parasite lines for the conditional

expression of PfHP1-GFP phosphomutants. We engineered (1) 3D7/N31DC_PfHP1-3M (3D7/HP1-3M) for expression of the S122/125/129A PfHP1 mutant; (2) 3D7/N31DC_PfHP1-HIM (3D7/HP1-HIM) for expression of the S89/92/122/125/129/136/174A PfHP1 mutant; and (3) 3D7/N31DC_PfHP1-Control (3D7/HP1-Control) for expression of wild type PfHP1-GFP. To obtain these cell lines we performed two subsequent transfection steps.

In the primary transfection, we generated the mother cell line 3D7-1G5DC/5'-loxPint-g31 (3D7/N31DC), which carries a *sera2* intron:loxP element (Jones et al., 2016) inserted into the 5' end of the *pfhp1* coding sequence. To achieve this, we constructed the pHF-gC-guide31 plasmid by inserting two annealed complementary oligonucleotides (F-g31 and R-g31) encoding the sgRNA target sequence and containing appropriate single-stranded overhangs into the *Bsa*I-digested pHF-gC SpCas9 plasmid (Filarsky et al., 2018) using T4 DNA ligase. The sgRNA target sequence (5'-ATTTATTTAGTAAAATGGAA-3') is positioned at bps +70 to +89 within the *pfhp1* coding sequence and was identified using the CHOPCHOP web tool (http://chopchop.cbu.uib.no) (Labun et al., 2016; Montague et al., 2014). The donor plasmid pFdon-N31 was generated by Gibson assembly joining four PCR fragments encoding (1) the pFdon plasmid backbone (Filarsky et al., 2018) digested with *Sal*I and *EcoR*I; (2) the 103 bp fragment encoding the *sera2* intron:loxP fragment amplified from pD_SIP2xGFP plasmid (I. Niederwieser, unpublished) using primers F139 and R143; (3) a 5' homology region (5' HR) spanning bps -490 upstream of the start codon to +87 in the *pfhp1* coding sequence amplified from 3D7 gDNA using primers F147 and R145; and (4) a 3' HR spanning bps +88 to +756 of the *pfhp1* coding sequence amplified from 3D7 gDNA using primers F146 and R144 (the *pfhp1* coding sequence is 798 bps long). For transfection, 50 µg of each plasmid (pHF-gC-guide31 and pFdon-N31) were mixed and co-electroporated into DiCre-expressing 3D7/1G5DC parasites (Collins et al., 2013). Transfected parasites were selected with 4 nM WR99210 for six days and then cultured in absence of drug selection until transgenic populations were established.

In the second step, 3D7/N31DC parasites were transfected again to generate parasite lines 3D7/HP1-3M, 3D7/HP1-HIM and 3D7/HP1-Control that carry a second *sera2* intron:loxP sequence directly downstream of the endogenous *pfhp1* STOP codon, followed by a recodonised mutated (HP1-3M and HP1-HIM) or wild type (HP1-Control) *pfhp1-gfp* sequence using the following cloning steps. First, we constructed the pBF-gC-guide250 plasmid by inserting two annealed complementary oligonucleotides (F-g250 and R-g250) encoding the sgRNA target sequence at the 3' end of the *pfhp1*

coding sequence and appropriate single-stranded overhangs into the *Bsa*I-digested pBF-gC SpCas9 plasmid (Filarsky et al., 2018) using T4 DNA ligase. The sgRNA target sequence (5'-AAAAAATTTAAGAGTTCCTG-3') is positioned at bps +751 to +770 within the *pfhp1* coding sequence (negative strand) and was identified using CHOPCHOP (http://chopchop.cbu.uib.no). Second, we constructed the three donor plasmids. The pD-HP1-Control plasmid was constructed by Gibson assembly joining two PCR fragments. The first fragment was amplified from the plasmid pD-PfHP1-KO (see Supplementary Methods) using primers F162 and R143 and contains, in the following order, the *gpf* coding sequence ending with a STOP codon, a 3' HR spanning the 824 bps directly downstream of the *pfhp1* STOP codon, the pD plasmid backbone (Brancucci et al., 2017), a 5' HR spanning bps +88 to +798 of the *pfhp1* coding sequence carrying eight synonymous mutations between bps +757 to +798 (see Supplementary Methods) and ending with a STOP codon followed by the 103 bp *sera2* intron:loxP element. The second PCR fragment was amplified from a plasmid containing a synthetic recodonized *pfhp1* sequence (pUC57-re-*pfhp1*) (GenScript™) (see Figure S3 and Supplementary Methods) using primers F164 and R165 and spans bps +88 to +798 of the *pfhp1* coding sequence omitting the STOP codon.

The pD-HP1-3M plasmid was constructed by Gibson assembly joining four PCR fragments encoding (1) the 5' HR spanning bps +88 to +798 of the *pfhp1* coding sequence ending with a STOP codon followed by the 103 bp *sera2* intron:loxP element and bps +88 to +384 of the recodonised *pfhp1* sequence amplified from the pD-PfHP1-Control plasmid using primers F158 and R168, the latter of which introduces the S122/125A mutations into PfHP1; (2) a fragment spanning bps +367 to +798 of the recodonised *pfhp1* sequence amplified from pUC57-re-*pfhp1* (GenScript™) using primers F91 and R165, the former of which introduces the S125/129A mutations into PfHP1; (3) the *gfp* coding sequence ending with a STOP codon followed by the 3' HR amplified from the pFdon-C-loxP-g250 vector (see Supplementary Methods) using primers F162 and R163; and (4) the pD plasmid backbone amplified from pUC19 using primers PCRA_F and PCRA_R (Brancucci et al., 2017).

Finally, the pD-HP1-HIM plasmid was constructed in a two-step process. First, a fragment containing, in the following order, bps +88 to +798 of the recodonised *pfhp1* sequence encoding the S89/92/122/125/129/136/174A mutations followed by the *gfp* sequence ending with a stop codon and the 3' HR was generated by Gibson assembly joining four fragments encoding (1) bps +88 to +280 of recodonised *pfhp1* amplified from pD-PfHP1-Control using primers F164 and R172, the latter of which introduces the

S89/92A mutations; (2) bps +261 to +409 of the recodonised *pfhp1* sequence amplified from pD-PfHP1-3M (containing the S122/125/129A mutations) using primers F171 and R174, the former of which introduces the S89/92A mutations and the latter of which introduces the S136A mutation; (3) bps +390 to +535 of the recodonised *pfhp1* sequence amplified from pD-PfHP1-Control using primers F173 and R176, the former of which introduces the S136A mutation and the latter of which introduces the S174A mutation; and (4) a fragment containing, in the following order, bps +520 to +798 of the recodonised *pfhp1* sequence, the *gfp* coding sequence ending with a STOP codon and 3' HR amplified from pD-PfHP1-Control using primers F175 and R163, the former of which introduces the S174A mutation. Second, the resulting fragment from the first step was used as template for a second round of PCR amplification using primers F164 and R163 and subjected to a second Gibson assembly joining with two other PCR fragments, namely the pD plasmid backbone amplified from pUC19 using primers PCRA_F and PCRA_R (Brancucci et al., 2017), and a fragment containing the 5' HR followed by the *sera2* intron:lox P amplified from the pD-PfHP1-Control using primers F158 and R143.

For each of the three transfections, 50 µg of the pBF-gC-guide250 plasmid was mixed with 50 µg of either pD-PfHP1-Control, pD-PfHP1-3M or pD-PfHP1-HIM and transfected by electroporation into the 3D7/N31DC parasite line as described above. Transfected parasites were selected with 5 µg/ml BSD-S-HCl for 10 days and then cultured in absence of drug pressure until transgenic populations were established. All oligonucleotide sequences used for the cloning of the CRISPR/Cas9 and donor plasmids are provided in Table S3. The nucleotide sequence of recodonized *pfhp1* is provided in Figure S3.

Nucleic acid isolation and diagnostic PCRs and reverse transcription PCRs

To confirm correct editing of the *pfhp1* locus we performed PCRs using the KAPA HiFi HotStart enzyme (Roche Sequencing Store) on gDNA isolated from the transgenic cell lines. To evaluate the excision efficiency after rapamycin treatment, diagnostic PCRs were performed on gDNA isolated 24-36 hours post rapamycin treatment (Knuepfer et al., 2017). To evaluate the splicing efficiency of the *sera 2* intron:loxP from the *pfhp1* open reading frame, total RNA from the 3D7/N31DC mother cell line and the rapamycin-treated phosphomutant cell lines were isolated using Ribozol (Amresco) according to the manufacturer's instruction. cDNA was then synthesized using oligo(dT) primers (RetroScript, Invitrogen) and PCRs on cDNA were performed using

primers F106 and R107 that amplify the entire coding sequence. All transfection plasmids generated in this study have been validated by Sanger sequencing. All transfection plasmids have been designed and Sanger sequencing results analysed using the SnapGene software (from GSL Biotech; available at snapgene.com). All primer sequences used for PCR are listed in Table S3.

Induction of DiCre recombinase-mediated DNA excision by rapamycin treatment

Parasites were synchronized twice 16 hours apart to obtain an eight-hour growth window (16-24 hpi). After re-invasion parasites were synchronized again at 0-8 hpi (generation 1) and split into two equal populations, one of which was treated with 0.02% v/v of DMSO (negative control) and the other half was treated with 100 nM rapamycin for 1 hour (Knuepfer et al., 2017). The cultures were then spun down, washed with an equal volume of culture medium, resuspended in culture medium and returned to culture.

SDS-PAGE and immunoblotting

After DMSO or rapamycin treatment in generation 1, parasites were allowed to complete schizogony and re-invasion. At 16-24 hpi in generation 2, parasites were released from infected RBCs (iRBCs) by 0.15% saponin/PBS complemented with 1X protease inhibitor (Roche Diagnostics). After washing 2-3 times in ice-cold PBS, parasite pellets were lysed in 70°C pre-heated Urea/SDS buffer (8 M Urea, 5% SDS, 50 mM Bis-Tris, 2 mM EDTA, 25 mM HCl at pH 6.5 supplemented with 2 mM DTT and 1X protease inhibitor). Whole parasite protein lysates were separated on NuPage 4-12% Bis-Tris gels (Novex) and analyzed by Western blot using mouse mAb α-GFP (Roche Diagnostics #11814460001), 1:1000; rabbit α-PfHP1 (Brancucci et al., 2014), 1:5'000; rabbit α-Histone 4 (Abcam ab10158), 1:10'000.

Live cell imaging and indirect immunofluorescence assay (IFA)

To quantify the efficiency of *pfhp1* excision after rapamycin treatment, live cell fluorescence microscopy was performed as described before (Witmer et al., 2012) with minor modifications using Hoechst (Merck) at a final concentration of 5 µg/ml to stain the nuclei. Excision efficiency was determined as the percentage of GFP-positive schizonts at 40-48 hpi in generation 1 (>100 schizonts counted per experiment). IFAs were performed on methanol-fixed cells using mouse IgG1 mAb α-ATS (Duffy et al., 2002), 1:150; and Alexa Fluor 488-conjugated α-mouse IgG (Molecular Probes), 1:250. Images were taken at 63-fold magnification on a Leica DM 5000B microscope with a

Leica DFC 300 FX camera, acquired via the Leica IM 1000 software, processed using ImageJ software (https://imagej.nih.gov/ij). For each experiment, images were acquired and processed with identical settings.

Parasite multiplication assay

Parasites were tightly synchronized twice 16 hours apart, split into two equal populations after re-invasion at 0-8 hpi (generation 1), of which one half was treated with DMSO (negative control) and the other half was induced for DiCre recombinase-mediated DNA excision by rapamycin treatment as described above. Giemsa smears were prepared to determine the parasitaemia at 16-24 hpi (generation 1). Giemsa-stained smears were prepared every second day onwards for three generations. Parasitaemia was counted by visual inspection of Giemsa-stained blood smears (>3'000 RBCs counted per experiment). Multiplication rates were determined as the parasitaemia observed in the following generation divided by the parasitaemia observed in the previous generation. The extrapolative growth curve was generated using a starting parasiteamia at 0.1%.

Gametocyte conversion assay

Parasites were tightly synchronized twice 16 hours apart and split into two equal populations after re-invasion at 0-8 hpi (generation 1), of which one half was treated with DMSO (negative control) and the other half was induced for DiCre recombinase-mediated DNA excision by rapamycin treatment as described above. At 16-24 hpi in the subsequent generation (day 1 of gametocytogenesis), cultures were treated with 50 mM N-acetyl-D-glucosamine (GlcNAc) for six days to eliminate asexual parasites (Fivelman et al., 2007; Ponnudurai et al., 1986) and then cultured with normal culture medium for another 4-6 days to observe gametocyte maturation. Gametocytaemia was determined on day 6 by visual inspection of Giemsa-stained blood smears. Sexual conversion rates were determined as the gametocytaemia observed on day 6 as a proportion of the total parasitaemia observed on day 1.

Acknowledgements

We are grateful to Mike Blackman and the Edinburgh Malaria Reagent Repository (http://www.malariaresearch.eu/) for providing the 3D7/1G5DiCre parasite line. This work was supported by the Swiss National Science Foundation (grant numbers 31003A_143916 and grant and 31003A_163258). I.S.L acknowledges support from the

Walter and Eliza Hall Institute of Medical Research and from the National Health and Medical Research Council for Operational Infrastructure Support (IRIISS 9000433).

Author contributions

H.T.N.B. designed and performed experiments, analysed data, prepared illustrations and wrote the paper. I.N. designed and performed experiments related to recombinant expression of PfHP1. N.M.B.B. performed sexual conversion assays. M.J.B, W.D. together with H.T.N.B performed the *in vitro* kinase assay. S.M. performed LC-MS/MS experiments. P.J., I.S.L. and C.D. supervised experiments and provided resources and conceptual advice. T.S.V. conceived of the study, designed, supervised, and analysed experiments, provided resources and wrote the paper. All authors contributed to editing of the manuscript.

Figure 1. Identification of phosphorylated residues in PfHP1. (A) Upper panel: silver-stained SDS-PAGE gel of protein samples from a PfHP1-GFP immunoprecipitation (IP) experiment using nuclear extracts from 3D7/HP1-GFP parasites and GFP-Trap®_A beads. Lower panel: Western blot analysis of the IP samples using a-PfHP1 antibodies showing the presence of PfHP1-GFP in the input and elution samples. FT, flow through; W1-W5, wash 1-5; E1/E2, eluates 1 and 2. **(B)** Overview of all phosphosites (yellow circles) identified in PfHP1, either in this study by LC-MS/MS of immunopurified native PfHP1-GFP or in other proteomics studies (Collins et al., 2014; Filarsky et al., 2018; Lasonder et al., 2012; Lasonder et al., 2015; Pease et al., 2013; Solyakov et al., 2011; Treeck et al., 2011). Phosphosites identified here and in at least one previous study are highlighted in red letters, those identified only in previous studies are highlighted in black letters, and the phosphosite exclusively identified here (S206) is highlighted by a green letter. Helices and ß-sheets predicted by the secondary structure prediction tool JPred4 (http://www.compbio.dundee.ac.uk/jpred4/index.html) (Drozdetskiy et al., 2015) are indicated by orange and green boxes, respectively. The approximate boundaries of the CD (brown), hinge domain (grey) and CSD (pink) are indicated (Flueck et al., 2009). Numbers refer to amino acid positions in the PfHP1 sequence.

Figure 2. PfCK2 phosphorylates PfHP1 and *in vitro*. (A) Coomassie-stained SDS-PAGE gel showing the purified recombinant PfHP1 and PfCD.H proteins. **(B)** *In vitro* ADP-Glo™ assay results reveal that PfCK2 phosphorylates PfHP1 and PfCD.H *in vitro*. The percentage of ADP converted back into ATP (y-axis) is a surrogate measure for kinase activity (i.e. the relative amount of ATP consumed in the kinase reaction). β-casein was included as a positive control substrate for PfCK2. Recombinant PfHP1 and PfCD.H in absence of PfCK2 were used as negative controls. Values represent the average of two replicate reactions. Error bars represent SD. **(C)** Coomassie-stained SDS-PAGE gel (top) and corresponding autoradiogram (bottom) of the *in vitro* γ-P^{32}-ATP PfCK2 kinase assay performed with recombinant PfHP1 and PfCD.H substrates. β-casein was used as a positive control substrate. 20 µM TBB was used as a specific inhibitor of PfCK2 (Holland et al., 2009; Sarno et al., 2001).

Figure 3. Generation of DiCre-inducible PfHP1 phosphomutants. (A) Schematics of the CRISPR/Cas9-edited *pfhp1* loci (left panel) and corresponding PfHP1 protein products (right panel) expressed in the 3D7/N31DC mother line (top) and the 3D7/HP1-3M,

3D7/HP1-HIM and 3D7/HP1-Control parasites (bottom) before (DMSO) and after (RAP) rapamycin-induced DiCre-dependent excision of the wild type *pfhp1* locus. HR, homology regions used for homology-directed repair of Cas9-induced DNA double-strand breaks. Blue arrowheads indicate the position of *sera2* intron:loxP elements (Jones et al., 2016). Red asterisks indicate STOP codons. Blue asterisks indicate the relative position of serine-to-alanine substitutions in the PfHP1 hinge region in the 3D7/HP1-3M and 3D7/HP1-HIM phosphomutants. Orange and blue boxes represent the wild type and recodonised *pfhp1*/PfHP1 sequences, respectively. Numbers in the gene and protein schematics refer to nucleotide and amino acid positions, respectively. The black arrowheads indicate the binding sites of the F119 and R157 primers used to confirm correct editing of the *pfhp1* locus and efficient DiCre-mediated excision upon rapamycin treatment by PCR on gDNA (see Figure 3B below). **(B)** PCR on gDNA confirms the correctly edited *pfhp1* loci and efficient excision of the endogenous *pfhp1* gene after rapamycin treatment in 3D7/HP1-3M, 3D7/HP1-HIM and 3D7/HP1-Control parasites. Using primers F119 and R157 (see Figure 3A) the correctly edited *pfhp1* locus delivers a PCR product of 3781 bps in the 3D7/HP1-3M (left panel), 3D7/HP1-HIM (middle panel) and 3D7/HP1-Control line (right panel). In the 3D7/N31DC mother line (i.e. prior to the insertion of a recodonised *pfhp1-gfp* fusion gene) this PCR reaction delivers a 2250 bps fragment (right panel). Correct excision of the endogenous *pfhp1* gene in rapamycin-treated 3D7/HP1-3M, 3D7/HP1-HIM and 3D7/HP1-Control parasites results in a decrease of the size of the PCR fragment from 3781 bps to 2964 bps. Primers targeting the *cg6* control locus (PF3D7_0709200) have been used as control. RAP, rapamycin. **(C)** The efficiency of DiCre-mediated excision of the endogenous *pfhp1* gene and resulting expression of the recodonised PfHP1-GFP fusion proteins has been quantified by counting the number of GFP-positive parasites in paired control (DMSO) and rapamycin-treated (RAP) populations in late schizont stages (40-48 hpi) (40 hrs after rapamycin treatment). Values represent the mean of three (3D7/HP1-HIM) and four (3D7/HP1-3M and 3D7/HP1-Control) independent biological replicate experiments (>100 iRBCs scored for each population). Error bars indicate SD. **(D)** Western blot showing the expression of endogenous untagged PfHP1 and recodonised PfHP1-GFP in the progeny of DMSO- and rapamycin-treated 3D7/HP1-3M, 3D7/HP1-HIM and 3D7/HP1-Control parasites (16-24 hpi, generation 2) (64 hrs after rapamycin treatment). α-histone 4 (H4) antibodies were used as loading control. RAP, rapamycin.

Figure 4. Sub-nuclear localization of PfHP1 phosphomutants. (A) Representative live cell fluorescence images showing the localization of the GFP-tagged PfHP1-3M and PfHP1-HIM phosphomutants and the PfHP1-Control protein in late schizonts (LS, 40-48 hpi, generation 1; 40 hrs after rapamycin treatment) and after re-invasion in the progeny at late ring stage (LR, 16-24 hpi, generation 2; 64 hrs after rapamycin treatment). Nuclei were stained with Hoechst. DIC, differential interference contrast. Scale bar, 5 µm.

Figure 5. Phenotypes of PfHP1 phosphomutants. (A) Growth curves of the control (DMSO) and rapamycin-treated (RAP) PfHP1-GFP phosphomutants and control line over three generations of intra-erythrocytic replication. Values are the mean of four (3D7/HP1-3M and 3D7/HP1-Control) and six (3D7/HP1-HIM) independent replicate experiments. Error bars represent SD. **(B)** Sexual conversion rates of DMSO- and rapamycin-treated (RAP) PfHP1-GFP phosphomutants, the PfHP1-Control line, the 3D7/1G5DiCre mother line and 3D7 wild type parasites. Values represent the mean of four (3D7/HP1-3M and 3D7/HP1-Control), six (3D7/HP1-HIM) and three (3D7/1G5DiCre and 3D7 wild type) independent replicate experiments. Error bars represent SD. Asterisks indicate significant differences in sexual conversion rates between RAP-treated and DMSO-treated parasites ($p<0.01$; unpaired two-tailed Student`s t-test). **(C)** Representative images showing PfEMP1 expression in control (DMSO) and rapamycin-treated (RAP) PfHP1-GFP phosphomutants and control line in the late ring stage progeny (LR, 16-24 hpi, generation 2; 64 hrs after rapamycin treatment) as determined by IFA using a-ATS antibodies recognizing the conserved ATS domain of PfEMP1 (Duffy et al., 2002). The percentage of PfEMP1-positive iRBCs are indicated for each population. Values represent the mean of two independent experiments (+/- SD) (3D7/HP1-3M and 3D7/HP1-Control) and a single experiment (3D7/HP1-HIM). Nuclei were stained with DAPI. DIC, differential interference contrast. Scale bar, 5 µm.

Figure 1

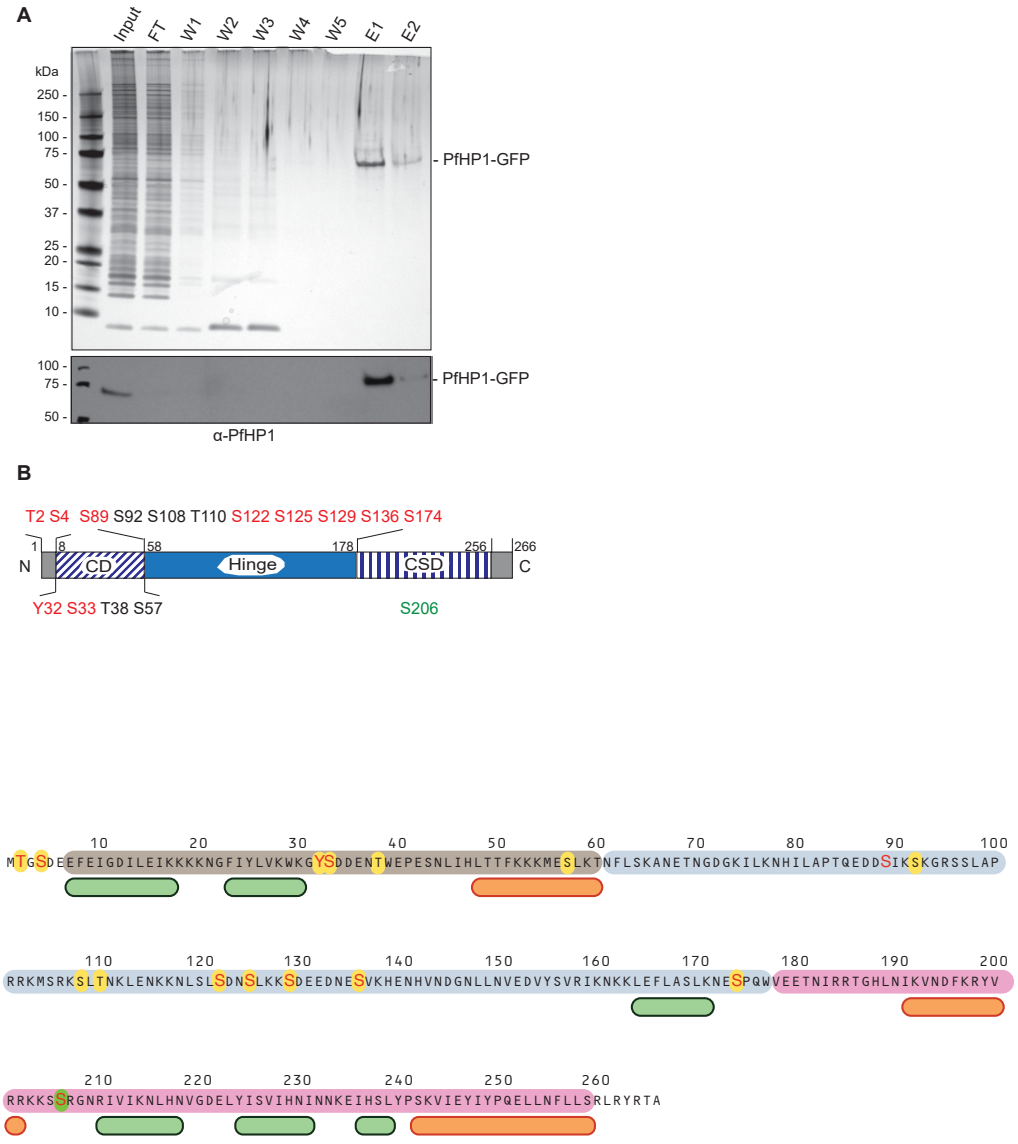
A
Input
FT
W1
W2
W3
W4
W5
E1
E2
kDa
250 -
150 -
100 -
75 -
50 -
37 -
25 -
20 -
15 -
10 -
- PfHP1-GFP
100 -
75 -
50 -
- PfHP1-GFP
α-PfHP1
B
T2 S4 S89 S92 S108 T110 S122 S125 S129 S136 S174
1
8
58
178
256
266
N
CD
Hinge
CSD
C
Y32 S33 T38 S57
S206
10 20 30 40 50 60 70 80 90 100
MTGSDEEFEIGDILEIKKKKNGFIYLVKWKGYSDDENTWEPESNLIHLTTFKKKMESLKTNFLSKANETNGDGKILKNHILAPTQEDDSIKSKGRSSLAP
110 120 130 140 150 160 170 180 190 200
RRKMSRKSLTNKLENKKNLSLSDNSLKKSDEEDNESVKHENHVNDGNLLNVEDVYSVRIKNKKLEFLASLKNESPQWVEETNIRRTGHLNIKVNDFKRYV
210 220 230 240 250 260
RRKKSSRGNRIVIKNLHNVGDELYISVIHNINNKEIHSLYPSKVIEYIYPQELLNFLLSRLRYRTA

Figure 2

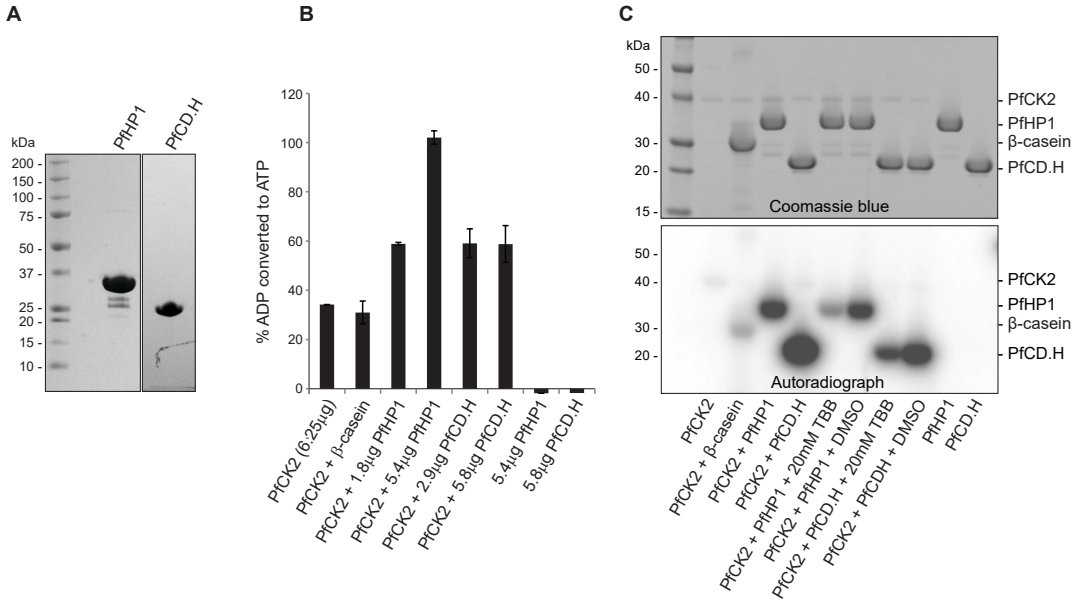
A
kDa
PfHP1
PfCD.H
200 -
150 -
100 -
75 -
50 -
37 -
25 -
20 -
15 -
10 -
B
% ADP converted to ATP
120
100
80
60
40
20
0
PfCK2 (6.25µg)
PfCK2 + β-casein
PfCK2 + 1.8µg PfHP1
PfCK2 + 5.4µg PfHP1
PfCK2 + 2.9µg PfCD.H
PfCK2 + 5.8µg PfCD.H
5.4µg PfHP1
5.8µg PfCD.H
C
kDa
50 -
40 -
30 -
20 -
15 -
PfCK2
PfHP1
β-casein
PfCD.H
Coomassie blue
Autoradiograph
PfCK2
PfCK2 + β-casein
PfCK2 + PfHP1
PfCK2 + PfCD.H
PfCK2 + PfHP1 + 20mM TBB
PfCK2 + PfHP1 + DMSO
PfCK2 + PfCD.H + 20mM TBB
PfCK2 + PfCDH + DMSO
PfHP1
PfCD.H

Figure 3

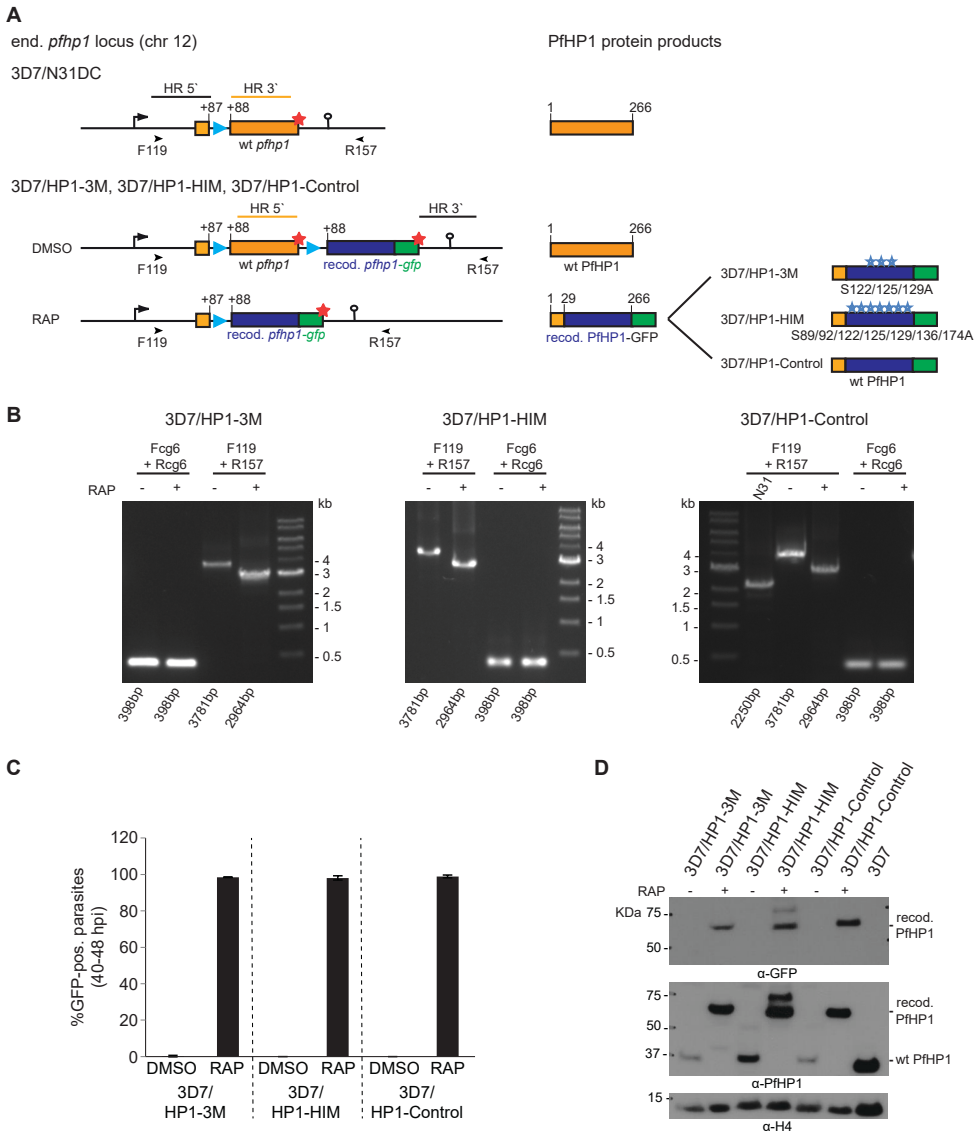
A
end. pfhp1 locus (chr 12)
3D7/N31DC
HR 5`
HR 3`
+87 +88
F119
wt pfhp1
R157
3D7/HP1-3M, 3D7/HP1-HIM, 3D7/HP1-Control
DMSO
RAP
recod. pfhp1-gfp
PfHP1 protein products
1
266
wt PfHP1
29
recod. PfHP1-GFP
3D7/HP1-3M
S122/125/129A
3D7/HP1-HIM
S89/92/122/125/129/136/174A
3D7/HP1-Control
B
3D7/HP1-3M
3D7/HP1-HIM
3D7/HP1-Control
Fcg6 + Rcg6
F119 + R157
RAP
kb
398bp
3781bp
2964bp
2250bp
C
%GFP-pos. parasites (40-48 hpi)
DMSO
RAP
3D7/ HP1-3M
3D7/ HP1-HIM
3D7/ HP1-Control
D
KDa
recod. PfHP1
α-GFP
wt PfHP1
α-PfHP1
α-H4

Figure 4

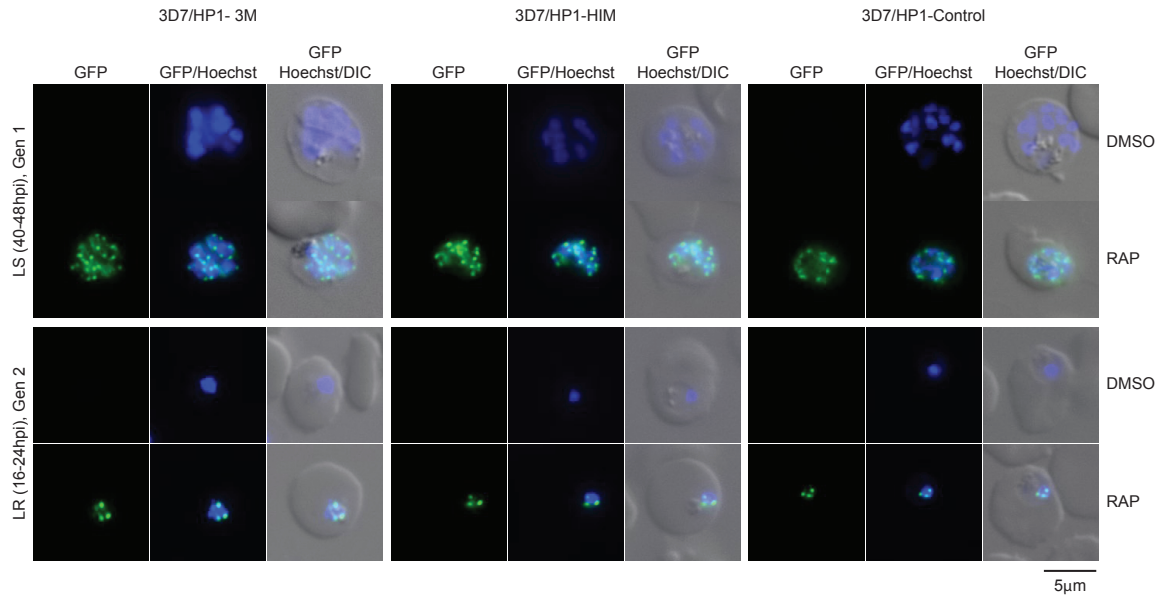
3D7/HP1- 3M
3D7/HP1-HIM
3D7/HP1-Control
GFP
GFP/Hoechst
GFP Hoechst/DIC
LS (40-48hpi), Gen 1
LR (16-24hpi), Gen 2
DMSO
RAP
DMSO
RAP
5µm

Figure 5

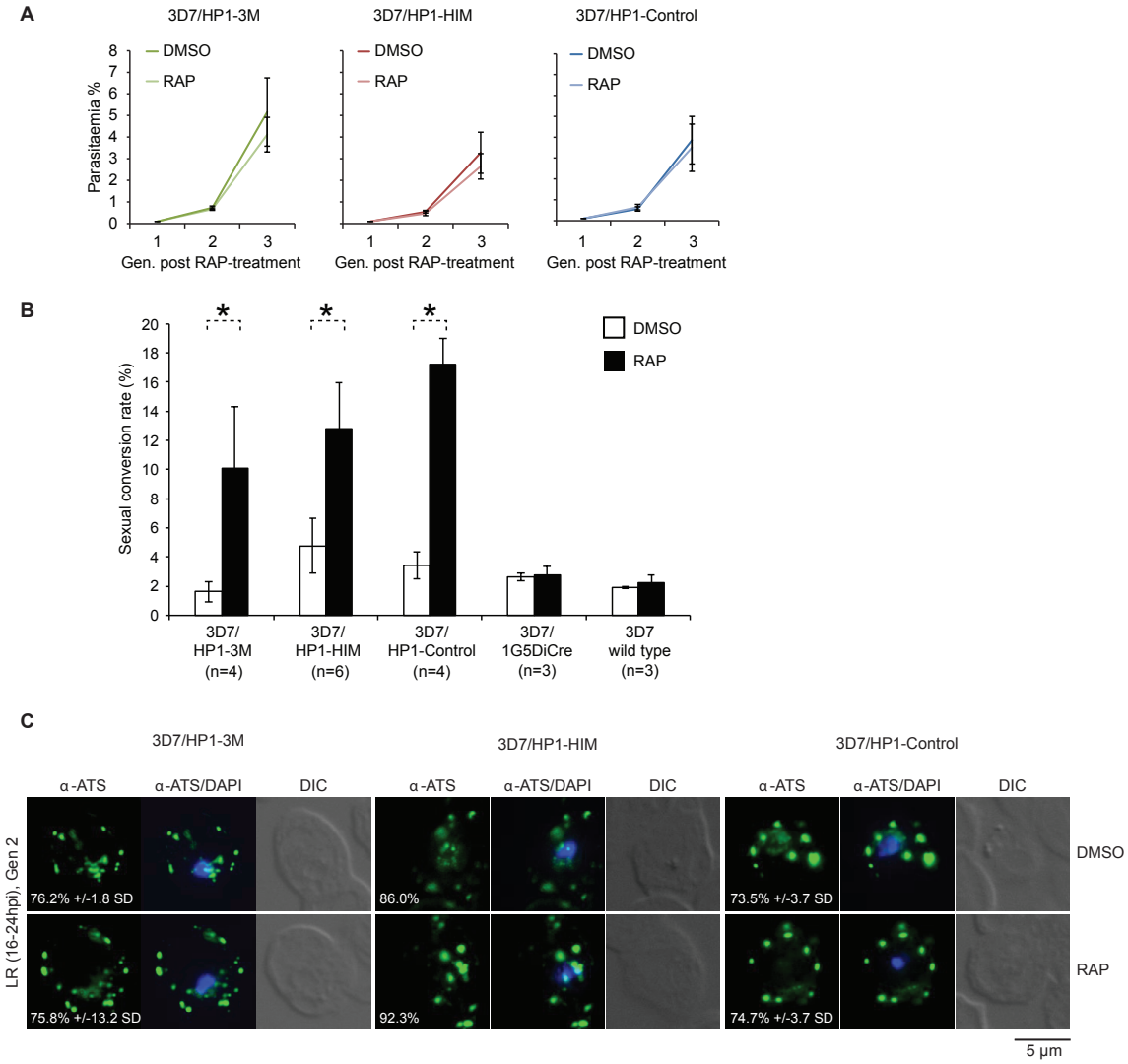
A
3D7/HP1-3M
3D7/HP1-HIM
3D7/HP1-Control
DMSO
RAP
Parasitaemia %
Gen. post RAP-treatment
B
Sexual conversion rate (%)
3D7/ HP1-3M (n=4)
3D7/ HP1-HIM (n=6)
3D7/ HP1-Control (n=4)
3D7/ 1G5DiCre (n=3)
3D7 wild type (n=3)
C
α-ATS
α-ATS/DAPI
DIC
LR (16-24hpi), Gen 2
76.2% +/-1.8 SD
86.0%
73.5% +/-3.7 SD
75.8% +/-13.2 SD
92.3%
74.7% +/-3.7 SD
5 µm

2.6 References

Amanchy, R., Periaswamy, B., Mathivanan, S., Reddy, R., Tattikota, S.G., and Pandey, A. (2007). A curated compendium of phosphorylation motifs. Nat Biotechnol *25*, 285-286.

Armstrong, C.M., and Goldberg, D.E. (2007). An FKBP destabilization domain modulates protein levels in Plasmodium falciparum. Nat Methods *4*, 1007-1009.

Ayoub, N., Jeyasekharan, A.D., Bernal, J.A., and Venkitaraman, A.R. (2008). HP1-beta mobilization promotes chromatin changes that initiate the DNA damage response. Nature *453*, 682-686.

Badugu, R., Yoo, Y., Singh, P.B., and Kellum, R. (2005). Mutations in the heterochromatin protein 1 (HP1) hinge domain affect HP1 protein interactions and chromosomal distribution. Chromosoma *113*, 370-384.

Banaszynski, L.A., Chen, L.C., Maynard-Smith, L.A., Ooi, A.G., and Wandless, T.J. (2006). A rapid, reversible, and tunable method to regulate protein function in living cells using synthetic small molecules. Cell *126*, 995-1004.

Bannister, A.J., Zegerman, P., Partridge, J.F., Miska, E.A., Thomas, J.O., Allshire, R.C., and Kouzarides, T. (2001). Selective recognition of methylated lysine 9 on histone H3 by the HP1 chromo domain. Nature *410*, 120-124.

Baruch, D.I., Pasloske, B.L., Singh, H.B., Bi, X., Ma, X.C., Feldman, M., Taraschi, T.F., and Howard, R.J. (1995). Cloning the P. falciparum gene encoding PfEMP1, a malarial variant antigen and adherence receptor on the surface of parasitized human erythrocytes. Cell *82*, 77-87.

Bertschi, N.L., Toenhake, C.G., Zou, A., Niederwieser, I., Henderson, R., Moes, S., Jenoe, P., Parkinson, J., Bartfai, R., and Voss, T.S. (2017). Malaria parasites possess a telomere repeat-binding protein that shares ancestry with transcription factor IIIA. Nat Microbiol *2*, 17033.

Bian, Y., Ye, M., Wang, C., Cheng, K., Song, C., Dong, M., Pan, Y., Qin, H., and Zou, H. (2013). Global screening of CK2 kinase substrates by an integrated phosphoproteomics workflow. Scientific reports *3*, 3460.

Bracchi-Ricard, V., Barik, S., Delvecchio, C., Doerig, C., Chakrabarti, R., and Chakrabarti, D. (2000). PfPK6, a novel cyclin-dependent kinase/mitogen-activated protein kinase-related protein kinase from Plasmodium falciparum. Biochem J *347 Pt 1*, 255-263.

Brancucci, N.M.B., Bertschi, N.L., Zhu, L., Niederwieser, I., Chin, W.H., Wampfler, R., Freymond, C., Rottmann, M., Felger, I., Bozdech, Z.*, et al.* (2014). Heterochromatin protein 1 secures survival and transmission of malaria parasites. Cell Host Microbe *16*, 165-176.

Brancucci, N.M.B., Gerdt, J.P., Wang, C., De Niz, M., Philip, N., Adapa, S.R., Zhang, M., Hitz, E., Niederwieser, I., Boltryk, S.D.*, et al.* (2017). Lysophosphatidylcholine Regulates Sexual Stage Differentiation in the Human Malaria Parasite Plasmodium falciparum. Cell *171*, 1532-1544 e1515.

Brasher, S.V., Smith, B.O., Fogh, R.H., Nietlispach, D., Thiru, A., Nielsen, P.R., Broadhurst, R.W., Ball, L.J., Murzina, N.V., and Laue, E.D. (2000). The structure of mouse HP1 suggests a unique mode of single peptide recognition by the shadow chromo domain dimer. EMBO J *19*, 1587-1597.

Chakraborty, A., Prasanth, K.V., and Prasanth, S.G. (2014). Dynamic phosphorylation of HP1alpha regulates mitotic progression in human cells. Nat Commun *5*, 3445.

Chakraborty, A., and Prasanth, S.G. (2014). Phosphorylation-dephosphorylation cycle of HP1alpha governs accurate mitotic progression. Cell Cycle *13*, 1663-1670.

Collins, C.R., Das, S., Wong, E.H., Andenmatten, N., Stallmach, R., Hackett, F., Herman, J.P., Muller, S., Meissner, M., and Blackman, M.J. (2013). Robust inducible Cre recombinase activity in the human malaria parasite Plasmodium falciparum enables efficient gene deletion within a single asexual erythrocytic growth cycle. Mol Microbiol *88*, 687-701.

Collins, M.O., Wright, J.C., Jones, M., Rayner, J.C., and Choudhary, J.S. (2014). Confident and sensitive phosphoproteomics using combinations of collision induced dissociation and electron transfer dissociation. J Proteomics *103*, 1-14.

Cowieson, N.P., Partridge, J.F., Allshire, R.C., and McLaughlin, P.J. (2000). Dimerisation of a chromo shadow domain and distinctions from the chromodomain as revealed by structural analysis. Curr Biol *10*, 517-525.

Daubenberger, C.A., Tisdale, E.J., Curcic, M., Diaz, D., Silvie, O., Mazier, D., Eling, W., Bohrmann, B., Matile, H., and Pluschke, G. (2003). The N'-terminal domain of glyceraldehyde-3-

phosphate dehydrogenase of the apicomplexan Plasmodium falciparum mediates GTPase Rab2-dependent recruitment to membranes. Biol Chem *384*, 1227-1237.

Deitsch, K.W., and Dzikowski, R. (2017). Variant Gene Expression and Antigenic Variation by Malaria Parasites. Annu Rev Microbiol *71*, 625-641.

Doble, B.W., and Woodgett, J.R. (2003). GSK-3: tricks of the trade for a multi-tasking kinase. J Cell Sci *116*, 1175-1186.

Dorin, D., Alano, P., Boccaccio, I., Ciceron, L., Doerig, C., Sulpice, R., Parzy, D., and Doerig, C. (1999). An atypical mitogen-activated protein kinase (MAPK) homologue expressed in gametocytes of the human malaria parasite Plasmodium falciparum. Identification of a MAPK signature. J Biol Chem *274*, 29912-29920.

Droucheau, E., Primot, A., Thomas, V., Mattei, D., Knockaert, M., Richardson, C., Sallicandro, P., Alano, P., Jafarshad, A., Baratte, B.*, et al.* (2004). Plasmodium falciparum glycogen synthase kinase-3: molecular model, expression, intracellular localisation and selective inhibitors. Biochim Biophys Acta *1697*, 181-196.

Drozdetskiy, A., Cole, C., Procter, J., and Barton, G.J. (2015). JPred4: a protein secondary structure prediction server. Nucleic Acids Res *43*, W389-394.

Duffy, M.F., Brown, G.V., Basuki, W., Krejany, E.O., Noviyanti, R., Cowman, A.F., and Reeder, J.C. (2002). Transcription of multiple var genes by individual, trophozoite-stage Plasmodium falciparum cells expressing a chondroitin sulphate A binding phenotype. Mol Microbiol *43*, 1285-1293.

Filarsky, M., Fraschka, S.A., Niederwieser, I., Brancucci, N.M.B., Carrington, E., Carrio, E., Moes, S., Jenoe, P., Bartfai, R., and Voss, T.S. (2018). GDV1 induces sexual commitment of malaria parasites by antagonizing HP1-dependent gene silencing. Science *359*, 1259-1263.

Fiol, C.J., Wang, A., Roeske, R.W., and Roach, P.J. (1990). Ordered multisite protein phosphorylation. Analysis of glycogen synthase kinase 3 action using model peptide substrates. J Biol Chem *265*, 6061-6065.

Fivelman, Q.L., McRobert, L., Sharp, S., Taylor, C.J., Saeed, M., Swales, C.A., Sutherland, C.J., and Baker, D.A. (2007). Improved synchronous production of Plasmodium falciparum gametocytes in vitro. Mol Biochem Parasitol *154*, 119-123.

Flueck, C., Bartfai, R., Volz, J., Niederwieser, I., Salcedo-Amaya, A.M., Alako, B.T., Ehlgen, F., Ralph, S.A., Cowman, A.F., Bozdech, Z.*, et al.* (2009). Plasmodium falciparum heterochromatin protein 1 marks genomic loci linked to phenotypic variation of exported virulence factors. PLoS Pathog *5*, e1000569.

Fraschka, S.A., Filarsky, M., Hoo, R., Niederwieser, I., Yam, X.Y., Brancucci, N.M.B., Mohring, F., Mushunje, A.T., Huang, X., Christensen, P.R.*, et al.* (2018). Comparative Heterochromatin Profiling Reveals Conserved and Unique Epigenome Signatures Linked to Adaptation and Development of Malaria Parasites. Cell Host Microbe *23*, 407-420.

Gardner, M.J., Hall, N., Fung, E., White, O., Berriman, M., Hyman, R.W., Carlton, J.M., Pain, A., Nelson, K.E., Bowman, S.*, et al.* (2002). Genome sequence of the human malaria parasite Plasmodium falciparum. Nature *419*, 498-511.

Grewal, S.I., and Moazed, D. (2003). Heterochromatin and epigenetic control of gene expression. Science *301*, 798-802.

Grzenda, A., Leonard, P., Seo, S., Mathison, A.J., Urrutia, G., Calvo, E., Iovanna, J., Urrutia, R., and Lomberk, G. (2013). Functional impact of Aurora A-mediated phosphorylation of HP1gamma at serine 83 during cell cycle progression. Epigenetics & chromatin *6*, 21.

Guizetti, J., and Scherf, A. (2013). Silence, activate, poise and switch! Mechanisms of antigenic variation in Plasmodium falciparum. Cell Microbiol *15*, 718-726.

Hiragami-Hamada, K., Shinmyozu, K., Hamada, D., Tatsu, Y., Uegaki, K., Fujiwara, S., and Nakayama, J. (2011). N-terminal phosphorylation of HP1{alpha} promotes its chromatin binding. Mol Cell Biol *31*, 1186-1200.

Hoeijmakers, W.A., Flueck, C., Francoijs, K.J., Smits, A.H., Wetzel, J., Volz, J.C., Cowman, A.F., Voss, T., Stunnenberg, H.G., and Bartfai, R. (2012). Plasmodium falciparum centromeres display a unique epigenetic makeup and cluster prior to and during schizogony. Cell Microbiol *14*, 1391-1401.

Holland, Z., Prudent, R., Reiser, J.B., Cochet, C., and Doerig, C. (2009). Functional analysis of protein kinase CK2 of the human malaria parasite Plasmodium falciparum. Eukaryot Cell *8*, 388-397.

Hviid, L., and Jensen, A.T. (2015). PfEMP1, A Parasite Protein Family of Key Importance in Plasmodium falciparum Malaria Immunity and Pathogenesis. Adv Parasitol *88*, 51-84.

Jacobs, S.A., Taverna, S.D., Zhang, Y., Briggs, S.D., Li, J., Eissenberg, J.C., Allis, C.D., and Khorasanizadeh, S. (2001). Specificity of the HP1 chromo domain for the methylated N-terminus of histone H3. EMBO J *20*, 5232-5241.

Jones, M.L., Das, S., Belda, H., Collins, C.R., Blackman, M.J., and Treeck, M. (2016). A versatile strategy for rapid conditional genome engineering using loxP sites in a small synthetic intron in Plasmodium falciparum. Sci Rep 6, 21800.

Knuepfer, E., Napiorkowska, M., van Ooij, C., and Holder, A.A. (2017). Generating conditional gene knockouts in Plasmodium - a toolkit to produce stable DiCre recombinase-expressing parasite lines using CRISPR/Cas9. Scientific reports *7*, 3881.

Kwon, S.H., and Workman, J.L. (2008). The heterochromatin protein 1 (HP1) family: put away a bias toward HP1. Mol Cells *26*, 217-227.

Kwon, S.H., and Workman, J.L. (2011). The changing faces of HP1: From heterochromatin formation and gene silencing to euchromatic gene expression: HP1 acts as a positive regulator of transcription. Bioessays *33*, 280-289.

Labun, K., Montague, T.G., Gagnon, J.A., Thyme, S.B., and Valen, E. (2016). CHOPCHOP v2: a web tool for the next generation of CRISPR genome engineering. Nucleic Acids Res *44*, W272-W276.

Lachner, M., O'Carroll, D., Rea, S., Mechtler, K., and Jenuwein, T. (2001). Methylation of histone H3 lysine 9 creates a binding site for HP1 proteins. Nature *410*, 116-120.

Lambros, C., and Vanderberg, J.P. (1979). Synchronization of Plasmodium falciparum erythrocytic stages in culture. J Parasitol *65*, 418-420.

Lasonder, E., Green, J.L., Camarda, G., Talabani, H., Holder, A.A., Langsley, G., and Alano, P. (2012). The Plasmodium falciparum schizont phosphoproteome reveals extensive phosphatidylinositol and cAMP-protein kinase A signaling. J Proteome Res *11*, 5323-5337.

Lasonder, E., Green, J.L., Grainger, M., Langsley, G., and Holder, A.A. (2015). Extensive differential protein phosphorylation as intraerythrocytic Plasmodium falciparum schizonts develop into extracellular invasive merozoites. Proteomics *15*, 2716-2729.

Lomberk, G., Wallrath, L., and Urrutia, R. (2006). The Heterochromatin Protein 1 family. Genome Biol *7*, 228.

Lopez-Rubio, J.J., Mancio-Silva, L., and Scherf, A. (2009). Genome-wide analysis of heterochromatin associates clonally variant gene regulation with perinuclear repressive centers in malaria parasites. Cell Host Microbe *5*, 179-190.

Malakhov, M.P., Mattern, M.R., Malakhova, O.A., Drinker, M., Weeks, S.D., and Butt, T.R. (2004). SUMO fusions and SUMO-specific protease for efficient expression and purification of proteins. J Struct Funct Genomics *5*, 75-86.

Meehan, R.R., Kao, C.F., and Pennings, S. (2003). HP1 binding to native chromatin in vitro is determined by the hinge region and not by the chromodomain. EMBO J *22*, 3164-3174.

Meggio, F., Marin, O., and Pinna, L.A. (1994). Substrate specificity of protein kinase CK2. Cell Mol Biol Res *40*, 401-409.

Montague, T.G., Cruz, J.M., Gagnon, J.A., Church, G.M., and Valen, E. (2014). CHOPCHOP: a CRISPR/Cas9 and TALEN web tool for genome editing. Nucleic Acids Res *42*, W401-W407.

Muchardt, C., Guilleme, M., Seeler, J.S., Trouche, D., Dejean, A., and Yaniv, M. (2002). Coordinated methyl and RNA binding is required for heterochromatin localization of mammalian HP1alpha. EMBO Rep *3*, 975-981.

Munari, F., Gajda, M.J., Hiragami-Hamada, K., Fischle, W., and Zweckstetter, M. (2014). Characterization of the effects of phosphorylation by CK2 on the structure and binding properties of human HP1beta. FEBS Lett *588*, 1094-1099.

Pease, B.N., Huttlin, E.L., Jedrychowski, M.P., Talevich, E., Harmon, J., Dillman, T., Kannan, N., Doerig, C., Chakrabarti, R., Gygi, S.P.*, et al.* (2013). Global analysis of protein expression and phosphorylation of three stages of Plasmodium falciparum intraerythrocytic development. J Proteome Res *12*, 4028-4045.

Perez-Toledo, K., Rojas-Meza, A.P., Mancio-Silva, L., Hernandez-Cuevas, N.A., Delgadillo, D.M., Vargas, M., Martinez-Calvillo, S., Scherf, A., and Hernandez-Rivas, R. (2009). Plasmodium falciparum heterochromatin protein 1 binds to tri-methylated histone 3 lysine 9 and is linked to mutually exclusive expression of var genes. Nucleic Acids Res *37*, 2596-2606.

Pinna, L.A. (2002). Protein kinase CK2: a challenge to canons. J Cell Sci *115*, 3873-3878.

Platero, J.S., Hartnett, T., and Eissenberg, J.C. (1995). Functional analysis of the chromo domain of HP1. EMBO J *14*, 3977-3986.

Ponnudurai, T., Lensen, A.H., Meis, J.F., and Meuwissen, J.H. (1986). Synchronization of Plasmodium falciparum gametocytes using an automated suspension culture system. Parasitology *93 (Pt 2)*, 263-274.

Reininger, L., Billker, O., Tewari, R., Mukhopadhyay, A., Fennell, C., Dorin-Semblat, D., Doerig, C., Goldring, D., Harmse, L., Ranford-Cartwright, L., *et al.* (2005). A NIMA-related protein kinase is essential for completion of the sexual cycle of malaria parasites. J Biol Chem *280*, 31957-31964.

Reininger, L., Tewari, R., Fennell, C., Holland, Z., Goldring, D., Ranford-Cartwright, L., Billker, O., and Doerig, C. (2009). An essential role for the Plasmodium Nek-2 Nima-related protein kinase in the sexual development of malaria parasites. J Biol Chem *284*, 20858-20868.

Rovira-Graells, N., Gupta, A.P., Planet, E., Crowley, V.M., Mok, S., Ribas de, P.L., Preiser, P.R., Bozdech, Z., and Cortes, A. (2012). Transcriptional variation in the malaria parasite Plasmodium falciparum. Genome Res *22*, 925-938.

Rusin, S.F., Adamo, M.E., and Kettenbach, A.N. (2017). Identification of Candidate Casein Kinase 2 Substrates in Mitosis by Quantitative Phosphoproteomics. Frontiers in cell and developmental biology *5*, 97.

Salcedo-Amaya, A.M., Hoeijmakers, W.A., Bartfai, R., and Stunnenberg, H.G. (2010). Malaria: could its unusual epigenome be the weak spot? Int J Biochem Cell Biol *42*, 781-784.

Sarno, S., Reddy, H., Meggio, F., Ruzzene, M., Davies, S.P., Donella-Deana, A., Shugar, D., and Pinna, L.A. (2001). Selectivity of 4,5,6,7-tetrabromobenzotriazole, an ATP site-directed inhibitor of protein kinase CK2 ('casein kinase-2'). FEBS Lett *496*, 44-48.

Scherf, A., Hernandez-Rivas, R., Buffet, P., Bottius, E., Benatar, C., Pouvelle, B., Gysin, J., and Lanzer, M. (1998). Antigenic variation in malaria: in situ switching, relaxed and mutually exclusive transcription of var genes during intra-erythrocytic development in Plasmodium falciparum. EMBO J *17*, 5418-5426.

Scherf, A., Lopez-Rubio, J.J., and Riviere, L. (2008). Antigenic variation in Plasmodium falciparum. Annu Rev Microbiol *62*, 445-470.

Schotta, G., Ebert, A., Krauss, V., Fischer, A., Hoffmann, J., Rea, S., Jenuwein, T., Dorn, R., and Reuter, G. (2002). Central role of Drosophila SU(VAR)3-9 in histone H3-K9 methylation and heterochromatic gene silencing. EMBO J *21*, 1121-1131.

Shimada, A., Dohke, K., Sadaie, M., Shinmyozu, K., Nakayama, J., Urano, T., and Murakami, Y. (2009). Phosphorylation of Swi6/HP1 regulates transcriptional gene silencing at heterochromatin. Genes Dev *23*, 18-23.

Shimada, A., and Murakami, Y. (2010). Dynamic regulation of heterochromatin function via phosphorylation of HP1-family proteins. Epigenetics *5*, 30-33.

Smith, J.D., Chitnis, C.E., Craig, A.G., Roberts, D.J., Hudson-Taylor, D.E., Peterson, D.S., Pinches, R., Newbold, C.I., and Miller, L.H. (1995). Switches in expression of Plasmodium falciparum var genes correlate with changes in antigenic and cytoadherent phenotypes of infected erythrocytes. Cell *82*, 101-110.

Solyakov, L., Halbert, J., Alam, M.M., Semblat, J.P., Dorin-Semblat, D., Reininger, L., Bottrill, A.R., Mistry, S., Abdi, A., Fennell, C., *et al.* (2011). Global kinomic and phospho-proteomic analyses of the human malaria parasite Plasmodium falciparum. Nat Commun *2*, 565.

St-Denis, N., Gabriel, M., Turowec, J.P., Gloor, G.B., Li, S.S., Gingras, A.C., and Litchfield, D.W. (2015). Systematic investigation of hierarchical phosphorylation by protein kinase CK2. J Proteomics *118*, 49-62.

Studier, F.W. (2005). Protein production by auto-induction in high density shaking cultures. Protein Expr Purif *41*, 207-234.

Su, X.Z., Heatwole, V.M., Wertheimer, S.P., Guinet, F., Herrfeldt, J.A., Peterson, D.S., Ravetch, J.A., and Wellems, T.E. (1995). The large diverse gene family var encodes proteins involved in cytoadherence and antigenic variation of Plasmodium falciparum-infected erythrocytes. Cell *82*, 89-100.

Sugimoto, K., Yamada, T., Muro, Y., and Himeno, M. (1996). Human homolog of Drosophila heterochromatin-associated protein 1 (HP1) is a DNA-binding protein which possesses a DNA-binding motif with weak similarity to that of human centromere protein C (CENP-C). J Biochem *120*, 153-159.

Tham, W.H., Lim, N.T., Weiss, G.E., Lopaticki, S., Ansell, B.R., Bird, M., Lucet, I., Dorin-Semblat, D., Doerig, C., Gilson, P.R., *et al.* (2015). Plasmodium falciparum Adhesins Play an Essential Role in Signalling and Activation of Invasion into Human Erythrocytes. PLoS Pathog *11*, e1005343.

Treeck, M., Sanders, J.L., Elias, J.E., and Boothroyd, J.C. (2011). The phosphoproteomes of Plasmodium falciparum and Toxoplasma gondii reveal unusual adaptations within and beyond the parasites' boundaries. Cell Host Microbe *10*, 410-419.

Van Voorhis, W.C., Adams, J.H., Adelfio, R., Ahyong, V., Akabas, M.H., Alano, P., Alday, A., Aleman, R.Y., Alsibaee, A., Alzualde, A., *et al.* (2016). Open Source Drug Discovery with the Malaria Box Compound Collection for Neglected Diseases and Beyond. PLoS Pathog *12*, e1005763.

Witmer, K., Schmid, C.D., Brancucci, N.M., Luah, Y.H., Preiser, P.R., Bozdech, Z., and Voss, T.S. (2012). Analysis of subtelomeric virulence gene families in Plasmodium falciparum by comparative transcriptional profiling. Mol Microbiol *84*, 243-259.

Zeng, W., Ball, A.R., Jr., and Yokomori, K. (2010). HP1: heterochromatin binding proteins working the genome. Epigenetics *5*, 287-292.

Zhao, T., and Eissenberg, J.C. (1999). Phosphorylation of heterochromatin protein 1 by casein kinase II is required for efficient heterochromatin binding in Drosophila. J Biol Chem *274*, 15095-15100.

2.7 Supplementary Information

This Supplementary Information includes:

Supplementary Methods

Figures S1 to S4

Tables S1 to S3

Supplementary Methods

Generation of the pFdon-C-loxP-g250 donor plasmid

The pFdon-C-loxP-g250 plasmid was constructed by Gibson assembly joining five DNA fragments. The first fragment represents the pFDon plasmid (Filarsky et al., 2018) digested with *Sal*I and *Eco*RI. The second fragment represents a *pfhp1* 5' HR spanning bps +88 to +798 omitting the stop codon and carrying eight synonymous mutations between bps +757 to +798 [(C→T)T(C→A)TTAAATTT(T→C)TTATTATCAAGA(C→T)TAAGATA(C→T)(C→A)G(T→A)AC AGC(T→G)], followed by 28 bps of the *sera2* intron:loxP element. This 5' HR was generated in a four-step PCR process. First, a PCR fragment containing six synonymous mutations within the region spanning bps +757 to + 790 of the *pfhp1* sequence (of which three are located within the sgRNA target sequence) was amplified from 3D7 gDNA using primers F133 and R138. This sequence was then used as template for a second round of amplification adding two more mutations within bps +792 to +798 of the *pfhp1* sequence followed by six bps of the *sera2* intron:loxP sequence (primers F133 and R138.1). The second sequence was then used as template for a third round of amplification adding nine more bps of the *sera2* intron:loxP sequence (primers F133 and R138.2). The third sequence was used as template for the final round of amplification to add in total 28 bps of the *sera2* intron:loxP sequence to serve as overhang for subsequent Gibson assembly (primers F133 and R138.3). The third fragment represents the *sera2* intron:loxP sequence followed by bps +1 to +356 of the *gpf* coding sequence amplified from the pD_SIP2xGFP plasmid (Igor Niederwieser, unpublished) using primers F139 and R148. The fourth fragment spans bps +336 to +714 of the *gfp* coding sequence ending with a stop codon and a Gibson assembly overhang amplified from the pD_SIP2xGFP plasmid (Igor Niederwieser, unpublished) using primers F149 and R136. The fifth and final fragment for Gibson assembly represents a *pfhp1* 3' HR spanning the 824 bps directly downstream of the stop codon amplified from 3D7 gDNA using primers F71 and R134. All oligonucleotide sequences used for the cloning of the pFdon-C-loxP-g250 plasmid are provided in Table S3.

Generation of the pD-PfHP1_KO donor plasmid

The pD-PfHP1-KO donor plasmid was constructed by Gibson assembly joining three PCR fragments encoding (1) the plasmid backbone pD amplified from pUC19 using

primers PCRA_F and PCRA_R (Brancucci et al., 2017), (2) a 5' HR spanning bps +88 to +798 of the *pfhp1* coding sequence ending with a stop codon carrying eight synonymous mutations within the region spanning bps +757 to +798 amplified from the pFdon-C-loxP-g250 plasmid (see above) using primers F158 and R159; and (3) a PCR product amplified from the pFdon-C-loxP-g250 plasmid using primers F139 and R163 and representing, in the following order, the 103 bp *sera2* intron:loxP element, the *gfp* coding sequence ending with a stop codon and a 3' HR sequence spanning 824 bps directly downstream of the *pfhp1* stop codon. All oligonucleotide sequences used for the cloning of the pD-PfHP1-KO plasmid are provided in Table S3.

Supplementary Figures

Figure S1. ADP Glo *in vitro* kinase assay results. Based on ADP-Glo™ kinase assays PfMAP2, PfPK6, PfNEK2 and PfNEK4 do not specifically phosphorylate PfHP1 and PfCD.H *in vitro*. The percentage of ADP converted back into ATP (y-axis) is a surrogate measure for kinase activity (i.e. the relative amount of ATP consumed in the kinase reaction). MBP was included as a positive control substrate for PfMAP2, PfPK6 and PfNEK2, β-casein was included as a positive control substrate for PfNEK4. Recombinant PfHP1 and PfCD.H in absence of recombinant kinases were used as negative controls. All kinases except PfNEK4 show substantial autophosphorylation activity. Values represent the results of a single experiment each.

Figure S2. PfGSK3 phosphorylates PfHP1 and PfCD.H *in vitro*. (A) ADP-Glo™ kinase assay. The percentage of ADP converted back into ATP (y-axis) is a surrogate measure for kinase activity (i.e. the relative amount of ATP consumed in the kinase reaction). Recombinant PfGSK3 showed strong autophosphorylation activity (column 1). Histones from calf thymus were used as positive control substrates (column 2). The addition of PfHP1 and PfCD.H increased the ATP consumption compared to addition of the control substrate (columns 3 to 6). Recombinant PfHP1 and PfCD.H in absence of PfGSK3 were used as negative controls (columns 7 and 8). The amount of PfGSK3 and substrates used in the assay is indicated. Values represent the results from two replicate reactions. Error bars represent SD. **(B)** γ-P^{32}-ATP kinase assay. Coomassie-stained gel (top) and corresponding autoradiogram (bottom) of the *in vitro* γ-P^{32}-ATP PfGSK3 kinase assay performed with recombinant PfHP1 and PfCD.H substrates. Recombinant PfGSK3 showed strong autophosphorylation activity (lanes 3-6).

Histones from calf thymus were used as positive control substrates (lane 4). PfGSK3 phosphorylated the control and the PfHP1 and PfCD.H test substrates (lanes 4-6). Recombinant PfHP1 and PfCD.H in absence of PfGSK3 were used as negative controls (lanes 1 and 2). 0.6 µg of PfGSK3 was used in each reaction.

Figure S3. Two-step CRISPR/Cas9-based gene editing strategy to generate DiCre-inducible PfHP1 phosphomutant cell lines. (A) First gene editing step: Schematic maps of the *pfhp1* locus (PF3D7_1220900) in 3D7/1G5DiCre parasites (Collins et al., 2013) (top), the co-transfected pFDon-N31 donor plasmid and pHF_gC-guide31 CRISPR/Cas9 transfection vector (center), and the modified *pfhp1* locus after CRISPR/Cas9-based gene editing in 3D7/N31DC parasites (bottom). The nucleotide positions of the sgt_*pfhp1-5'* sgRNA target sequence is indicated (chromosome 12 coordinates). The pFDon-N31 donor plasmid contains a 103 bp *sera2* intron:loxP element (light blue triangle) (Jones et al., 2016) flanked by two homology regions (HR) (orange, black) for homology-directed repair. The pHF_gC-guide31 plasmid contains expression cassettes for SpCas9 (dark grey), the sgRNA (purple) and the h*dhfr*-y*fcu* fusion selection marker (light grey-brown). Second gene editing step: Schematic maps of the *pfhp1* locus in 3D7/N31DC parasites (top), the co-transfected pD_HP1 donor plasmid (pD_HP1-Control is shown as an example) and pBF_gC-guide250 CRISPR/Cas9 transfection vector (center), and the modified *pfhp1* locus after CRISPR/Cas9-based gene editing in 3D7/HP1-3M, 3D7/HP1-HIM and 3D7/HP1-Control parasites (3D7/HP1-Control is shown as an example) (bottom). The nucleotide positions of the sgt_*pfhp1-3'* sgRNA target sequence is indicated (chromosome 12 coordinates). The pD_HP1 donor plasmids contain an assembly of the 103 bp *sera2* intron:loxP element (light blue triangle) (Jones et al., 2016) and the recodonised *pfhp1* sequence (dark blue) fused to *gfp* (green) flanked by two homology regions (HR) (orange, black) for homology-directed repair. The pBF_gC-guide250 plasmid contains expression cassettes for SpCas9 (dark grey), the sgRNA (purple) and the *bsd*-y*fcu* fusion selection marker (light grey-brown). Red stars represent STOP codons. Numbers refer to the nucleotide position within the *pfhp1* coding sequence. **(B)** Nucleotide sequences of the wild type (*pfhp1*) and recodonised (*pfhp1* re) *pfhp1* genes and amino acid sequence of PfHP1. Bases altered in the *pfhp1* re are highlighted in red letters. Numbers refer to the nucleotide position within the *pfhp1* coding sequence.

Figure S4. Confirmation of successful gene editing by PCR and Sanger sequencing. (A) Top: Schematic of the CRISPR/Cas9-edited *pfhp1* locus in the 3D7/N31DC mother line carrying a 103 bp *sera2* intron:loxP element (Jones et al., 2016) inserted into the 5' end of the gene. The homology regions (HR) used for homology-directed repair of the Cas9-induced DNA double-strand break are indicated. The blue arrowhead indicates the position of *sera2* intron:loxP element. The red asterisk indicates the STOP codon. Numbers refer to nucleotide positions within the *pfhp1* coding sequence. The black arrowheads indicate the binding sites of the primers used to confirm correct gene editing of the *pfhp1* locus by PCR on gDNA. Bottom: PCR on gDNA isolated from 3D7/N31DC parasites and 3D7/1G5DiCre control parasites (Collins et al., 2013) confirms the correctly edited *pfhp1* locus in the 3D7/N31DC mother line. Primer pairs F156/R143 and F139/R265 deliver PCR products only from the 3D7/N31DC but not from the parental 3D7/1G5DiCre line (note that F139 and R143 bind specifically to the *sera2* intron:loxP element). Using primers F156 and R265, the correctly edited *pfhp1* locus delivers a PCR product of 1893 bps in the 3D7/N31DC line and of 1790 bps in the parental 3D7/1G5DiCre line (i.e. prior to the insertion of the *sera 2* intron:loxP element). Primers targeting the *cg6* control locus (PF3D7_0709200) have been used as control. **(B)** Top: Schematic maps of the CRISPR/Cas9-edited *pfhp1* gene locus in the 3D7/N31DC mother line carrying a 103 bp *sera2* intron:loxP element (left) and the corresponding mRNA/cDNA sequence after splicing of the *sera2* intron:loxP element (right). The blue arrowhead indicates the position of *sera2* intron:loxP element. The red asterisk indicates the STOP codon. The black arrowheads indicate the binding sites of the F106 and R107 primers used to confirm splicing of the *sera2* intron:loxP element. Bottom left: PCR on gDNA and cDNA from 3D7/N31DC parasites confirms the correct splicing of the *sera2* intron:loxP element. The F106 and R107 primers bind up- and downstream of the *pfhp1* open reading frame and amplify a 1020 bp and 917 bp fragment from gDNA and cDNA, respectively. Bottom right: Sanger sequencing of PCR products amplified from gDNA and cDNA confirms the correct insertion of the *sera2* intron:loxP element into the *pfhp1* gene in 3D7/N31DC parasites and correct splicing of the *sera2* intron:loxP element, respectively. **(C)** Top: schematics of the CRISPR/Cas9-edited *pfhp1* locus in 3D7/HP1-3M parasites after rapamycin-induced DiCre-dependent replacement of endogenous wild type *pfhp1* with a recodonised mutated *pfhp1-3m-gfp* fusion gene and the corresponding mRNA/cDNA sequence after splicing of the *sera 2* intron:loxP element. The blue arrowhead indicates the position of *sera2* intron:loxP element. The red asterisk indicates the STOP codon. The blue asterisks

indicate the relative position of mutations encoding serine-to-alanine substitutions in the 3D7/HP1-3M phosphomutant. Orange and blue boxes represent the wild type and recodonised *pfhp1* sequences, respectively. The black arrowheads indicate the binding sites of the F106 and R107 primers used to confirm splicing of the *sera2* intron:loxP element. Bottom left: PCR on gDNA and cDNA from rapamycin-treated 3D7/HP1-3M parasites confirms the correct splicing of the *sera2* intron:loxP element. The F106 and R107 primers bind up- and downstream of the *pfhp1-gfp* open reading frame and amplify a 1734 bp and 1631 bp fragment from gDNA and cDNA, respectively. Bottom right: Sanger sequencing of the RT-PCR product amplified from cDNA from rapamycin-treated 3D7/HP1-3M parasites confirms the successful introduction of the mutations encoding the S122A/S125A/S129A substitutions in the 3D7/HP1-3M phosphomutant.

Figure S1

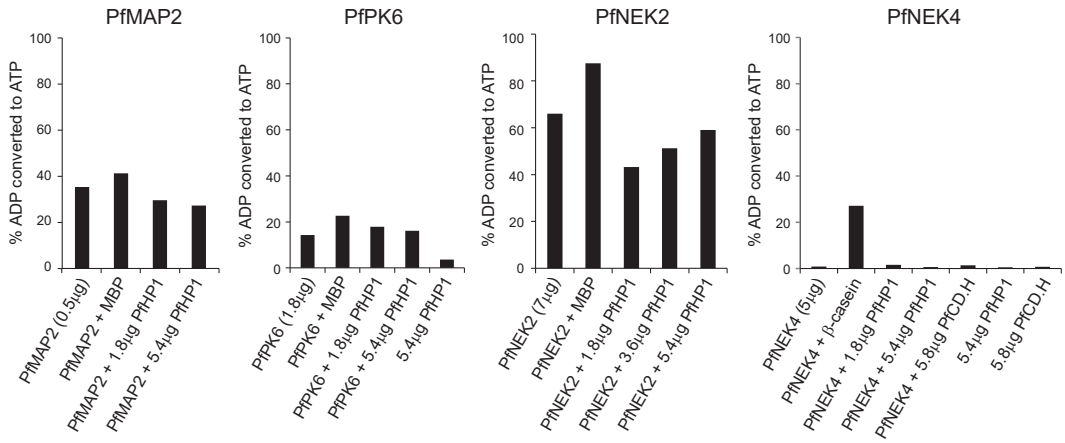
PfMAP2
PfPK6
PfNEK2
PfNEK4
% ADP converted to ATP
0
20
40
60
80
100
PfMAP2 (0.5µg)
PfMAP2 + MBP
PfMAP2 + 1.8µg PfHP1
PfMAP2 + 5.4µg PfHP1
PfPK6 (1.8µg)
PfPK6 + MBP
PfPK6 + 1.8µg PfHP1
PfPK6 + 5.4µg PfHP1
5.4µg PfHP1
PfNEK2 (7µg)
PfNEK2 + MBP
PfNEK2 + 1.8µg PfHP1
PfNEK2 + 3.6µg PfHP1
PfNEK2 + 5.4µg PfHP1
PfNEK4 (5µg)
PfNEK4 + β-casein
PfNEK4 + 1.8µg PfHP1
PfNEK4 + 5.4µg PfHP1
PfNEK4 + 5.8µg PfCD.H
5.4µg PfHP1
5.8µg PfCD.H

Figure S2

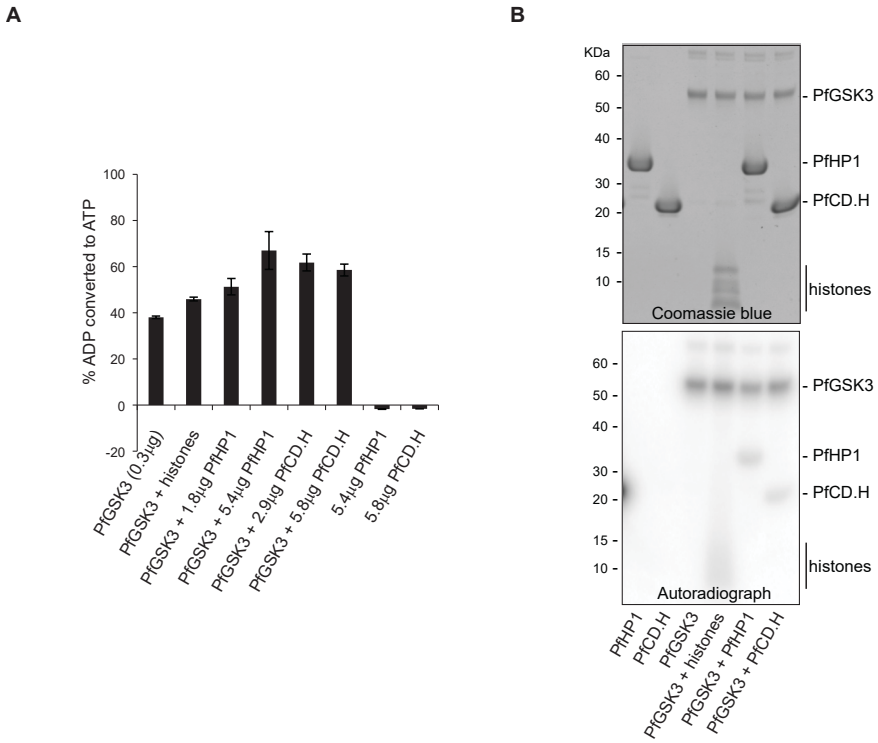
A
% ADP converted to ATP
100
80
60
40
20
0
-20
PfGSK3 (0.3µg)
PfGSK3 + histones
PfGSK3 + 1.8µg PfHP1
PfGSK3 + 5.4µg PfHP1
PfGSK3 + 2.9µg PfCD.H
PfGSK3 + 5.8µg PfCD.H
5.4µg PfHP1
5.8µg PfCD.H
B
KDa
60
50
40
30
20
15
10
- PfGSK3
- PfHP1
- PfCD.H
histones
Coomassie blue
Autoradiograph
PfHP1
PfCD.H
PfGSK3
PfGSK3 + histones
PfGSK3 + PfHP1
PfGSK3 + PfCD.H

Figure S3

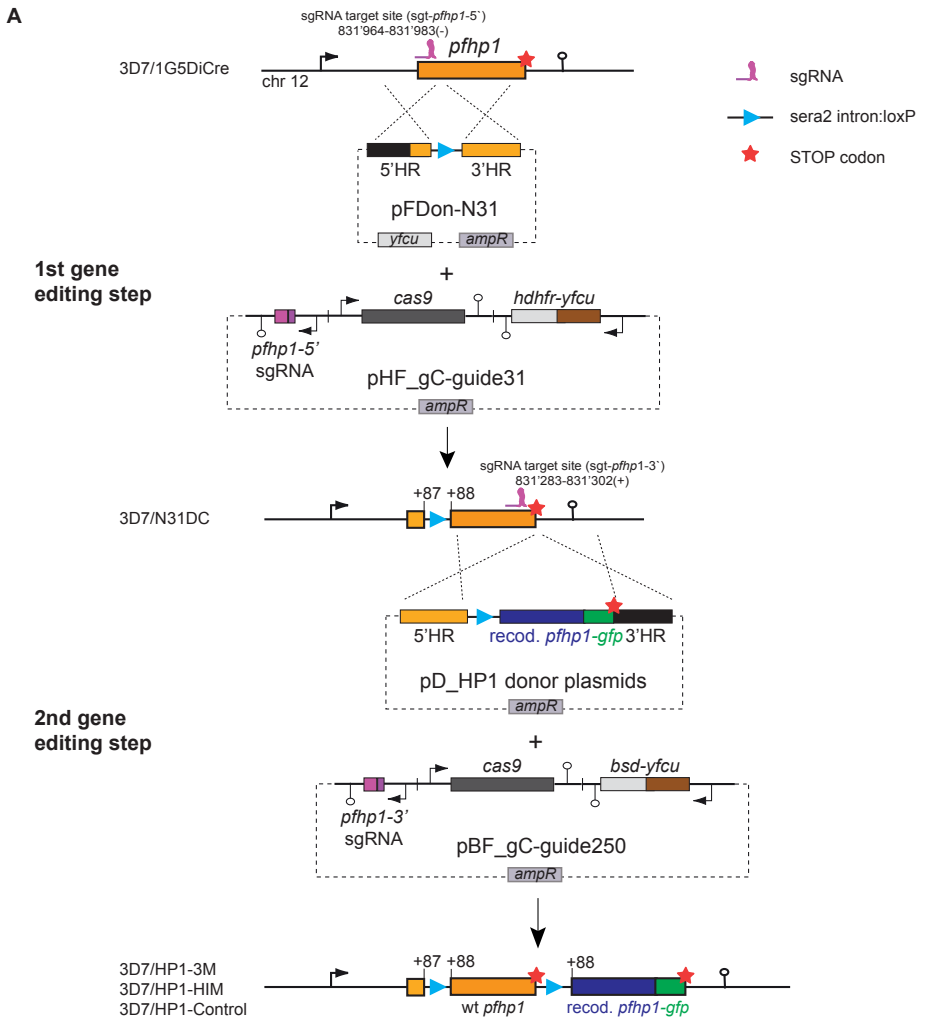

B

```
pfhp1      ATGACAGGGTCAGATGAAGAATTTGAAATTGGTGATATACTTGAAATAAAAAAAAAGAAGAATGGTTTTATTTATTTAGTAAAATGGAAAGGAT   94
             M  T  G  S  D  E  E  F  E  I  G  D  I  L  E  I  K  K  K  K  N  G  F  I  Y  L  V  K  W  K  G
pfhp1   re ATGACAGGTAGTGATGAAGAATTTGAAATTGG AGATATATTAGAAATTAAAAAGAAGAAAATGGTTTTAT CTACTTAGTAAAATGGAAAGGAT   94
pfhp1      ATTCAGATGATGAGAATACTTGGGAACCCGAAAGTAATTTAATACATTTGACAACATTTAAGAAAAAGATGGAAAGCTTAAAAACGAATTTTTT   188
             Y  S  D  D  E  N  T  W  E  P  E  S  N  L  I  H  L  T  T  F  K  K  K                    M  E  S  L  K  T  N  F  L
pfhp1   re ATAGTGATGATGAAATACATGGGAACCAGAATCAAATTT GATTCATTTGACAAC TTTTAA AAAGAAAATGGAATCATTAAAAAC AAATTT CTT   188
pfhp1      ATCGAAAGCTAATGAGACAAATGGTGATGGGAAAATTTTGAAAAATCATATATTAGCACCAACACAAGAAGACGATAGTATTAAATCAAAAGGT   282
             S  K  A  N  E  T  N  G  D  G  K  I  L  K  N  H  I                    L  A  P  T  Q  E  D  D  S  I  K  S  K  G
pfhp1   re ATCTAAAGCAAATGAAACAAATGGAGATGGTAAAATATT AAAGAATCATAT TTTAGC TCCAACACAAGAAGATGATAGTAT AAAATCAAAAGGT   282
pfhp1      AGAAGTTCCTTAGCACCCCGACGAAAAATGAGTAGAAAAAGTTTAACGAACAAACTAGAAAATAAAAAGAACTTATCTTTATCAGACAATTCTT   376
             R  S  S  L  A  P  R  R  K  M  S  R  K  S  L  T  N  K  L  E  N  K  K  N  L  S  L  S  D  N  S
pfhp1   re AGAAGTTC ATTAGCACC TAGAAGAAAAATGTC TAGAAAAAGTTTAAC AAATAAGTTAGAAAATAA GAAAAATTT GTC ATTATC TGAT AATTC AT   376
pfhp1      TAAAAAAAAGTGATGAAGAAGATAATGAATCTGTAAAACATGAGAATCACGTTAATGATGGAAATTTATTAAATGTTGAAGATGTATATAGCGT   470
             I  K  K  S  D  E  E  D  N  E  S  V  K  H  E  N  H  V  N  D  G  N  L  L                    N  V  E  D  V  Y  S  V
pfhp1   re TAAAGAAAAGTGATGAAGAAGATAATGAATCTGT TAAACATGAAAATCA TGTAAATGATGGAAATTT GTTAAATGT AGAAGATGTTTATAG TGT   470
pfhp1      TCGTATTAAAAATAAGAAATTGGAGTTTTTGGCTAGCTTGAAAAATGAATCTCCACAATGGGTAGAAGAAACAAATATTAGAAGAACTGGACAT   564
             R  I  K  N  K  K  L  E  F  L  A  S  L  K  N  E  S  P  Q  W  V  E  E  T  N  I  R  R  T                    G  H
pfhp1   re AAGAATTAAAAATAAGAAATT AGAATTTTT AGCTTCT TT AAAGAATGAAAGTCCACAATGGGT TGAAGAAACAAATATTAGAAGAACAGGTCAT   564
pfhp1      TTAAATATTAAAGTCAATGATTTTAAAAGATATGTAAGAAGAAAAAAAAGTTCTAGGGGTAATAGAATAGTTATCAAAAATCTACACAACGTTG   658
             L  N  I  K  V  N  D  F  K  R  Y  V  R  R  K  K  S  S  R  G  N  R  I  V  I  K  N  L  H  N  V
pfhp1   re TT GAATATTAAAGT TAATGATTTTAAAAGATATGT TAGAAGAAAGAAAAGTAGTAGAGGAAATAGAATAGT AATTAAAAATTTGCAT AATGTAG   658
pfhp1      GAGATGAATTATATATTTCGGTTATTCATAATATAAATAATAAAGAAATTCATAGTTTATATCCTTCCAAAGTTATTGAATATATTTATCCACA   752
             G  D  E  L  Y  I  S  V  I  H  N  I  N  N                    K  E  I  H  S  L  Y  P  S  K  V  I  E  Y  I  Y  P  Q
pfhp1   re GAGATGAATTATATAT AAGTGTTATTCATAATATAAATAATAA GGAAATTCATAGTTTATATCCTTC AAAAGTAATAGAATATAT ATATCC TCA   752
pfhp1      GGAACTCTTAAATTTTTTATTATCAAGACTAAGATACCGTACAGCT                                                   798
             E  L  L  N  F  L  L  S  R  L  R  Y  R  T  A
pfhp1   re AGAATTATTAAATTT CTTATT ATCAAGATTAAGATATAGAACAGCA                                                   798
```

Figure S4

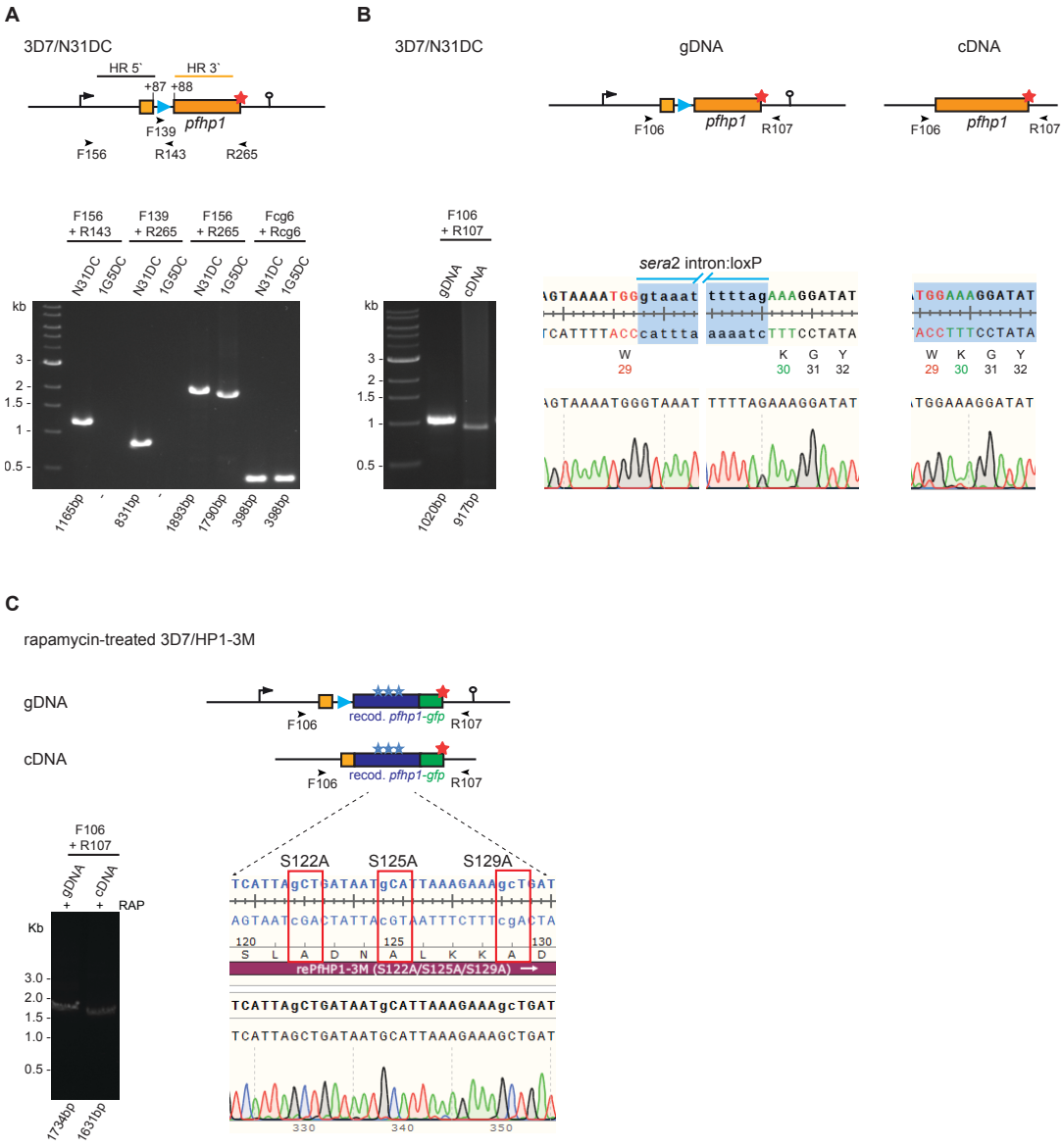
A
3D7/N31DC
HR 5`
HR 3`
+87 +88
pfhp1
F139
F156
R143
R265
F156 + R143
F139 + R265
F156 + R265
Fcg6 + Rcg6
N31DC
1G5DC
kb
3
2
1.5
1
0.5
1165bp
831bp
1893bp
1790bp
398bp
398bp
B
3D7/N31DC
gDNA
cDNA
F106
pfhp1
R107
F106 + R107
1020bp
917bp
sera2 intron:loxP
W 29
K 30
G 31
Y 32
C
rapamycin-treated 3D7/HP1-3M
gDNA
cDNA
recod. pfhp1-gfp
F106
R107
F106 + R107
+ gDNA
+ cDNA
RAP
Kb
3.0
2.0
1.5
1.0
0.5
1734bp
1631bp
S122A
S125A
S129A
rePfHP1-3M (S122A/S125A/S129A)
330
340
350

Supplementary Tables

Table S1. Mass spectrometry results of the PfHP1-GFP immunoprecipitation experiments (*Table not inserted into the thesis due to size. Data available on request (Gene Regulation Laboratory - Till S. Voss, Swiss TPH))*.

Table S2. Mass spectrometry results of the PfCK2 and PfGSK3 ADP-Glo™ *in vitro* kinase assays

(*Table not inserted into the thesis due to size. Data available on request (Gene Regulation Laboratory - Till S. Voss, Swiss TPH))*.

Table S3. List of all oligonucleotides used in this study.

Application	Oligo name	Sequence (5'-3')
Annealing	F-g31	TATTATTTATTTAGTAAAATGGAA
	R-g31	AAACTTCCATTTTACTAAATAAAT
	F-g250	TATTCATAATAAAATTAAGCTGTA
	R-g250	AAACCAGGAACTCTTAAATTTTTT
	R107	CTTATATAAATAAATTTACTACAG
	F119	GTGTGTGTTTAAGAAAAAATATG
	F156	GCAATAAGAAAAAAAATGGGAGG
	R157	CATGTAGCCAAAATATGTG
	R265	TATTCATAATAAAATTAAGCTGTA
	F-cg6	GTTCATGCTCCTCAACAAAG
	R-cg6	GAACAAATACATAAGAGCGC
PCR cloning transfection vectors	F71	TTTTATTATGCAAATATACATATATAC
	F91	GATAATGCATTAAAGAAAGCTGATGAAGAAGATAATGAATCTG
	F133	CAGTGAGCGAGGAAGCTTGTCGACAAAGGATATTCAGATGATGAG
	R134	CTTTTCTCTTGTGGATCCGAATTCGAGGTTAAAATTCTAAACTATATG
	R136	GTATATATGTATATTTGCATAATAAAATTATTTGTATAGTTCATCCATG
	R138	TATATCTTAATCTTGATAATAAGAAATTTAATAATTCCTGTGGATAAATATATTC
	R138.1	ATTTACCGCTGTTCTATATCTTAATCTTGATAATAAG
	R138.2	ATTTTTTTTATTTACCGCTGTTCTATATCTTAATC
	R138.3	GTTATTGTATATTATTTTTTTTATTTACCGCTGTTC
	F139	GTAAATAAAAAAAAATAATATACAATAAC
	R143	CTAAAAGAATATAAAATATATAAATAT
	R144	CTTTTCTCTTGTGGATCCGAATTCTTCCTGTGGATAAATATATTC
	R145	GTTATTGTATATTATTTTTTTTATTTACCCATTTTACTAAATAAATAAAAC
	F146	ATATTTATATATTTTATATTCTTTTAGAAAGGATATTCAGATGATGAG
	F147	CAGTGAGCGAGGAAGCTTGTCGACACACCCCCAAAAGGCCGA
	R148	AGGGTATCACCTTCAAACTTGACTTCAGCACGTGTCTTGTAG
	F149	CAAGTTTGAAGGTGATACCCT
	F158	CGTTGGCCGATTCATTAATGAAAGGATATTCAGATGATGAG
	R159	GTTATTGTATATTATTTTTTTTATTTACTTACGCTGTTCTATATCTTAATC
	F162	ATGAGTAAAGGAGAAGAAC
	R163	CCTCTTCGCTATTACGCCAGGAGGTTAAAATTCTAAACTATATG
	F164	ATATTTATATATTTTATATTCTTTTAGAAAGGATATAGTGATGATGA
	R165	GTTCTTCTCCTTTACTCATTGCTGTTCTATATCTTAATC
	R168	TTTCTTTAATGCATTATCAGCTAATGACAAATTTTTCTTATTTTC
	F171	TGATGCAATAAAAGCTAAAGGTAGAAGTTCATTAG
	R172	CTTTAGCTTTTATTGCATCATCTTCTTGTGTTGGAG
	F173	TGAAGAAGATAATGAAGCAGTTAAACATGAAAATCATGTAAATG
	R174	CTGCTTCATTATCTTCTTCATCAG

	F175	GCACCACAATGGGTTGAAGAAAC
	R176	CAACCCATTGTGGTGCTTCATTCTTTAAAGAAGCTAAAAATTC
	PCRA_F	CTGGCGTAATAGCGAAGAGG
	PCRA_R	CATTAATGAATCGGCCAACG
PCR cloning expression vectors	Bsa_His_f	AAGGTCTCGGATCTCATCATCATCATCATCACGGG
	T7term	TGCTAGTTATTGCTCAGCGG
	HP1_F	ATGACAGGCTCAGATGAAGAATTTGAAATTGG
	HP1_Xho_R	ATATTTGCATTCTCGAGTTAAGCTGTACGG
	CDH_Xho_R	GTTCCTCGAGTTTATGTTTCTTCTACCCATTGTGG

Chapter 3. In-depth functional analysis of heterochromatin protein 1 in *Plasmodium falciparum*

Hai T. N. Bui[1,2], Eilidh Carrington[1,2], Nicolas M. B. Brancucci[1,2], Till S. Voss[1,2,*]

[1]Department of Medical Parasitology and Infection Biology, Swiss Tropical and Public Health Institute, 4051 Basel, Switzerland

[2]University of Basel, 4003 Basel, Switzerland

[*]Corresponding author: till.voss@swisstph.ch

Manuscript in preparation

This chapter presents results that will form the major part of a future manuscript detailing the functional contribution and conservation of PfHP1 domains. I generated the cell lines and performed all experiments described in this chapter. I prepared the original manuscript and the figures. Till S. Voss edited the manuscript.

3.1 Abstract

The human malaria protozoan *Plasmodium falciparum* has a unique ortholog of heterochromatin protein 1, called PfHP1, which has been shown to cooperate in the regulation of various cellular processes through a sophisticated epigenetic mechanism. PfHP1 has been reported to play an important role in mitotic progression, transcriptional silencing of heterochromatin-associated genes and sexual differentiation. However, the precise functional contribution and conservation of each domain of PfHP1 protein have not been studied until now. Here, we employed CRISPR/Cas9-mediated genome editing and the DiCre/LoxP system to dissect the function of individual PfHP1 domains. First, we showed that the N-terminal 29 residues (aas 1-29) and the C-terminal 76 residues (aas 191-266) are responsible for targeting PfHP1 to nucleus, in which the later polypeptide has a stronger effect required for the efficient nuclear targeting. Second, we revealed that each of the three structural domains of the intact PfHP1 are required for proper heterochromatin binding, normal asexual proliferation and *ap2-g* gene silencing. Third, we successfully generated a PfHP1 knock out cell line that highly produces gametocytes once inducted (more than 82% of sexual conversion rate). Finally, we discovered that the HP1 Hinge and CSD domains are functionally conserved between *P. falciparum* and *P. berghei* in terms of heterochromatin binding, normal asexual proliferation, *var* gene - and *ap2-g* gene silencing. Our study not only represents a major insight into PfHP1 function and conservation but also provides a tool for further studies on gametocyte biology in the human malaria parasites.

3.2 Introduction

Heterochromatin protein 1 (HP1) was initially described in *Drosophila melanogaster* as a non-histone chromosomal protein associated with heterochromatin and essential for gene silencing in position effect variegation (Eissenberg et al., 1990; James et al., 1989; James and Elgin, 1986). The well-known function of HP1 lies in the formation and spreading of heterochromatin region via its recognition of methylated lysine 9 on histone 3 tails (H3K9me3) (Maison and Almouzni, 2004; Zeng et al., 2010). Chromatin-bound HP1 serves as a platform for the recruitment of downstream chromatin modifiers including H3K9me-specific histone methyltransferases which methylate H3K9 in neighbouring nucleosomes, facilitating the binding of further HP1 proteins (Maison and Almouzni, 2004). The self-propagation of HP1 results in the spread of regional heterochromatin, thereby promoting silencing of heterochromatin-associated genes (Grewal and Moazed, 2003; J. Wang et al., 2016).

HP1 is a small protein and well conserved among eukaryotes (Zeng et al., 2010). Its orthologs have been identified in a broad range of organisms from fission yeast (*Schizosacharomyces pombe)* to humans (Lomberk et al., 2006; Zeng et al., 2010). In *S. pombe*, Switching 6 (Swi6) and Chromo domain-containing protein 2 (Chp2) are two important homologs of the HP1 protein family involved in gene silencing and heterochromatin formation (Zeng et al., 2010). In mammals, there are three HP1 variants encoded by a class of genes called *chromobox* (*cbx*) genes. They are *cbx5*/HP1a, *cbx1*/HP1β and *cbx3*/HP1γ, which are highly similar in amino acid (aa) sequences (Vermaak et al., 2005). In general, HP1 is characterized by three structural domains: (1) a conserved chromo domain (CD) at the N-terminus, which binds H3K9me3; (2) a conserved chromo shadow domain (CSD) at the C-terminus, which mediates HP1 dimerization and HP1 interaction with other nuclear chromatin modifiers and (3) a variable intervening region or hinge domain linking CD and CSD, which interacts with Histone H1, DNA, RNA as well as native chromatin (Aasland and Stewart, 1995; Kwon and Workman, 2011; Lomberk et al., 2006).

HP1 has been well characterized in many eukaryotes. In mammalian models, localization of HP1 proteins has been shown to be variant-specific. While mammalian HP1a and HP1β are found at centromeric heterochromatin regions, HP1γ is found in both heterochromatic and euchromatic regions (Horsley et al., 1996; Minc et al., 1999; 2000). The domain responsible for targeting HP1 to the nucleus has been reported to

be species-dependent. In *Drosophila melanogaster*, the nuclear targeting ability is highlighted in the C-terminal 54 residues of the protein (aas 152-206) (Powers and Eissenberg, 1993). This finding is surprising as the polypeptide does not bear a consensus nuclear localization signal (NLS) (Dingwall and Laskey, 1991; Powers and Eissenberg, 1993). In contrast, the hinge region of Swi6 demonstrates nuclear targeting function and carries canonical consensus NLS motifs (G. Wang et al., 2000). Additionally, the Swi6 C-terminus acts as a second, albeit weaker, nuclear targeting domain without predicted consensus NLS (G. Wang et al., 2000). Heterochromatin binding domains in HP1 also show inter-species difference. In fission yeast, the chromo domain (CD domain) was shown to direct Swi6 to heterochromatin (G. Wang et al., 2000). Meanwhile, in mice this function additionally requires RNA binding by the hinge domain (Muchardt et al., 2002). *Drosophila* HP1 carries two redundant domains for pericentric heterochromatin targeting: the first lies in the N-terminal 95 residues (aas 1-95) (Platero et al., 1995) and the second in the C-terminal 112 residues (aas 95-206) (Powers and Eissenberg, 1993).

The human malaria parasite *Plasmodium falciparum* possesses only one HP1 homolog, designated as PfHP1 (Flueck et al., 2009; Pérez-Toledo et al., 2009). PfHP1 is mainly enriched at subtelomeric regions of all 14 chromosomes and some chromosome-internal islands (Flueck et al., 2009) where H3K9me3 occupies (Lopez-Rubio et al., 2009; Salcedo-Amaya et al., 2009). However, PfHP1 is absent from peri-centromeric regions (Flueck et al., 2009), possibly because these regions lack H3K9me3 (Lopez-Rubio et al., 2009; Salcedo-Amaya et al., 2009). This demarcated localization indicates that PfHP1 might not contribute to the formation and maintenance of centromere structure and function as observed for HP1 proteins in other eukaryotes (Allshire et al., 1995; Bernard et al., 2001; Fischer et al., 2009; Nonaka et al., 2002; Yi et al., 2018). Further, PfHP1 covers a large number of protein-coding genes and most of them belong to gene families encoding exported virulence proteins specific for *P. falciparum* including *var* gene family (Flueck et al., 2009). The *var* gene family consists of 60 genes encoding antigenically and functionally distinct variants of erythrocyte membrane protein 1 (PfEMP1) (Brancucci et al., 2014; Flueck et al., 2009; Pérez-Toledo et al., 2009). The interaction of PfEMP1 with receptors such as ICAM-1, CD-36 on blood endothelial cells and with uninfected RBCs (rosetting) results in cellular adherence and sequestration of infected red blood cells (iRBCs) (Cowman et al., 2016; Newbold et al., 1997; Reeder

and Brown, 1996; Rowe et al., 2009). Antigenic variation and diversity of PfEMP1 contribute significantly to immune evasion and hence, to the establishment of chronic infection (Cowman et al., 2016; Reeder and Brown, 1996). At any given time, there is only one *var* gene expressed while the rest are simultaneously transcriptional silenced (Dzikowski et al., 2006; Voss et al., 2006). The mutually exclusive expression of *var* genes is regulated by sophisticated epigenetic mechanisms including repressive histone modification (Jiang et al., 2013; Lopez-Rubio et al., 2009; 2007), histone-modifying enzymes like HDACs (Duraisingh et al., 2005; Tonkin et al., 2009)and HKMTs (Jiang et al., 2013; Volz et al., 2012), dynamic remodelling of chromatin and perinuclear locus reposition (Dzikowski et al., 2006; Freitas-Junior et al., 2005; Ralph et al., 2005; Voss et al., 2006), repressive long non-coding RNAs (Amit-Avraham et al., 2015; Epp et al., 2009) and PfHP1 (Brancucci et al., 2014).

Additionally, the roles of PfHP1 in three important cellular processes have been inferred through the use of a conditional loss-of-function mutant by targeting *pfhp1* gene with a sequence encoding FKPB destabilization domain (Armstrong and Goldberg, 2007; Brancucci et al., 2014). First, a massive de-repression of most of *var* genes was observed in the PfHP1-depleted parasites, leading to 52 out of 60 genes in this family to be highly upregulated (Brancucci et al., 2014). PfHP1 interacts with the histone mark H3K9me3 to obtain repressive heterochromatic state as well as to maintain the repressive cluster of silenced *var* genes while permissive state of a *var* gene is achieved by being devoid of PfHP1 (Brancucci et al., 2014; Bunnik et al., 2018; Voss et al., 2014). The study identified a central role of PfHP1 in epigenetic regulation of the mutually exclusive expression and inheritance of *var* gene family (Brancucci et al., 2014). Second, PfHP1 has been showed to be indispensable for normal growth of asexual parasites (Brancucci et al., 2014). Nearly 50% of the PfHP1-depleted parasites were unable to enter schizogony stage because of defective DNA replication one generation after stimulation (Brancucci et al., 2014). Instead, these parasites entered a reversible arrested trophozoite stage (Brancucci et al., 2014). Finally, a remarkable induction in sexual conversion of approximately 52% was found in the PfHP1-depleted parasites (Brancucci et al., 2014). The sexual conversion resulted from the derepression of *pfap2-g* locus (Brancucci et al., 2014). p*fap2-g* is a member of the *apiap2* family and encodes for PfAP2-G, the master transcriptional regulator of gametocytogenesis (Kafsack et al., 2014). *pfap2-g* was identified as a heterochromatic island covered by

H3K9me3 (Lopez-Rubio et al., 2009) and is the only PfHP1-regulated member of the *apiap2* family (Flueck et al., 2009). In *P. falciparum*, GDV1 (gametocyte development 1 protein) has been shown to bind PfHP1 *in vivo* and *in vitro* and form a putative regulatory complex that initiates gametocytogenesis (Filarsky et al., 2018). Using an *ap2-g* loss-of-function mutant in the gametocyte-non-producible *P. falciparum* clone, F12, the authors have revealed that *ap2-g* and some other genes that are occupied by PfHP1 was upregulated after the overexpression of GDV-1 (Filarsky et al., 2018). Together, GDV-1 was suggested to activate sexual commitment process by antagonizing HP1-dependent silencing of the *ap2-g* locus (Filarsky et al., 2018). The depletion of PfHP1 initiates de-repression of *pfap2-g* in committed schizonts, which then release sexually committed merozoites that re-invade and undergo full gametocyte maturation over the next 8-10 days (Brancucci et al., 2014). Thus, these studies have reinforced the central role of PfHP1 in controlling the differentiation switch from asexual to sexual stage of the human malaria parasites in its IDC.

Here, we conducted the first in-depth functional analysis of PfHP1 domains using CRISPR/Cas9-mediated genome editing and the DiCre/LoxP system. First, we showed that the N-terminal 29 residues (aas 1-29) and the C-terminal 76 residues (aas 191-266) are responsible for targeting PfHP1 to nucleus. The later polypeptide presents a stronger effect required for the full delivery of PfHP1 to nucleus. Software analysis addressed KKKK (aas 17-20) at the N-terminus and RRKK (aas 201-204) at the C-terminus as putative functional NLSs. Second, we found that intact PfHP1 containing all three structural domains is required for heterochromatin localization and the normal asexual growth of blood stage malaria parasites. Our results indicate that individual domains of PfHP1 confer precise functional contribution and/or have specific interaction with heterochromatin. Third, we successfully generated a PfHP1 knock out cell line with more pronounced morphological phenotype that allows massive production of more than 82% gametocytes once induced. Finally, we addressed that the HP1 Hinge and CSD domains are functionally conserved between *P. falciparum* and *P. berghei*.

3.3 Results

Investigation of the roles of PfHP1 domains in PfHP1 localization

To begin studying the functional contribution of individual PfHP1 domains, we engineered parasites that allow conditional expression of PfHP1 mutants based on the DiCre-loxP system (Collins et al., 2013) using CRISPR-Cas9-based gene editing. In these parasites, the endogenous *pfhp1* gene is excised upon rapamycin (RAP)-induced activation of the DiCre recombinase and replaced with a recodonised *pfhp1* gene encoding a mutated PfHP1 protein carrying a C-terminal GFP tag (Figures 1 and S1). We generated four such conditional PfHP1 mutant cell lines called 3D7/HP1-KO, 3D7/HP1-ΔCD, 3D7/HP1-ΔHinge, 3D7/HP1-ΔCSD, where aas 30-266 (full-length PfHP1 is 266 aas), 30-58 (CD domain), 75-177 (hinge domain) or 191-266 (CSD domain), respectively, have been deleted (Figure 1B). In the 3D7/HP1-ΔHinge cell line, aas 75-177 is substituted by a peptide representing aas 232-254 of PfSIP2, a member of the ApiAP2 family of transcription factors specific for *Plasmodium* and related Apicomplexan parasites (Flueck et al., 2009). In PfSIP2, this short polypeptide links two adjacent AP2-binding domains (Flueck et al., 2010) and was used in the 3D7/HP1-ΔHinge mutant line as a linker separating the CD and CSD domains (Figure 1C). We also used a control cell line where endogenous *pfhp1* is replaced by a recodonized *pfhp1* wild type sequence (3D7/HP1-Control) (Bui et al., manuscript submitted) (Figure 1C). The CRISPR-Cas9-based gene editing strategy used to generate these parasite lines is explained in detail in the Materials and Methods section and Figure S1.

PCR on parasite genomic DNA (gDNA) was performed to confirm the correct integration of the recodonised *pfhp1-gfp* gene variants directly downstream of the endogenous *pfhp1* gene and the successful DiCre-mediated excision of the floxed endogenous *pfhp1* gene upon RAP treatment in all five cell lines (Figure S2A). After RAP treatment, GFP-tagged PfHP1 mutants were expressed under the control of the endogenous *pfhp1* promoter (Figure S1). The conditional expression of PfHP1-GFP fusions allowed us to identify the roles of each of the three PfHP1 domains in targeting PfHP1 to nucleus and peri-nuclear heterochromatin. Live cell fluorescence imaging at 40-48 hpi in the same intra-erythrocytic cell cycle (generation 1, 40 hrs post RAP treatment) showed that RAP treatment resulted in the highly efficient excision of the endogenous *pfhp1* gene and expression of PfHP1-GFP fusion proteins in ~86% to 99% of parasites in the populations (Figures 2 and S2B). In contrast, parasites in the DMSO-treated control populations did not express the GFP-tagged PfHP1 mutants as expected (Figures 2 and S2B). Consistent with the live fluorescence imaging results,

analysis of whole parasite protein lysates by Western Blot showed that the RAP-treated parasites exclusively expressed the truncated PfHP1-GFP fusions while DMSO-treated control parasites exclusively expressed untagged wild-type PfHP1 (~31KDa) (Figure S2C). The expression levels of GFP fusions from PfHP1 mutant lines were similar to that of GFP fusion from PfHP1 control cell line, with the exception of GFP fusions from 3D7/HP1-ΔHinge and 3D7/HP1-ΔCD lines (Figure S2C). Since all GFP fusion proteins were expressed under control of the endogenous *pfhp1* promoter, the lower expression of GFP fusions observed in 3D7/HP1-ΔHinge and 3D7/HP1-ΔCD lines was likely result of mRNA instability, inefficient protein translation because of mRNA secondary structures or reduced protein stability. However, we were able to obtain a sufficient level of GFP signal in 3D7/HP1-ΔCD and 3D7/HP1-ΔHinge cell lines at schizont stage when protein expression peaks (Figure 2D-E).

The PfHP1 domain(s) responsible for nuclear targeting was determined as below. First, the ΔCD-GFP (deletion of aas 30-58) and ΔHinge-GFP (deletion of aas 75-177) localized to the nucleus (Figure 2D-E), suggesting that the sequences they share, i.e. aas 1-29, 59-74 and 178-266, are responsible for this function. Second, the ΔCSD-GFP in which the aas 191-266 are deleted, localized to both cytosol and preferably to nucleus (Figure 2C). Thus, the C-terminal polypeptide (aas 191-266) is required for efficient nuclear delivery. Third, GFP signal in 3D7/HP1-KO (deletion of aas 30-266) localized to both compartments (Figure 2B). Hence, the short N-terminal polypeptide (aas 1-29) is likely insufficient to target PfHP1 to nucleus.

We next used the NuPred (Brameier et al., 2007) and PSORTII (https://psort.hgc.jp/form2.html) algorithms to identify putative NLS elements. These analyses demonstrated NLSs in each of PfHP1 domains (Figure 1A): a KKKK motif (aas 17-20) in CD domain, a RRKK motif (aas 201-204) in CSD domain and PRRK motif (aas 100-103) or/and PRRKMSR motif (aa 100-106) in Hinge domain. These NLSs match 4-residue or 7-residue pattern of the PKKKRKV NLS motif exemplified from simian virus 40 (SV-40) (Kalderon et al., 1984). There was no potential NLSs predicted in the PfSIP2 linker sequence, thus, the localization of ΔHinge-GFP lies in PfHP1 intrinsic sequence (aas 1-78 and 178-266). Since the fusion ΔHinge-GFP protein was still imported into nucleus (Figure 2D), predicted NLSs within Hinge domain are not necessary for this function.

From our approach, only GFP fusion of 3D7/HP1-Control cell line localized to heterochromatin foci, representing by punctuated patterns at nuclear periphery (Figure 2A). Although the GFP fusions of 3D7/HP1-ΔCD and 3D7/HP1-ΔHinge cell lines localize to the nucleus, their ability to target heterochromatin is abolished (Figure 2D-E). Thus, an entire CD domain and Hinge domain are obligatory for heterochromatin targeting. Furthermore, GFP-ΔCSD fusion expressing CD-Hinge domains was partially diffused from nucleus to cytosol and was not concentrated in perinuclear foci (Figure 2C, 3D7/HP1-ΔCSD). Together, CD-Hinge domain is insufficient for targeting PfHP1 to heterochromatin but additionally requires CSD domain.

In summary, our live imaging data indicated that the N-terminal 29 aas (1-29) and C-terminal 76 aas (191-266) are responsible for targeting PfHP1 to nucleus. The later polypeptide presents a stronger effect required for the full delivery of PfHP1 to nucleus. Software analysis addressed KKKK (aas 17-20) in CD and RRKK (aas 201-204) in CSD as putatively functional NLSs. As only intact PfHP1 is able to bind heterochromatin, our result implied essential and precise functional contribution and/or specific interaction of each structural domain with heterochromatin components.

Each of PfHP1 domains is indispensable for normal asexual growth

In a recent study, we showed that PfHP1 is required for (1) progression through schizogony and thus parasite multiplication; (2) silencing of the *pfap2-g* locus and thus inhibition of sexual commitment; and (3) *var* mutually exclusive expression and thus the PfEMP1 expression (Brancucci et al., 2014). Here, we asked if the individual domains of PfHP1 are required for any of these processes. The 3D7/HP1-Control (Bui et al., manuscript submitted, Chapter 2) was used as a control to evaluate the function of PfHP1 mutants.

First, we investigated the proliferation of the four PfHP1 truncation cell lines and the control cell line. As shown in Figure 3A, in the 3D7/HP1-Control cell line, the multiplication of DMSO- and RAP-treated parasites was highly comparable. As expected, the multiplication of DMSO-treated parasites from four PfHP1 truncation mutant lines was also comparable to that of the control. In contrast, the RAP-treated parasites of four PfHP1 truncation mutant lines consistently drew a same pattern of proliferation defect in the following cycle after RAP treatment, showing a failure in entering schizogony in generation 2 (Figure 3A). In generation 3 of the RAP-treated

population (112 hrs post RAP treatment), we were able to select a relative fraction of about ~4.5 to 18% of total infected parasites as proliferating asexual subpopulation (RAPSUR subpopulations) (Figure S3). However, these proliferating asexual subpopulations did not display GFP signal (data not show), indicating that the DNA excision did not occur after RAP treatment. Further examination of RAPSUR subpopulations revealed the lack of Cre recombinase activity, thus, resulting in the failure of DNA excision and presence of proliferating asexual parasites (Figure S3). Although the mechanism how PfHP1 regulates asexual mitosis is unknown, the results indicated that individual domains of PfHP1 are required for proper function of PfHP1 in controlling the virtual proliferation of asexual blood stage parasites. This data is consistent with previously reported data (Brancucci et al., 2014).

Second, we examined a possible role of individual PfHP1 domains in controlling *pfap2-g* silencing by comparing the sexual commitment rates between DMSO- and RAP-treated parasites for all PfHP1 truncation mutant lines. As shown in Figure 3B, left panel, RAP-treated 3D7/HP1-KO, 3D7/HP1-ΔCD, 3D7/HP1-ΔHinge and 3D7/HP1-ΔCSD parasites showed significantly higher sexual conversion rates compared to the DMSO-treated populations (*p*-value < 0.01, unpaired two-tailed Student' t-test). The result is consistent with previously described result (Brancucci et al., 2014) except that we obtained extremely higher conversion rate of approximately 82-95% in RAP treated populations in these PfHP1 truncation lines. However, we also found a significant increase in sexual conversion rate for the RAP-treated 3D7/HP1-Control parasites expressing a recodonised wild-type *pfhp1* gene (*p*-value < 0.01, unpaired two-tailed Student' t-test) (Figure 3B, left panel). Comparing the fold changes of sexual conversion rates between RAP- versus DMSO-treated parasites showed significant differences between parasites expressing truncated PfHP1 variants compared to the 3D7/HP1-Control cell line (Figure 3B right panel).

An a-Pfs16 IFA study (30-38 to 40-48 hpi, generation 2) and overview images of a Giemsa-stained blood smear (10 days post invasion) confirmed high proportion of stage I and stage IV/V gametocytes, respectively, in 3D7/HP1-KO cell line (Figures 3C). Gametocytes in the RAP-treated sample of 3D7/HP1-KO and other PfHP1 mutant cell lines completed sexual development within 8–10 days, similar to DMSO-treated gametocytes. Together, the result suggested that each of PfHP1 individual domains is

essential for controlling *ap2-g* silencing and reinforced the central role of PfHP1 in epigenetic regulation of sexual commitment process in the human malaria parasites.

The function of the HP1 Hinge and Chromo shadow domains is conserved between *P. falciparum* and *P. berghei*

It has been shown that in *S. pombe*, replacement of Swi6 CD domain by CD domain of mouse HP1-like protein, M31 retained Swi6 function in sporulation phenotype, normal zygote asci formation and mitotic stability ability while CSD substitution did not (G. Wang et al., 2000). Thus, chromodomain function is conserved between fission yeast and mouse (G. Wang et al., 2000). We also pointed out if such conservation occurs within *Plasmodium* using a domain swap experiment. Among HP1 orthologs within *Plasmodium* genus, we chose *P.berghei* HP1 (PbPH1) to perform domain swap experiment with *P.falciparum* HP1 because of the similarity in controlling sexual conversion switch through *ap-2g* derepression in the two malaria parasites (Brancucci et al., 2014; Kafsack et al., 2014; Sinha et al., 2014).

To this end, we generated three HP1-hybrid cell lines namely 3D7/HP1-hyb-PbHinge, 3D7/HP1-hyb-PbCSD, 3D7/HP1-hyb-PbHP1 in which the PfHP1 Hinge, CSD or full length PfHP1 were conditionally substituted by PbHP1 Hinge, CSD domain and full length PbHP1, respectively using similar approach described above (Figures 4A-B and S1). A CD domain swap was not performed because of high degree in identity and similarity between PfHP1- and PbHP1 CD sequences after RAP induction (only six residues different) [Figure S4B and (Fraschka et al., 2018)]. We successfully generated two PfHP1 hybrid mutant lines, 3D7/HP1-hyb-PbHinge and 3D7/HP1-hyb-PbCSD. Despite a number of efforts, we failed to obtain the 3D7/HP1-hyb-PbHP1 line. The 3D7/HP1-Control cell line was also used as a control to evaluate the function of the PfHP1 hybrid mutants in three PfHP1-dependent processes mentioned above.

To assess the ability of hybrid HP1s in heterochromatin binding, we performed live imaging at 40-48 hpi in generation 1 and at 16-24 hpi in generation 2 to observe the localization of GFP fusion proteins after RAP treatment. None of the DMSO-treated parasites expressed the GPF-tagged proteins as expected, whereas in the RAP-treated populations, the GFP-tagged PfHP1-hyb-PbHinge and PfHP1-hyb-PbCSD hybrids localized to nucleus and to heterochromatin loci indistinguishable to the GFP-

tagged PfHP1 control (Figures 4C, 2A and S2A). Thus, replacement of PfHP1 Hinge or CSD domain by that of PbHP1 retains proper heterochromatin localization of PfHP1.

We next evaluated proliferation rates of the HP1 hybrid cell lines and control cell line over three consecutive generations after RAP treatment. In our static culture condition, DMSO- and RAP-treated parasites in both 3D7/HP1-hyb-PbHinge, 3D7/HP1-hyb-PbCSD and 3D7/HP1-Control lines proved highly comparable rate of multiplication (Figures 5A and 3A), revealing proper function of the PfHP1-PbHP1 hybrids in controlling cell cycle progression and growth.

To study the possible role of HP1 hybrid mutants in regulating *pfap2-g* silencing, sexual conversion rate between DMSO- and RAP- treated parasites were examined. As shown in Figure 5B, left panel, RAP-treated population always revealed higher sexual conversion rate compared to DMSO-treated population. Comparing the fold changes of sexual conversion rates between RAP- versus DMSO-treated parasites showed insignificant differences between mutant lines expressing PfHP1-PbHP1 hybrids compared to the 3D7/HP1-Control line (Figure 5B, right panel) (p value > 0.05, unpaired two-tailed Student' t-test). Hence, the Hinge and CSD domain exchange between PfHP1 and PbHP1 does not affect the regulation of *ap2-g* silencing in the human malaria parasites.

Finally, to probe the ability of HP1 hybrids in maintaining singular *var* gene expression, immunofluorescence study was performed to compare the expression of PfEMP1 in the progeny of DMSO- and RAP-treated 3D7/HP1-hyb-PbHinge, 3D7/HP1-hyb-PbCSD and the control cell lines at 16-24 hpi, generation 2. IFAs showed comparable intensity for PfEMP1 signal between RAP-treated and DMSO-treated paired samples from these three cell lines (Figure 5C), implying a preserved function of the PfHP1-PbHP1 hybrids in regulating *var* gene expression.

Taken together, these data reflect the functional conservation of Hinge and CSD domains in PfHP1 and PbHP1. However, our study did not rule out if HP1 function is conserved between the two parasites because of the failure in obtaining 3D7/HP1-hyb-PbHP1 line expressing full length PbHP1.

3.4 Discussion

Previous studies have indicated that domains targeting HP1s to nucleus are species-dependent and do not always possess canonical NLS sequences (Powers and

Eissenberg, 1993; G. Wang et al., 2000). Therefore, we could not rely on sequence homology to predict the nuclear targeting sequence within PfHP1. Instead, we had to determine the nuclear localization sequence empirically. We identified that the C-terminal 76 residue-polypeptide (aas 191-266) presents strong and effective nuclear targeting ability while the N-terminal 29 residue-polypeptide (aas 1-29) expresses weaker ability. Fusion proteins lacking the C-terminal polypeptide (aas 191-266) were not fully imported into nucleus. Although the N-terminal 29 residue-polypeptide was insufficient for fully targeting PfHP1 to nucleus, our results cannot indicate whether the CSD alone is sufficient for this function because the former polypeptide was always present in all of PfHP1 truncation variants.

Heterochromatin binding function has been well studied in many model organisms (Muchardt et al., 2002; Platero et al., 1995; Powers and Eissenberg, 1993; G. Wang et al., 2000). Studies employing different experimental systems have highlighted the contribution of more than one structural HP1 domain for proper heterochromatin targeting. In mouse, heterochromatin-targeting ability of HP1α is underlined by RNA binding via a conserved region of Hinge together with the binding to methylated histone via CD (Muchardt et al., 2002). Additionally, in *Drosophila*, the domain directing HP1 to heterochromatin was first assigned to the C-terminal half of the protein (aas 95-206) that contains the CSD region (aas 142-206) and a substantial length of the hinge domain (Powers and Eissenberg, 1993). In the study of J. A. Powers and C. Eissenberg, in order to determine the domain targeting HP1 to nucleus, a number of *lacZ*/*hp1* gene fusion sequences were used to express HP1 deletions that were N-terminally tagged with β-galactosidase (Powers and Eissenberg, 1993). Protein fusions containing CD and/or Hinge domain failed to target nucleus while protein fusions containing majority of CSD region (aas 152-206; CSD domain is from aas 142 to 206) showed nuclear localization (Powers and Eissenberg, 1993). However, heterochromatin localization was only found in the protein fusions that contained at least a substantial length/part of the Hinge domain plus CSD region (aas 95-206) (Powers and Eissenberg, 1993). Specify that β-galactosidase fusion HP1 variants were expressed in a wild-type HP1 background *in vivo* in the study of J. A. Powers and C. Eissenberg, heterochromatin-binding function in this scenario could result from dimerization between CSD-containing fusion protein and endogenous HP1 protein. In our approach, HP1-GFP fusions were expressed in a null PfHP1 background. We found

that only full length PfHP1 was properly recruited to heterochromatin foci and that CD-Hinge was insufficient for this function. Although CD-Hinge region is able to bind existing H3K9me3 (Bannister et al., 2001; Lachner et al., 2001), it is possible that the lack of CSD domain has prevented PfHP1 homo-dimerization as well as the recruitment of histone lysine methyl transferase (HKMT). In turns, these events impede PfHP1 self-propagation and *de novo* H3K9me3 establishment during cell division, resulting in deficiency in heterochromatin compaction and cohesion in schizont stage of generation 1 and the ring progeny in generation 2. In consequence, parasites expressing truncated PfHP1 variants were unable to enter schizogony and committed to gametocytes, emphasising that PfHP1 is indispensable for normal growth of asexual blood-stage malaria parasites.

By successful generating an inducible *pfhp1* knockout cell line, we obtained interesting pronounced morphology with (1) exiguous number/ exclusion of arrested trophozoite population and (2) more than 82% of the population synchronously switch to sexual commitment pathway. Notably, while gametocyte production is labouring (S. Duffy et al., 2016; Saliba and Jacobs-Lorena, 2013), the gametocyte highly producible line in our study presents a robust tool for further studies on gametocytogenesis, gametocyte development and biology, anti-malaria gametocyte drug discovery as well as transmission-block strategies.

Although HP1 has been studied in *P. falciparum* (Brancucci et al., 2014; Flueck et al., 2009; Pérez-Toledo et al., 2009), function of HP1 in *P. berghei* is still little known. It has been reported that HP1 was enriched at all subtelomeric regions of 14 chromosomes in all *Plasmodium* species (Fraschka et al., 2018). However, heterochromatin organization is different between *P. falciparum* and *P. berghei* during parasite developments (Fraschka et al., 2018; Witmer et al., 2019). During progression from asexual developmental stages to sexual conversion process, subtelomeric heterochromatin expansion was observed in *P. falciparum* while heterochromatin landscape was remained between developmental stages in *P. berghei* (Fraschka et al., 2018; Witmer et al., 2019). Genes driving iRBC remodeling become heterochromatic during gametocytogenesis in *P. falciparum* (Fraschka et al., 2018). The difference is explained by the fact that *P. berghei* does not encode for such similar orthologues. Intriguingly, *ap2-g* locus was enriched in HP1 in all *Plasmodium* species (Fraschka et al., 2018). Additionally, *ap2-g* has been identified as a conserved master

regulator of gametocytogenesis in both of *P. falciparum* and *P. berghei* (Brancucci et al., 2014; Kafsack et al., 2014; Sinha et al., 2014). The removal of H3K9me3-bound PfHP1 from *ap2-g* locus is mediated by the upstream regulator of sexual commitment, PfGDV1, thus triggering sexual commitment (Filarsky et al., 2018). The similarity in controlling gametocytogenesis through *ap2-g* derepression in *P. falciparum* and *P. berghei* has prompted us to investigate on the functional conservation of HP1 domains in the two parasites. However, there is no GDV-1 ortholog in *P. berghei*, suggesting an alternative regulatory mechanism in controlling the *pbap2-g* silencing in this rodent malaria parasites (Eksi et al., 2012). From our study, the PbHP1-PfHP1 hybrids are inferred to interact with PfGDV-1 to evict HP1 hybrids from *pfap2-g* locus. These results are possibly explained by the high conservation in PfHP1 and PbHP1 sequences as well as individual domain sequences (Figure S5, >82% similarity in protein sequences and (Fraschka et al., 2018)). Although we do not know the exact domain(s) of PfHP1 interacting with GDV-1, such interaction was likely retained in our domain swapping experiment, emphasizing the functional conservation of HP1 between the human and rodent malaria parasites.

In conclusion, our study identified that the N-terminal 29 residues (aas1-29) and C-terminal 76 residues (aas 191-266) are responsible for targeting PfHP1 to nucleus. In parallel, we revealed that each of the three structural domains of PfHP1 protein is required for PfHP1 proper function in heterochromatin binding, normal asexual proliferation and *ap2-g* gene silencing. Finally, we discovered that the Hinge and CSD domains are functionally conserved between the *P. falciparum* and *P. berghei*. Our study not only represents a major insight into PfHP1 function and conservation but also provides a tool for robust production of gametocytes used in further studies on gametocyte biology or high-throughput anti-malaria gametocyte drug screen.

3.5 Materials and Methods

Parasite culture and transfection

The transgenic cell lines generated in this study were cultured at 5% hematocrit in RPMI-1640 medium supplemented with 25 mM HEPES, 100 mM hypoxanthine, 24 mM sodium bicarbonate, 0.5% Albumax II supplemented with 2mM choline to reduce background sexual conversion rates as demonstrated recently (Brancucci et al., 2014; Trager and Jensen, 1976). Parasite cultures were synchronized using 5% sorbitol as

described previously (Lambros and Vanderberg, 1979). Cotransfection of CRISPR/Cas9 and donor plasmids into the DiCre-expressing line 3D7/1G5DiCre (Collins et al., 2013) and selection of transfected populations were performed as described recently (Filarsky et al., 2018) and (Bui et al, submitted).

Transfection constructs

We applied CRISPR/Cas9-mediated genome editing and the DiCre/LoxP system (Collins et al., 2013) to generate cell lines conditionally expressing truncated PfHP1 and hybrid PfHP1 variants. We engineered (1) 3D7/HP1-KO for expression of full-length PfHP1 deletion (deletion of aas 30- 266. The PfHP1 is 266 aas in length (PF3D7_1220900)); (2) 3D7/HP1-ΔCD for expression of PfHP1 CD deletion (deletion of aas 30-58); (3) 3D7/HP1-ΔHinge for the expression of PfHP1 Hinge deletion (aas 75-177 of PfHP1 was replaced with a peptide representing aas 232-254 of PfSIP2. The PfSIP2 is 1979 aas in length (PF3D7_0604100)); (4) 3D7/HP1-ΔCSD for the expression of PfHP1 CSD deletion (deletion of aas 191-266); (4) 3D7/hyb-PbHinge for the expression of chimeric PfHP1 in which PfHP1 Hinge domain (aas 75-177) was replaced by PbHP1 Hinge domain (aas 75-192); (6) 3D7/hyb-PbCSD for the expression of chimeric PfHP1 in which PfHP1 CSD domain (aas 191-266) was replaced by PbHP1 CSD domain (aas 206-281). The PbHP1 is 281 aas in length (PBANKA_1436100); (7) 3D7/HP1-hyb-PbHP1 for expression of full length PbHP1 (aas 30-266) and (8) 3D7/HP1-Control for expression of wild type PfHP1 [Bui et al, manuscript submitted] (See Figs S1, 1C and 3A for schematic illustrations). To obtain these cell lines, we performed two subsequent transfection steps.

In the primary transfection, the mother cell line 3D7-1G5DC/5'-loxPint-g31 (or 3D7/N31DC) which carries a *sera2* intron:loxP element (Jones et al., 2016) inserted into the 5'of *pfhp1* coding sequence was generated as described previously [Bui et al, manuscript submitted, Chapter 2].

In the second transfection, the mother cell line 3D7/N31DC parasites were transfected again to generate seven parasite lines: 3D7/HP1-KO, 3D7/HP1-ΔCD, 3D7/HP1-ΔHinge, 3D7/HP1-ΔCSD, 3D7/hyb-PbHinge, 3D7/hyb-PbCSD, 3D7/HP1-Control. These transgenic parasite lines carry a second *sera2* intron: loxP sequence directly downstream of the endogenous *pfhp1* stop codon, followed by GFP coding sequence (HP1-KO), a recodonised mutated PfHP1 (HP1-ΔCD, HP1-ΔHinge, HP1-ΔCSD,

HP1-hyb-PbHinge, HP1-hyb-PbCSD) or wild type (HP1-Control) *pfhp1-gfp* sequence. The transgenic parasite lines were generated using the following cloning steps.

First, we constructed the pBF-gC-guide250 plasmid carrying the sgRNA target sequence at the 3' end of the *pfhp1* coding sequence [Bui et al., manuscript submitted].

Second, we constructed the seven donor plasmids.

The pD-PfHP1-Control donor plasmid and pD-PfHP1-KO were constructed as described previously [Bui et al., manuscript submitted].

The pD-PfHP1-ΔCD donor plasmid was constructed by Gibson assembly joining three PCR fragments encoding (1) the pD plasmid backbone amplified from pUC19 using primers PCRA_F and PCRA_R (Brancucci et al., 2017), (2) a 5` homologous region (HR) followed by a 103bp- *sera2* intron:loxP sequence amplified from pD-PfHP1-Control using primers F158 and R143, (3) a fragment amplified from pD-PfHP1-Control using primers F177 and R163 spanning, in the following order, base pairs (bps) +175 to +798 of a synthetic recodonized *pfhp1* coding sequence (*re-pfhp1*, GenScript™) omitting the stop codon (the *pfhp1* coding sequence is 798 bp long), a *gfp* coding sequence ending with stop codon and a 3`HR spanning 824 bps downstream of the *pfhp1* stop codon.

The pD-PfHP1-ΔHinge donor plasmid was constructed by Gibson assembly joining four PCR fragments encoding (1) the pD plasmid backbone amplified from pUC19 using primers PCRA_F and PCRA_R (Brancucci et al., 2017), (2) 5` HR followed by the *sera2* intron: loxP sequence amplified from pD-PfHP1-Control using primers F158 and R143, (3) a fragment amplified from the pBCam-ΔHinge-3HA-Cherry plasmid (supplementary method) using primers F164 and R165 spanning, in the following order, bps +88 to +222 of the *re-pfhp1* coding sequence, bps +694 to +762 of the *pfsip2* coding sequence (the *pfsip2* coding sequence is 5937 bp long) and bps +532 to +798 of the *re-pfhp1* coding sequence omitting stop codon, (4) a fragment amplified from pFdon C-loxP-g250 [Bui et al, manuscript submitted] using primers F162 and R163 spanning, in the following order, a *gfp* coding sequence ending with stop codon and the 3`HR.

The pD-PfHP1-ΔCSD donor plasmid was constructed by Gibson assembly joining three PCR fragments encoding (1) the pD plasmid backbone amplified from pUC19 using

primers PCRA_F and PCRA_R (Brancucci et al., 2017), (2) a fragment amplified from pD-PfHP1-Control using primers F158 and R178 spanning, in the following order, the 5`HR, the *sera2* intron: loxP, bps +88 to +570 of the *re-pfhp1* coding sequence (3) a fragment amplified from pFdon C-loxP-g250 [Bui et al, manuscript submitted] using primers F162 and R163 spanning, in the following order, a *gfp* coding sequence ending with stop codon and the 3' HR.

The pD-hyb-PbHinge donor plasmid was constructed by Gibson assembly joining two PCR fragments encoding (1) the pD-HP1-KO plasmid backbone was amplified from its own template using primers F162 and R143, (2) a fragment amplified from the pBCam-hyb-PbHinge-3HA-Cherry (supplementary method) using primers F164 and R165 spanning, in the following order, bps +88 to +222 of the *re-pfhp1* coding sequence, bps +223 to +576 of the *hp1* from *P. berghei* coding sequence (*pbhp1,* the *pbhp1* coding sequence is 843 bp long), bps +532 to +798 of the *re-pfhp1* coding sequence omitting the stop codon.

The pD-hyb-PbCSD donor plasmid was constructed by Gibson assembly joining two PCR fragments encoding (1) the pD-HP1-KO plasmid backbone was amplified from its own template using primers F162 and R143, (2) a fragment amplified from the pBCam-hyb-PbCSD-3HA-Cherry (supplementary method) using primers F164 and R161 spanning, in the following order, bps +88 to +570 of the *re-pfhp1* coding sequence, bps +616 to +843 of the *pbhp1* omitting the stop codon.

Finally, the pD-hyb-PbHP1 donor plasmid was constructed by Gibson assembly joining five PCR fragments encoding (1) the 5' HR spanning bps +88 to +798 of the *pfhp1* coding sequence ending with a stop codon amplified from pFdon C-loxP-g250 [Bui et al, manuscript submitted] using primers F158 and R159; (2) 103 bp *sera2* intron:loxP element was amplified from pD-SIP2-loxP-GFP plasmid (I. Niederwieser, unpublished; see also Hai BUI et al, manuscript submitted, Chapter 2) using primers F139 and R143; (3) bps +88 to +843 of the *pbhp1* amplified from *P. berghei* gDNA using primers F160 and R161; (4) a fragment containing the *gfp* sequence ending with a stop codon followed by the 3' HR was amplified from pFdon C-loxP-g250 [Bui et al, manuscript submitted] using primers F162 and R163 and (5) the pD plasmid backbone amplified from pUC19 using primers PCRA_F and PCRA_R (Brancucci et al., 2017).

For each of the seven transfections, 50 µg of the pBF-gC-guide250 plasmid was mixed with 50 µg of a donor plasmid above and electroporated into the 3D7/N31DC mother parasite line. Transfected parasites were selected as described previously [(Filarsky et al., 2018) and (Bui et al, manuscript submitted)].

All oligonucleotide sequences used for the cloning of the CRISPR/Cas9 and donor plasmids are provided in Table S1. The nucleotide sequence of recodonized *pfhp1* and *pbhp1* are provided in Figure S4.

Induction of DiCre recombinase mediated DNA excision by Rapamycin

Parasites were synchronized twice 16 hours apart to obtain an eight-hour growth window (16-24 hpi). After re-invasion parasites were synchronized again at 0-8 hpi (generation 1) and split into two equal populations, of which one half was treated with 0.02%v/v of DMSO (negative control) and the other half was treated with 100 nM RAP for 1 hour (Knuepfer et al., 2017). The cultures were then spun down, washed with an equal volume of culture medium, resuspended in culture medium and returned to culture.

Live cell imaging and indirect immunofluorescence assay (IFA)

To quantify the efficiency of *pfhp1* excision after RAP treatment, live cell fluorescence microscopy was performed as described before [Witmer et al., 2012] with minor modification using 5 µg/ml Hoechst (supplied by Merk, Darmstadt, DE) to stain the nuclei. Excision efficiency was determined as the percentage of GFP-positive schizonts at 40-48 hpi in generation 1 (>200 schizonts counted per experiment).

IFAs were performed on methanol-fixed cells using mouse IgG1 mAb a-ATS (M. F. Duffy et al., 2002),1:150; mouse mAb a-Pfs16 (kind gift from Robert W. Sauerwein), 1:250; and Alexa Fluor 488-conjugated a-mouse IgG (Molecular Probes), 1:250. Images were taken at 63-fold magnification on a Leica DM 5000B microscope with a Leica DFC 300 FX camera, acquired via the Leica IM 1000 software, processed using ImageJ software [https://imagej.nih.gov/ij/]. For each experiment, images were acquired and processed with identical settings.

Parasite multiplication assay

Parasites were tightly synchronized twice 16 hours apart. At 0-8 hpi, generation 1, parasites were split into two equal populations, of which one half was treated with

DMSO (negative control) and the other half was induced for DiCre recombinase-mediated DNA excision by RAP treatment as described above. Giemsa smears were prepared to determine the parasitaemia at 16-24 hpi (generation 1). Giemsa-stained smears were prepared every second day onwards for three generations. Parasitaemia was counted by visual inspection of Giemsa-stained blood smears (≥ 3'000 RBCs counted per experiment). Multiplication rates were determined as the parasitaemia observed in the following generation divided by the parasitaemia observed in the previous generation. The extrapolative growth cure was generated using starting parasitaemia at 0.1%.

Gametocyte conversion assay

After DMSO or RAP treatment in generation 1, parasites were allowed to complete schizogony and re-invasion. At 16-24 hpi in generation 2, each pair of cultured (DMSO- and RAP-treated) were treated with 50 mM N-acetyl-D-glucosamine (GlcNAc) for five days to eliminate asexual parasites (Ponnudurai et al., 1986) and then cultured with normal culture medium for another 4-6 days to observe the maturation of gametocytes. Gametocytaemia was determined on day 6 of GlcNAc treatment by visual inspection of Giemsa-stained blood smears. Sexual conversion rates were determined as the gametocytaemia observed on the day 6 as a proportion of the total parasitaemia observed on day 1 of GlcNAc treatment.

SDS-PAGE and immunoblotting

After DMSO or RAP treatment in generation 1, parasites were allowed to complete schizogony and re-invasion. At 16-24 hpi in generation 2 parasites were released from infected RBCs (iRBCs) by 0.15% saponin/PBS complemented with 1X protease inhibitor (Roche Diagnostics). After washing 2-3 times in ice-cold PBS, parasite pellets were lysed in 70°C pre-heated Urea/SDS buffer (8 M Urea, 5% SDS, 50 mM Bis-Tris, 2 mM EDTA, 25 mM HCl at pH 6.5 supplemented with 2 mM DTT and 1X protease inhibitor). Whole parasite protein lysates were separated on NuPage 4-12% Bis-Tris gels (Novex) and analyzed by Western blot using mouse mAb α-GFP (Roche Diagnostics #11814460001), 1:1000; rabbit α-PfHP1(Brancucci et al., 2014), 1:5'000; rabbit α-Histone 4 (Abcam ab10158).

Nucleic acid isolation and polymerase chain reaction

To evaluate the correct editing of the *pfhp1* locus, we performed PCRs on genomic DNAs (gDNAs) of transgenic cell lines, which were sampled and isolated as described previously (Witmer et al., 2012).

To evaluate the DNA excision efficiency after RAP treatment, diagnostic PCRs were performed on gDNAs after 24-36 hours post treatment. Primers were designed to allow the PCR amplification to span over the 5`to 3` homologous regions.

All transfection plasmids generated in this study have been validated by Sanger sequencing. All transfection plasmids have been designed and Sanger sequencing results analysed using the SnapGene software (from GSL Biotech; available at snapgene.com). All primer sequences used for PCR are listed in Table S1.

Acknowledgements

We are grateful to Mike Backman and the Edinburgh Malaria Reagent Repository (http://www.malariaresearch.eu/) for providing the 3D7/1G5DiCre parasite line. This work has been supported by the Swiss National Science Foundation (grant numbers 31003A_143916 and 31003A_163258).

Figure 1. Generation of DiCre-inducible PfHP1 truncation mutants. (A) Organization of PfHP1 (Flueck et al 2009). The amino acid sequence of CD and CSD domains are indicated. Red letters indicate predicted functional NLS motifs in CD and CSD domains by NucPred and PSORTII. **(B)** Schematics of the CRISPR/Cas9-edited *pfhp1* locus (upper panel) and corresponding PfHP1 protein products (lower panel) before (DMSO) and after (RAP) rapamycin-induced DiCre-dependent excision of the wild type *pfhp1* locus. Blue arrowheads indicate the position of *sera2* intron:loxP elements. Red stars indicate STOP codons. Brown and blue boxes represent the wild type *pfhp1*/PfHP1 and the replacing cassette sequences/replacing protein sequences, respectively. Green boxes represent *gfp*/GFP sequence. Numbers in the gene and protein schematics refer to nucleotide and amino acid positions, respectively. RAP, rapamycin. **(C)** Diagrams showing organization of recodonized PfHP1 (top panel) and PfHP1 protein products expressed in the 3D7/HP1-Control, 3D7/HP1-KO, 3D7/HP1-ΔCD, 3D7/HP1-ΔHinge and 3D7/HP1-ΔCSD after RAP-treatment (lower panels). Dashed lines represent corresponding deletion in PfHP1 protein sequence. Purple curve represents a short polypeptide of the PfSIP2 protein known to link two adjacent Ap2-binding domains of the protein. The amino acid sequence and position of this polypeptide are indicated. Localization and heterochromatin binding function of corresponding PfHP1 control- and truncated PfHP1 proteins are summarized on the right. N: nuclei. C: cytosol.

Figure 2. Subcellular localization of PfHP1 truncation mutants. (A – E) Representative live cell fluorescence images showing localization of the GFP-fusions in (A) 3D7/HP1-Control, (B) 3D7/HP1-KO, (C) 3D7/HP1-ΔCSD, (D) 3D7/HP1-ΔHinge and (E) 3D7/HP1-ΔCD in late schizonts (LS, 40-48 hpi, generation 1; 40 hrs after rapamycin treatment). Nuclei were stained with Hoechst. DIC, differential interference contrast. Scale bar (black), 5 µm. Magnificent bar (white), 2.5 µm.

Figure 3. Phenotypes of PfHP1 truncation mutants. (A) Growth curves of the DMSO- and RAP-treated PfHP1 truncation mutant lines and control cell line over three consecutive generations. Values are the mean of four replicates for 3D7/HP1-Control and three biological replicates for other cell lines (>3.000 RBCs counted per sample). Error bars indicate SD. **(B)** Sexual conversion rate of the 3D7/HP1-Control and PfHP1 truncation mutant lines accessed by GlucNAc assay and inspected by Giemsa at day 6 of the treatment (left panel) and the corresponding fold change in sexual conversion rates

between the RAP-treated versus DMSO-treated control populations (right panel). Results are the mean of at least three replicates (>3.000 RBCs counted per sample. n indicates number of replicates). Error bars indicate SD. Asterisks indicate significant differences in sexual commitment rates between RAP-treated and DMSO-treated parasites (right panel, $p<0.01$; unpaired two-tailed Student's t-test). **(C)** Overview images of IFAs and Giemsa stains of DMSO- and RAP- treated population of 3D7/HP1-KO (left panel). IFAs were performed on methanol-fixed cultures at 30-38 hpi, generation 2 using a-Pfs16 antibodies. Giemsa stains were taken at 10 days post invasion (10dpi). Images of IFAs and Giemsa stains highlight the large proportion of stage I gametocytes (green) and stage IV-V gametocytes in RAP-treated population compared to DMSO-treated population of 3D7/HP1-KO. Sexual conversion rate of 3D7/HP1-KO and 3D7/HP1-Control was accessed by Pfs16 IFAs at 30-38 to 40-48 hpi, generation 2 (right panel). Results are the mean of replicates (>200 iRBCs counted per sample. n indicates number of replicates). Error bars indicate SD.

Figure 4. Generation of DiCre-inducible PfHP1-PbHP1 hybrid mutants. (A) Organization of PfHP1 and PbHP1 based on protein sequence alignment using Global Alignment EMBOSS Needle (https://www.ebi.ac.uk/Tools/psa/emboss_needle/)(see also Figure S4B). **(B)** Diagrams showing GFP-tagged PfHP1 hybrid protein products expressed in the 3D7/HP1-hyb-PbHinge, 3D7/HP1-hyb-PbCSD and 3D7/HP1-hyb-PbHP1 cell lines after RAP-treatment. **(C)** Representative live cell fluorescence images showing the localization of GFP-fusions in 3D7/HP1-hyb-PbHinge and 3D7/HP1-hyb-PbCSD cell lines in late schizonts (LS, 40-48 hpi, generation 1, 40 hrs after DMSO/RAP- treatment) and in late ring (LR, 16-24 hpi, generation 2, 64 hrs after DMSO/RAP treatment). Scale bar (black), 5µm. Magnificent bar (white), 2.5 µm.

Figure 5. Phenotype of PfHP1-PbHP1 hybrid mutant lines. (A) Growth curves of the DMSO- and RAP-treated 3D7/HP1-hyb-PbHinge and 3D7/HP1-hyb-PbCSD parasites over three consecutive generations. Values are the mean of three (3D7/HP1-hyb-PbHinge) and four (3D7/HP1-hyb-PbCSD) independent replicate experiments. Error bars represent SD. **(B)** Sexual conversion rates of the DMSO- and RAP-treated PfHP1-PbHP1 hybrid mutants and the control cell line (left panel) and the corresponding fold change in sexual conversion rates between the RAP-treated versus DMSO-treated control population (right panel). Values represent the mean of three (3D7/HP1-hby-PbHinge) and four (3D7/HP1-Control and 3D7/HP1-hyb-PbCSD) independent

replicate experiments. Error bars represent SD. There is no significant difference in the fold induction in sexual conversion rates of the 3D7/HP1-hyb-PbHinge and 3D7/HP1-hyb-PbCSD compared to the 3D7/HP1-Control cell line (right panel, *p* value > 0.05; unpaired two-tailed Student' t-test). **(C)** PfEMP1 expression in DMSO- and RAP-treated PfHP1-PbHP1 hybrid mutants and control cell lines in the progeny at late ring stage (LR, 16-24 hpi, generation 2; 64 hrs after rapamycin treatment) as determined by IFA using a-ATS antibodies recognizing the conserved ATS domain of PfEMP1 (M. F. Duffy et al., 2002). The percentages of PfEMP1-positive iRBCs are indicated for each population. Values represent the mean of two independent experiments (+/-SD) (3D7/HP1-Control) and a single experiment (3D7/HP1-hyb-PbHinge and 3D7/HP1-hyb-PbCSD). At least 200 iRBCs counted per sample. Nuclei were stained with DAPI. DIC, differential interference contrast. Scale bar, 5µm.

Figure 1

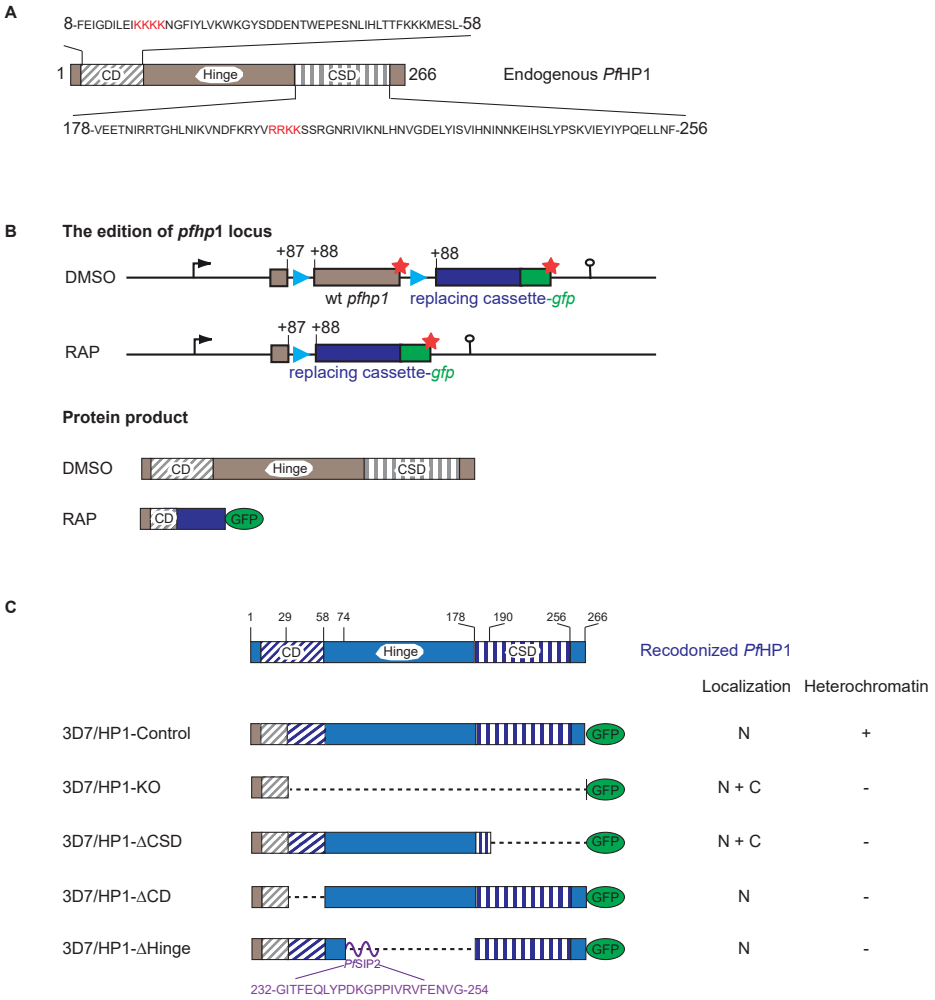
A
8-FEIGDILEIKKKKNGFIYLVKWKGYSDDENTWEPESNLIHLTTFKKKMESL-58
1
CD
Hinge
CSD
266
Endogenous PfHP1
178-VEETNIRRTGHLNIKVNDFKRYVRRKKSSRGNRIVIKNLHNVGDELYISVIHNINNKEIHSLYPSKVIEYIYPQELLNF-256
B
The edition of pfhp1 locus
DMSO
+87 +88
+88
wt pfhp1
replacing cassette-gfp
RAP
+87 +88
replacing cassette-gfp
Protein product
DMSO
CD
Hinge
CSD
RAP
CD
GFP
C
1 29 58 74 178 190 256 266
CD
Hinge
CSD
Recodonized PfHP1
Localization
Heterochromatin
3D7/HP1-Control
GFP
N
+
3D7/HP1-KO
GFP
N + C
-
3D7/HP1-ΔCSD
GFP
N + C
-
3D7/HP1-ΔCD
GFP
N
-
3D7/HP1-ΔHinge
GFP
N
-
PfSIP2
232-GITFEQLYPDKGPPIVRVFENVG-254

Figure 2

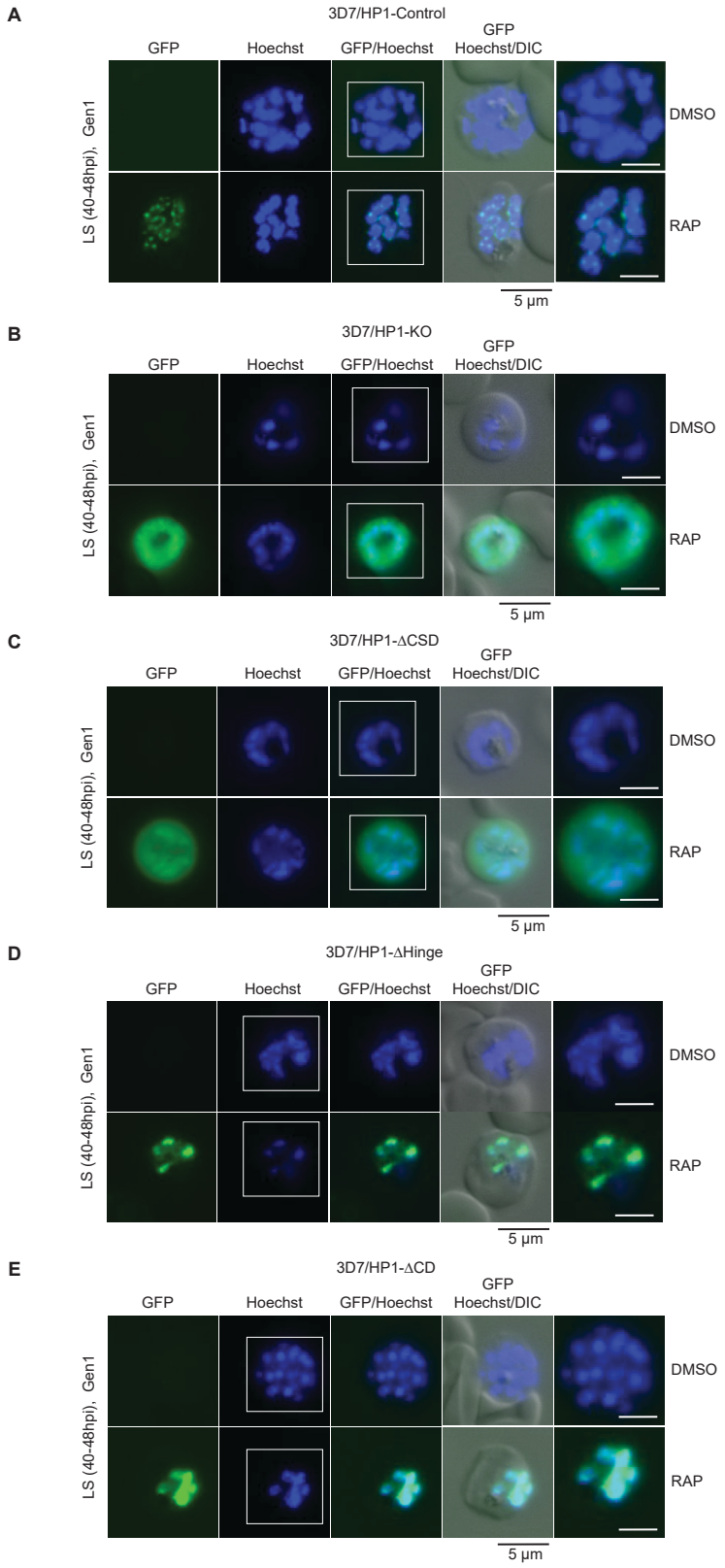
A
3D7/HP1-Control
GFP
Hoechst
GFP/Hoechst
GFP
Hoechst/DIC
LS (40-48hpi), Gen1
DMSO
RAP
5 µm
B
3D7/HP1-KO
C
3D7/HP1-ΔCSD
D
3D7/HP1-ΔHinge
E
3D7/HP1-ΔCD

Figure 3

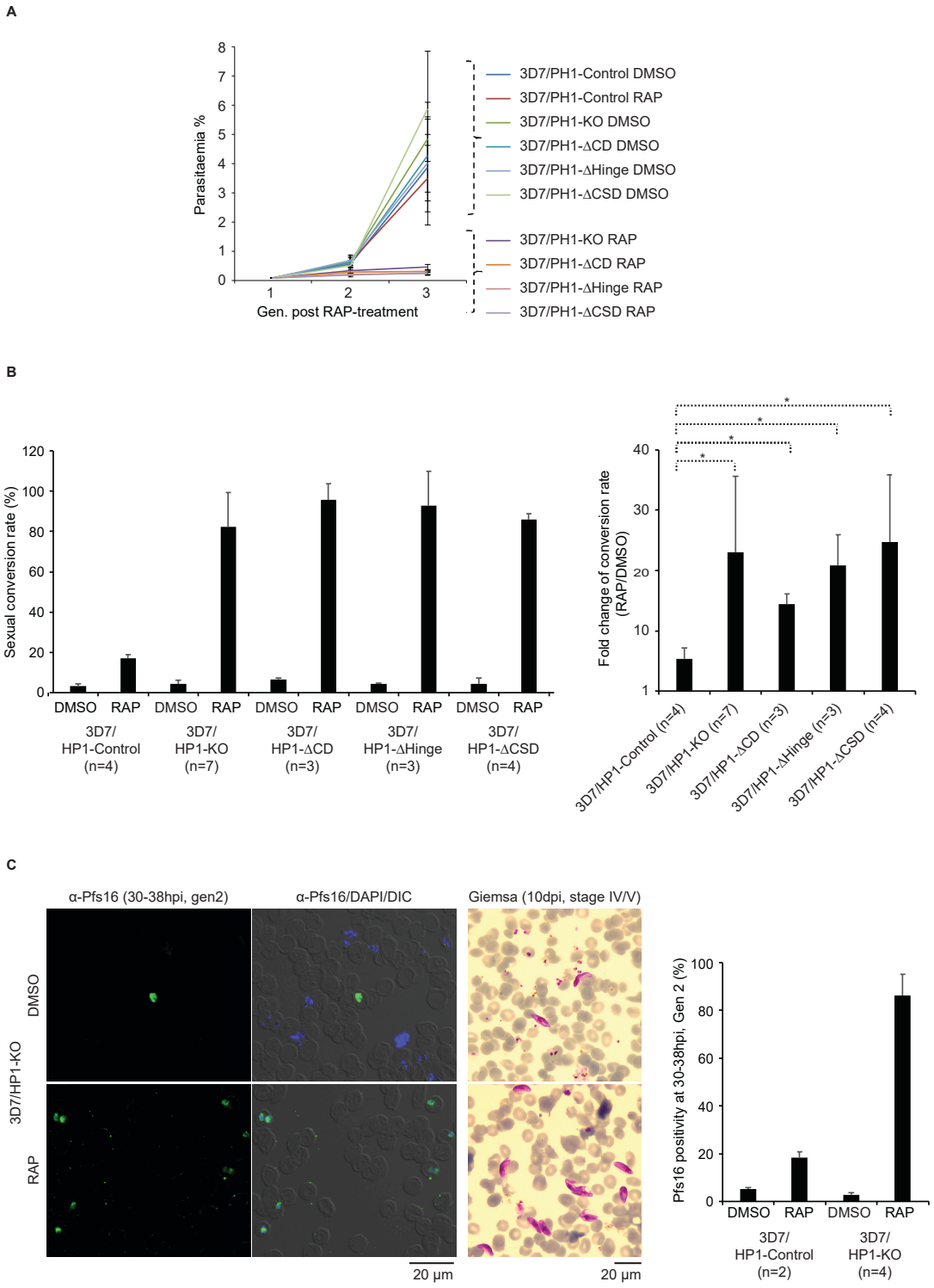
A
Parasitaemia %
Gen. post RAP-treatment
3D7/PH1-Control DMSO
3D7/PH1-Control RAP
3D7/PH1-KO DMSO
3D7/PH1-ΔCD DMSO
3D7/PH1-ΔHinge DMSO
3D7/PH1-ΔCSD DMSO
3D7/PH1-KO RAP
3D7/PH1-ΔCD RAP
3D7/PH1-ΔHinge RAP
3D7/PH1-ΔCSD RAP
B
Sexual conversion rate (%)
DMSO RAP DMSO RAP DMSO RAP DMSO RAP DMSO RAP
3D7/ HP1-Control (n=4)
3D7/ HP1-KO (n=7)
3D7/ HP1-ΔCD (n=3)
3D7/ HP1-ΔHinge (n=3)
3D7/ HP1-ΔCSD (n=4)
Fold change of conversion rate (RAP/DMSO)
3D7/HP1-Control (n=4)
3D7/HP1-KO (n=7)
3D7/HP1-ΔCD (n=3)
3D7/HP1-ΔHinge (n=3)
3D7/HP1-ΔCSD (n=4)
C
α-Pfs16 (30-38hpi, gen2)
α-Pfs16/DAPI/DIC
Giemsa (10dpi, stage IV/V)
3D7/HP1-KO
DMSO
RAP
20 µm
20 µm
Pfs16 positivity at 30-38hpi, Gen 2 (%)
DMSO RAP DMSO RAP
3D7/ HP1-Control (n=2)
3D7/ HP1-KO (n=4)

Figure 4

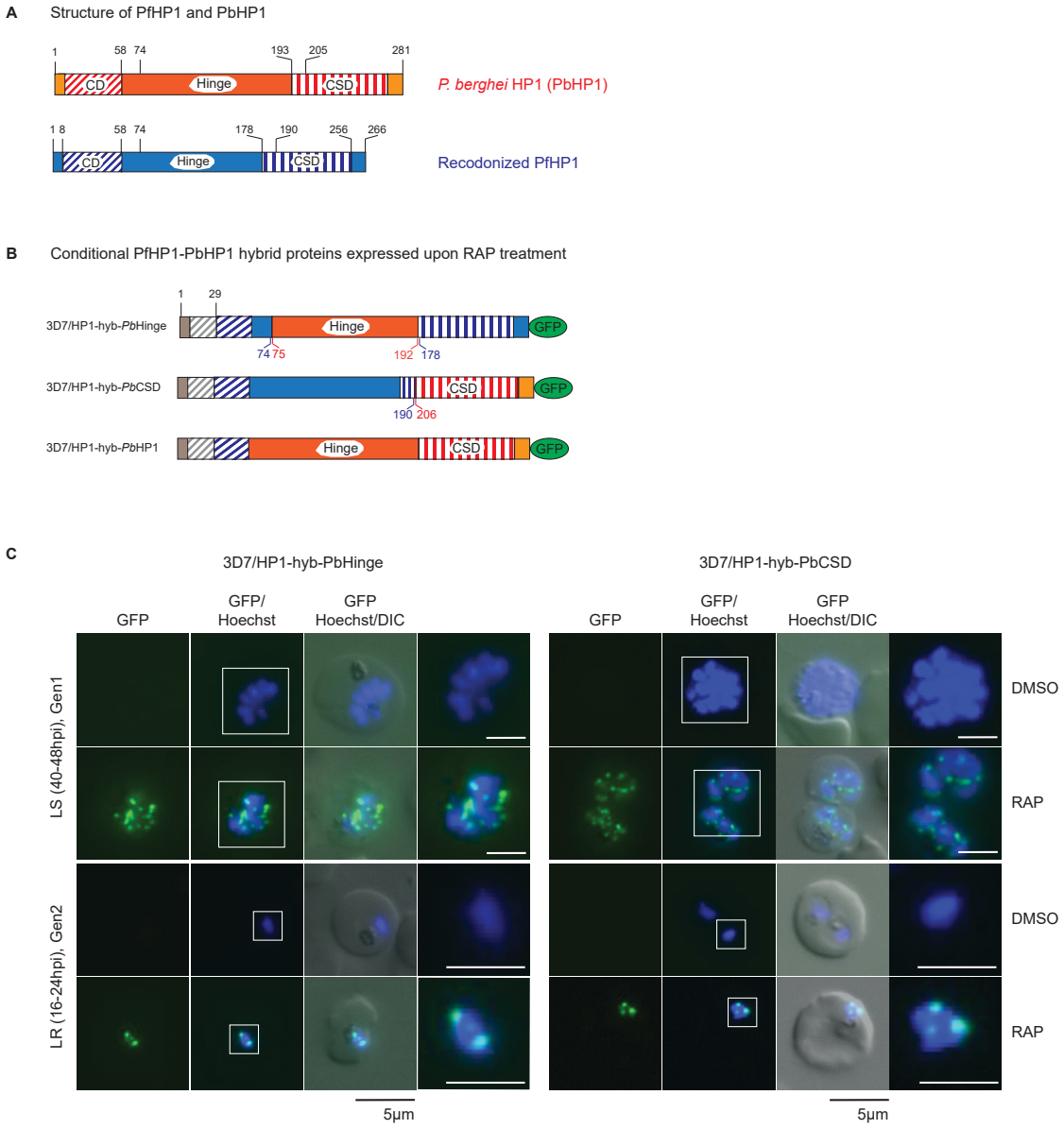
A
Structure of PfHP1 and PbHP1
1
58
74
193
205
281
CD
Hinge
CSD
P. berghei HP1 (PbHP1)
1 8
58
74
178
190
256
266
CD
Hinge
CSD
Recodonized PfHP1
B
Conditional PfHP1-PbHP1 hybrid proteins expressed upon RAP treatment
1
29
3D7/HP1-hyb-PbHinge
Hinge
GFP
74 75
192 178
3D7/HP1-hyb-PbCSD
CSD
GFP
190 206
3D7/HP1-hyb-PbHP1
Hinge
CSD
GFP
C
3D7/HP1-hyb-PbHinge
3D7/HP1-hyb-PbCSD
GFP
GFP/ Hoechst
GFP Hoechst/DIC
LS (40-48hpi), Gen1
LR (16-24hpi), Gen2
DMSO
RAP
DMSO
RAP
5µm
5µm

Figure 5

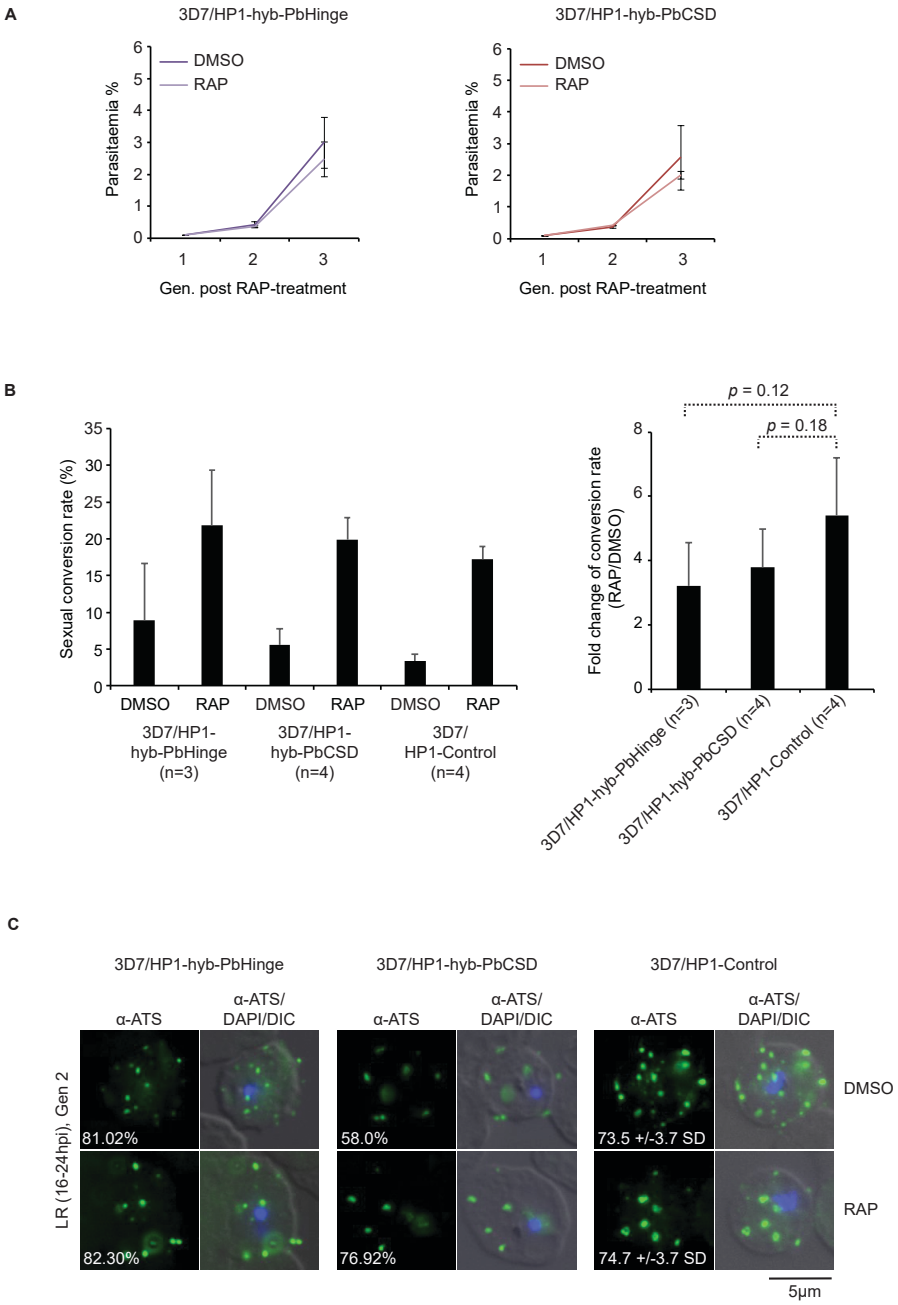
A
3D7/HP1-hyb-PbHinge
3D7/HP1-hyb-PbCSD
DMSO
RAP
Parasitaemia %
Gen. post RAP-treatment
B
Sexual conversion rate (%)
DMSO
RAP
3D7/HP1-hyb-PbHinge (n=3)
3D7/HP1-hyb-PbCSD (n=4)
3D7/HP1-Control (n=4)
p = 0.12
p = 0.18
Fold change of conversion rate (RAP/DMSO)
C
3D7/HP1-hyb-PbHinge
3D7/HP1-hyb-PbCSD
3D7/HP1-Control
α-ATS
α-ATS/ DAPI/DIC
LR (16-24hpi), Gen 2
DMSO
RAP
81.02%
58.0%
73.5 +/-3.7 SD
82.30%
76.92%
74.7 +/-3.7 SD
5µm

3.6 References

Aasland, R., Stewart, A.F., 1995. The chromo shadow domain, a second chromo domain in heterochromatin-binding protein 1, HP1. Nucleic Acids Res. 23, 3168–3173.

Allshire, R.C., Nimmo, E.R., Ekwall, K., Javerzat, J.P., Cranston, G., 1995. Mutations derepressing silent centromeric domains in fission yeast disrupt chromosome segregation. Genes Dev 9, 218–233. doi:10.1101/gad.9.2.218

Amit-Avraham, I., Pozner, G., Eshar, S., Fastman, Y., Kolevzon, N., Yavin, E., Dzikowski, R., 2015. Antisense long noncoding RNAs regulate var gene activation in the malaria parasite Plasmodium falciparum. Proc. Natl. Acad. Sci. U.S.A. 112, E982–91. doi:10.1073/pnas.1420855112

Armstrong, C.M., Goldberg, D.E., 2007. An FKBP destabilization domain modulates protein levels in Plasmodium falciparum. Nat Meth. 4, 1007–1009. doi:10.1038/nmeth1132

Bannister, A.J., Zegerman, P., Partridge, J.F., Miska, E.A., Thomas, J.O., Allshire, R.C., Kouzarides, T., 2001. Selective recognition of methylated lysine 9 on histone H3 by the HP1 chromo domain. Nature 410, 120–124. doi:10.1038/35065138

Bernard, P., Maure, J.F., Partridge, J.F., Genier, S., Javerzat, J.P., Allshire, R.C., 2001. Requirement of heterochromatin for cohesion at centromeres. Science 294, 2539–2542. doi:10.1126/science.1064027

Brameier, M., Krings, A., MacCallum, R.M., 2007. NucPred--predicting nuclear localization of proteins. Bioinformatics 23, 1159–1160. doi:10.1093/bioinformatics/btm066

Brancucci, N.M.B., Bertschi, N.L., Zhu, L., Niederwieser, I., Chin, W.H., Wampfler, R., Freymond, C., Rottmann, M., Felger, I., Bozdech, Z., Voss, T.S., 2014. Heterochromatin protein 1 secures survival and transmission of malaria parasites. Cell Host Microbe 16, 165–176. doi:10.1016/j.chom.2014.07.004

Brancucci, N.M.B., Gerdt, J.P., Wang, C., De Niz, M., Philip, N., Adapa, S.R., Zhang, M., Hitz, E., Niederwieser, I., Boltryk, S.D., Laffitte, M.-C., Clark, M.A., Grüring, C., Ravel, D., Blancke Soares, A., Demas, A., Bopp, S., Rubio-Ruiz, B., Conejo-Garcia, A., Wirth, D.F., Gendaszewska-Darmach, E., Duraisingh, M.T., Adams, J.H., Voss, T.S., Waters, A.P., Jiang, R.H.Y., Clardy, J., Marti, M., 2017. Lysophosphatidylcholine Regulates Sexual Stage Differentiation in the Human Malaria Parasite Plasmodium falciparum. Cell 171, 1532–1544.e15. doi:10.1016/j.cell.2017.10.020

Bunnik, E.M., Cook, K.B., Varoquaux, N., Batugedara, G., Prudhomme, J., Cort, A., Shi, L., Andolina, C., Ross, L.S., Brady, D., Fidock, D.A., Nosten, F., Tewari, R., Sinnis, P., Ay, F., Vert, J.-P., Noble, W.S., Le Roch, K.G., 2018. Changes in genome organization of parasite-specific gene families during the Plasmodium transmission stages. Nat Commun 9, 1910–15. doi:10.1038/s41467-018-04295-5

Collins, C.R., Das, S., Wong, E.H., Andenmatten, N., Stallmach, R., Hackett, F., Herman, J.-P., Müller, S., Meissner, M., Blackman, M.J., 2013. Robust inducible Cre recombinase activity in the human malaria parasite Plasmodium falciparum enables efficient gene deletion within a single asexual erythrocytic growth cycle. Mol. Microbiol. 88, 687–701. doi:10.1111/mmi.12206

Cowman, A.F., Healer, J., Marapana, D., Marsh, K., 2016. Malaria: Biology and Disease. Cell 167, 610–624. doi:10.1016/j.cell.2016.07.055

Dingwall, C., Laskey, R.A., 1991. Nuclear targeting sequences--a consensus? Trends Biochem. Sci. 16, 478–481.

Duffy, M.F., Brown, G.V., Basuki, W., Krejany, E.O., Noviyanti, R., Cowman, A.F., Reeder, J.C., 2002. Transcription of multiple var genes by individual, trophozoite-stage Plasmodium falciparum cells expressing a chondroitin sulphate A binding phenotype. Mol. Microbiol. 43, 1285–1293.

Duffy, S., Loganathan, S., Holleran, J.P., Avery, V.M., 2016. Large-scale production of Plasmodium falciparum gametocytes for malaria drug discovery. Nat Protoc 11, 976–992. doi:10.1038/nprot.2016.056

Duraisingh, M.T., Voss, T.S., Marty, A.J., Duffy, M.F., Good, R.T., Thompson, J.K., Freitas-Junior, L.H., Scherf, A., Crabb, B.S., Cowman, A.F., 2005. Heterochromatin silencing and locus

repositioning linked to regulation of virulence genes in Plasmodium falciparum. Cell 121, 13–24. doi:10.1016/j.cell.2005.01.036

Dzikowski, R., Frank, M., Deitsch, K., 2006. Mutually exclusive expression of virulence genes by malaria parasites is regulated independently of antigen production. PLoS Pathog. 2, e22. doi:10.1371/journal.ppat.0020022

Eissenberg, J.C., James, T.C., Foster-Hartnett, D.M., Hartnett, T., Ngan, V., Elgin, S.C., 1990. Mutation in a heterochromatin-specific chromosomal protein is associated with suppression of position-effect variegation in Drosophila melanogaster. Proc. Natl. Acad. Sci. U.S.A. 87, 9923–9927.

Eksi, S., Morahan, B.J., Haile, Y., Furuya, T., Jiang, H., Ali, O., Xu, H., Kiattibutr, K., Suri, A., Czesny, B., Adeyemo, A., Myers, T.G., Sattabongkot, J., Su, X.-Z., Williamson, K.C., 2012. Plasmodium falciparum gametocyte development 1 (Pfgdv1) and gametocytogenesis early gene identification and commitment to sexual development. PLoS Pathog. 8, e1002964. doi:10.1371/journal.ppat.1002964

Epp, C., Li, F., Howitt, C.A., Chookajorn, T., Deitsch, K.W., 2009. Chromatin associated sense and antisense noncoding RNAs are transcribed from the var gene family of virulence genes of the malaria parasite Plasmodium falciparum. RNA 15, 116–127. doi:10.1261/rna.1080109

Filarsky, M., Fraschka, S.A., Niederwieser, I., Brancucci, N.M.B., Carrington, E., Carrió, E., Moes, S., Jenoe, P., Bartfai, R., Voss, T.S., 2018. GDV1 induces sexual commitment of malaria parasites by antagonizing HP1-dependent gene silencing. Science 359, 1259–1263. doi:10.1126/science.aan6042

Fischer, T., Cui, B., Dhakshnamoorthy, J., Zhou, M., Rubin, C., Zofall, M., Veenstra, T.D., Grewal, S.I.S., 2009. Diverse roles of HP1 proteins in heterochromatin assembly and functions in fission yeast. Proc. Natl. Acad. Sci. U.S.A. 106, 8998–9003. doi:10.1073/pnas.0813063106

Flueck, C., Bartfai, R., Niederwieser, I., Witmer, K., Alako, B.T.F., Moes, S., Bozdech, Z., Jenoe, P., Stunnenberg, H.G., Voss, T.S., 2010. A major role for the Plasmodium falciparum ApiAP2 protein PfSIP2 in chromosome end biology. PLoS Pathog. 6, e1000784. doi:10.1371/journal.ppat.1000784

Flueck, C., Bartfai, R., Volz, J., Niederwieser, I., Salcedo-Amaya, A.M., Alako, B.T.F., Ehlgen, F., Ralph, S.A., Cowman, A.F., Bozdech, Z., Stunnenberg, H.G., Voss, T.S., 2009. Plasmodium falciparum heterochromatin protein 1 marks genomic loci linked to phenotypic variation of exported virulence factors. PLoS Pathog. 5, e1000569.

Fraschka, S.A., Filarsky, M., Hoo, R., Niederwieser, I., Yam, X.Y., Brancucci, N.M.B., Mohring, F., Mushunje, A.T., Huang, X., Christensen, P.R., Nosten, F., Bozdech, Z., Russell, B., Moon, R.W., Marti, M., Preiser, P.R., Bartfai, R., Voss, T.S., 2018. Comparative Heterochromatin Profiling Reveals Conserved and Unique Epigenome Signatures Linked to Adaptation and Development of Malaria Parasites. Cell Host Microbe 23, 407–420.e8. doi:10.1016/j.chom.2018.01.008

Freitas-Junior, L.H., Hernandez-Rivas, R., Ralph, S.A., Montiel-Condado, D., Ruvalcaba-Salazar, O.K., Rojas-Meza, A.P., Mancio-Silva, L., Leal-Silvestre, R.J., Gontijo, A.M., Shorte, S., Scherf, A., 2005. Telomeric heterochromatin propagation and histone acetylation control mutually exclusive expression of antigenic variation genes in malaria parasites. Cell 121, 25–36. doi:10.1016/j.cell.2005.01.037

Grewal, S.I.S., Moazed, D., 2003. Heterochromatin and epigenetic control of gene expression. Science 301, 798–802. doi:10.1126/science.1086887

Horsley, D., Hutchings, A., Butcher, G.W., Singh, P.B., 1996. M32, a murine homologue of Drosophila heterochromatin protein 1 (HP1), localises to euchromatin within interphase nuclei and is largely excluded from constitutive heterochromatin. Cytogenet. Cell Genet. 73, 308–311. doi:10.1159/000134363

James, T.C., Eissenberg, J.C., Craig, C., Dietrich, V., Hobson, A., Elgin, S.C., 1989. Distribution patterns of HP1, a heterochromatin-associated nonhistone chromosomal protein of Drosophila. Eur. J. Cell Biol. 50, 170–180.

James, T.C., Elgin, S.C., 1986. Identification of a nonhistone chromosomal protein associated with heterochromatin in Drosophila melanogaster and its gene. Mol. Cell. Biol. 6, 3862–3872.

Jiang, L., Mu, J., Zhang, Q., Ni, T., Srinivasan, P., Rayavara, K., Yang, W., Turner, L., Lavstsen, T., Theander, T.G., Peng, W., Wei, G., Jing, Q., Wakabayashi, Y., Bansal, A., Luo, Y., Ribeiro, J.M.C., Scherf, A., Aravind, L., Zhu, J., Zhao, K., Miller, L.H., 2013. PfSETvs methylation of histone H3K36 represses virulence genes in Plasmodium falciparum. Nature 499, 223–227. doi:10.1038/nature12361

Jones, M.L., Das, S., Belda, H., Collins, C.R., Blackman, M.J., Treeck, M., 2016. A versatile strategy for rapid conditional genome engineering using loxP sites in a small synthetic intron in Plasmodium falciparum. Sci Rep 6, 21800. doi:10.1038/srep21800

Kafsack, B.F.C., Rovira-Graells, N., Clark, T.G., Bancells, C., Crowley, V.M., Campino, S.G., Williams, A.E., Drought, L.G., Kwiatkowski, D.P., Baker, D.A., Cortés, A., Llinás, M., 2014. A transcriptional switch underlies commitment to sexual development in malaria parasites. Nature 507, 248–252. doi:10.1038/nature12920

Kalderon, D., Roberts, B.L., Richardson, W.D., Smith, A.E., 1984. A short amino acid sequence able to specify nuclear location. Cell 39, 499–509. doi:10.1016/0092-8674(84)90457-4

Knuepfer, E., Napiorkowska, M., van Ooij, C., Holder, A.A., 2017. Generating conditional gene knockouts in Plasmodium - a toolkit to produce stable DiCre recombinase-expressing parasite lines using CRISPR/Cas9. Sci Rep 7, 3881–12. doi:10.1038/s41598-017-03984-3

Kwon, S.H., Workman, J.L., 2011. The changing faces of HP1: From heterochromatin formation and gene silencing to euchromatic gene expression: HP1 acts as a positive regulator of transcription. Bioessays 33, 280–289. doi:10.1002/bies.201000138

Lachner, M., O'Carroll, D., Rea, S., Mechtler, K., Jenuwein, T., 2001. Methylation of histone H3 lysine 9 creates a binding site for HP1 proteins. Nature 410, 116–120. doi:10.1038/35065132

Lambros, C., Vanderberg, J.P., 1979. Synchronization of Plasmodium falciparum erythrocytic stages in culture. J. Parasitol. 65, 418–420.

Lomberk, G., Wallrath, L., Urrutia, R., 2006. The Heterochromatin Protein 1 family. Genome Biol. 7, 228. doi:10.1186/gb-2006-7-7-228

Lopez-Rubio, J.J., Gontijo, A.M., Nunes, M.C., Issar, N., Hernandez-Rivas, R., Scherf, A., 2007. 5' flanking region of var genes nucleate histone modification patterns linked to phenotypic inheritance of virulence traits in malaria parasites. Mol. Microbiol. 66, 1296–1305. doi:10.1111/j.1365-2958.2007.06009.x

Lopez-Rubio, J.J., Mancio-Silva, L., Scherf, A., 2009. Genome-wide analysis of heterochromatin associates clonally variant gene regulation with perinuclear repressive centers in malaria parasites. Cell Host Microbe 5, 179–190. doi:10.1016/j.chom.2008.12.012

Maison, C., Almouzni, G., 2004. HP1 and the dynamics of heterochromatin maintenance. Nat. Rev. Mol. Cell Biol. 5, 296–304. doi:10.1038/nrm1355

Minc, E., Allory, Y., Worman, H.J., Courvalin, J.C., Buendia, B., 1999. Localization and phosphorylation of HP1 proteins during the cell cycle in mammalian cells. Chromosoma 108, 220–234.

Minc, E., Courvalin, J.C., Buendia, B., 2000. HP1gamma associates with euchromatin and heterochromatin in mammalian nuclei and chromosomes. Cytogenet. Cell Genet. 90, 279–284.

Muchardt, C., Guilleme, M., Seeler, J.-S., Trouche, D., Dejean, A., Yaniv, M., 2002. Coordinated methyl and RNA binding is required for heterochromatin localization of mammalian HP1alpha. EMBO Rep. 3, 975–981. doi:10.1093/embo-reports/kvf194

Newbold, C., Warn, P., Black, G., Berendt, A., Craig, A., Snow, B., Msobo, M., Peshu, N., Marsh, K., 1997. Receptor-specific adhesion and clinical disease in Plasmodium falciparum. Am. J. Trop. Med. Hyg. 57, 389–398. doi:10.4269/ajtmh.1997.57.389

Nonaka, N., Kitajima, T., Yokobayashi, S., Xiao, G., Yamamoto, M., Grewal, S.I.S., Watanabe, Y., 2002. Recruitment of cohesin to heterochromatic regions by Swi6/HP1 in fission yeast. Nat. Cell Biol. 4, 89–93. doi:10.1038/ncb739

Pérez-Toledo, K., Rojas-Meza, A.P., Mancio-Silva, L., Hernández-Cuevas, N.A., Delgadillo, D.M., Vargas, M., Martínez-Calvillo, S., Scherf, A., Hernandez-Rivas, R., 2009. Plasmodium

falciparum heterochromatin protein 1 binds to tri-methylated histone 3 lysine 9 and is linked to mutually exclusive expression of var genes. Nucleic Acids Res. 37, 2596–2606. doi:10.1093/nar/gkp115

Platero, J.S., Hartnett, T., Eissenberg, J.C., 1995. Functional analysis of the chromo domain of HP1. EMBO J. 14, 3977–3986.

Ponnudurai, T., Lensen, A.H., Meis, J.F., Meuwissen, J.H., 1986. Synchronization of Plasmodium falciparum gametocytes using an automated suspension culture system. Parasitology 93 (Pt 2), 263–274. doi:10.1017/s003118200005143x

Powers, J.A., Eissenberg, J.C., 1993. Overlapping domains of the heterochromatin-associated protein HP1 mediate nuclear localization and heterochromatin binding. J. Cell Biol. 120, 291–299. doi:10.1083/jcb.120.2.291

Ralph, S.A., Scheidig-Benatar, C., Scherf, A., 2005. Antigenic variation in Plasmodium falciparum is associated with movement of var loci between subnuclear locations. Proc. Natl. Acad. Sci. U.S.A. 102, 5414–5419. doi:10.1073/pnas.0408883102

Reeder, J.C., Brown, G.V., 1996. Antigenic variation and immune evasion in Plasmodium falciparum malaria. Immunol. Cell Biol. 74, 546–554. doi:10.1038/icb.1996.88

Rowe, J.A., Claessens, A., Corrigan, R.A., Arman, M., 2009. Adhesion of Plasmodium falciparum-infected erythrocytes to human cells: molecular mechanisms and therapeutic implications. Expert Rev Mol Med 11, e16. doi:10.1017/S1462399409001082

Salcedo-Amaya, A.M., van Driel, M.A., Alako, B.T., Trelle, M.B., van den Elzen, A.M.G., Cohen, A.M., Janssen-Megens, E.M., van de Vegte-Bolmer, M., Selzer, R.R., Iniguez, A.L., Green, R.D., Sauerwein, R.W., Jensen, O.N., Stunnenberg, H.G., 2009. Dynamic histone H3 epigenome marking during the intraerythrocytic cycle of Plasmodium falciparum. Proc. Natl. Acad. Sci. U.S.A. 106, 9655–9660. doi:10.1073/pnas.0902515106

Saliba, K.S., Jacobs-Lorena, M., 2013. Production of Plasmodium falciparum gametocytes in vitro. Methods Mol. Biol. 923, 17–25. doi:10.1007/978-1-62703-026-7_2

Sinha, A., Hughes, K.R., Modrzynska, K.K., Otto, T.D., Pfander, C., Dickens, N.J., Religa, A.A., Bushell, E., Graham, A.L., Cameron, R., Kafsack, B.F.C., Williams, A.E., Llinás, M., Berriman, M., Billker, O., Waters, A.P., 2014. A cascade of DNA-binding proteins for sexual commitment and development in Plasmodium. Nature. 507, 253-257. doi:10.1038/nature12970

Tonkin, C.J., Carret, C.K., Duraisingh, M.T., Voss, T.S., Ralph, S.A., Hommel, M., Duffy, M.F., Silva, L.M.D., Scherf, A., Ivens, A., Speed, T.P., Beeson, J.G., Cowman, A.F., 2009. Sir2 paralogues cooperate to regulate virulence genes and antigenic variation in Plasmodium falciparum. PLoS Biol 7, e84. doi:10.1371/journal.pbio.1000084

Trager, W., Jensen, J.B., 1976. Human malaria parasites in continuous culture. Science 193, 673–675.

Vermaak, D., Henikoff, S., Malik, H.S., 2005. Positive selection drives the evolution of rhino, a member of the heterochromatin protein 1 family in Drosophila. PLoS Genet. 1, 96–108. doi:10.1371/journal.pgen.0010009

Volz, J.C., Bartfai, R., Petter, M., Langer, C., Josling, G.A., Tsuboi, T., Schwach, F., Baum, J., Rayner, J.C., Stunnenberg, H.G., Duffy, M.F., Cowman, A.F., 2012. PfSET10, a Plasmodium falciparum methyltransferase, maintains the active var gene in a poised state during parasite division. Cell Host Microbe 11, 7–18. doi:10.1016/j.chom.2011.11.011

Voss, T.S., Bozdech, Z., Bartfai, R., 2014. Epigenetic memory takes center stage in the survival strategy of malaria parasites. Curr. Opin. Microbiol. 20, 88–95. doi:10.1016/j.mib.2014.05.007

Voss, T.S., Healer, J., Marty, A.J., Duffy, M.F., Thompson, J.K., Beeson, J.G., Reeder, J.C., Crabb, B.S., Cowman, A.F., 2006. A var gene promoter controls allelic exclusion of virulence genes in Plasmodium falciparum malaria. Nature 439, 1004–1008. doi:10.1038/nature04407

Wang, G., Ma, A., Chow, C.M., Horsley, D., Brown, N.R., Cowell, I.G., Singh, P.B., 2000. Conservation of heterochromatin protein 1 function. Mol. Cell. Biol. 20, 6970–6983.

Wang, J., Jia, S.T., Jia, S., 2016. New Insights into the Regulation of Heterochromatin. Trends Genet. 32, 284–294. doi:10.1016/j.tig.2016.02.005

Witmer, K., Fraschka, S.A., Vlachou, D., Bartfai, R., Christophides, G.K., 2019. Epigenetic regulation underlying Plasmodium berghei gene expression during its developmental transition from host to vector. bioRxiv 41, 646430. doi:10.1101/646430

Witmer, K., Schmid, C.D., Brancucci, N.M.B., Luah, Y.-H., Preiser, P.R., Bozdech, Z., Voss, T.S., 2012. Analysis of subtelomeric virulence gene families in Plasmodium falciparum by comparative transcriptional profiling. Mol. Microbiol. 84, 243–259. doi:10.1111/j.1365-2958.2012.08019.x

Yi, Q., Chen, Q., Liang, C., Yan, H., Zhang, Z., Xiang, X., Zhang, M., Qi, F., Zhou, L., Wang, F., 2018. HP1 links centromeric heterochromatin to centromere cohesion in mammals. EMBO Rep. 19, 120. doi:10.15252/embr.201745484

Zeng, W., Ball, A.R., Yokomori, K., 2010. HP1: heterochromatin binding proteins working the genome. Epigenetics 5, 287–292.

3.7 Supplementary Information

This Supplementary Information includes:

Supplementary method 1

Figure S1 to S5

Tables S1

Supplementary method 1. The generation of pBCam-ΔHinge-3HA-Cherry, pBCam-hyb-PbHinge-3HA-Cherry and pBCam-hyb-PbCSD-3HA-Cherry plasmids

The pBCam-ΔHinge-3HA-Cherry was constructed as follows. The fragment PfCD spanning bps +1 to +222 of the re-*pfhp1* sequence was amplified from a pUC57 plasmid containing a synthetic recodonized *pfhp1* coding sequence (pUC57-re-*pfhp1)* (GenScript™) using primers F11 and R148. The fragment PfSIP2.linker spanning bps +694 to +762 of the *pfsip2* coding sequence was amplified from 3D7 gDNA using primers F4 and R5. The fragment PfCSD spanning bps +532 to +798 of the *re-pfhp1* sequence, omitting stop codon was amplified from pUC57-re-*pfhp1* using primers F2 and R3. A hybrid fragment of PfSIP2.linker/PfCSD was amplified by fusion PCR from a mixture of PfSIP2.linker and PfCSD PCR templates using primer F4 and R3. The final hybrid fragment of PfCD/PfSIP2.linker/PfCSD was amplified by fusion PCR from a mixture of PfCD and PfSIP2.linker/PfCSD PCR templates using primers F11 and R3 and cloned into pBCam-3HA –Cherry using *Bam*HI and *Nhe*I and T4 DNA ligase.

The pBCam-hyb-PbHinge-3HA-Cherry was constructed as follows. The fragment PfCD spanning bps +1 to +222 of the *re-pfhp1* sequence was amplified from pUC57-re-*pfhp1* using primers F11 and R1. The fragment PbHinge spanning bps +223 to +576 of the *pbhp1* sequence was amplified from *P. berghei* gDNA using primers F35 and R36. The fragment PfCSD spanning bps +532 to +798 of the *re-pfhp1* sequence, omitting stop codon was amplified from pUC57-re-*pfhp1* using primers F2 and R42. A hybrid fragment of PfCD/PbHinge was amplified by fusion PCR from a mixture of PfCD and PbHinge PCR templates using primer F11 and R36. The final hybrid fragment of PfCD/PbHinge/PfCSD was amplified by fusion PCR from a mixture of PfCD/PbHinge and PfCSD PCR templates using primers F11 and R42 and cloned into pBCam-3HA – Cherry using *Bam*HI and *Not*I.

The pBCam-hyb-PbCSD-3HA-Cherry was constructed as follows. The fragment PfCD.Hinge spanning bps +1 to +570 of the *re-pfhp1* sequence was amplified from pUC57-re-*pfhp1* using primers F11 and R12. The fragment PbCSD spanning bps +616 to +843 of the *pbhp1* sequence, omitting stop codon was amplified from *P. berghei* gDNA using primers F38 and R41. A hybrid fragment of PfCD.Hinge/PbCSD was amplified by fusion PCR from a mixture of PfCD.Hinge and PbCSD PCR templates using primers F11 and R41 and cloned into pBCam-3HA–Cherry using *Bam*HI and *Not*I.

Supplementary Figures

Figure S1. Two-step CRISP/Cas9-based gene editing strategy to generate DiCre-inducible PfHP1 truncation and PfHP1-PbHP1 hybrid cell lines.

(A) First gene editing step: Schematic maps of the *pfhp1* locus (PF3D7_1220900) in 3D7/1G5DiCre parasites (top), the co-transfected pFDon-N31 donor plasmid and pHF_gC-guide31 CRISPR/Cas9 transfection vector (center), and the modified *pfhp1* locus after CRISPR/Cas9-based gene editing in 3D7/N31DC parasites (bottom). The nucleotide positions of the sgt_*pfhp1*-5' sgRNA target sequence is indicated (chromosome 12 coordinates). The pFDon-N31 donor plasmid contains a 103 bp *sera2* intron:loxP element (light blue triangle) (Jones et al., 2016) flanked by two homology regions (HR) (brown, black) for homology-directed repair. The pHF_gC-guide31 plasmid contains expression cassettes for SpCas9 (dark grey), the sgRNA (purple) and the h*dhfr-yfcu* fusion selection marker (light grey-dark brown). Second gene editing step: Schematic maps of the *pfhp1* locus in 3D7/N31DC parasites (top), the co-transfected pD_HP1 donor plasmids and pBF_gC-guide250 CRISPR/Cas9 transfection vector (center), and the modified *pfhp1* locus after CRISPR/Cas9-based gene editing in 3D7/HP1-Control, 3D7/HP1-KO and 3D7/HP1-hyb-PbCSD are shown as examples (bottom). The nucleotide positions of the sgt_*pfhp1*-3' sgRNA target sequence is indicated (chromosome 12 coordinates). The pD_HP1 donor plasmids contain an assembly of the 103 bp *sera2* intron:loxP element (light blue triangle) and the replacing cassette (dark blue) fused to *gfp* (green) flanked by two homology regions (HR) (brown, black) for homology-directed repair. The pBF_gC-guide250 plasmid contains expression cassettes for SpCas9 (dark grey), the sgRNA (purple) and the *bsd-yfcu* fusion selection marker (light grey-brown). Red stars represent STOP codons. Numbers refer to the nucleotide position within the *pfhp1* coding sequence. The black arrowheads indicate the binding sites of the F119 and R157 primers used to confirm correct gene editing of the *pfhp1* locus and efficient DiCre-mediated excision upon rapamycin treatment by PCR on genomic DNA.

Figure S2. Confirmation of successful generation of DiCre-inducible PfHP1 truncation and hybrid cell lines. (A) PCR confirmation of correct editing of the *pfhp1* locus and efficient excision of the endogenous *pfhp1* gene after RAP treatment. PCRs were

amplified from gDNA of 3D7/HP1-Control, 3D7/HP1-hyb-PbHinge, 3D7/HP1-hyb-PbCSD, 3D7/HP1-KO, 3D7/HP1-ΔCD, 3D7/HP1-ΔHinge, 3D7/HP1-ΔCSD cell lines in DMSO (-) and RAP (+) treated conditions. Using primers F119 and R157 (see Figure S1), correct editing of the *pfhp1* locus delivers a PCR product of 2250 bps in the 3D7/N31DC mother line prior to insertion of a replacing cassette-*gfp* fusion sequence. The length of the correctly edited *pfhp1* locus (-) and the length of the locus after efficient excision upon RAP treatment (+) from PfHP1 mutant cell lines were indicated at the bottom of the figure. The correct excision of floxed DNA after RAP treatment resulted in a decrease in the size of the corresponding PCR fragments in DMSO treated condition (-). **(B)** The efficiency of DiCre-mediated excision and resulting expression of GFP-tagged PfHP1s were quantified by the proportion of GFP-positive parasites in the paired DMSO- and RAP-treated samples in late schizonts (40-48 hpi, generation 1, 40 hrs after RAP-treatment). Values represent the mean of three independent biological replicates (>140 iRBCs scored for 3D7/HP1-hyb-PbHinge and 3D7/HP1-hyb-PbCSD populations and >200 iRBCs scored for other cell lines). Error bars indicate SD. The GFP-positive parasites in the DMSO- and RAP-treated populations of the 3D7/HP1-ΔCD and 3D7/HP1-ΔHinge were not determined. **(C)** Expression of GFP fusion from PfHP1 mutant cell lines were examined by Western blot in the ring progeny of DMSO- and RAP-treated populations from all seven transgenic cell lines (16-24 hpi, generation 2, 64 hrs after DMSO/RAP treatment). Immunoblot using α-PfHP1 antibodies revealed untagged wild type PfHP1 (~31 KDa) expressed in all DMSO treated samples. Immunoblot using α-GFP antibodies revealed GFP fusion proteins expressed in all RAP treated samples of 3D7/HP1-Control (57.87 KDa), 3D7/HP1-ΔCD (54.45 KDa), 3D7/HP1-ΔHinge (47.51 KDa), 3D7/HP1-ΔCSD (47.70 KDa), 3D7/HP1-KO (30.09 KDa), 3D7/HP1-hyb-PbHinge (57.72 KDa) and 3D7/HP1-hyb-PbCSD (56.77 KDa). The molecular weight of GFP fusion proteins were predicted using Protein Molecular Weight tool at genecorner.ugent.be. α-histone 4 (H4) antibodies were used as loading control.

Figure S3. Lack of Cre recombinase activity in a small subpopulations of transgenic cell lines. (A) The relative proportion of sexual and asexual subpopulation (RAPSUR) of RAP-treated 3D7/HP1-KO, 3D7/HP1-ΔCD, 3D7/HP1-ΔHinge, 3D7/HP1-ΔCSD populations in generation 3 (112 hrs after RAP treatment). Results are the mean of three independent replicates (>100 iRBCs counted per sample). Error bars indicate SD. **(B)** Examination of the *pfhp1* locus and the presence of DiCre cassette at *sera5* locus in

3D7/1G5DiCre, 3D7/N31DC lines and RAPSUR subpopulation of 3D7/HP1-KO, 3D7/HP1-ΔCD, 3D7/HP1-ΔHinge and 3D7/HP1-ΔCSD. PCR amplification using F119 and R157 revealed the correctly edited *pfhp1* locus in tested RAPSUR subpopulations. Primers *sera5* +27 and -25 confirmed wild type *sera5* locus, i.e absence of DiCre cassette (1.7 kb PCR products) while the primers *sera5* +27 and -11 confirmed correctly edited *sera5* locus, i.e presence of the DiCre cassette (1.9 kb PCR products) (Collins et al., 2013) in tested cell lines. The lack of DiCre cassette and/or ineffective activity of Cre recombinase resulted in the failure of DNA excision, thus, generating a proliferating asexual subpopulation in PfHP1 truncation cell lines after RAP treatment.

Figure S4. PfHP1 and PbHP1 are highly conserved in protein sequence. **(A)** Nucleotide sequences of the wild type (*pfhp1*) and recodonised (*pfhp1* re) *pfhp1* genes and amino acid sequence of PfHP1. Bases altered in the *pfhp1* re are highlighted in red letters. Numbers refer to the nucleotide position within the *pfhp1* coding sequence. **(B)** Alignment of PfHP1 and PbHP1 by EMBOSS Needle (https://www.ebi.ac.uk/Tools/psa/emboss_needle/). Conserved residues are marked by asterisks. The positions of the PfHP1 chromo- and chromoshadow domains are indicated (Flueck et al., 2009).

Figure S1

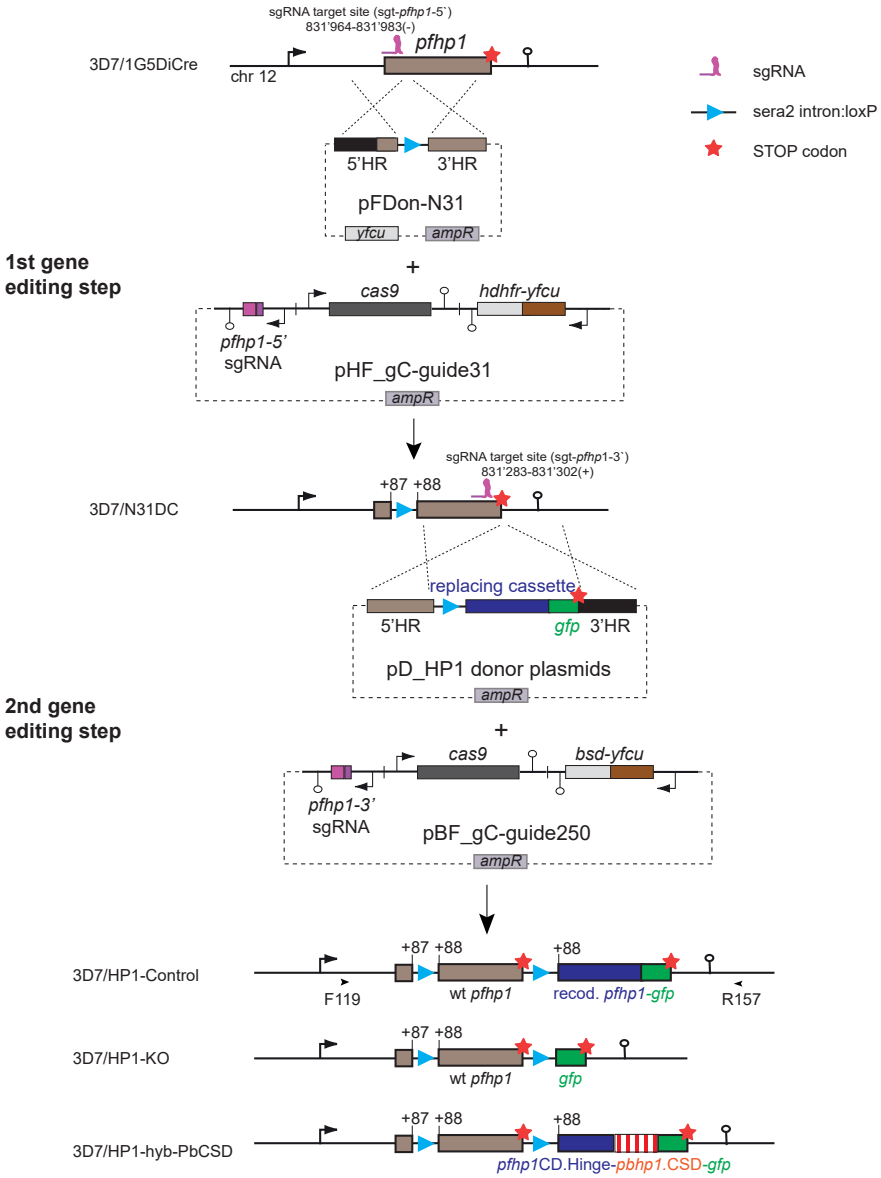
sgRNA target site (sgt-pfhp1-5')
831'964-831'983(-)
pfhp1
3D7/1G5DiCre
chr 12
sgRNA
sera2 intron:loxP
STOP codon
5'HR
3'HR
pFDon-N31
yfcu
ampR
1st gene editing step
+
cas9
hdhfr-yfcu
pfhp1-5'
sgRNA
pHF_gC-guide31
ampR
sgRNA target site (sgt-pfhp1-3')
831'283-831'302(+)
+87 +88
3D7/N31DC
replacing cassette
5'HR
gfp
3'HR
pD_HP1 donor plasmids
ampR
2nd gene editing step
+
cas9
bsd-yfcu
pfhp1-3'
sgRNA
pBF_gC-guide250
ampR
3D7/HP1-Control
+87 +88
+88
F119
wt pfhp1
recod. pfhp1-gfp
R157
3D7/HP1-KO
+87 +88
wt pfhp1
gfp
3D7/HP1-hyb-PbCSD
+87 +88
+88
pfhp1CD.Hinge-pbhp1.CSD-gfp

Figure S2

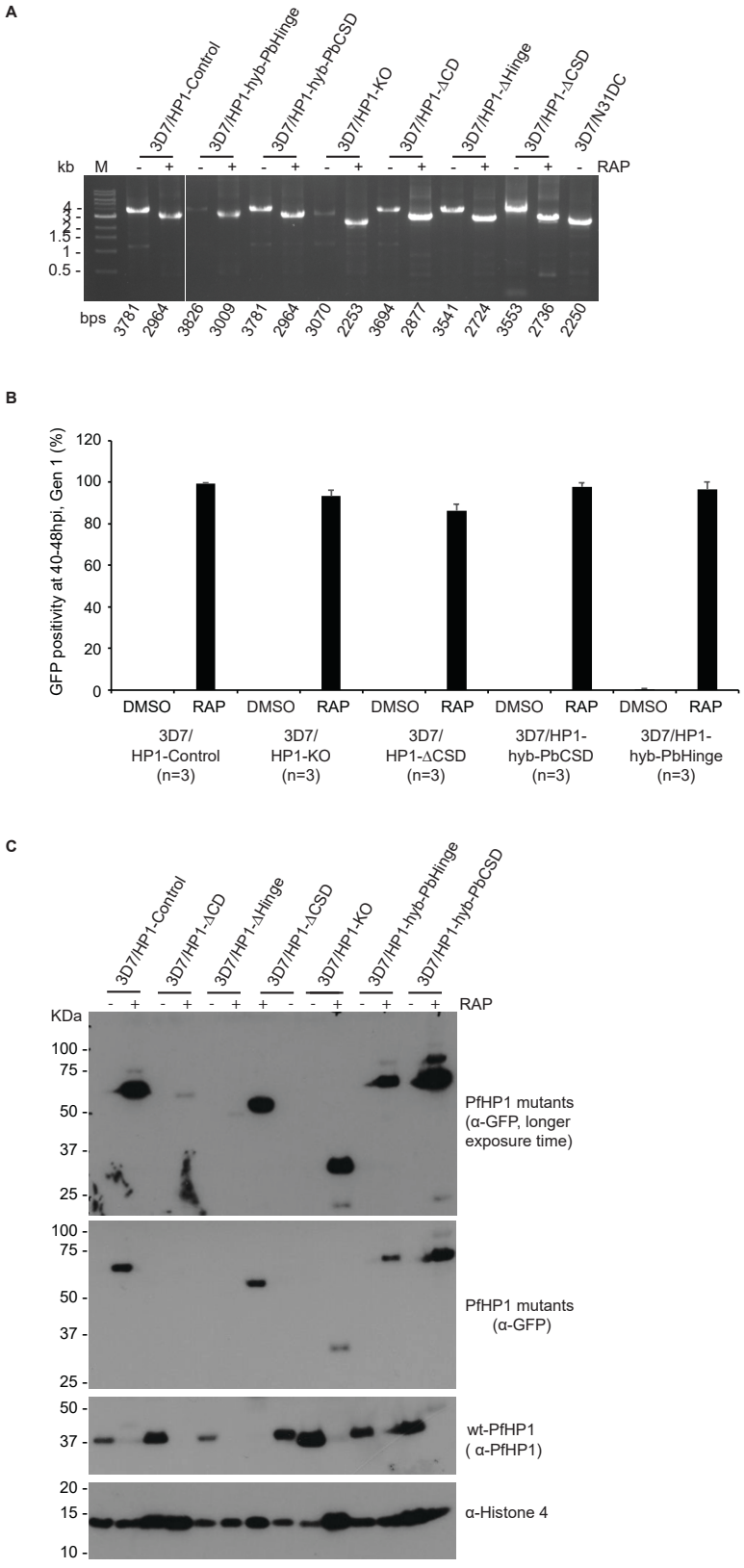
A
3D7/HP1-Control
3D7/HP1-hyb-PbHinge
3D7/HP1-hyb-PbCSD
3D7/HP1-KO
3D7/HP1-ΔCD
3D7/HP1-ΔHinge
3D7/HP1-ΔCSD
3D7/N31DC
kb M - + - + - + - + - + - + - + - RAP
4
3
2
1.5
1
0.5
bps 3781 2964 3826 3009 3781 2964 3070 2253 3694 2877 3541 2724 3553 2736 2250
B
GFP positivity at 40-48hpi, Gen 1 (%)
120
100
80
60
40
20
0
DMSO RAP DMSO RAP DMSO RAP DMSO RAP DMSO RAP
3D7/ HP1-Control (n=3)
3D7/ HP1-KO (n=3)
3D7/ HP1-ΔCSD (n=3)
3D7/HP1-hyb-PbCSD (n=3)
3D7/HP1-hyb-PbHinge (n=3)
C
3D7/HP1-Control
3D7/HP1-ΔCD
3D7/HP1-ΔHinge
3D7/HP1-ΔCSD
3D7/HP1-KO
3D7/HP1-hyb-PbHinge
3D7/HP1-hyb-PbCSD
- + - + - + + - - + - + - + RAP
KDa
100
75
50
37
25
PfHP1 mutants (α-GFP, longer exposure time)
PfHP1 mutants (α-GFP)
wt-PfHP1 (α-PfHP1)
20
15
10
α-Histone 4

Figure S3

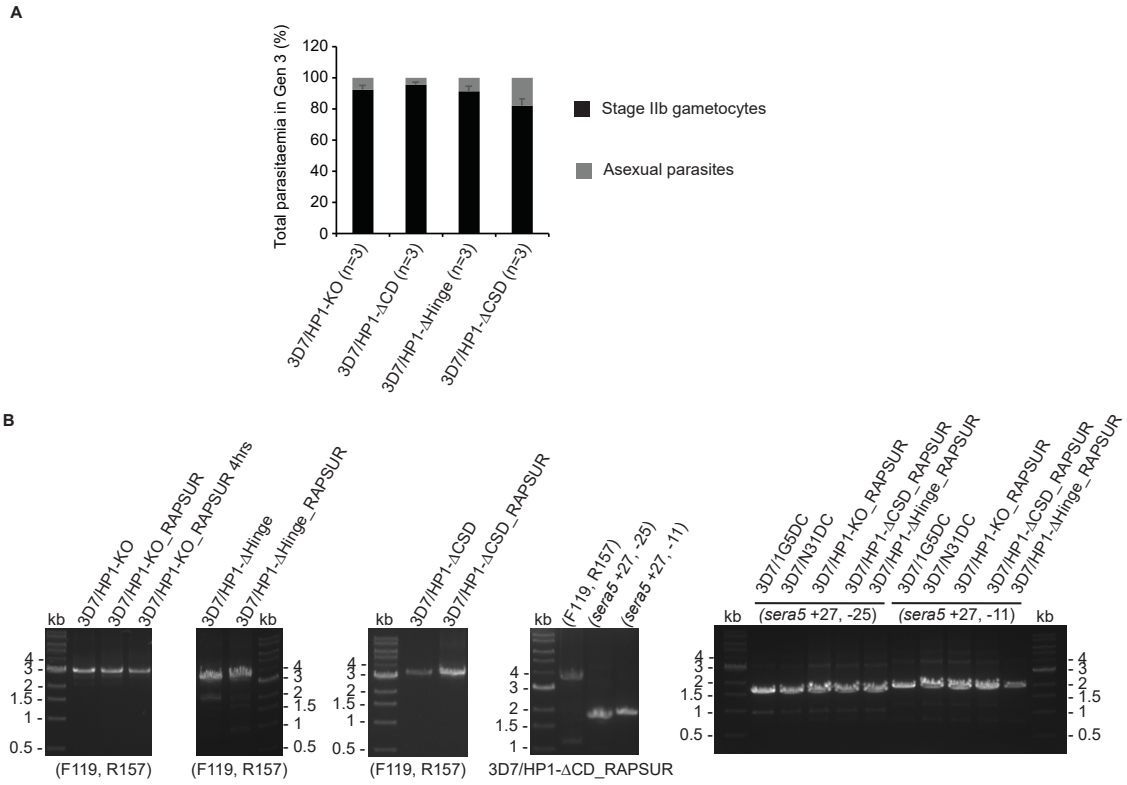
A
Total parasitaemia in Gen 3 (%)
120
100
80
60
40
20
0
Stage IIb gametocytes
Asexual parasites
3D7/HP1-KO (n=3)
3D7/HP1-ΔCD (n=3)
3D7/HP1-ΔHinge (n=3)
3D7/HP1-ΔCSD (n=3)
B
kb
3D7/HP1-KO
3D7/HP1-KO_RAPSUR
3D7/HP1-KO_RAPSUR 4hrs
(F119, R157)
3D7/HP1-ΔHinge
3D7/HP1-ΔHinge_RAPSUR
(F119, R157)
3D7/HP1-ΔCSD
3D7/HP1-ΔCSD_RAPSUR
(F119, R157)
(F119, R157)
(sera5 +27, -25)
(sera5 +27, -11)
3D7/HP1-ΔCD_RAPSUR
3D7/1G5DC
3D7/N31DC
3D7/HP1-KO_RAPSUR
3D7/HP1-ΔCSD_RAPSUR
3D7/HP1-ΔHinge_RAPSUR
3D7/1G5DC
3D7/N31DC
3D7/HP1-KO_RAPSUR
3D7/HP1-ΔCSD_RAPSUR
3D7/HP1-ΔHinge_RAPSUR
(sera5 +27, -25)
(sera5 +27, -11)
4
3
2
1.5
1
0.5

Figure S4

A

```
pfhp1      ATGACAGGGTCAGATGAAGAATTTGAAATTGGTGATATACTTGAAATAAAAAAAAAGAAGAATGGTTTTATTTATTTAGTAAAATGGAAAGGAT   94
             M T G S D E E F E I G D I L E I K K K K N G F I Y L V K W K G
pfhp1  re  ATGACAGGTAGTGATGAAGAATTTGAAATTGG AGATATA TT AGAAATT AAAAAGAAGAAAAATGGTTTTAT CTA CTTAGTAAAATGGAAAGGAT   94
pfhp1      ATTCAGATGATGAGAATACTTGGGAACCCGAAAGTAATTTAATACATTTGACAACATTTAAGAAAAAGATGGAAAGCTTAAAAACGAATTTTTT   188
             Y S D D E N T W E P E S N L I H L T T F K K K                                   M E S L K T N F L
pfhp1  re  AT AGTGATGATGA AAATAC ATGGGAACC AGAATCA AATTT GATT CATTTGACAAC TTTTAA AAAGAAAATGGAATCA TTAAAAAC AAATTT CTT  188
pfhp1      ATCGAAAGCTAATGAGACAAATGGTGATGGGAAAATTTTGAAAAATCATATATTAGCACCAACACAAGAAGACGATAGTATTAAATCAAAAGGT   282
             S  K A N E T N G D G K I L K N H I                       L  A  P  T  Q  E  D  D  S  I  K  S  K  G
pfhp1  re  ATCT AAAGCAAATGAAACAAATGGAGATGGT AAAATATT AAAGAATCATAT TTTAGCT CCAACACAAGAAGAT GATAGTAT AAAATCAAAAGGT  282
pfhp1      AGAAGTTCCTTAGCACCCCGACGAAAAATGAGTAGAAAAAGTTTAACGAACAAACTAGAAAATAAAAAGAACTTATCTTTATCAGACAATTCTT   376
             R  S  S  L  A  P  R  R  K  M  S  R  K  S  L  T  N  K  L  E  N  K  K  N  L  S  L  S  D  N  S
pfhp1  re  AGAAGTTC ATTAGCACC TA GAAGAAAAATGTC TAGAAAAAGTTTAAC AAATAAGTT AGAAAATAA GAAAAATTT GTC ATTATC T GAT AATTC AT  376
pfhp1      TAAAAAAAAGTGATGAAGAAGATAATGAATCTGTAAAACATGAGAATCACGTTAATGATGGAAATTTATTAAATGTTGAAGATGTATATAGCGT   470
             I K K S D E E D N E S V K H E N H V N D G N L L                                   N V E D V Y S V
pfhp1  re  TAAA GAAAAGTGATGAAGAAGATAATGAATCTGT TAAACATGA AATCA TGT AAATGATGGAAATTT GTTAAATGT AGAAGATGTT TATAG TGT  470
pfhp1      TCGTATTAAAAATAAGAAATTGGAGTTTTTGGCTAGCTTGAAAAATGAATCTCCACAATGGGTAGAAGAAACAAATATTAGAAGAACTGGACAT   564
             R  I K N K K L E F L A S L K N E S P Q W V E E T N I R R T                                 G H
pfhp1  re  AAGAATTAAAAATAAGAAATT AGAATTTTT AGCTTCT TT AAAGAATGAA AGTCCACAATGGGT TGAAGAAACAAATATTAGAAGAAC AGGT CAT  564
pfhp1      TTAAATATTAAAGTCAATGATTTTAAAAGATATGTAAGAAGAAAAAAAAAGTTCTAGGGGTAATAGAATAGTTATCAAAAATCTACACAACGTTG   658
             L N I K V N D F K R Y V R R K K S S R G N R I V I K N L H N V
pfhp1  re  TT GAATATTAAAGT TAATGATTTTAAAAGATATGT TAGAAGAAAGAAAAGT AGTAGAGGAAATAGAATAGATAGT AATT AAAAATTTGCAT AATGT AG  658
pfhp1      GAGATGAATTATATATTTCGGTTATTCATAATATAAATAATAAAGAAATTCATAGTTTATATCCTTCCAAAGTTATTGAATATATTTATCCACA   752
             G D E L Y I S V I H N I N N                       K E I H S L Y P S K V I E Y I Y P Q
pfhp1  re  GAGATGAATTATATAT AAGTGTTATTCATAATATAAATAATAA GGAAATTCATAGTTTATATCCTTC AAAAGTAAT AGAATATAT ATATCC TCA  752
pfhp1      GGAACTCTTAAATTTTTTATTATCAAGACTAAGATACCGTACAGCT                                                  798
             E  L L N F L L S R L R Y R T A
pfhp1  re  AGAATT ATTAAATTT CTTATT ATCAAGA TTAAGATA TA GAACAGCA                                               798
```

B

```
                                  Chromo domain
PfHP1     MTGSDEEFEIGDILEIKKKKNGFIYLVKWKGYSDDENTWEPESNLIHLTTFKKKMESLKT      60
PbHP1     MTGSDEEFEIGDILDVKRKKNGFIYLVKWKGYSDDENTWEPESNLLHLTDFKKKMEYLKS      60
          **************::*:*****************************:*** ****** **:

PfHP1     NFLSKANETNGDGKILKNHILAPTQED----DSIKSKGRSSLAPRRKMSRKSLTNKLEN-      115
PbHP1     IYLNKIDRTSSDSKIMKKNNVQLFDQDDMGNTLMKPKGRTTLISRKRGHKRGMRNRMRNR      120
           :*.* :.*..*.**:*:: :   ::*      :* ***::*  *::  ::.: *::.*

PfHP1     --------KKNLSLSDNSLKKSDEEDNESVKHENHVN--DGNLLNVEDVYSVRIKNKKLE      165
PbHP1     MRNRIGNKSSASSVTDGSLKKSDDDDNQSIKKESSSNNYNNTLLNIEDVYSVRIKNRKME      180
                  ..  *::*.******::**:*:*:*.  *  :..***:**********:*:*
                                 Chromoshadow domain
PfHP1     FLASLKNESPQWVEETNIRRTGHLNIKVNDFKRYVRRKKSSRGNRIVIKNLHNVGDELYI      225
PbHP1     FLASLKNASPQWVEESNIRSTGHLNIKVNDFKKYIKRKKTSKGSRIVIKNLHNVGDELYI      240
          ******* *******:*** ************:*::***:*:*.****************

          ____________________________________
PfHP1     SVIHNINNKEIHSLYPSKVIEYIYPQELLNFLLSRLRYRTA       266
PbHP1     SVIHNINNKEIHSLYPSKVIEYIYPQELLNFLLSRLRYRTV       281
          ***************************************.
```

Table S1. Primers and primer sequences used in the study of in-depth functional analysis of heterochromatin protein 1 in *Plasmodium falciparum*

Application	Primer	Sequence 5'-3'
PCR cloning transfection vectors	R1	TTT ACC ATC TCC ATT TGT TTC ATT TG
	F2	GTTGAAGAAACAAATATTAGAAGAAC
	R3	CAGT GCTAGC TGC TGT TCT ATA TCT TAA TCT TG
	F4	GAA ACA AAT GGA GAT GGT AAA GGA ATA ACC TTT GAA CAA TTA TAT C
	R5	CTA ATA TTT GTT TCT TCA AC ACC TAC ATT TTC AAA TAC TCG TAC
	F11	CAGT GGATCC AAAAA *ATGACAGGTAGTGATGAAG*
	R12	ATT CAA ATG ACC TGT TCT TC
	F35	CAAATGAAACAAATGGAGATGGTAAAATTATGAAAAAAAACAATGTACAG
	R36	GTT CTT CTA ATA TTT GTT TCT TCA ACC CAT TGT GGT GAT GCA TTT TTT AAG
	F38	*GAAGAACAGGTCATTTGAATATAAAAGTTAACGATTTTAAAAAA*
	R41	CAATGCGGCCGCAACCGTTCTATATCTAAGTCTTG
	R42	CAATGCGGCCGCTGCTGTTCTATATCTTAATCTTG
	F119	GTGTGTGTTTAAGAAAAAATATG
	F139	GTAAATAAAAAAAATAATATACAATAAC
	R143	CTAAAAGAATATAAAATATATAAATAT
	R148	AGGGTATCACCTTCAAACTTGACTTCAGCACGTGTCTTGTAG
	R157	CATGTAGCCAAAATATGTG
	F158	CGTTGGCCGATTCATTAATGAAAGGATATTCAGATGATGAG
	R159	GTTATTGTATATTATTTTTTTTATTTACTTACGCTGTTCTATATCTTAATC
	F160	ATATTTATATATTTTATATTCTTTTAGAAAGGCTATTCAGATGATG
	R161	GTTCTTCTCCTTTACTCATAACCGTTCTATATCTAAGTC
	F162	ATGAGTAAAGGAGAAGAAC
	R163	CCTCTTCGCTATTACGCCAGGAGGTTAAAATTCTAAACTATATG
	F164	ATATTTATATATTTTATATTCTTTTAGAAAGGATATAGTGATGATGA
	R165	GTTCTTCTCCTTTACTCATTGCTGTTCTATATCTTAATC
	F177	ATATTTATATATTTTATATTCTTTTAGAAAACAAATTTCTTATCTAAAG
	R178	GTTCTTCTCCTTTACTCATATTCAAATGACCTGTTCTTC
	PCRA_F	CTGGCGTAATAGCGAAGAGG
	PCRA_R	CATTAATGAATCGGCCAACG
Annealing	F-g31	TATTATTTATTTAGTAAAATGGAA
	R-g31	AAACTTCCATTTTACTAAATAAAT
	F-g250	TATTCATAATAAAATTAAGCTGTA
	R-g250	AAACCAGGAACTCTTAAATTTTTT
PCR gDNA	F-cg6	GTTCATGCTCCTCAACAAAG
	R-cg6	GAACAAATACATAAGAGCGC
	F119	GTGTGTGTTTAAGAAAAAATATG
	R157	CATGTAGCCAAAATATGTG
	sera5+27	CAATATCATTTGAATCAAACAGTGGT
	sera5 -11	CTTTGCCATCCAGGCTGTTC
	sera5 -25	CCATTGGACTAGAACCTTCAT

Chapter 4. Preliminary results about the roles of individual PfHP1 domains in regulating *var* gene silencing

4.1 Aim of study

As mentioned before, Brancucci and colleagues have employed a PfHP1 knock-down cell line to show that PfHP1 is required for three important cellular processes: (1) progression through schizogony and thus, normal parasite replication; (2) silencing of the *pfap2-g* locus and thus, inhibition of sexual commitment; and (3) *var* gene silencing and thus, ensuring the singular choice of *var* gene expression (Brancucci et al., 2014). In Chapter 3, I have shown that each of three PfHP1 domains is essential for (1) the proliferation of asexual blood stage parasites and (2) the silencing of *ap2-g*/inhibition of the sexual conversion, which is consistent with the previous results (Brancucci et al., 2014).

Here, I aimed to investigate if individual domains of PfHP1 also play a role in regulating *var* gene silencing, as previously shown for full length PfHP1 (Brancucci et al., 2014). My preliminary results showed that an extremely high percentage of stage I gametocytes in the generation after rapamycin treatment did not express PfEMP1 in all four mutant cell lines: 3D7/HP1-KO, 3D7/HP1-ΔCD, 3D7/HP1-ΔHinge and 3D7/HP1-ΔCSD. My preliminary data suggest a possibility that sexual committed parasites might execute alternative mechanism to regulate *var* gene silencing independent to PfHP1.

4.2 Methods

Cell lines used in this study

The following cell lines were used in this study: 3D7/HP1-KO, 3D7/HP1-ΔCD, 3D7/HP1-ΔHinge, 3D7/HP1-ΔCSD and 3D7/HP1-Control. These cell lines have been generated, cultured and induced to express GFP-tagged PfHP1 mutants as described in Chapter 3 of this thesis.

Indirect immunofluorescence assay (IFA)

IFAs were performed on methanol-fixed cells in the progeny of rapamycin-treated parasites (30-38h to 40-48 hpi, generation 2) using mouse IgG or IgG1 mAb a-ATS (Duffy et al., 2002),1:150; mouse mAb a-Pfs16 (kind gift from Robert W. Sauerwein),

1:250; and Alexa Fluor 488-conjugated a-mouse IgG or IgG1 (Molecular Probes), 1:250. Images were taken at 63-fold magnification on a Leica DM 5000B microscope with a Leica DFC 300 FX camera, acquired via the Leica IM 1000 software, processed using ImageJ software [https://imagej.nih.gov/ij/]. For each experiment, images were acquired and processed with identical settings.

4.3 Results

To address the functional contribution of individual domains of PfHP1 in controlling *var* gene expression, parasites were split at 0-8 hpi in generation 1 and treated either with DMSO or RAP. Immunofluorescence imaging was performed to compare the expression of PfEMP1 in the progeny of DMSO- and RAP-treated parasites (40-48 hpi, generation 2).

In the 3D7/HP1-Control cell line, the majority of both RAP- and DMSO-treated parasites were schizonts and comparable in fluorescence intensity signals for PfEMP1 (Figure 4.1A). Similarly, approximately 100% of DMSO-treated 3D7/HP1-KO, 3D7/HP1-ΔCD, 3D7/HP1-ΔHinge and 3D7/HP1-ΔCSD parasites were schizonts and PfEMP1-positive as expected (Figure 4.1A and C). Notably, the proportion of schizonts in the corresponding RAP-treated samples dropped to 0.7 - 2.58% and these were also positive for PfEMP1. In contrast, undetectable PfEMP1 signal was observed in the rest of the parasites in the RAP-treated populations (Figure 4.1A and C).

In order to characterize if the PfEMP1-negative parasites in these RAP-treated populations indeed correspond to early gametocytes, I performed independent Pfs16 IFAs since the a-ATS and a-Pfs16 antibodies are both mouse-derived monoclonal antibodies. The Pfs16 IFAs showed that only ~ 4 to 6% of the progeny of DMSO-treated parasites were Pfs16-positive in 3D7/HP1-KO, 3D7/HP1-ΔCD, 3D7/HP1-ΔHinge and 3D7/HP1-ΔCSD cell lines. In contrast, this population was observed at ~85 to 98% in the corresponding RAP-treated parasites (Figure 4.1B-C). These extremely high percentage of early gametocytes is very similar to the proportion of PfEMP1-negative parasites observed in the RAP-treated samples of 3D7/HP1-KO, 3D7/HP1-ΔCD, 3D7/HP1-ΔHinge and 3D7/HP1-ΔCSD cell lines.

Together, two independent immunofluorescence studies showed that at early stage of gametocytogenesis, PfEMP1 expression is strongly reduced even in the absence of PfHP1.

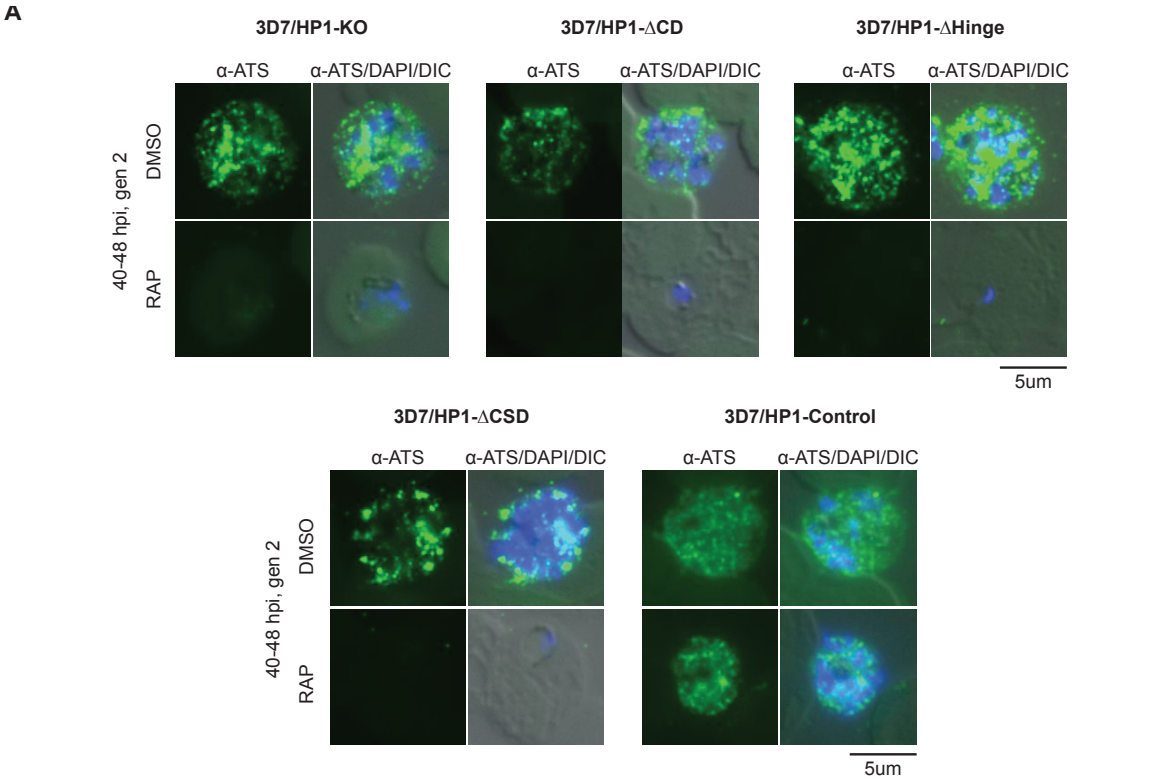
A
3D7/HP1-KO
3D7/HP1-ΔCD
3D7/HP1-ΔHinge
α-ATS
α-ATS/DAPI/DIC
40-48 hpi, gen 2
DMSO
RAP
5um
3D7/HP1-ΔCSD
3D7/HP1-Control

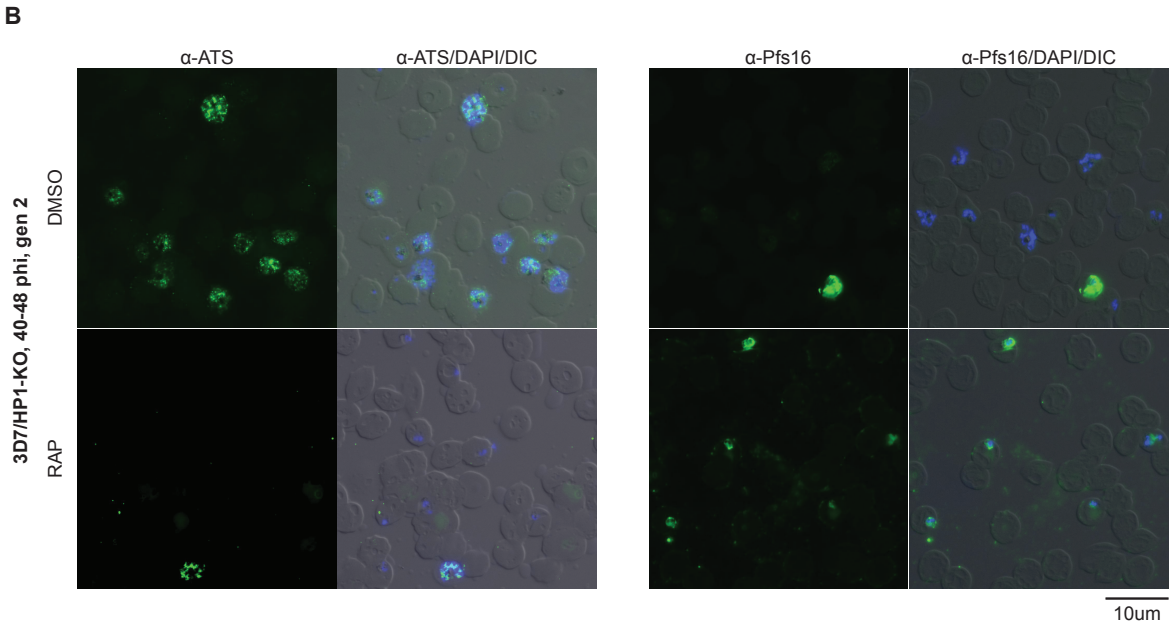
B
α-ATS
α-ATS/DAPI/DIC
α-Pfs16
α-Pfs16/DAPI/DIC
3D7/HP1-KO, 40-48 phi, gen 2
DMSO
RAP
10um

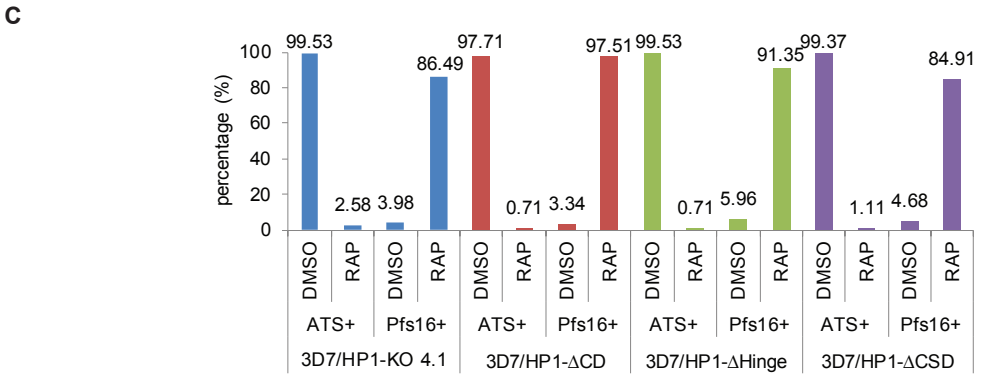
C
percentage (%)
100
80
60
40
20
0
99.53
2.58
3.98
86.49
97.71
0.71
3.34
97.51
99.53
0.71
5.96
91.35
99.37
1.11
4.68
84.91
DMSO
RAP
ATS+
Pfs16+
3D7/HP1-KO 4.1
3D7/HP1-ΔCD
3D7/HP1-ΔHinge
3D7/HP1-ΔCSD

Figure 4.1. PfEMP1 expression is reduced at early stage of gametocytogenesis. (A) Representative images showing PfEMP1 expression in the progeny of DMSO- and RAP-treated PfHP1 truncation mutant and control cell lines (40-48 hpi, generation 2) as determined by IFA using a-ATS antibodies recognizing the conserved ATS domain of PfEMP1. Nuclei were stained with DAPI. DIC, differential interference contrast. Scale bar 5 µm. **(B)** Representative examples of independent PfEMP1 and Pfs16 IFAs in the progeny of DMSO- and RAP-treated 3D7/HP1-KO parasites (40-48 hpi, generation 2) as determined by IFA using a-ATS antibodies and a-Pfs16 antibodies. Scale bar 10 µm. **(C)** Proportion of PfEMP1-positive parasites and proportion Pfs16-positive parasites in DMSO- and RAP-treated PfHP1 truncation mutant lines (40-48 hpi, generation 2) as determined by independent IFAs using a-ATS antibodies and a-Pfs16 antibodies. Values were obtained from a single experiment each (>200 iRBCs counted per sample except for 3D7/HP1-ΔCSD DMSO with >150 iRBCs counted).

In order to better study the expression of PfEMP1 in the early stage I gametocytes, I performed a double labelling IFA using a-Pfs16 and a-ATS antibodies simultaneously using 3D7/HP1-ΔCD parasites as a representative cell line. Although both of a-Pfs16 and a-ATS antibodies are mouse-derived, a-Pfs16 antibodies mark the parasitophorous vacuole membrane (PVM) (Bruce et al., 1994; Eksi and Williamson, 2011; Kongkasuriyachai et al., 2004; Maier et al., 2009) while a-ATS antibodies visualize PfEMP1 that is exported beyond the parasite boundaries (Horrocks et al., 2005; Marti and Spielmann, 2013). Hence, using a single secondary labelled anti-mouse IgG antibody type still allows the differentiation the two labelling patterns, of which one comes from PfEMP1 and the other comes from Pfs16 antigens. As shown in Figure 4.2, only schizonts expressed PfEMP1 in both DMSO-/RAP-treated conditions. In contrast, neither gametocytes with wild type PfHP1 background (DMSO-treated condition, Pfs16-positive parasites) nor the induced gametocytes with mutant PfHP1 background (RAP-treated condition, Pfs16-positive parasites) expressed PfEMP1. This result was consistent with the observation from the two independent IFAs shown above.

This preliminary result is somehow contradictory to the result described previously where the progeny of PfHP1-GFP-DD knockdown parasites showed increased PfEMP1 expression because of de-repression of the *var* gene family (Brancucci et al., 2014).

However, in the previous study, the proportion of PfHP1-depleted parasites in the population showing upregulated PfEMP1 was not specified. It has been reported that approximately 50% of the ring progeny from PfHP1-depleted parasites were early stage I- gametocytes (Pfs16-positive) and the rest was arrested trophozoites (Brancucci et al., 2014). Hence, this gametocyte subpopulation in the PfHP1-depleted parasites was speculated to not express PfEMP1 while the arrested asexual trophozoites was speculated to highly express PfEMP1. I have repeated the PfEMP1 IFA on the 3D7/HP1-GFP-DD line in ON and OFF Shield-1 conditions in order to quantify the proportion of parasites that expressing high level of PfEMP1. However, I was unsuccessful to generate these results since there have been high background or very faint PfEMP1 signal intensity obtained from IFA samples that interfered with evaluation of *bona fide* PfEMP1 signal as well as the quantification. The possible reasons for this failure could be the differences in experimental conditions compared to the previous study, including the use of different Shield-1 stocks and especially different batches of a-ATS antibodies for which I indeed experienced large variabilities in quality (for example, one batch with aggregation of antibodies in -20°C storage condition) (data not shown).

Although the results presented in this chapter are preliminary and need to be repeated in biological replicates, the PfEMP1 and Pfs16 expression patterns were very consistent in all four cell lines, the 3D7/HP1-KO, 3D7/HP1-ΔCD, 3D7/HP1-ΔHinge and 3D7/HP1-ΔCSD. This initial result therefore suggests that *var* gene expression during the onset of gametocytogenesis is downregulated independently of PfHP1, probably because of the low abundance/absence of transcription factor(s) that previously activated permissive *var* locus in asexual stage parasites.

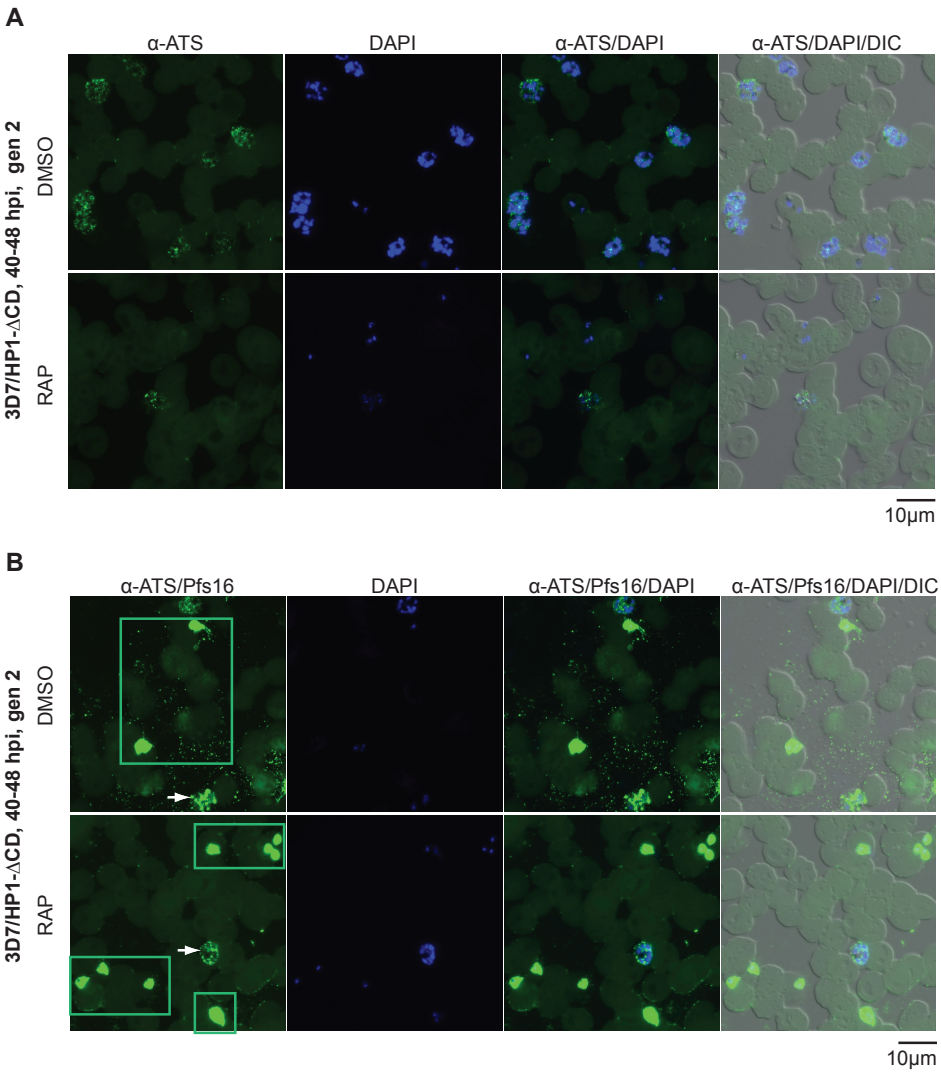

Figure 4.2. PfEMP1 and Pfs16 co-labelling in 3D7/HP1-ΔCD cell line. (A) Representative overview images showing PfEMP1 expression in the progeny of DMSO- and RAP-treated 3D7/HP1-ΔCD at 40-48 hpi, generation 2 as determined by IFA using α-ATS antibodies recognizing the conserved ATS domain of PfEMP1. Nuclei were stained with DAPI. DIC, differential interference contrast. Scale bar 10 μm. **(B)** Double labelling IFA using α-Pfs16 and α-ATS antibodies for 3D7/HP1-ΔCD cell line at 40-48 hpi, generation 2. The white arrows indicate PfEMP1 staining pattern in schizonts. The green boxes indicate Pfs16 staining pattern of stage I gametocytes. The proportion of each labelled subpopulation was not determined. Scale bar 10 μm.

4.4 References

Brancucci, N.M.B., Bertschi, N.L., Zhu, L., Niederwieser, I., Chin, W.H., Wampfler, R., Freymond, C., Rottmann, M., Felger, I., Bozdech, Z., Voss, T.S., 2014. Heterochromatin protein 1 secures survival and transmission of malaria parasites. Cell Host Microbe 16, 165–176. doi:10.1016/j.chom.2014.07.004

Bruce, M.C., Carter, R.N., Nakamura, K., Aikawa, M., Carter, R., 1994. Cellular location and temporal expression of the Plasmodium falciparum sexual stage antigen Pfs16. Mol. Biochem. Parasitol. 65, 11–22.

Duffy, M.F., Brown, G.V., Basuki, W., Krejany, E.O., Noviyanti, R., Cowman, A.F., Reeder, J.C., 2002. Transcription of multiple var genes by individual, trophozoite-stage Plasmodium falciparum cells expressing a chondroitin sulphate A binding phenotype. Mol. Microbiol. 43, 1285–1293.

Eksi, S., Williamson, K.C., 2011. Protein targeting to the parasitophorous vacuole membrane of Plasmodium falciparum. Eukaryotic Cell 10, 744–752. doi:10.1128/EC.00008-11

Horrocks, P., Pinches, R.A., Chakravorty, S.J., Papakrivos, J., Christodoulou, Z., Kyes, S.A., Urban, B.C., Ferguson, D.J.P., Newbold, C.I., 2005. PfEMP1 expression is reduced on the surface of knobless Plasmodium falciparum infected erythrocytes. J. Cell. Sci. 118, 2507–2518. doi:10.1242/jcs.02381

Kongkasuriyachai, D., Fujioka, H., Kumar, N., 2004. Functional analysis of Plasmodium falciparum parasitophorous vacuole membrane protein (Pfs16) during gametocytogenesis and gametogenesis by targeted gene disruption. Mol. Biochem. Parasitol. 133, 275–285.

Maier, A.G., Cooke, B.M., Cowman, A.F., Tilley, L., 2009. Malaria parasite proteins that remodel the host erythrocyte. Nat. Rev. Microbiol. 7, 341–354. doi:10.1038/nrmicro2110

Marti, M., Spielmann, T., 2013. Protein export in malaria parasites: many membranes to cross. Curr. Opin. Microbiol. 16, 445–451. doi:10.1016/j.mib.2013.04.010

Chapter 5. Studying PfHP1 function using a genetic complementation approach

This chapter presents some initial analyses on the functional contribution of PfHP1 domains to overall PfHP1 function and the functional conservation of PfHP1 domains among different species, using a genetic complementation approach. In this study, I employed the previously published PfHP1 knockdown cell line, 3D7/HP1-GFP-DD (Brancucci et al., 2014), to ectopically express a series of PfHP1 mutants and evaluate their ability to complement three PfHP1-dependent processes: (1) maintenance of mutually exclusive expression of *var* genes, (2) mitotic progression of asexual blood stage parasites and (3) sexual differentiation switch (Brancucci et al., 2014).

5.1 Methods

Parasite culture and transfection

3D7/HP1-GFP-DD parasites (Brancucci et al., 2014) were cultured at 5% hematocrit in RPMI-1640 medium supplemented with 25 mM HEPES, 100 mM hypoxanthine, 24 mM sodium bicarbonate and 0.5% Albumax II, 4 nM WR99210 (WR) and 625 nM Shield-1. (Brancucci et al., 2014; Lambros and Vanderberg, 1979; Trager and Jensen, 1976; Voss et al., 2006). Transfection was performed as described (Brancucci et al., 2014; Voss et al., 2006).

Transfection cell lines and transfection constructs

I employed the pBcam-3xHA-Cherry vector (Witmer et al., 2012) to generate a series of complementation constructs expressing mutant PfHP1 proteins C-terminally tagged with a sequence encoding the 3xHA-CherryFP epitope-fluorophore tag. These complementation constructs were expressed under the control of the constitutive *P. falciparum* calmodulin (*cam)* promoter. The pBcam-3xHA-Cherry vector can be selected on blasticidin for stable episomal maintenance. I have successfully generated seven such complementation cell lines by transfecting pBcam-3xHA-Cherry-derived PfHP1 complementation plasmids into 3D7/HP1-GFP-DD parasites. They are listed below.

(1) 3D7/HP1-Control-HAC that ectopically expresses full-length wild type PfHP1 (aas 1-266).

(2) 3D7/HP1-ΔCD-HAC that ectopically expresses a PfHP1 mutant consisting only of the Hinge and CSD regions (aas 55-266).

(3) 3D7/HP1-ΔHinge-HAC that ectopically expresses a PfHP1 mutant in which the hinge region (aas 75-177) is replaced by a linker polypeptide derived from the ApiAP2 factor PfSIP2 (aas 232-254 of PfSIP2 that connect two AP2 domains) (Flueck et al., 2009).

(4) 3D7/HP1-ΔCSD-HAC that ectopically expresses a PfHP1 mutant consisting only of the CD and Hinge regions (aas 1-190).

(5) 3D7/hsHP1-N-HAC that ectopically expresses a chimeric PfHP1 containing, in the following order, the human HP1a CD (aas 1-75) followed by the PfHP1 Hinge and CSD regions (aas 55-266, encoded by a recodonized *pfhp1* sequence, Genscript™, see Chapter 2 for more details).

(6) 3D7/Swi6-N-HAC that ectopically expresses a chimeric PfHP1 containing, in the following order, the *S.pombe* Swi6 CD (aas 1-139) followed by the PfHP1 Hinge and CSD regions (aas 55-266, encoded by a recodonized *pfhp1* sequence, Genscript™).

(7) 3D7/Swi6-C-HAC that ectopically expresses a chimeric PfHP1 containing, in the following order, the PfHP1 CD and Hinge regions (aas 1-190, encoded by a recodonized *pfhp1* sequence, Genscript™) followed by the Swi6 CSD region (aas 260-328).

The corresponding transfection constructs are listed below.

The pBcam-PfHP1 full-3xHA-Cherry carrying full-length wild type PfHP1 (aas 1-266) was obtained from N.Brancucci [N.Brancucci PhD dissertation, 2014]

To generate the pBcam-ΔCD-3xHA-Cherry, a fragment named PfHP1.HingeCSD encoding aas 55-266 of the endogenous PfHP1 was amplified from 3D7 gDNA using primers 5fwd and 5rev and cloned into the pBcam-3xHA-Cherry plasmid using *Bam*HI and *Not*I and T4 ligase.

The pBcam-ΔHinge-3xHA-Cherry was constructed as described in Chapter 3 (Supplementary Information).

To generate the pBcam-ΔCSD-3xHA-Cherry plasmid, a fragment named PfHP1.CDHinge encoding aas 1-190 of the endogenous PfHP1 was amplified from 3D7 gDNA using primers 2fwd and 2rev and cloned into the pBcam-3xHA-Cherry plasmid using *Bam*HI and *Not*I and T4 ligase.

The pBcam-HsHP1-N-3xHA-Cherry was constructed as follows. A fragment named HsHP1.CD encoding aas 1-75 of the human HP1a was amplified from cDNA of human Jurkat cells using primers F6 and R7. A fragment named PfHP1.HingeCSD encoding aas 55-266 of recodonized PfHP1 (rePfHP1) was amplified from pUC57-rePfHP1 (Genscript™) using primers F10 and R3. The resulting hybrid fragment HsCD/PfHP1.HingeCSD was amplified by fusion PCR from a mixture of HsHP1.CD and PfHP1.HingeCSD PCR products (at 1:100 dilution) using primers F6 and R3 and cloned into pBCam-3xHA–Cherry using *Bam*HI and *Nhe*I and T4 ligase.

The pBcam-Swi6-N-3xHA-Cherry was constructed as follows. A fragment named Swi6.CD encoding aas 1-139 of the *S. pombe* Swi6 was amplified from plasmid pMB117-Swi6 (kind gift of M. Bühler, Friedrich-Miescher Institute, Basel, Switzerland) using primers F8 and R9. The resulting hybrid fragment Swi6CD/PfHP1.HingeCSD was amplified from a mixture of Swi6.CD and PfHP1.HingeCSD PCR products (at 1:100 dilution) by fusion PCR using primers F8 and R3 and cloned into pBcam-3xHA–Cherry using *Bam*HI and *Nhe*I and T4 ligase.

The pBcam-Swi6-C-3xHA-Cherry was constructed as follows. A fragment named Swi6.CSD encoding aas 260-328 of the *S.pombe* Swi6 was amplified from plasmid pMB117-Swi6 using primers F15 and R16. The resulting hybrid fragment PfHP1.CDHinge/Swi6.CSD was amplified from a mixture of PfHP1.CDHinge and Swi6.CSD PCR products (at 1:100 dilution) by fusion PCR using primers F11 and R16 and cloned into pBcam-3xHA –Cherry using *Bam*HI and *Nhe*I and T4 ligase.

All primer sequences are listed in Table 1.

For each of the seven transfections, 100 µg of the corresponding pBcam-3xHA-Cherry-derived complementation vector described above was electroporated into the 3D7/HP1-GFP-DD parasite line. Transfectants were selected in the presence of the indicated combinations of 625 nM Shield-1 and 4 nM WR99210 (to maintain 3D7/HP1-GFP-DD parasites stably expressing PfHP1-GFP-DD from the endogenous locus) and 5 µg/ml BSD (to maintain the pBcam-3xHA-Cherry-derived complementation vector).

Once obtained, transfectants were continuously cultured in the presence of 625 nM Shield-1, 4 nM WR99210 and 10 µg/ml BSD.

Western Blot analysis

Transfectants cultured under ON Shield-1 conditions (625 nM Shield-1, 4nM WR and 10 µg/ml BSD) were synchronized twice 16 hrs apart to obtain an 8 hrs growth window. The parasites were then synchronized at 0-8 hpi generation 1 and split into two populations, one cultured with Shield-1 and one without Shield-1. Nuclei were isolated at 40-48 hpi generation 1 as described in Chapters 2 and 3. Proteins were detected using mouse mAb a-GFP (Roche Diagnostics #11814460001), 1:1'000; rat mAb a-HA (3F10, Roche Diagnostics #11867423001), 1:1'000; rabbit a-PfHP1 (Brancucci et al., 2014), 1:5'000; rabbit a-Histone 4 (Abcam ab10158), 1:10'000.

Fluorescence microscopy

IFAs were performed on methanol-fixed cells using the following antibodies: rat mAb a-HA (3F10, Roche Diagnostics #11867423001), 1:100; mouse mAb a-GFP (Roche Diagnostics #11814460001), 1:100; mouse IgG1 mAb a-ATS (Duffy et al., 2002), 1:150, Secondary antibodies: Alexa Fluor 568-conjugated a-rat IgG (Molecular Probes #A11077), 1:250; Alexa Fluor 488-conjugated a-mouse IgG (Molecular Probes), 1:250. Nuclei were stained with DAPI. Images were taken at 63-fold magnification on a Leica DM 5000B microscope with a Leica DFC 300 FX camera, acquired via the Leica IM 1000 software, processed using ImageJ software [https://imagej.nih.gov/ij/]. For each experiment, images were acquired and processed with identical settings.

Parasite multiplication assay

Parasites were tightly synchronized (0-8 hpi, generation 1), split into two equal populations, of which one half was maintained with 625 nM Shield-1, 4 nM WR99210 and 10 µg/ml BSD (negative control) and the other half was induced for the depletion of endogenous PfHP1-GFP-DD by Shield-1 removal (4 nM WR99210 and 10 µg/ml BSD). Giemsa smears were prepared to determine the parasitaemia at 16-24 hpi (generation 1). Giemsa-stained smears were prepared every second day onwards for three generations. Parasitaemia was counted by visual inspection of Giemsa-stained blood smears (≥ 1'000 RBCs counted per experiment). Multiplication rates were determined as the parasitaemia observed in the following generation divided by the parasitaemia observed in the previous generation. The extrapolative growth cure was generated using a starting parasiteamia at 0.1%.

Gametocyte conversion assay

Parasites were tightly synchronized (0-8 hpi, generation 1), split into two equal populations, of which one half was maintained with 625 nM Shield-1, 4 nM WR99210 and 10 µg/ml BSD (negative control) and the other half was induced for the depletion of endogenous PfHP1-GFP-DD by Shield-1 removal as described above. Gametocytaemia and arrested parasitaemia was determined on day seven after Shield-1 removal by visual inspection of Giemsa-stained blood smears. Sexual conversion rates were determined as the gametocytaemia observed on day seven as a proportion of the total parasitaemia observed at 16-24 hpi in generation 2. Arrested parasitaemia was determined as the arrested trophozoites observed on day seven as a proportion of the total parasitaemia observed at 16-24 hpi in generation 2.

5.2 Results and discussion

Validation of complementation PfHP1 cell lines

To begin studying the *in vivo* functional contribution and conservation of structural domains of PfHP1, I employed the conditional PfHP1 knockdown cell line, 3D7/HP1-GFP-DD (Brancucci et al., 2014) and expressed a series of episomal complementation PfHP1 constructs cloned into the pBcam-3xHA-Cherry vector (Witmer et al., 2012). There were seven complementation cell lines generated successfully. The control cell line is 3D7/HP1-Control-HAC. Three truncated PfHP1 mutant cell lines are 3D7/HP1-ΔCD-HAC, 3D7/HP1-ΔHinge-HAC and 3D7/HP1-ΔCSD-HAC. Three chimeric PfHP1 mutant cell lines are 3D7/hsHP1-N-HAC, 3D7/Swi6-N-HAC and 3D7/Swi6-C-HAC. The generation of complementation cell lines and transfection constructs are explained in detail in the Methods section above and in Figure 5.1.

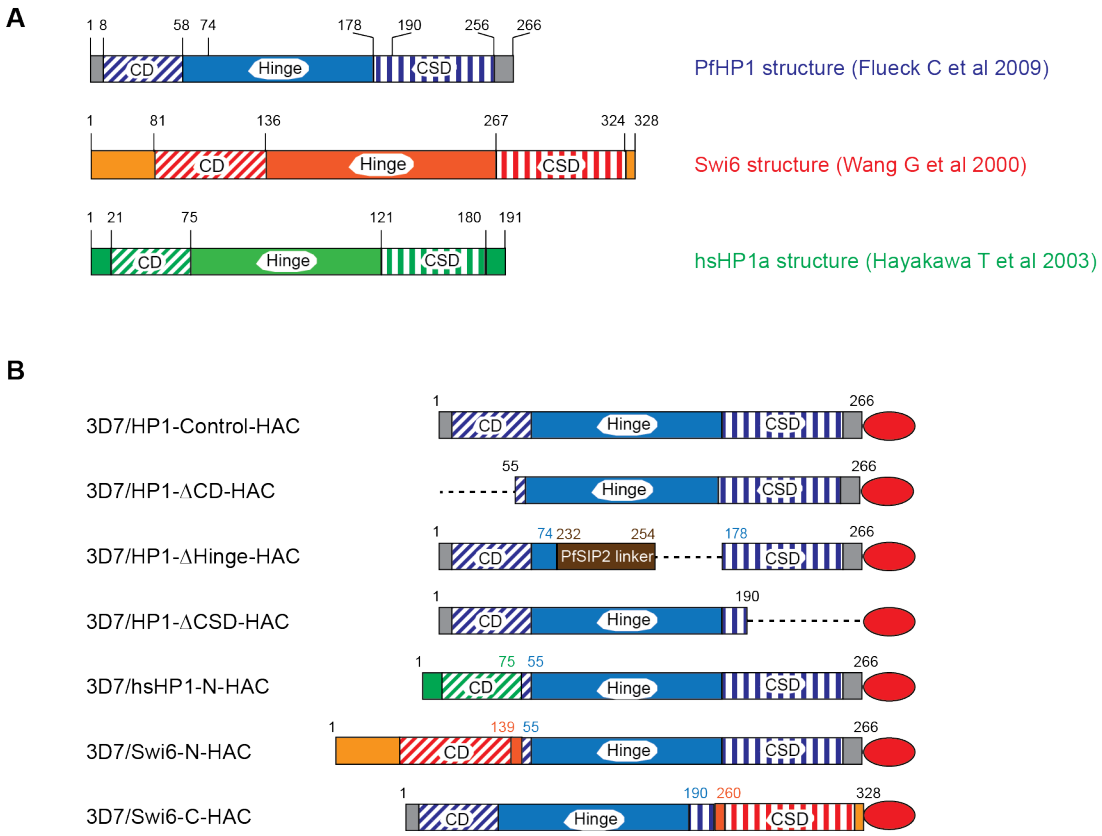

Figure 5.1. **The generation of PfHP1 complementation cell lines**. **(A)** Structure of PfHP1, Swi6 and hsHP1a (Flueck et al., 2009; Hayakawa et al., 2003; Wang et al., 2000). **(B)** Names of the complementation cell lines (left) and schematics of the ectopically expressed PfHP1 protein products (right) used in this study. The red oval represents 3xHA-CherryFP. The dashed lines represent deletions. The numbers indicate positions of amino acid residues. The blue, green, orange and brown colors represent domains from PfHP1, HsHP1, Swi6 and PfSIP2, respectively.

When transfectants were obtained, expression of ectopic proteins was analyzed by immunoblot using whole parasite protein lysates harvested at 40-48 hpi in generation 1. In the immunoblot analysis, the a-HA antibodies recognize ectopic proteins which were C-terminally tagged with 3xHA-CherryFP (or shortly HAC-tag), the a-GFP antibodies recognize endogenous the PfHP1-GFP-DD protein at ~70 KDa. Note that the rabbit polyclonal a-PfHP1 antibodies recognize mostly the CD and the Hinge region of PfHP1 (I. Niederwieser, personal communication). The immunoblot analysis with a-HA antibodies revealed the correct expression of all seven ectopic PfHP1

mutants: (1) HP1-Control-HAC at ~63KDa; (2) HP1-ΔCD-HAC at ~58KDa; (3) HP1-ΔHinge-HAC at ~54.9KDa; (4) HP1-ΔCSD-HAC at ~55.1KDa; (5) hsHP1-N-HAC at ~66KDa; (6) Swi6-N-HAC at ~73.5KDa; (7) Swi6-C-HAC at ~72KDa. Protein molecular weight was predicted using Protein Calculator free software (http://protcalc.sourceforge.net/). As shown in Figure 5.2A, under ON Shield-1 conditions (1) all cell lines expressed similar levels of the endogenous PfHP1-GFP-DD shown by analysis with a-GFP; (2) similar amounts of protein lysates were loaded as shown by analysis with a-H4 (histone H4); (3) the endogenous and ectopic PfHP1s in the 3D7/HP1-Control-HAC were expressed at similar levels shown by the analysis with a-PfHP1 antibodies, giving an indirect standard to compare the expression level of other ectopic PfPH1 mutants to that of endogenous PfHP1. However, ectopic PfHP1s from the other six complementation cell lines were expressed at different levels (Figure 5.2A). To be specific, the expression level of ectopic PfHP1s from 3D7/HP1-ΔCSD-HAC, 3D7/hsHP1-N-HAC; 3D7/Swi6-N-HAC and 3D7/Swi6-C-HAC were similar to that of endogenous PfHP1-GFP-DD. In contrast, the expression levels of ectopic PfHP1s from 3D7/HP1-ΔCD-HAC and 3D7/HP1-ΔHinge-HAC were much lower than that of endogenous PfHP1-GFP-DD. In order to possibly increase the expression level of ectopic PfHP1s, PfHP1 mutant cell lines were challenged with a higher amount of BSD up to 20 µg/ml. However, under this condition, parasites revealed low multiplication rates, prolonged cell cycle and cell death (data not shown). Therefore, the culture condition with 10 µg/ml of BSD was selected as the standard condition for the optimal expression of ectopic PfHP1 mutants. In brief, the immunoblot assay showed that with the low level expression of ectopic PfHP1 mutants in 3D7/HP1-ΔCD-HAC and 3D7/HP1-ΔHinge-HAC parasites, these cell lines were not suitable for further studies, while the 3D7/HP1-Control-HAC, 3D7/HP1-ΔCSD-HAC, 3D7/hsHP1-N-HAC, 3D7/Swi6-N-HAC and 3D7/Swi6-C-HAC were suitable for further analysis.

In parallel to the Western blot analysis, localization IFA studies were also performed at trophozoite stage (around 24-32 hpi, generation 1) to analyze the localization of ectopic PfHP1 mutants. In the presence of endogenous PfHP1-GFP-DD (ON Shield-1 condition), ectopic PfHP1s from 3D7/HP1-Control-HAC, 3D7/hsHP1-N-HAC, 3D7/Swi6-N-HAC, 3D7/HP1-ΔCD-HAC and 3D7/HP1-ΔHinge-HAC were concentrated into foci at nuclear periphery indistinguishable to endogenous PfHP1. In contrast, when the PfHP1 CSD domain is deleted (3D7/HP1-ΔCSD-HAC) or replaced by the CSD from Swi6 (3D7/Swi6-C-HAC), the heterochromatin localization was hampered at different

levels. First, in the 3D7/Swi6-C-HAC line a subpopulation (percentage not determined) showed cytosolic localization and punctate nuclear localization, i.e. not heterochromatin-restricted localization. Second, in the 3D7/HP1-ΔCSD-HAC line the CSD-truncated PfHP1 localised to the cytosol (Figure 5.2B). Together, these results indicate an important role of the PfHP1 CSD domain in targeting the protein to nucleus. In addition, the results also suggest that the replacement of the PfHP1 CD domain with that from other HP1 proteins (Swi6 and hsHP1a) could retain the correct localization of PfHP1, which is possibly obtained by dimerization of chimeric PfHP1s with endogenous PfHP1 via the CSD. On the contrary, it seems that replacement of the PfHP1 CSD domain with that from Swi6 only partly fulfilled this function. Thus, the IFA results corroborated the central role of the CSD domain in HP1 homodimerisation (Cowieson et al., 2000), specific for each species.

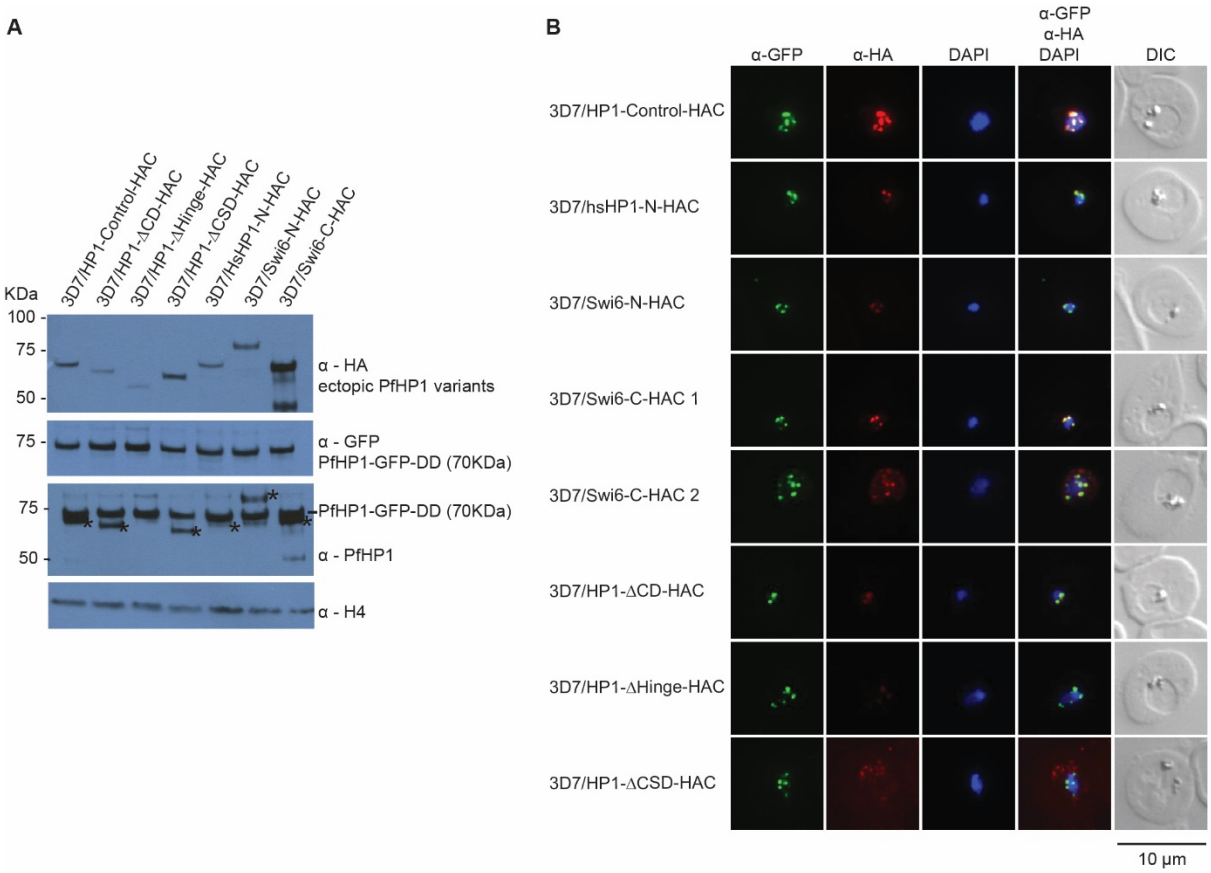

Figure 5.2. Validation of PfHP1 complementation cell lines. (A) Expression of ectopic PfHP1s in transgenic cell lines. a-HA antibodies recognized ectopic PfHP1 proteins, a-GFP antibodies recognized endogenous PfHP1-GFP-DD protein at ~70 KDa. a-H4 antibodies recognized histone H4 and used for loading control. a-HP1 antibodies recognized both endogenous PfHP1-GFP-DD and ectopic PfHP1 proteins. The asterisks represent ectopic PfHP1s recognized by a-PfHP1 antibodies (note that the a-HP1 antibodies do not efficiently bind to the PfHP1 CSD domain). The hyphens represent endogenous PfHP1-GFP-DD protein at ~70 KDa. **(B)** Localization of ectopic PfHP1s in the presence of endogenous PfHP1 in trophozoites (ON Shield-1). Scale bar 10 µm.

In the absence of endogenous PfHP1-GFP-DD (OFF Shield-1 cultures, 24-32 hpi, generation 2), in 3D7/HP1-Control-HAC and 3D7/hsHP1-N-HAC parasites ectopic PfHP1s localized to heterochromatin foci. In contrast, the hybrid PfHP1 protein in the 3D7/Swi6-C-HAC line mislocalized to cytoplasm and no heterochromatin foci were observed (Figure 5.3 left panel). Unfortunately, in 3D7/Swi6-N-HAC, 3D7/HP1-ΔCD-HAC, 3D7/HP1-ΔHinge-HAC and 3D7/HP1-ΔCSD-HAC parasites the signal intensity for CherryFP-tagged PfHP1 mutants was not above the background so that the localization of these ectopic PfHP1 mutants could not be determined in parasites depleted of wild type PfHP1 (Figure 5.3 left panel). This was expected for 3D7/HP1-ΔCD-HAC and 3D7/HP1-ΔHinge-HAC parasites that expressed the ectopic PfHP1 mutants at very low levels (see Figure 5.2 above). However, the ectopic PfHP1 mutants in 3D7/Swi6-N-HAC and 3D7/HP1-ΔCSD-HAC were expressed at levels similar to that of endogenous PfHP1-GFP-DD so it was unexpected that these two HP1 mutants could not be detected by IFA. Hence, I asked if there were some problems during the IFA performance that did not allow the visualization of these ectopic PfHP1 mutants under OFF Shield-1 conditions. To this end, I conducted an immunoblot analysis using whole parasite protein lysates from the 3D7/HP1-Control-HAC, 3D7/Swi6-N-HAC and 3D7/HP1-ΔCSD-HAC lines to examine protein expression levels in both ON and OFF Shield-1 conditions. As shown in Figure 5.4, the immunoblot analysis revealed that in OFF Shield-1 condition, when endogenous PfHP1-GFP-DD was depleted, the ectopic PfHP1s in 3D7/Swi6-N-HAC and 3D7/HP1-ΔCSD-HAC lines were expressed at extremely low levels compared to that of the 3D7/HP1-Control-HAC line. In ON Shield-1 condition, the ectopic PfHP1s in 3D7/Swi6-N-HAC and 3D7/HP1-ΔCSD-HAC lines were expressed at lower levels compared to that of the 3D7/HP1-Control-HAC line (Figure 5.4), which was different to previous observation (Figure 5.2). Thus, the 3D7/Swi6-N-HAC and 3D7/HP1-ΔCSD-HAC expressed ectopic PfHP1 mutants at uneven levels. Therefore, alternative transgenic lines with higher and unfluctuating expression level of ectopic PfHP1 variants would be needed for the localization study and further studies of PfHP1 mutants. The other cell lines, 3D7/hsHP1-N-HAC and 3D7/Swi6-C-HAC should also be re-examined in term of ectopic PfHP1 expression. Nevertheless, the immunofluorescence study once again emphasized that (1) CD replacement does not severely alter the capacity of PfHP1 to localize to heterochromatin; and (2) CSD replacement cannot fulfil this function, probably because of the differences in CSD-specific binding properties present in each species.

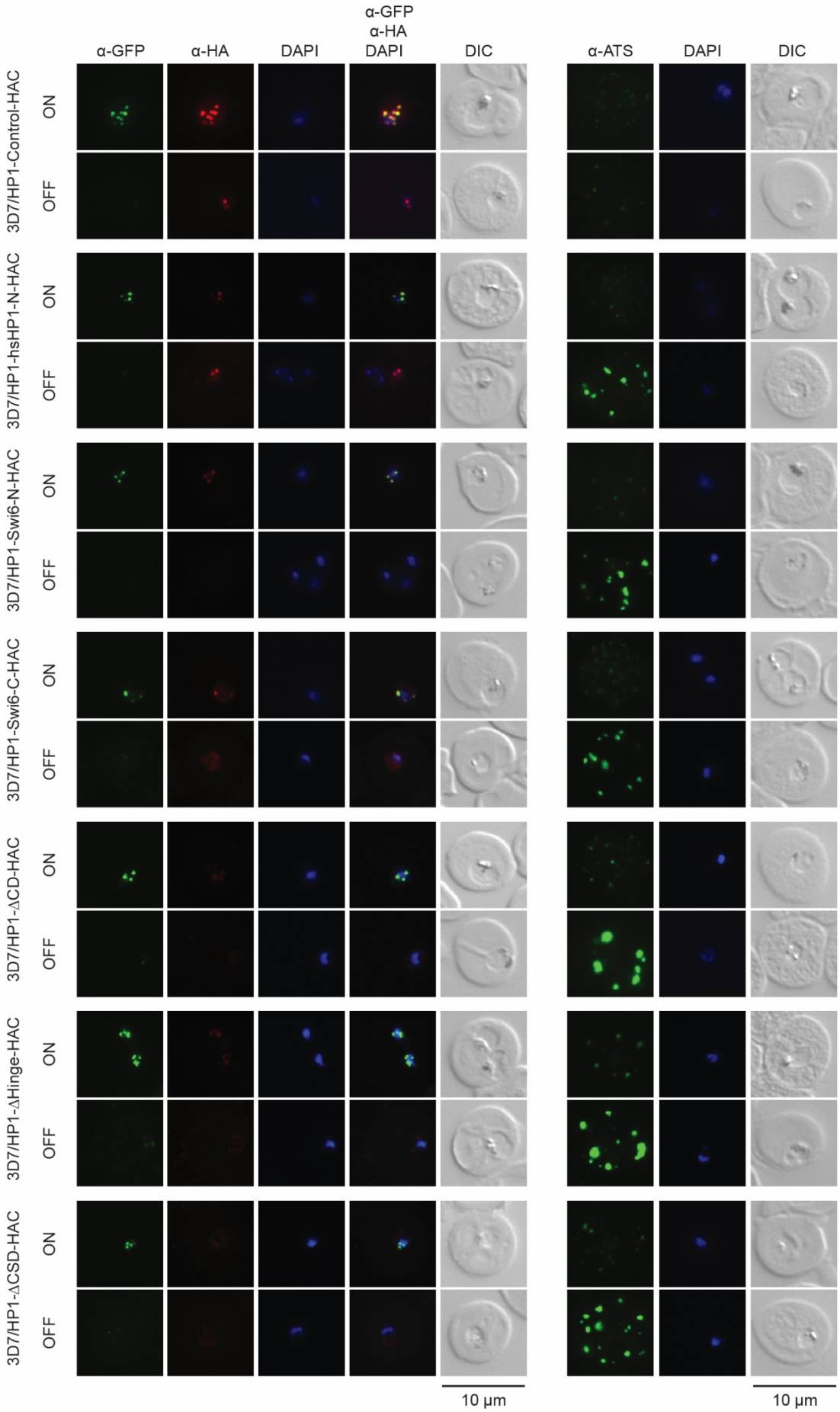
α-GFP
α-HA
DAPI
α-GFP
α-HA
DAPI
DIC
α-ATS
DAPI
DIC
3D7/HP1-Control-HAC
3D7/HP1-hsHP1-N-HAC
3D7/HP1-Swi6-N-HAC
3D7/HP1-Swi6-C-HAC
3D7/HP1-ΔCD-HAC
3D7/HP1-ΔHinge-HAC
3D7/HP1-ΔCSD-HAC
ON
OFF
10 μm
10 μm

Figure 5.3. Localization of ectopic PfHP1 mutants and PfEMP1 expression in PfHP1 complementation cell lines. (A) Localization study of ectopic PfHP1 mutants. **(B)** PfEMP1 expression of complementation cell lines in the presence (ON Shield-1) and absence (OFF Shield-1) of endogenous PfHP1-GFP-DD at 24-32 hpi, generation 2.

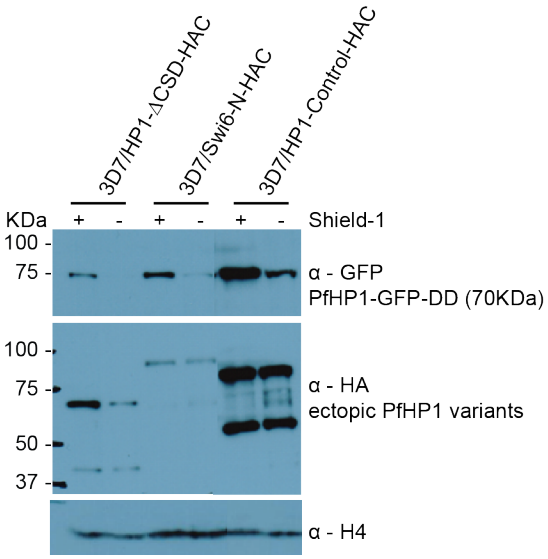

Figure 5.4. Ectopic PfHP1 expression in some PfHP1complementation cell lines. Immunoblot analysis revealed low expression of ectopic PfHP1 mutants in 3D7/HP1-ΔCSD-HAC and 3D7/Swi6-N-HAC compared to that of the 3D7/HP1-Control-HAC line.

In a recent study, it has been observed in PfHP1-depleted 3D7/HP1-GFP-DD parasites that (1) PfEMP1 expression is upregulated because of the derepression of *var* gene family; (2) sexual conversion rate is increased because of the derepression of the *pfap2-g* gene, which encodes for PfAP2-G, a master regulator of sexual differentiation (Kafsack et al., 2014) and (3) a subpopulation of parasites arrested at the trophozoite stage as a result of a failure in DNA replication preventing progression through schizogony (Brancucci et al., 2014). In parallel with the localization study, I investigated the functional contribution and conservation of the CD, hinge and CSD domains of PfHP1 in these three main PfHP1-dependent processes (*var* gene silencing, mitotic proliferation, sexual commitment).

First, to probe the ability of PfHP1 mutants in maintaining singular choice of *var* gene, IFAs were performed to compare the expression levels of PfEMP1 in the progeny of ON and OFF Shield-1 parasites at 24-32 hpi in generation 2. As shown in Figure 5.3 (right

panel), in both the ON and OFF Shield-1 conditions, the 3D7/HP1-Control-HAC cell line expressed PfEMP1 at low level, represented by comparable fluorescence intensity. As expected, in the ON Shield-1 condition, the other complementation cell lines expressed comparably low levels of PfEMP1 similarly to that seen for the control cell line. In contrast, in the OFF Shield-1 condition strong upregulation of PfEMP1 expression was observed for all six other complementation lines 3D7/HP1-ΔCD-HAC, 3D7/HP1-ΔHinge-HAC, 3D7/HP1-ΔCSD-HAC, 3D7/hsHP1-N-HAC, 3D7/Swi6-N-HAC and 3D7/Swi6-C-HAC. This result is similar to the result previously presented for the PfHP1-depleted cell line (Brancucci et al., 2014).

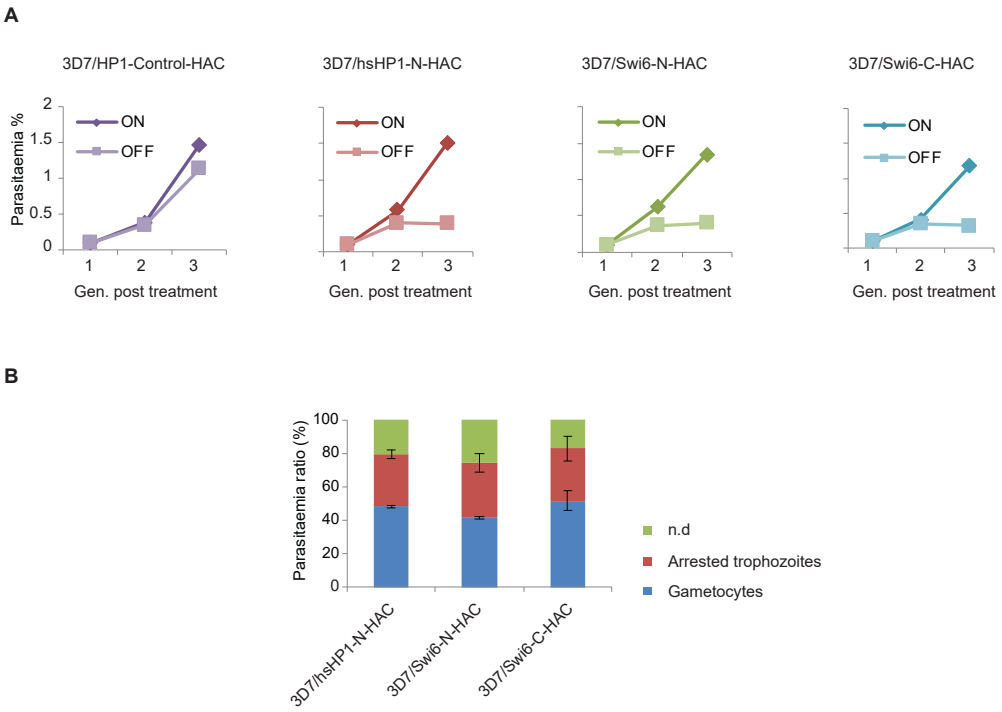

Figure 5.5. Phenotypes of PfHP1 complementation cell lines. (A) Growth curves of three PfHP1 complementation cell lines and the control cell line over three generations under ON/OFF Shield-1 condition. Values were obtained from one experiment (>1000 RBCs counted for each sample). **(B)** Sexual conversion rates and proportion of arrested trophozoites determined on day seven after Shield-1 removal in the OFF Shield-1 population of three complementation cell lines. Values represent mean of two independent experiments (>2000 cells counted for each sample). Error bars represent SD. n.d means not determined.

Second, I evaluated the growth phenotype of the PfHP1 complementation cell lines by determining replication rates over three consecutive generations. In the 3D7/HP1-Control-HAC line, parasites in the ON and OFF Shield-1 condition showed a highly comparable rate of multiplication as expected (Figure 5.5A). Meanwhile, in the 3D7/hsHP1-N-HAC, 3D7/Swi6-N-HAC and 3D7/Swi6-C-HAC lines, parasites in the OFF Shield-1 condition consistently showed a proliferation defect in the cycle after Shield-1 removal (generation 2) (Figure 5.5A). From those OFF Shield-1 populations, I obtained approximately 31% of arrested trophozoites at day seven after Shield-1 removal (Figure 5.5B). These phenotypes are again similar to the growth defect of the 3D7/HP1-GFP-DD line under OFF Shield-1 condition as described previously (Brancucci et al., 2014).

Third, I examined a possible role of chimeric PfHP1s in controlling *pfap2-g* silencing by examining the sexual commitment rates in three PfHP1 complementation cell lines, 3D7/hsHP1-N-HAC, 3D7/Swi6-N-HAC and 3D7/Swi6-C-HAC. As shown in Figure 5.5B, the gametocyte populations comprised of approximately 41-51% of all infected RBCs in the OFF Shield-1 populations. These high rates of sexual commitment are comparable to that of the PfHP1-depeleted parasites (Brancucci et al., 2014).

On the one hand, these preliminary results seemingly suggest that (1) full-length PfHP1, or in other words, every single domain of PfHP1 is required for normal growth of asexual parasites as well as for controlling singular choice of *var* gene; (2) the replacement of either CD or CSD domain with that of human HP1a or *S. pombe* Swi6 fails to restore PfHP1's roles in controlling cell cycle progression, *var*- and *ap2-g* gene silencing, or in other words, the CD and CSD functions are not conserved among *P. falciparum*, fission yeast and human. On the other hand, it is worth noting that HP1 operates position-effect variegation in a dose-dependent manner (Eissenberg et al., 1990; Eissenberg et al., 1992). Since the two independent immunoblots showed fluctuating and/or low expression levels of ectopic PfHP1 mutants in the major of transgenic cell lines (3D7/HP1-ΔCD-HAC and 3D7/HP1-ΔHinge-HAC, 3D7/HP1-ΔCSD-HAC and 3D7/Swi6-N-HAC), the dosage effect of PfHP1 possibly explained the failure of ectopic PfHP1 mutants in fulfilling wild type PfHP1 functions. As mentioned above, there needs alternative transgenic cell lines with higher and unfluctuating expression level of PfHP1 mutants for further studies in order to obtain firm conclusions on the functional contribution and conservation of PfHP1 domains among species. Nevertheless, the preliminary localization study indicated an important role of the PfHP1 CSD domain in

targeting the protein to nucleus and this function is underlined by the homodimerization and/or interaction that is specific for each species. This result is consistent with investigated role of CSD presented in Chapter 3 of this thesis.

Table 1. List of primers

Application	Primer	Sequence 5'-3'
PCR cloning	2wd	CAGT GGATCCAAAAAATGACAGGGTCAGATGAAGA
	2rev	CAGTGCGGCCGCATTTAAATGTCCAGTTCTTCTAA
	5fwd	CAGT GGATCCAAAAA ATGACAGGGTCAGATGAAGA
	5rev	CAGTGCGGCCGCATTTAAATGTCCAGTTCTTCTAA
	R3	CAGTGCTAGCTGCTGTTCTATATCTTAATCT TG
	F6	CAGTGGATCCAAAAAATGGGAAAGAAAACCAAGCGGAC
	R7	GAAATTTGTTTTTAATGATTCCATCTCCTTCATCTTCTTATAC
	F8	CAGTGGATCCAAAAAATGAAGAAAGGAGGTGTTC
	R9	GAAATTTGTTTTTAATGATTCCATTGGTCTTCCTCCATGTTC
	F10	ATGGAATCATTAAAAACAAATTTC
	F15	GAAGAACAGGTCATTTGAATGTTAAACAAGTAGAAAACTATG
	R16	CAGT GCTAGCTTCATTTTCACGGAACGTTAAG

5.3 References

Brancucci, N.M.B., Bertschi, N.L., Zhu, L., Niederwieser, I., Chin, W.H., Wampfler, R., Freymond, C., Rottmann, M., Felger, I., Bozdech, Z., Voss, T.S., 2014. Heterochromatin protein 1 secures survival and transmission of malaria parasites. Cell Host Microbe 16, 165–176. doi:10.1016/j.chom.2014.07.004

Cowieson, N.P., Partridge, J.F., Allshire, R.C., McLaughlin, P.J., 2000. Dimerisation of a chromo shadow domain and distinctions from the chromodomain as revealed by structural analysis. Curr. Biol. 10, 517–525.

Duffy, M.F., Brown, G.V., Basuki, W., Krejany, E.O., Noviyanti, R., Cowman, A.F., Reeder, J.C., 2002. Transcription of multiple var genes by individual, trophozoite-stage Plasmodium falciparum cells expressing a chondroitin sulphate A binding phenotype. Mol. Microbiol. 43, 1285–1293.

Eissenberg J. C., James T. C., Foster-Hartnett D. M., Hartnett T., Ngan V., Elgin S. C. R. (1990) Mutation in a heterochromatin-specific chromosomal protein is associated with suppression of position-effect variegation in Drosophila melanogaster. Proc. Natl. Acad. Sci. U. S. A. 87, 9923–9927.

Eissenberg, J. C., G. D. Morris, G. Reuter, and T. Hartnett. 1992. The heterochromatin-associated protein HP-1 is an essential protein in Drosophila with dosage-dependent effects on position-effect variegation. Genetics 131, 345-352.

Flueck, C., Bartfai, R., Volz, J., Niederwieser, I., Salcedo-Amaya, A.M., Alako, B.T.F., Ehlgen, F., Ralph, S.A., Cowman, A.F., Bozdech, Z., Stunnenberg, H.G., Voss, T.S., 2009. Plasmodium falciparum heterochromatin protein 1 marks genomic loci linked to phenotypic variation of exported virulence factors. PLoS Pathog. 5, e1000569. doi:10.1371/journal.ppat.1000569

Hayakawa, T., Haraguchi, T., Masumoto, H., Hiraoka, Y., 2003. Cell cycle behavior of human HP1 subtypes: distinct molecular domains of HP1 are required for their centromeric localization during interphase and metaphase. J. Cell. Sci. 116, 3327–3338. doi:10.1242/jcs.00635

Kafsack, B.F.C., Rovira-Graells, N., Clark, T.G., Bancells, C., Crowley, V.M., Campino, S.G., Williams, A.E., Drought, L.G., Kwiatkowski, D.P., Baker, D.A., Cortés, A., Llinás, M., 2014. A transcriptional switch underlies commitment to sexual development in malaria parasites. Nature 507, 248–252. doi:10.1038/nature12920

Lambros, C., Vanderberg, J.P., 1979. Synchronization of Plasmodium falciparum erythrocytic stages in culture. J. Parasitol. 65, 418–420.

Trager, W., Jensen, J.B., 1976. Human malaria parasites in continuous culture. Science 193, 673–675.

Voss, T.S., Healer, J., Marty, A.J., Duffy, M.F., Thompson, J.K., Beeson, J.G., Reeder, J.C., Crabb, B.S., Cowman, A.F., 2006. A var gene promoter controls allelic exclusion of virulence genes in Plasmodium falciparum malaria. Nature 439, 1004–1008. doi:10.1038/nature04407

Wang, G., Ma, A., Chow, C.M., Horsley, D., Brown, N.R., Cowell, I.G., Singh, P.B., 2000. Conservation of heterochromatin protein 1 function. Mol. Cell. Biol. 20, 6970–6983.

Witmer, K., Schmid, C.D., Brancucci, N.M.B., Luah, Y.-H., Preiser, P.R., Bozdech, Z., Voss, T.S., 2012. Analysis of subtelomeric virulence gene families in Plasmodium falciparum by comparative transcriptional profiling. Mol. Microbiol. 84, 243–259. doi:10.1111/j.1365-2958.2012.08019.x

Chapter 6. General discussion and Outlook

6.1 PfHP1 phosphorylation and speculation

It has been well observed in other model eukaryotes that HP1 is subject to phosphorylation to regulate its various functions including progression through mitosis (Chakraborty and Prasanth, 2014; Hiragami-Hamada et al., 2011) and heterochromatic gene silencing (Hiragami-Hamada et al., 2011; Shimada et al., 2009; Zhao and Eissenberg, 1999; Zhao et al., 2001). The hinge domain of HP1 has been known for DNA/RNA binding activity in the human, mouse and *Xenopus laevis* HP1 family proteins (Meehan et al., 2003; Muchardt et al., 2002; Sugimoto et al., 1996). In *P. falciarpum*, most of the phosphosites in PfHP1 identified by MS/MS intriguingly clusters in the hinge region, proposing a possible link between hinge domain phosphorylation and PfHP1 function at first impression.

Focusing on investigating the role of the PfHP1 hinge phosphorylation in parasite biology *in vivo*, I have successfully applied the CRISPR/Cas9-mediated genome editing technique to generate a number of conditional PfHP1 phospho-mutants based on the DiCre/LoxP system. One of the advantages of this method is the conditional expression of the PfHP1 mutants in absence of wild type PfHP1, ensuring that dimerization between wild type and mutated PfHP1 does not occur. Thus, the system allows precise interpretation on the localization of PfHP1 mutants. Although western blot results showed high expression of PfHP1 phosphomutants and absence of endogenous PfHP1 (Chapter 2 of this thesis), I did not observe any clear differences in the localization of phosphomutated PfHP1s compared to wild type PfHP1 in my IFAs as well as in the three major PfHP1-dependent processes of *var* gene silencing, sexual commitment and S-phase entry (Brancucci et al., 2014).

Considering the methodology for studying *in vivo* function of PfHP1 phosphorylation in particular, and protein phosphorylation in general, alanine is largely used as a non-phosphoryltable residue to substitute serine, and is a powerful approach to mimic the effect of non-phosphorylation (Chen and Cole, 2015). Although serine and alanine are both small amino acids, serine is polar amino acid, meaning it is hydrophilic, while alanine is non-polar and hydrophobic. Furthermore, the side chain from serine can form hydrogen bonds with a variety of polar substrates in contrast to the non-active

side chain from alanine (Chen and Cole, 2015). The serine-to-alanine substitution might, therefore, alter the hydrophobicity or secondary structure of the PfHP1 hinge region. However, since the hinge region is unstructured (Lomberk et al., 2006), it is possible that the serine-to-alanine substitution does not largely affect PfHP1 global structure, hence, PfHP1 functions. In my study, all phosphomutants (3D7/HP1-3M and 3D7/HP1-HIM) retain PfHP1 functions, suggesting that the serine-to-alanine substitutions did not negatively impact on PfHP1 function.

So, the question is: what role do these phosphosites in the hinge region play? I raise a hypothesis that the phosphorylation of PfHP1 hinge domain might contribute to regulate PfHP1 interaction with (1) DNA/RNA and/or (2) a so far unknown interactor. The first hypothesis could be tested *in vitro* by mobility shift electrophoresis assay - EMSA using purified recombinant wtPfHP1 and hinge-phosphomutated PfHP1s. The second hypothesis could be tested by PfHP1 pull-down experiments between the DMSO- and RAP-treated conditions using the 3D7/HP1-HIM cell line. However, such factors could appear in only a certain stage among many stages during the *P. falciparum* life cycle, so nuclear protein extraction should be conducted in time course. Together with the fact that no major effects were observed by the non-phosphorylatable PfHP1 hinge domain during blood stages, such pull-down experiments should also be performed in mosquito stage of the parasites. Beside the localization, interaction and the three major PfHP1-dependent cellular processes, the function of PfHP1 hinge phosphorylation could be tested on the fitness of parasites during cellular stress such as heat shock or anti-malaria drug susceptibility.

Of course, with the experimental design system and "knock-in" technique I established by the CRISPR/Cas9 and DiCre/loxP systems, my study provides an elegant approach to allow studying the functional contribution of other phosphosites within the PfHP1 CD and CSD domains. One of the most interesting phosphosite to me is S206, whose position is next to a predicted NLS motif (aas 201-204) residing in the CSD region (Chapter 3 of this thesis). It is worth noting that the S206 residue was detected only once in our four MS/MS experiments mapping phosphorylated residues in native PfHP1-GFP purified by immunoprecipitation (IP) from protein extracts of blood stage parasites (Bui et al., manuscript submitted). The apparent low frequency of the S206 phosphorylation is possibly due to its phosphorylation state occurring in a narrow time window or in a very small subpopulation of the parasites. From this point of view, the phosphorylation state of S206 itself in the CSD domain possibly regulates the

interaction of PfHP1 with other effectors to modulate a special process occurring only in such a short time period or small subpopulation. To enlighten this hypothesis, a cell line carrying a serine-to-alanine substitution at S206 could be easily generated. It is certainly worth to generate a phosphomimetic control cell line of by serine-to-glutamate substitution (Chen and Cole, 2015; Hiragami-Hamada et al., 2011; Shimada et al., 2009; Zhao and Eissenberg, 1999) at S206 in order to compare the effects of phosphorylation (DMSO control condition) versus constitutive phosphorylation (serine-to-glutamate) and non-phosphorylation (serine-to-alanine).

In summary, successful identification of PfHP1-associated processes with PfHP1 phosphorylation will undoubtedly contribute to our understanding about PfHP1 and its function in malaria pathology.

6.2 Functional contribution of PfHP1 individual domains and speculation

While the hinge phosphorylation is likely not involved in PfHP1 function during the parasitic IDC (Bui et al., manuscript submitted), it can be predicted that hinge domain replacement should not influence PfHP1 functions. In fact, the replacement of PfHP1 hinge domain by PbHP1 hinge domain retained PfHP1 function (Chapter 3 of this thesis). It is probably because of the high similarity in length (the PbHP1 hinge domain is 15 residues longer than the PfHP1 hinge domain) and in the sequences (Chapter 3 of this thesis). However, the replacement of PfHP1 hinge domain by a shorter linker prevented PfHP1 heterochromatin localization and induced gametocytogenesis (Chapter 3 of this thesis). Furthermore, when the hinge domain was preserved and the CD was partly shortened (deletion of residues 30-58, 3D7/HP1-ΔCD line), heterochromatin targeting was also hampered, probably because of the abolishment in H3K9me3 binding ability. Together, these results emphasized the CD and hinge regions as targeting module of PfHP1 to heterochromatin. In addition, this function also likely depends on the length of the hinge domain as implied in an *in vivo* study in *S. pombe* (Wang et al., 2000). In *S. pombe*, when the hinge domain was 72-residues shortened to the length of mouse HP1a (M31), the truncated protein still fully functioned as opposed to a longer removal of 95 residues in the hinge that resulted in a major reduction of Swi6 functions in normal zygote asci formation and mitotic stability (Wang et al., 2000).

In my study, I tackled the functional contribution of the hinge domain by the substitution of the hinge domain with a short linker from another protein (PfSIP2). At first

glance, this replacement was a good solution since the small linker between two AP2 domains of PfSIP2 has fulfilled the purpose of mimicking a spacer between CD and CSD domain from PfHP1. However, going beyond this aim and in order to incorporate other scientific questions, for example which residues of the hinge domain are essential for PfHP1 function or to what extent the hinge domain reduction in length is tolerable for PfHP1 functions, my approach employed here cannot answer. In general, the insertion of another gene fragment into *pfhp1* could interfere with downstream analysis, for example the interpretation of localization results since PfSIP2 also localizes to nucleus at heterochromatin loci and co-localizes with PfHP1 (Flueck et al., 2009). Fortunately, PSORTII prediction did not reveal any NLS in the PfSIP2 linker. In any case, to fulfil the research aims more comprehensively, the methodology would be more optimal to preserve PfHP1 hinge sequences and study its functional contribution by a series of hinge deletion.

In summary, although there have been some disadvantages in the method applied, my study still implies the essence of the CD-hinge region in targeting PfHP1 to heterochromatin, in which the contribution of the hinge domain as a spacer is still an open question that can be investigated in future.

6.3 PfHP1 and *var* gene regulation during gametocytogenesis

Chronic malaria is caused by the persistence of the parasites during blood stage infection (Buffet et al., 2011; Cowman et al., 2016; Kyes et al., 2001). The underlying reason for this persistence is the antigenic variation of the variant surface adhesion antigens, especially PfEMP1 expressing on iRBCs that allows immune evasion (Buffet et al., 2011; Cowman et al., 2016; Kyes et al., 2001). Further, PfEMP1 also mediates parasite rosetting (attachment of iRBCs to uninfected RBCs and the cytoadhesion to the microvasculature (Cowman et al., 2016; Newbold et al., 1997; Reeder and Brown, 1996; Rowe et al., 2009). Once sequestered, the parasites escape from splenic clearance, causing severe symptoms (Buffet et al., 2011; Cowman et al., 2016; Kyes et al., 2001). Thus, PfEMP1 is considered the major virulence factor of *P. falciparum* and the study on controlling mechanisms of *var* gene expression would contribute to understanding on pathology and assist malaria prevention. PfEMP1 is encoded by the *var* gene family that contains 60 members but only one *var* gene is transcribed by a single parasite (Dzikowski and Deitsch, 2009; Scherf et al., 1998; Voss et al., 2006). This is known as mutually exclusive expression. The expression switch of PfEMP1/*var* gene

in mutually exclusive expression is a key component of antigenic variation (Reeder and Brown, 1996; Scherf et al., 2008). The mutually exclusive expression of *var* genes has been shown to be regulated by different epigenetic mechanisms including lncRNAs (Amit-Avraham et al., 2015; Jiang et al., 2013; Ralph et al., 2005), chromatin structure changes involving histone variants (Petter et al., 2011; 2013) and histone post-translational modifications (Lopez-Rubio et al., 2007; Westenberger et al., 2009), subnuclear compartmentalisation/genome organization (Brolin et al., 2009; Marty et al., 2006; Ralph et al., 2005; Voss et al., 2006), histone-modifying enzymes like HDACs (Duraisingh et al., 2005; Tonkin et al., 2009), HKMTs (Jiang et al., 2013; Volz et al., 2012) and PfHP1 (Brancucci et al., 2014). Among the epigenetic factors that maintain singular choice of *var* gene expression, PfHP1 has been shown to be a key regulator of antigenic variation as conditional depletion of PfHP1 (3D7/HP1-GFP-DD in OFF Shield-1 condition) disrupted transcriptional silencing of almost all of *var* genes as well as the *ap2-g* gene encoding for PfAP2-G (Brancucci et al., 2014). In repressive state, internal and subtelomeric *var* genes were tethered at nuclear periphery while in permissive state, an actively transcribed *var* gene was disassociated with telomeric clusters and repositioned to another site of the nuclear periphery (Ralph et al., 2005; Voss et al., 2006). Interestingly, using the same PfHP1-depleted cell line (3D7/HP1-GFP-DD in OFF Shield-1 condition) and applying the Hi-C (chromosome conformation capture coupled with next-generation sequencing) technique, recently Bunnik and colleagues showed a complete loss of tethering between internal and subtelomeric *var* genes, suggesting a role for PfHP1 in maintaining the structure of repressive *var* clusters (Bunnik et al., 2018). While these studies clearly demonstrated the important role of PfHP1 in derepression of *var* genes, I still propose some aspects need to be revisited. First, is there any correlation between the induction in *var* gene transcription and PfEMP1 protein translation? Brancucci and colleagues revealed the hyper-expression of PfEMP1 in the PfHP1-depleted cell line both by IFA and by immunoblot analysis. However, since there are two subpopulations in the investigated progeny of PfHP1-depleted parasites (approximately 50% each of arrested trophozoites and early gametocytes), it is unclear whether both of the two subpopulations hyper-expressed PfEMP1. In my preliminary results about the expression of PfEMP1, I consistently observed lack of PfEMP1 expression in the progeny of all RAP-treated PfHP1-GFP mutant cell lines (3D7/HP1-KO, 3D7/HP1-ΔCD, 3D7/HP1-ΔHinge and 3D7/HP1-ΔCSD). Hence, my preliminary results are seemingly in contrast to the results previously

presented (Brancucci et al., 2014). The major difference between the PfHP1 depleted cell line (3D7/HP1-GFP-DD in OFF Shield-1 condition) and the PfHP1 knockout cell line (3D7/HP1-KO in RAP treated condition) resides in the sexual conversion rate that the former one produced ~50% (Brancucci et al., 2014) while later one produced up to nearly 100% gametocytes (Chapter 3-4 of this thesis). Therefore, I speculate that in PfHP1 depleted cell line, the subpopulation hyper-expressing PfEMP1 likely derives from the arrested trophozoites. To confirm the observation of my study, microarray or qRT-PCR would be practical methods to examine the *var* transcription profile in gametocytes produced by PfHP1 knockout cell line. Nevertheless, my preliminary results suggest an unknown mechanism employed by early gametocytes to suppress the expression of *var*/PfEMP1 even in a PfHP1-depleted background. In other words, during onset of gametocytogenesis the repression of *var* gene transcription possibly follows another regulatory mechanism that is PfHP1-independent. The downregulation of *var* gene at the onset of gametocytogenesis could be due to the low abundance (or absence) of the transcription factor(s) activating *var* gene, which is previously abundant in asexual stage parasites. Further, this result is highly consistent with previously reported result (Tibúrcio et al., 2013). Gametocytes with wild type PfHP1 background have been shown to minimally express PfEMP1 on the membrane of knob-less gametocyte-iRBCs (Tibúrcio et al., 2013). It has also been shown that stage I/II gametocyte-iRBCs were unable to bind to the host ligands used by PfEMP1 expressed by the asexual parasites to bind endothelial cells such as ICAM1 and CD36 by cytoadhesion assays (Tibúrcio et al., 2013). Although a defined subset of nonsubtelomeric type C var genes were selectively transcribed during gametocyte development (early stage II and III) independent to the phenotype of asexual progenitors (Sharp et al., 2006; Tibúrcio et al., 2013), global transcription of *var* genes was dramatically reduced at early gametocytogenesis in 3D7 (Tibúrcio et al., 2013). Additionally, the PfEMP1 reduction phenotype is not surprising because of the need of low antigenicity of immature gametocytes during their long residence in the bone marrow in order to avoid destruction by the reticulo-endothelial system (Alano, 2007; Rogers et al., 2000).

In a PfHP1-depleted cell line with almost all of *var* gene transcription upregulated (Brancucci et al., 2014), the proportion of parasites hyper-expressing PfEMP1 was not specified (Brancucci et al., 2014). As there is limitation for the physical purification of gametocytes stage I and arrested trophozoites as well as changes in experimental

conditions as mentioned before (chapter 4 of this PhD thesis), I was not able to repeat the PfEMP1 expression experiments of the 3D7/HP1-GFP-DD cell line (Brancucci et al., 2014). I therefore suggest experimental methods that would allow to resolve these obstacles. The first and easier method is to repeat a double-labelling IFA using α-ATS antibodies recognizing the conserved ATS domain of PfEMP1 and antibodies recognizing the early gametocyte marker; Pfs16 (Bruce et al., 1994) and PfGEXP5 (Tibúrcio et al., 2015) are such early gametocyte markers. However, antibodies available for those are all mouse-derived (Tibúrcio et al., 2015), causing problems for co-labelling with the mouse-derived α-ATS antibodies. We later determined by ELISA that α-ATS is mouse IgG1-κ antibodies while α-Pfs16 is mouse IgG1-λ antibodies (with help from Julia Hauser, Swiss TPH). Thus, Pfs16 and PfEMP1 double-labelling IFA using different antibody subtypes could be feasible. Alternatively, a second method is to regenerate a PfHP1 loss-of-function mutant as Brancucci and colleagues described previously, however in a conditional PfAP2-G overexpression cell line. Such a cell line could be obtained by the insertion of a *pfap-2g* gene targeted with a sequence encoding the *glmS* ribozyme (Prommana et al., 2013) and a fluorescent tag like CherryFP or the tandem dimer Tomato (tdTomato) (Morris et al., 2010) into the non-essential *cg6* locus (Nkrumah et al., 2006). I expect a homogenous sexually committed population when Shield-1 is removed to deplete PfHP1 while PfAP2-G is simultaneously overexpressed by glucosamine removal (Prommana et al., 2013) at early ring stage (Bancells et al., 2019; Brancucci et al., 2014) to drive sexual commitment. In this case, the non-overexpression of PfAP2-G by the continuous presence of glucosamine is considered as control condition, in which I expect two subpopulations of gametocytes and arrested trophozoites as described previously in the PfHP1-depleted cell line (Brancucci et al., 2014). Moreover, another external control cell line could be added to the study by generating a PfHP1 loss-of-function mutant in a null PfAP2-G background cell line, where the sexual conversion is blocked. In the latter control cell line, I expect that the PHP1 depletion results in a pure arrested trophozoite population. α-PfEMP1 IFAs among three conditions (pure gametocytes, pure arrested trophozoites and mixed of the two populations) would hopefully allow concluding on the actual overexpression of PfEMP1 whether in gametocytes and/or only in arrested trophozoites with a PfHP1-depleted background.

6.4 Significance of the research

Although there is tremendous amount of research in the field of malaria, this tropical disease is still a burden to developing countries and claims over 400.000 deaths in 2017 (World malaria report 2018, WHO). This is mainly because of the impressive biology of the parasite as it lives a very complex life cycle, changing between different hosts and various environments as well as combining both asexual proliferation and sexual differentiation within the human blood stream. Another striking feature is that this human malaria parasite can express highly stage-specific and variable antigens, allowing the parasite to escape the human immune response. Together, this causes a lot of difficulties in malaria eradication unless there is deep understanding in the underlying mechanisms that take part in regulating its transmission and antigenic variation. In this theme, epigenetics in general and PfHP1 in particular has emerged as a central part that needs to be studied in much more detail.

For the first time, I have conducted a detailed study on the function of PfHP1 as well as its central contribution to the three main PfHP1-dependent processes (*var* gene silencing, mitotic proliferation, sexual commitment) through the conditional expression of truncated and chimeric PfHP1s in a DiCre recombinase-expressing 3D7 cell line (1G5DC) (Collins et al., 2013). Following up on this aspect, PfCK2 was revealed to phosphorylate PfHP1 *in vitro* at a cluster of serines in the hinge region. In addition, PfHP1 phosphorylation was also analyzed for the first time although the phosphorylation of the hinge region showed unimportant to control PfHP1 function in blood stage parasites. In this study, the success in generating an inducible PfHP1-knockout parasite line that produces gametocytes at high levels is indeed an important tool to perform further research on gametocyte biology and development or applied research to prevent malaria transmission such as identifying anti-malarial gametocyte drug screen. Beside relevant research prospection, the method for the generation of conditional knockout cell lines presented in this study by combining CRISPR/Cas9-based gene editing and conditional gene replacements using the DiCre/loxP system presents an elegant and versatile approach to analyze function and phosphorylation also of other important proteins. Furthermore, this study may also be relevant to study pathogenesis and transmission in general and the underlying epigenetic mechanisms in particular, in some other unicellular pathogenic eukaryotes since they also share common features such as changing living environments and mutually exclusive expression of surface antigens.

6.5 References

Alano, P., 2007. Plasmodium falciparum gametocytes: still many secrets of a hidden life. Mol. Microbiol. 66, 291–302. doi:10.1111/j.1365-2958.2007.05904.x

Amit-Avraham, I., Pozner, G., Eshar, S., Fastman, Y., Kolevzon, N., Yavin, E., Dzikowski, R., 2015. Antisense long noncoding RNAs regulate var gene activation in the malaria parasite Plasmodium falciparum. Proc. Natl. Acad. Sci. U.S.A. 112, E982–91. doi:10.1073/pnas.1420855112

Bancells, C., Llorà-Batlle, O., Poran, A., Nötzel, C., Rovira-Graells, N., Elemento, O., Kafsack, B.F.C., Cortés, A., 2019. Revisiting the initial steps of sexual development in the malaria parasite Plasmodium falciparum. Nat Microbiol 4, 144–154. doi:10.1038/s41564-018-0291-7

Brancucci, N.M.B., Bertschi, N.L., Zhu, L., Niederwieser, I., Chin, W.H., Wampfler, R., Freymond, C., Rottmann, M., Felger, I., Bozdech, Z., Voss, T.S., 2014. Heterochromatin protein 1 secures survival and transmission of malaria parasites. Cell Host Microbe 16, 165–176. doi:10.1016/j.chom.2014.07.004

Brolin, K.J.M., Ribacke, U., Nilsson, S., Ankarklev, J., Moll, K., Wahlgren, M., Chen, Q., 2009. Simultaneous transcription of duplicated var2csa gene copies in individual Plasmodium falciparum parasites. Genome Biol. 10, R117–16. doi:10.1186/gb-2009-10-10-r117

Bruce, M.C., Carter, R.N., Nakamura, K., Aikawa, M., Carter, R., 1994. Cellular location and temporal expression of the Plasmodium falciparum sexual stage antigen Pfs16. Mol. Biochem. Parasitol. 65, 11–22.

Buffet, P.A., Safeukui, I., Deplaine, G., Brousse, V., Prendki, V., Thellier, M., Turner, G.D., Mercereau-Puijalon, O., 2011. The pathogenesis of Plasmodium falciparum malaria in humans: insights from splenic physiology. Blood 117, 381–392. doi:10.1182/blood-2010-04-202911

Bunnik, E.M., Cook, K.B., Varoquaux, N., Batugedara, G., Prudhomme, J., Cort, A., Shi, L., Andolina, C., Ross, L.S., Brady, D., Fidock, D.A., Nosten, F., Tewari, R., Sinnis, P., Ay, F., Vert, J.-P., Noble, W.S., Le Roch, K.G., 2018. Changes in genome organization of parasite-specific gene families during the Plasmodium transmission stages. Nat Commun 9, 1910–15. doi:10.1038/s41467-018-04295-5

Chakraborty, A., Prasanth, S.G., 2014. Phosphorylation-dephosphorylation cycle of HP1a governs accurate mitotic progression. Cell Cycle 13, 1663–1670. doi:10.4161/cc.29065

Chen, Z., Cole, P.A., 2015. Synthetic approaches to protein phosphorylation. Curr Opin Chem Biol 28, 115–122. doi:10.1016/j.cbpa.2015.07.001

Collins, C.R., Das, S., Wong, E.H., Andenmatten, N., Stallmach, R., Hackett, F., Herman, J.-P., Müller, S., Meissner, M., Blackman, M.J., 2013. Robust inducible Cre recombinase activity in the human malaria parasite Plasmodium falciparum enables efficient gene deletion within a single asexual erythrocytic growth cycle. Mol. Microbiol. 88, 687–701. doi:10.1111/mmi.12206

Cowman, A.F., Healer, J., Marapana, D., Marsh, K., 2016. Malaria: Biology and Disease. Cell 167, 610–624. doi:10.1016/j.cell.2016.07.055

Duraisingh, M.T., Voss, T.S., Marty, A.J., Duffy, M.F., Good, R.T., Thompson, J.K., Freitas-Junior, L.H., Scherf, A., Crabb, B.S., Cowman, A.F., 2005. Heterochromatin silencing and locus repositioning linked to regulation of virulence genes in Plasmodium falciparum. Cell 121, 13–24. doi:10.1016/j.cell.2005.01.036

Dzikowski, R., Deitsch, K.W., 2009. Genetics of antigenic variation in Plasmodium falciparum. Curr. Genet. 55, 103–110. doi:10.1007/s00294-009-0233-2

Flueck, C., Bartfai, R., Volz, J., Niederwieser, I., Salcedo-Amaya, A.M., Alako, B.T.F., Ehlgen, F., Ralph, S.A., Cowman, A.F., Bozdech, Z., Stunnenberg, H.G., Voss, T.S., 2009. Plasmodium falciparum heterochromatin protein 1 marks genomic loci linked to phenotypic variation of exported virulence factors. PLoS Pathog. 5, e1000569. doi:10.1371/journal.ppat.1000569

Hiragami-Hamada, K., Shinmyozu, K., Hamada, D., Tatsu, Y., Uegaki, K., Fujiwara, S., Nakayama, J.-I., 2011. N-terminal phosphorylation of HP1{alpha} promotes its chromatin binding. Mol. Cell. Biol. 31, 1186–1200. doi:10.1128/MCB.01012-10

Jiang, L., Mu, J., Zhang, Q., Ni, T., Srinivasan, P., Rayavara, K., Yang, W., Turner, L., Lavstsen, T., Theander, T.G., Peng, W., Wei, G., Jing, Q., Wakabayashi, Y., Bansal, A., Luo, Y., Ribeiro, J.M.C., Scherf, A., Aravind, L., Zhu, J., Zhao, K., Miller, L.H., 2013. PfSETvs methylation of histone H3K36 represses virulence genes in Plasmodium falciparum. Nature 499, 223–227. doi:10.1038/nature12361

Kyes, S., Horrocks, P., Newbold, C., 2001. Antigenic variation at the infected red cell surface in malaria. Annu. Rev. Microbiol. 55, 673–707. doi:10.1146/annurev.micro.55.1.673

Lomberk, G., Wallrath, L., Urrutia, R., 2006. The Heterochromatin Protein 1 family. Genome Biol. 7, 228. doi:10.1186/gb-2006-7-7-228

Lopez-Rubio, J.J., Gontijo, A.M., Nunes, M.C., Issar, N., Hernandez-Rivas, R., Scherf, A., 2007. 5' flanking region of var genes nucleate histone modification patterns linked to phenotypic inheritance of virulence traits in malaria parasites. Mol. Microbiol. 66, 1296–1305. doi:10.1111/j.1365-2958.2007.06009.x

Marty, A.J., Thompson, J.K., Duffy, M.F., Voss, T.S., Cowman, A.F., Crabb, B.S., 2006. Evidence that Plasmodium falciparum chromosome end clusters are cross-linked by protein and are the sites of both virulence gene silencing and activation. Mol. Microbiol. 62, 72–83. doi:10.1111/j.1365-2958.2006.05364.x

Meehan, R.R., Kao, C.-F., Pennings, S., 2003. HP1 binding to native chromatin in vitro is determined by the hinge region and not by the chromodomain. EMBO J. 22, 3164–3174. doi:10.1093/emboj/cdg306

Morris, L.M., Klanke, C.A., Lang, S.A., Lim, F.-Y., Crombleholme, T.M., 2010. TdTomato and EGFP identification in histological sections: insight and alternatives. Biotech Histochem 85, 379–387. doi:10.3109/10520290903504753

Muchardt, C., Guilleme, M., Seeler, J.-S., Trouche, D., Dejean, A., Yaniv, M., 2002. Coordinated methyl and RNA binding is required for heterochromatin localization of mammalian HP1alpha. EMBO Rep. 3, 975–981. doi:10.1093/embo-reports/kvf194

Newbold, C., Warn, P., Black, G., Berendt, A., Craig, A., Snow, B., Msobo, M., Peshu, N., Marsh, K., 1997. Receptor-specific adhesion and clinical disease in Plasmodium falciparum. Am. J. Trop. Med. Hyg. 57, 389–398. doi:10.4269/ajtmh.1997.57.389

Nkrumah, L.J., Muhle, R.A., Moura, P.A., Ghosh, P., Hatfull, G.F., Jacobs, W.R., Fidock, D.A., 2006. Efficient site-specific integration in Plasmodium falciparum chromosomes mediated by mycobacteriophage Bxb1 integrase. Nat. Methods 3, 615–621. doi:10.1038/nmeth904

Petter, M., Lee, C.C., Byrne, T.J., Boysen, K.E., Volz, J., Ralph, S.A., Cowman, A.F., Brown, G.V., Duffy, M.F., 2011. Expression of P. falciparum var genes involves exchange of the histone variant H2A.Z at the promoter. PLoS Pathog. 7, e1001292. doi:10.1371/journal.ppat.1001292

Petter, M., Selvarajah, S.A., Lee, C.C., Chin, W.H., Gupta, A.P., Bozdech, Z., Brown, G.V., Duffy, M.F., 2013. H2A.Z and H2B.Z double-variant nucleosomes define intergenic regions and dynamically occupy var gene promoters in the malaria parasite Plasmodium falciparum. Mol. Microbiol. 87, 1167–1182. doi:10.1111/mmi.12154

Prommana, P., Uthaipibull, C., Wongsombat, C., Kamchonwongpaisan, S., Yuthavong, Y., Knuepfer, E., Holder, A.A., Shaw, P.J., 2013. Inducible knockdown of Plasmodium gene expression using the glmS ribozyme. PLoS ONE 8, e73783. doi:10.1371/journal.pone.0073783

Ralph, S.A., Scheidig-Benatar, C., Scherf, A., 2005. Antigenic variation in Plasmodium falciparum is associated with movement of var loci between subnuclear locations. Proc. Natl. Acad. Sci. U.S.A. 102, 5414–5419. doi:10.1073/pnas.0408883102

Reeder, J.C., Brown, G.V., 1996. Antigenic variation and immune evasion in Plasmodium falciparum malaria. Immunol. Cell Biol. 74, 546–554. doi:10.1038/icb.1996.88

Rogers, N.J., Hall, B.S., Obiero, J., Targett, G.A., Sutherland, C.J., 2000. A model for sequestration of the transmission stages of Plasmodium falciparum: adhesion of gametocyte-infected erythrocytes to human bone marrow cells. Infect. Immun. 68, 3455–3462. doi:10.1128/iai.68.6.3455-3462.2000

Rowe, J.A., Claessens, A., Corrigan, R.A., Arman, M., 2009. Adhesion of Plasmodium falciparum-infected erythrocytes to human cells: molecular mechanisms and therapeutic implications. Expert Rev Mol Med 11, e16. doi:10.1017/S1462399409001082

Scherf, A., Hernandez-Rivas, R., Buffet, P., Bottius, E., Benatar, C., Pouvelle, B., Gysin, J., Lanzer, M., 1998. Antigenic variation in malaria: in situ switching, relaxed and mutually exclusive

transcription of var genes during intra-erythrocytic development in Plasmodium falciparum. EMBO J. 17, 5418–5426. doi:10.1093/emboj/17.18.5418

Scherf, A., Lopez-Rubio, J.J., Riviere, L., 2008. Antigenic variation in Plasmodium falciparum. Annu. Rev. Microbiol. 62, 445–470. doi:10.1146/annurev.micro.61.080706.093134

Sharp, S., Lavstsen, T., Fivelman, Q.L., Saeed, M., McRobert, L., Templeton, T.J., Jensen, A.T.R., Baker, D.A., Theander, T.G., Sutherland, C.J., 2006. Programmed transcription of the var gene family, but not of stevor, in Plasmodium falciparum gametocytes. Eukaryotic Cell 5, 1206–1214. doi:10.1128/EC.00029-06

Shimada, A., Dohke, K., Sadaie, M., Shinmyozu, K., Nakayama, J.-I., Urano, T., Murakami, Y., 2009. Phosphorylation of Swi6/HP1 regulates transcriptional gene silencing at heterochromatin. Genes Dev. 23, 18–23. doi:10.1101/gad.1708009

Sugimoto, K., Yamada, T., Muro, Y., Himeno, M., 1996. Human homolog of Drosophila heterochromatin-associated protein 1 (HP1) is a DNA-binding protein which possesses a DNA-binding motif with weak similarity to that of human centromere protein C (CENP-C). The Journal of Biochemistry 120, 153–159. doi:10.1093/oxfordjournals.jbchem.a021378

Tibúrcio, M., Dixon, M.W.A., Looker, O., Younis, S.Y., Tilley, L., Alano, P., 2015. Specific expression and export of the Plasmodium falciparum Gametocyte EXported Protein-5 marks the gametocyte ring stage. Malar. J. 14, 334–12. doi:10.1186/s12936-015-0853-6

Tibúrcio, M., Silvestrini, F., Bertuccini, L., Sander, A.F., Turner, L., Lavstsen, T., Alano, P., 2013. Early gametocytes of the malaria parasite Plasmodium falciparum specifically remodel the adhesive properties of infected erythrocyte surface. Cell. Microbiol. 15, 647–659. doi:10.1111/cmi.12062

Tonkin, C.J., Carret, C.K., Duraisingh, M.T., Voss, T.S., Ralph, S.A., Hommel, M., Duffy, M.F., Silva, L.M.D., Scherf, A., Ivens, A., Speed, T.P., Beeson, J.G., Cowman, A.F., 2009. Sir2 paralogues cooperate to regulate virulence genes and antigenic variation in Plasmodium falciparum. PLoS Biol 7, e84. doi:10.1371/journal.pbio.1000084

Volz, J.C., Bartfai, R., Petter, M., Langer, C., Josling, G.A., Tsuboi, T., Schwach, F., Baum, J., Rayner, J.C., Stunnenberg, H.G., Duffy, M.F., Cowman, A.F., 2012. PfSET10, a Plasmodium falciparum methyltransferase, maintains the active var gene in a poised state during parasite division. Cell Host Microbe 11, 7–18. doi:10.1016/j.chom.2011.11.011

Voss, T.S., Healer, J., Marty, A.J., Duffy, M.F., Thompson, J.K., Beeson, J.G., Reeder, J.C., Crabb, B.S., Cowman, A.F., 2006. A var gene promoter controls allelic exclusion of virulence genes in Plasmodium falciparum malaria. Nature 439, 1004–1008. doi:10.1038/nature04407

Wang, G., Ma, A., Chow, C.M., Horsley, D., Brown, N.R., Cowell, I.G., Singh, P.B., 2000. Conservation of heterochromatin protein 1 function. Mol. Cell. Biol. 20, 6970–6983.

Westenberger, S.J., Cui, L., Dharia, N., Winzeler, E., Cui, L., 2009. Genome-wide nucleosome mapping of Plasmodium falciparum reveals histone-rich coding and histone-poor intergenic regions and chromatin remodeling of core and subtelomeric genes. BMC Genomics 10, 610–17. doi:10.1186/1471-2164-10-610

Zhao, T., Eissenberg, J.C., 1999. Phosphorylation of heterochromatin protein 1 by casein kinase II is required for efficient heterochromatin binding in Drosophila. J Biol Chem 274, 15095–15100. doi:10.1074/jbc.274.21.15095

Zhao, T., Heyduk, T., Eissenberg, J.C., 2001. Phosphorylation site mutations in heterochromatin protein 1 (HP1) reduce or eliminate silencing activity. J Biol Chem 276, 9512–9518. doi:10.1074/jbc.M010098200